

The expression and function of axon guidance circular RNAs during neuronal development

Daniëlle van Rossum

Colofon

PhD thesis, Utrecht University, the Netherlands
Copyright © 2021 Daniëlle van Rossum

Author: Daniëlle van Rossum
Layout: Daniëlle van Rossum
Cover: Bart van Dijk & Daniëlle van Rossum
Press: Proefschrift-All In One | www.proefschrift-aio.nl
ISBN: 978-90-393-7392-7

Printing of this thesis was financially supported by the UMC Utrecht Brain Center and Zeiss

Squaring the circle: The expression and function of axon guidance circular RNAs during neuronal development

De expressie en functie van axon guidance
circulaire RNAs tijdens de neuronale ontwikkeling

(met een samenvatting in het Nederlands)

Proefschrift

ter verkrijging van de graad van doctor aan de Universiteit Utrecht op gezag van de rector magnificus, prof.dr. H.R.B.M. Kummeling, ingevolge het besluit van het college voor promoties in het openbaar te verdedigen op donderdag 2 september 2021 des middags te 2.15 uur

door Daniëlle Samantha van Rossum

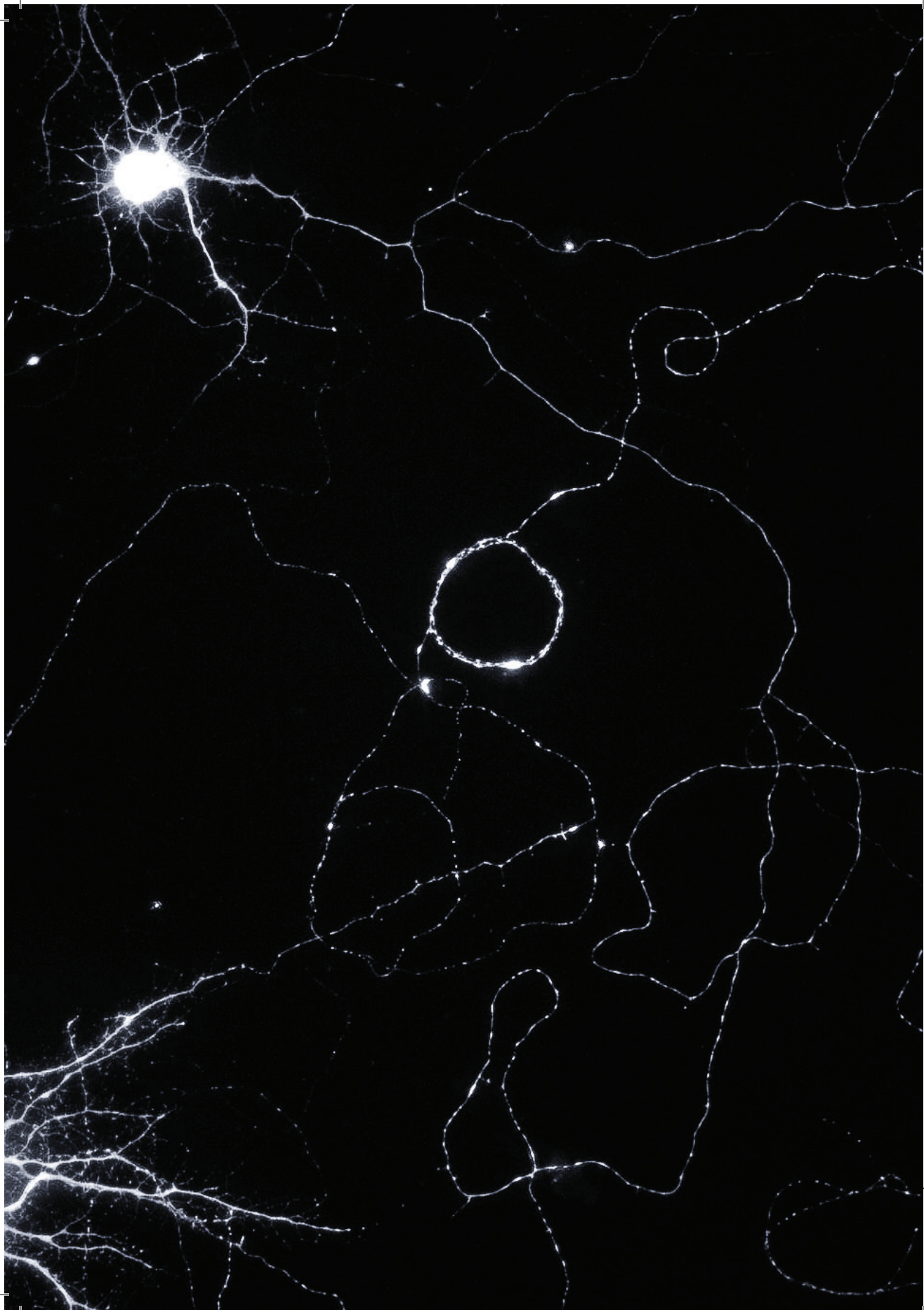
geboren op 2 februari 1991 te Zoetermeer

Promotor:

Prof. dr. R.J. Pasterkamp

Contents

INTRODUCTION	7
General introduction and outline of the thesis	
CHAPTER 1	39
Axon guidance circRNAs are conserved in the human brain and dynamically expressed in the developing and adult mouse brain	
CHAPTER 2	85
Characterization of the spatiotemporal expression of axon guidance circRNAs in the developing mouse brain using <i>in situ</i> hybridization	
CHAPTER 3	113
Manipulation and functional assessment of axon guidance circRNA <i>in vitro</i> and <i>in vivo</i>	
CHAPTER 4	161
CiRS-7 miRNA interactome and function in the healthy and epileptic brain	
DISCUSSION	193
Summary & general discussion	
ADDENDA	213
Nederlandse Samenvatting	
Curriculum Vitae	
Acknowledgements	
Samenstelling beoordelingscommissie	



INTRODUCTION

General introduction and outline of the thesis

The axons of these primary cortical neurons seem to 'run in circles' (Image taken with an epifluorescent microscope).

PREFACE

Squaring the circle is a phenomenon that has mesmerized many great minds since ancient times. The question is whether it is possible to construct a circle with exactly the same surface area as a given square. Although the impossibility of the phenomenon was proven in 1882, many more countless attempts to solve the question were made and the expression "*squaring the circle*" slowly evolved as a metaphor for trying to do the impossible. The story of studying circular RNAs (circRNAs) has some resemblances to the 'squaring the circle' phenomenon. CircRNAs were initially discovered in the late 1970s but received little attention as they were thought to be useless byproducts of aberrant splicing. Nonetheless, at the beginning of the 2010s circRNAs re-emerged as potential regulators of gene expression due to the development of RNA sequencing techniques. Since then, many minds have bended their heads over these circular molecules, as these seemed promising players in the complex network of gene regulation. Although circRNAs were reported to be highly expressed in the developing brain, still little is known about circRNA function in the brain in health and disease. In this thesis we therefore aimed to explore the expression and function of circRNAs (generated from axon guidance genes specifically) in the developing (mouse) brain using various molecular and cellular approaches. The work presented in this thesis provides new insights into tools to study the expression of (axon guidance) circRNAs and makes a first step towards dissecting their function in neuronal development. Nonetheless, not all of our results are conclusive and the question remains: Are circRNAs the long hidden players of important neuronal developmental processes, or might this perhaps be a story about trying to square a circular RNA...?

GENERAL INTRODUCTION

Adapted from: van Rossum D, Verheijen BM and Pasterkamp RJ (2016) Circular RNAs: Novel Regulators of Neuronal Development. Front. Mol. Neurosci. 9:74. doi: 10.3389/fnmol.2016.00074

Here, we introduce axon guidance and summarize our current knowledge of the molecular characteristics, functions and mechanism-of-action of circular RNAs (circRNAs) in neurons. We discuss the relevance of studying circRNAs from axon guidance genes specifically and introduce the aim and outline of this thesis.

Axon guidance: Target finding in a complex network

The human brain is more complex than any other known structure on earth. It embodies a complicated network of a large number of nerve cells, also known neurons, and glia cells, which are important for the (physical) support and protection of neurons. Neurons are distinguished by their branch-like projections called axons and dendrites (together known as neurites) which gather and transmit electrochemical signals. By growing their neurites to other cells, each neuron can connect with hundreds of other neurons nearby, or with cells that are much further away. This facilitates cellular communication between cells in different brain areas and allows the brain to produce all of the thoughts, actions, memories, feelings and experiences of the world. Given that the brain consists of billions of cells, it is fascinating that each individual neuron knows how to grow its axon to the proper target cell, leading to correct brain function. The famous neuroscientist Ramón y Cajal already racked his brain over this phenomenon more than 100 years ago. Since then, many proteins and RNAs have been identified that are involved in establishing the complex anatomical organization of the brain, but much of the toolbox of brain development and functioning remains to be explored.

Axon guidance is the developmental process by which neurons extend their neurites to the appropriate targets. At the leading tip of their growing axons, neurons have a specialized structure called the growth cone. This growth cone is a highly dynamic structure, that changes shape and direction based on interaction with surrounding cues. Through proteins, called receptors, that are localized on their membrane, growth cones can sense guidance cues present in the surrounding environment. The size and direction of growth

of the growth cone is influenced upon interaction with guidance cues. After interplay between axon guidance cues, cell-and tissue-type specific responses are triggered, and intracellular signaling pathways are activated that change cytoskeleton organization. This way, axon guidance cues can either act as an attractant or repellent for growing axons, steering them towards or away from specific targets (Figure 1). Moreover, some axon guidance cues are secreted and can direct the growth cone toward or away from specific regions over long distances in the brain, while other cues are membrane-associated and can influence the direction of growing axons nearby¹. This already indicates how different axon guidance cues each play their own role in axonal pathfinding. When axons finally reach their target area, the growth cone collapses and the formation of a synapse (the point of connection between two neurons) starts, laying the foundation a functional neural circuit.

Canonical axon guidance cues

Over the past decades more than 100 guidance molecules and receptors have been identified. For Netrins, Slits, Semaphorins, and Ephrins, the major axon guidance families (also known as canonical axon guidance cues), roles in neural circuit formation have been established. Netrins are a small family of conserved axon guidance cues involved in directing cell migration and axonal outgrowth in the developing nervous system² (Figure 1). Where Netrins were initially identified as attractants and Slits, Semaphorins and Ephrins as repellents, it became clear that, depending on the cellular context, they can also act in the opposite way^{3,4}. A key player in axon guidance, and a variety of other cellular processes, is the Netrin receptor deleted in colorectal cancer (DCC). Netrin binding to DCC results in attractive responses, while if uncoordinated-5 (UNC5) co-exists with DCC binding of Netrin results in repulsive responses⁵. Down's syndrome Cell Adhesion Molecule (DSCAM) also functions as a Netrin receptor in collaboration with DCC⁶. Another receptor that assists in axon guidance by binding to Netrin is the transmembrane protein Neogenin⁷. Neogenin is implicated in cell proliferation and differentiation, and mediates the repulsive effect on multiple guidance molecules including repulsive guidance molecule (RGM) and Netrins^{8,9}. Where Netrins are secreted or membrane-bound, Slits are secreted proteins that repel axons after binding to roundabout (Robo) receptors^{5,10-12}. Both Slits and Robos are highly conserved and besides their role in attracting and repelling axons across the midline, they play an important role in cell migration and proliferation of neurons and glia and various other processes outside of the nervous system¹³.

Semaphorins are a large conserved family of axon guidance molecules that are secreted or bound to the membrane of the growth cone¹⁴. Plexins, which are large conserved proteins, are the most prominent semaphorin receptors in neurons, but some Semaphorins require Neuropilin (Nrp) as a co-receptor¹⁵. Depending on their environment, Semaphorins and Plexins can act as ligands and induce forward signaling, or as receptors resulting in reverse signaling. Like Semaphorins, Ephrins can function as receptors by participating in reverse signaling. Ephrins are membrane-bound, short-range signaling molecules that are important for a large number of developmental events, including axonal branching and synaptogenesis¹⁶. Depending on how they are attached to the membrane they are classified into two subfamilies, GPI-linked (A) or transmembrane (B)¹⁷. Ephrins bind to a large group of Eph receptors and can function as attractants for some axons and repellents for others, thereby activating a variety of intracellular signaling cascades that instruct growth of the axon into the right direction¹⁸.

A key function of axon guidance cues is regulating the direction of migrating neurons and developing axons through changes in cellular morphology. When these axon guidance processes are executed properly and neurons have reached their destination, the connections between neurons are refined through electrical signaling. Bundles of individual axons from many different neurons within one region of the brain can form fiber bundles that can make connections with neurons in other regions of the brain. This way neuronal networks between neurons are formed that can direct our thoughts and actions, like the prefrontal cortex and the hippocampus. When a machine as complex as the brain malfunctions during development or gets injured, problems in the neuronal network and cellular communication arise. This can result in various neurodevelopmental disorders like epilepsy, autism spectrum disorders and schizophrenia, but also play a role in the development of neuronal disorders at an adult stage like amyotrophic lateral sclerosis (ALS) and Alzheimer's or Parkinson's disease¹⁹. Therefore, understanding the complexity and molecular mechanisms of neural circuit development is important as they can be the foundation of the cause and potential treatment of the disorders.

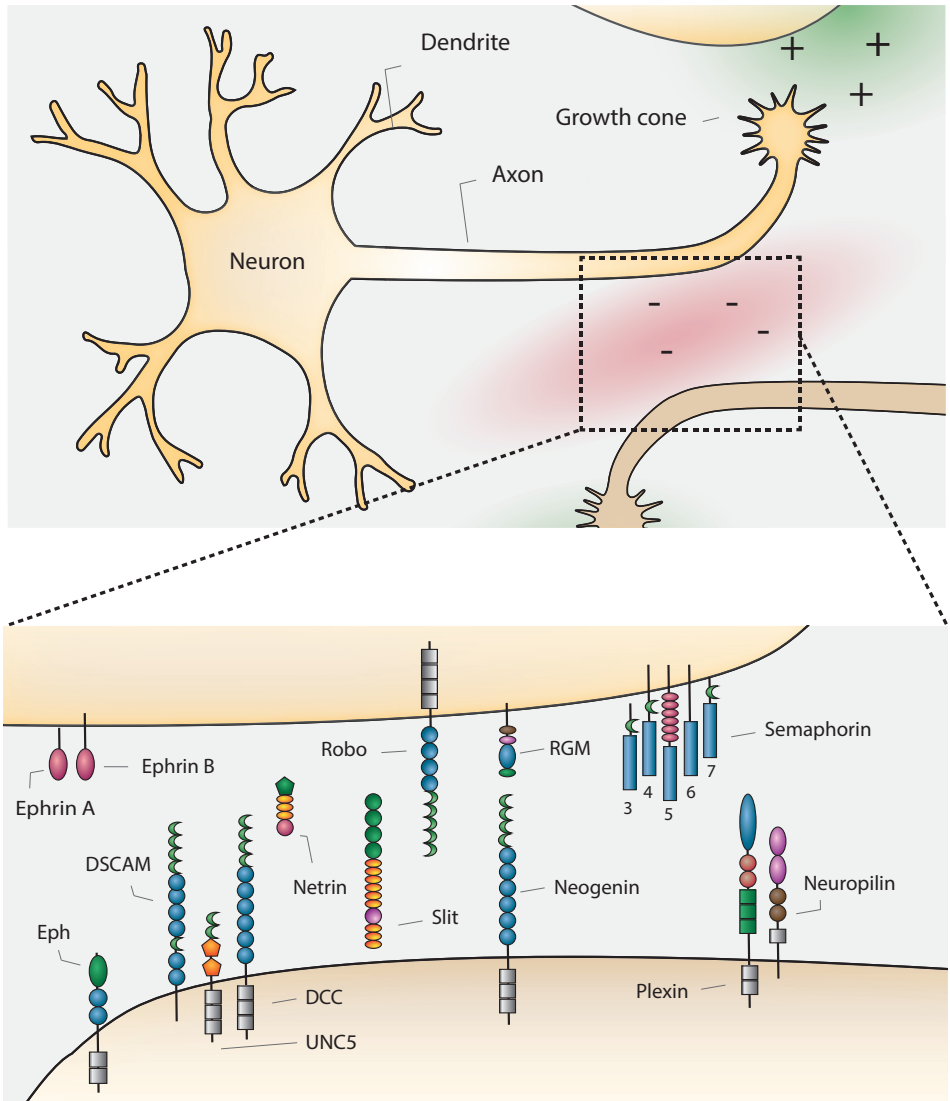


Figure 1 | Axonal growth mediated by attractive and repulsive axon guidance cues.

Axon guidance is the developmental process by which neurons extend their axons to the appropriate targets. At the leading tip of their growing axons, neurons have a specialized structure called the growth cone. This growth cone is a highly dynamic structure, that changes shape and direction based on interaction with surrounding cues. Through proteins, called receptors, that are localized on their membrane, growth cones can sense guidance cues present in the surrounding environment. Upon interaction with guidance cues, intracellular signaling pathways in the neuron are activated that change cytoskeleton organization and determine which way the growth cone will grow. Axon guidance cues can either act as an attractant (positive, green) or repellent (negative, red) for growing axons. Over the years approximately 100 guidance molecules have been identified, these include Netrins, Slits, Semaphorins, Ephrins, DCC, UNC5, DSCAM, Robos, Plexins, Neuropilins and Ephs.

Axon guidance and non-coding RNAs

The process of axon guidance is key to the formation of a neuronal network. Hence, it is fascinating that with a limited set of axon guidance genes (approximately 100), complex neuronal circuits (the adult human brain is estimated to have more than 60 trillion neuronal connections) can be established. Since new axon guidance cues are still being discovered, it is likely that there are more unknown players involved in the process of neuronal wiring besides guidance proteins, morphogens, growth factors, and cell-adhesion molecules that are key to axon guidance. For instance, alternative splicing, a process that allows the generation of a large number of isoforms from a single gene, and the transcription of non-coding transcripts are thought to also contribute to shaping complex neuronal networks, which adds a layer of gene expression regulation that is only starting to be explored²⁰⁻²².

An estimated 80% of the human genome consists of non-coding elements such as small non-coding RNAs (sncRNAs; <200 nucleotides) and long non-coding RNA (lncRNAs; >200 nucleotides). These non-coding RNAs (ncRNAs) do not code for proteins, but have been reported to serve as key transcriptional and post-transcriptional regulators of gene expression. For instance, one group of sncRNAs, microRNAs (miRNAs), can induce mRNA degradation or translational repression, which alters the expression of specific genes. It is even estimated that about 60% of translated protein coding genes are negatively regulated by miRNAs²³. miRNAs have also been reported to play a role in the regulation of axon guidance genes, e.g. by regulation of either guidance receptors at the transcriptional level or by affecting their downstream signaling at the post-transcriptional level²⁴⁻²⁶. For example, Robo1 and Robo2 are negatively regulated by miR-218, and the sensitivity of retinal ganglion cell axons to the repellent Sema3A is regulated by translational control of Neuropilin1 and miR-124^{24,27}.

lncRNAs are prominently expressed in the brain and have been implicated in neuronal development, function and disease²¹. One type of lncRNAs that has attracted growing attention are circular RNAs (circRNAs), that have recently been detected in large numbers in the brain. Interestingly, axon guidance genes can also give rise to circRNAs and these transcripts were reported to be specifically upregulated during certain (embryonic) stages of the developing porcine brain²⁸. Many of the axon guidance circRNAs were reported to be expressed in a tissue/developmental stage-specific manner and revealed a striking

(up)regulation of circRNAs, not only during brain development but also during neuronal maturation and differentiation. Although the importance of the role of non-coding RNAs in neuronal development has started to emerge, no systematic investigation or studies on the specific expression or function of individual circRNAs from axon guidance genes have been reported up until now. This raised the question whether circRNAs from axon guidance genes may also play a role in neural circuit formation. Understanding the role of axon guidance circRNA in brain development is important as it may help to enhance our insight into the mechanisms of neuronal circuit formation and disease.

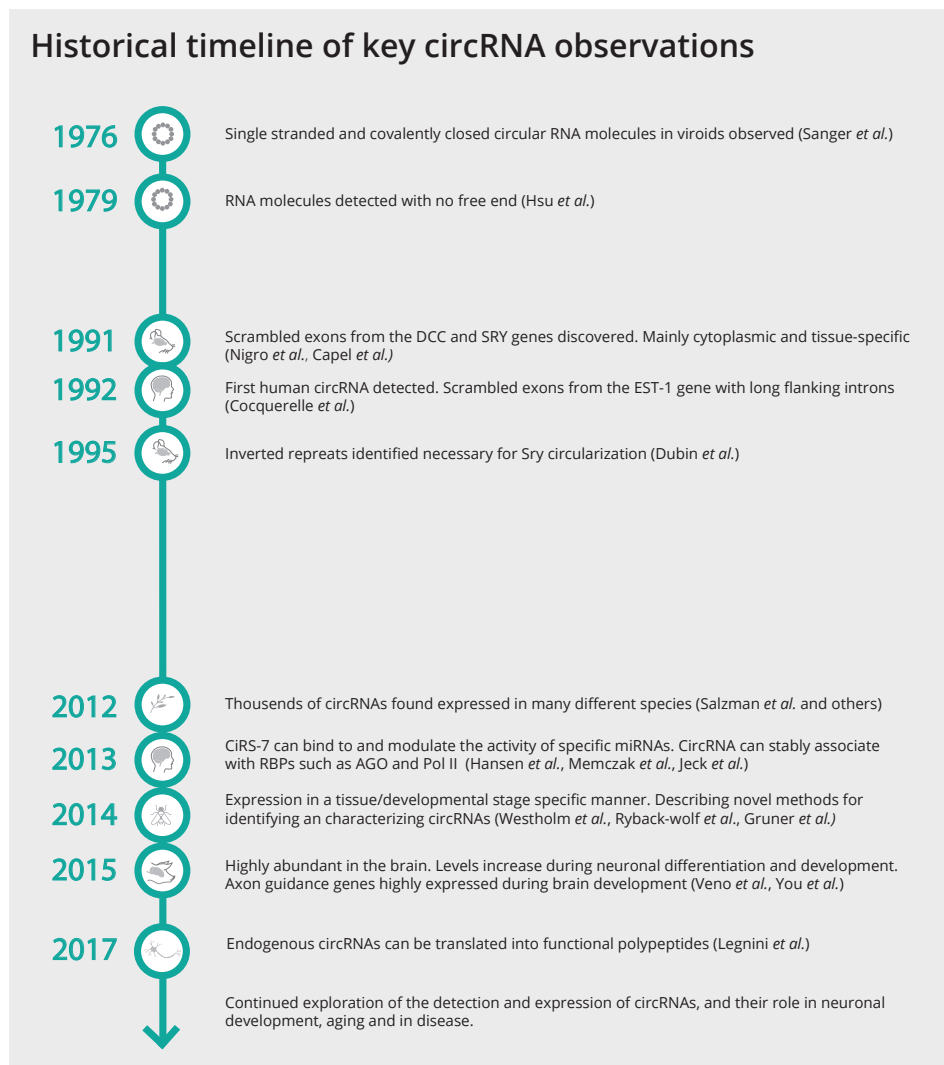


Figure 2 | Historical timeline of key circRNA observations

Circular RNAs

CircRNA transcripts were originally described in the late 1970s (Figure 2). They were first detected in human cell lines using electron microscopy, adding to a number of observations of circRNAs in viroids and other experimental models²⁹⁻³¹. The serendipitous discovery of circular transcripts generated from the gene *DCC* demonstrated that circRNAs can actually originate from transcribed genes³². In the following years, circRNA isoforms derived from several other loci were found in cells, including from the *ETS-1*, *Dystrophin* and *Cytochrome P-450 2C18* genes³³⁻³⁶. Initially, these circRNAs were thought to be potentially pathogenic byproducts of aberrant splicing or 'transcriptional/splicing noise' and did not receive much attention. However, skepticism toward the existence and significance of circRNAs faded away with the development of new and improved transcriptomics and bioinformatics approaches. High-throughput sequencing of ribosome-depleted RNA convincingly showed that human fibroblasts contain more than 25,000 unique and stable circRNAs³⁷. These circRNAs originate from 14,4% of expressed genes, which came as a surprise, as circRNAs were initially considered a rare phenomenon. Estimates indicate that circRNAs may actually account for about 1% of total RNA in human³⁸.

Recently, a plethora of studies reported the expression of a variety of circRNAs in different species ranging from human and mouse to *Drosophila* and *C. elegans*^{28,37-42}. These studies demonstrate that circRNAs are evolutionary conserved and expressed in a time-, cell type- and gene-specific manner. While most circRNAs are lowly abundant, some are ubiquitously expressed and are present at higher copy numbers (>10-fold), as compared to their linear transcripts^{37,38}. Interestingly, these studies also revealed that circRNAs are regulated during neuronal differentiation and nervous system development, while also highlighting specific subcellular distributions of certain circRNAs in neurons, e.g., at the synapse^{28,43,44}. These findings hint at important roles for circRNAs in neural development and function.

CircRNA Biogenesis: Back-Splicing and Composition

CircRNAs can be distinguished from their linear counterparts by their remarkable continuous closed loop structure, formed by a 'back-splicing' event wherein a covalent bond is formed between 5' (splice donor) and 3' (splice acceptor) splice-sites of a pre-mRNA^{37,40}. Back-splicing leads to the formation of a 'head-to-tail junction' or 'black-splice junction' that contains a unique sequence not present in mRNAs (Figure 3). Because

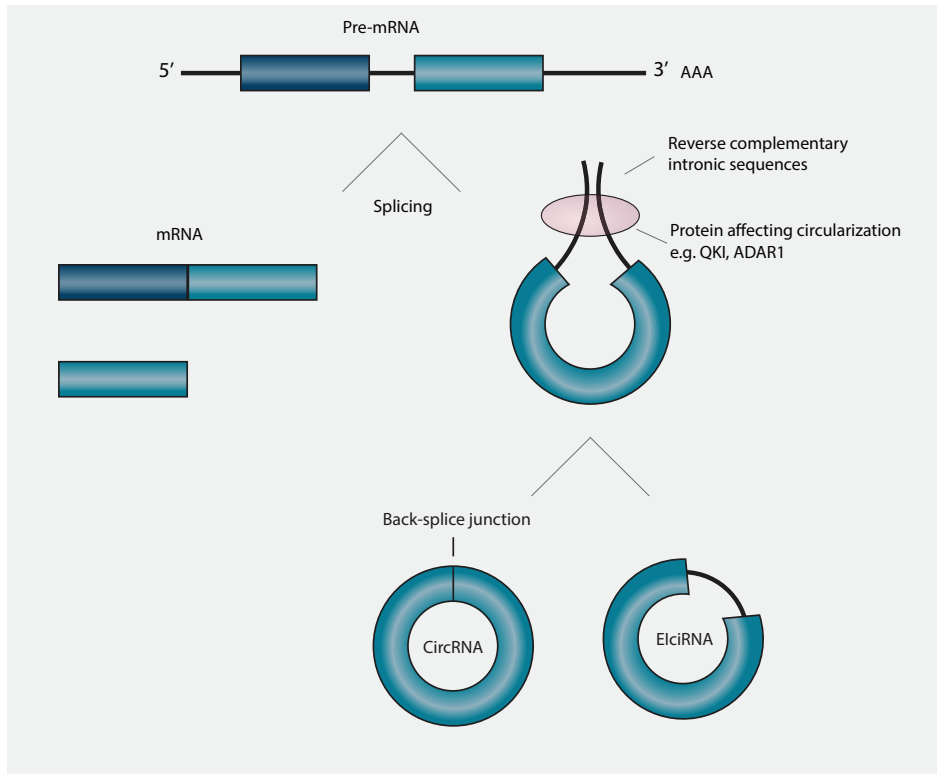


Figure 3 | Schematic representation of circRNA biogenesis.

The canonical splicing machinery generates mature linear mRNA from pre-mRNA by removing intervening introns. CircRNAs are generated from pre-mRNAs when a downstream splice donor is joined to an upstream splice acceptor, forming a covalent bond between the 3' and 5' ends. This process is called back-splicing and results in a 'back-splice junction'. circRNAs can be exonic, intronic or a combination of both. Back-splicing coupled with splicing removes the intervening introns to generate exonic circRNAs. Although less common, some exonic circRNAs with retained intron are generated by back-splicing and are called ElcircRNAs. MBL (muscleblind) can bind to its own circRNA and QKI (Quaking) and ADAR1 (Adenosine deaminase acting on RNA 1) bind circRNAs to regulate circRNA biogenesis.

they lack 5' and 3' termini, circRNAs do not show typical features of mRNA processing, such as 5' capping and a poly(A)-tail, making them highly resistant to degradation by exonucleases. The biogenesis of circRNAs is poorly understood, but appears to be distinct from canonical pre-mRNA splicing that occurs during the maturation of mRNA transcripts. However, back-splicing reactions do seem to be dependent on canonical splicing machinery^{45,46}. circRNAs are very heterogeneous and can (1) consist of coding or scrambled coding sequences only, (2) contain exonic and intronic segments, i.e., in

exon-intron circRNAs (EicRNA) that retain flanking intronic sequences or (3) be derived from untranslated regions (UTRs), intergenic loci, and antisense sequences. It is evident that these structurally diverse circRNAs could fulfill pleiotropic functions^{47,48}. A detailed overview of mechanisms for circRNA formation is beyond the scope of this thesis, but readers are directed to other articles on this subject⁴⁹⁻⁵¹.

Regulation of CircRNA Biogenesis

CircRNA biogenesis and expression likely depend on various *cis*-regulatory elements and *trans*-acting factors. Evidence for the regulation of circRNA formation in *cis* comes from the identification of inverted repeat sequences bracketing the region that produces circRNAs. Highly abundant circRNAs have significantly longer flanking introns, and genes giving rise to circRNA transcripts generally contain longer intronic sequences as compared to genes that do not^{39,47}. In line with this, circRNAs originating from genes with neuronal functions in *Drosophila* often have long introns⁴². Similarly, genes involved in axon guidance and Wnt signaling give rise to a disproportionately large number of circRNAs in the developing pig brain and have, on average, long intronic sequences²⁸. These long intronic regions may act to slow down canonical splicing, allowing back-splicing to occur. In this way, circRNA formation competes with pre-mRNA splicing. Intronic elements flanking circRNA transcripts, such as ALU-repeats, have been demonstrated to be involved in the circularization of exons^{37,39,46,52-54}. Importantly, circRNA expression is not always correlated with expression of linear RNA from the same locus. Therefore, *cis* motifs alone are not sufficient to explain the dynamic expression patterns of circRNA.

Trans-acting factors that can affect circRNA biogenesis are RNA-binding proteins (RBPs), including splicing factors. RBPs carry out essential roles during neural development and their dysregulation contributes to neural disorders. For example, deficiency of the RBP Quaking (QKI) may contribute to the pathogenesis of schizophrenia and the development of human inherited ataxia^{55,56}. Interestingly, knockdown of QKI reduces the production of circRNAs, while integration of QKI binding sites into linear RNAs induces exon circularization. These observations indicate a role for QKI in the formation of circRNAs⁵⁷. In contrast to the agonistic effect of QKI, the RBP ADAR1 (Adenosine deaminase acting on RNA 1) inhibits the formation of circRNAs by binding double stranded RNA (Figure 2)^{53,58-61}. It will be interesting to determine whether QKI's and ADAR1's role in neural development and disease are directly mediated through their ability to control circRNA biogenesis.

Functions of CircRNAs and mechanism of action in Neurons

The functional role of most circRNAs remains elusive. For a few circRNAs, interesting functions have been uncovered and these have fueled speculations regarding general functions of circRNAs.

miRNA Sponging and Binding to RBPs

The relatively well-studied circRNAs sex determining region Y (SRY) and cerebellar degeneration-related protein 1 antisense (CDR1as; also known as ciRS-7: Circular RNA Sponge for miR-7) have multiple binding sites for miR-138 and miR-7, respectively. Binding of specific miRNAs by these circRNAs can modulate miRNA expression levels competitively and thereby suppress their function, a process known as 'miRNA sponging' (Figure 3 (1))^{40,62}. More recently, circHIPK3, generated from the HIPK3 gene, was shown to mediate sponging of miR-124, thereby modulating human cell growth⁶³. Both ciRS-7 and miR-7 have been linked to nervous system development and disease. miR-7 represses α -synuclein, a protein involved in Parkinson's pathogenesis, and miR-7 downregulation is observed in human glioblastoma^{64,65}. Increased levels of miR-7 have been detected in neuropsychiatric disorders and evidence for ciRS-7-mediated regulation of dendritic spine density via a miR-7-SHANK3 axis has been found^{66,67}. Expression of human ciRS-7 in zebrafish causes impaired midbrain development and knockdown of ciRS-7 leads to migration defects *in vitro*, as shown in a wound-healing assay using HEK293 cells^{40,62}. Interestingly, a circRNA knockout mouse for ciRS-7 was generated that revealed altered excitatory synaptic transmission and defects in sensomotor gating and in this knockout mouse decreased expression of miR-7 and up-regulation of its mRNA targets were observed⁶⁸. In another study these findings were explained by the suggestion that when ciRS-7 levels are reduced, miR-7 is not 'sponged' and free to bind to the lncRNA Cyran0 that can degrade miR-7⁶⁹. In all, these data implicate a role for circRNAs and their interaction with other ncRNAs in neurite growth and neuron migration (Figure 4 (2)).

CircRNAs might not only act as competitive RNAs for miRNAs, but could also be involved in their storage, sorting, and localization. Interestingly, ciRS-7 binds to Argonaute (AGO), an effector protein in the RNA-induced silencing complex (RISC). ciRS-7 is not cleaved by AGO upon miR-7 binding, because none of the miR-7 binding sites is complementary for more than 12 nucleotides. However, CiRS-7 contains a binding site for another miRNA, miR-671, which is fully complementary and can induce AGO-mediated cleavage of this circRNA⁷⁰.

This may have several co-regulatory consequences. For example, cleavage of the circRNA may result in the (local) release of binding partners (miR-7), which would indicate a role in miRNA transport and delivery (Figure 4 (3)). In addition, a cleaved antisense circRNA might bind its linear sense transcript, potentially resulting in RNA destabilization and silencing.

In addition to miRNAs, circRNAs bind to, sequester and transport RBPs, which may regulate the interaction of RBPs with their RNA targets (Figure 4 (4,5))^{39,71,72}. Examples include circRNAs from the muscleblind (mbl) and FOXO3 genes^{46,73}. Interestingly, alternative splicing of circRNAs may also lead to the formation of new binding sequences for specific RBPs and give rise to a number of different protein decoys. circRNAs are likely to not only bind single RBPs but actually have been proposed to act as scaffolds for the assembly of large protein complexes (Figure 4 (6))^{28,74,75}.

Currently, it is not clear whether miRNA sponging and RBP binding are shared functions of circRNAs. Some studies demonstrate that only a few circRNAs have properties similar to the previously described miRNA sponges, but that these are not features of circRNAs as a group⁴¹. The existence of circRNAs in species that lack RNA interference (RNAi) pathways also points toward other mechanisms. Therefore, miRNA sponging and protein binding might be exceptional properties of select circRNAs that are not shared by the majority of circRNAs.

Transcriptional Control

As functional circRNAs have been shown to act as miRNA sponges or protein decoys in the cytoplasm, it is tempting to speculate that circRNAs primarily act as post-transcriptional regulators of gene expression^{40,76}. However, circRNAs do not only localize to the cytoplasm, but can also be present in the nucleus. circRNAs containing introns, like ElciRNAs, are retained in the nucleus, and can interfere with gene transcription, including the transcription of their parental genes. This process can be mediated by direct interaction with U1 snRNP: an ElciRNA-U1 complex can recruit RNA polymerase II (Pol II) to the promoter region of a gene, stimulating initiation of transcription (Figure 4 (7)). Nuclear circRNAs could therefore be specifically involved in the regulation of transcriptional activity in neurons^{47,77}. For example, upregulation of PAIP2 by circPAIP2 may affect contextual memory⁷⁸.

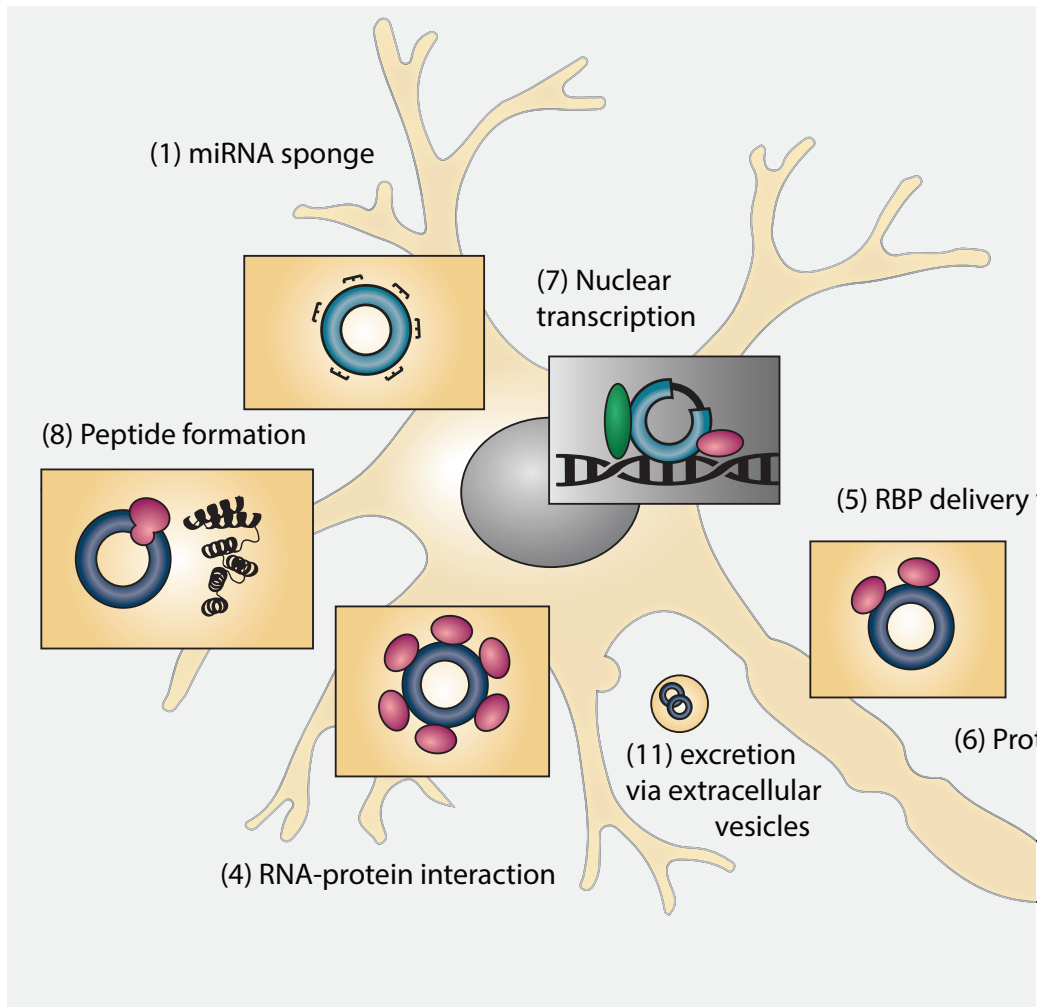
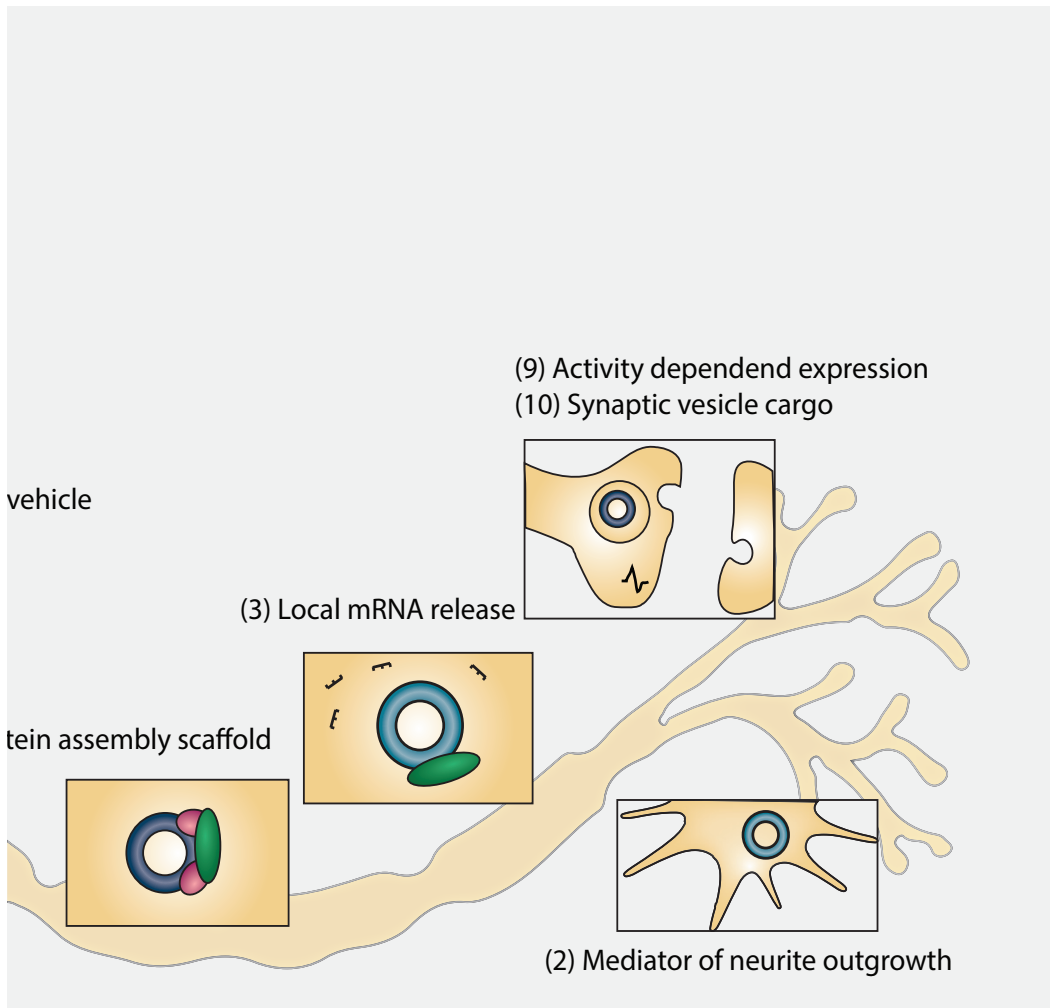


Figure 4 | (Putative) functions of circRNAs in neurons.

Schematic representation of a neuron, indicating established and putative general and neuron-specific functions of circRNAs: (1) circRNAs such as *ciRS-7* (Cerebellar degeneration-related protein 1 antisense) and *SRY* (Sex determining region Y) have binding sites for specific miRNAs, e.g., miR-7. By binding these miRNAs they act as 'miRNA sponges' and inhibit miRNA function. (2) circRNAs may affect neurite outgrowth and neuronal migration. For example, ectopic *ciRS-7* expression causes migration defects in vitro. (3) miR-671 can bind *ciRS-7* to induce AGO-mediated cleavage of this circRNA. This may result in the local release of other miRNAs bound by *ciRS-7*. (4) Various RNA-binding proteins (RBPs) bind circRNAs. For example, *MBL* (muscleblind) can bind to its own circRNA. *QKI* (Quaking) and *ADAR1* (Adenosine deaminase acting on RNA 1) bind circRNAs to regulate circRNA biogenesis. circRNAs may 'sponge' RBPs (such as *TDP-43*) in the nucleus to regulate gene expression. (5) Binding of RBPs by circRNAs may facilitate RBP transport to distal compartments in neurons, e.g., synapses. (6) circRNAs have been proposed to act as scaffolds for



protein complex assembly. By binding multiple RBPs, circRNAs might facilitate stable interactions between proteins. **(7)** Exon-intron circRNAs (EicRNAs) are associated with RNA polymerase II in the nucleus. EicRNAs recruit Pol II to regulate host gene transcription via U1 snRNA. **(8)** It has been proposed that small peptides and/or proteins may be generated from circRNAs in the cytoplasm. **(9)** The expression of certain circRNAs is affected by neuronal activity. **(10)** circRNAs are present in synaptic vesicles. **(11)** circRNAs are present in extracellular vesicles and could act as long range signaling molecules.

Translation

CircRNAs often contain coding exons (e.g., for protein structural domains) and carry open reading frames 39,79. First it was only reported that synthetic exonic circRNAs can be translated *in vitro* and *in vivo* when internal ribosome entry sites (IRES) or prokaryotic binding sites are introduced⁸⁰⁻⁸². But recent experimental evidence supports the speculation that endogenous circRNAs also have translation potential (Figure 4 (8))⁸³⁻⁸⁶. A group of endogenously expressed circRNAs were reported to generate small peptides in cancer cell lines, human fibroblasts, drosophila heads and mammalian muscle cells^{84,85}. Using Ribosome foot printing, researchers observed that circRNAs can be translated by membrane-associated ribosomes⁸⁴. However, as only for a limited set of circRNAs their translation into peptides has been reported, it remains unclear whether all circRNAs can be endogenously translated into protein under normal conditions and whether they exert specific biological effects or interfere with protein-protein interactions. Interestingly, the inhibition of circZNF60 (reported to generate peptide in mouse and human skeletal muscle cells) caused a strong reduction in myoblast proliferation, suggesting that peptides from circRNAs can affect cell growth⁸³. Many RNAs and proteins are transported into neurites, axons and dendrites, where they are locally translated or activated upon stimulation by specific intra- or extracellular cues. It is plausible that some circRNAs act as local regulators of gene expression at distal neuronal sites, such as growth cones and synapses, and contribute to different aspects of neural development. For example, circRNAs generated from the axon guidance receptor gene DCC contain a substantial number of open reading frames encoding for ligand-binding domains. It is tempting to speculate that, if generated, these circRNA-derived protein fragments may interfere with DCC ligand binding.

The variety of studies reporting on the (putative) functions of certain circRNA suggest that circRNAs could fulfill numerous functions in the developing nervous system, depending on (1) their expression in a specific species, (2) which gene they are originated, (3) when they are expressed in the brain, and (4) their (sub)cellular localization. Thus, in order to investigate the roles and mechanism-of-action of axon guidance circRNAs during neural development and plasticity, more information on their conservation and spatiotemporal expression in the developing brain need is necessary.

Neuronal Development and Plasticity

Several studies have demonstrated that circRNAs are specifically enriched in brain tissue. Intriguingly, circRNAs are not homogeneously distributed throughout the nervous system but are differentially expressed in different brain regions and subcellular compartments, and at specific embryonic and postnatal stages^{28,40,43,44,87}. For instance, the abundance and expression profiles of human circRNAs changed during different embryonic developmental stages and circRNAs in the developing porcine brain are generally display higher expression in the cerebellum as compared to the brainstem^{44,88}. Which factors exactly drive circRNA expression at a certain time or place is largely unclear. But what has been reported is that circRNAs can be up- or downregulated in cultured neurons in response to changes in neuronal activity, for instance by addition of the GABAA receptor antagonist bicuculline, indicating that neuronal expression of circRNA is activity-dependent (Figure 4 (9))⁴⁴. Neuronal activity is known to affect gene expression in multiple ways, and one potential novel way may thus be by modulating circRNA levels.

Recent studies reveal that many of the circRNAs expressed in neural tissues derive from synaptic genes such as *Dscam* and *Homer1*, or from genes with prominent roles in early neural development, e.g., genes implicated in Wnt signaling, axon guidance, and TGF- β signaling²⁸. A large group of circRNA transcripts, especially from axon guidance cues (e.g., from the Eph and Robo gene families) are observed to be upregulated at specific developmental time points, e.g., during synaptogenesis^{28,44,89}. Interestingly, circRNAs from genes with synaptic functions (e.g., *Dscam* and *Homer 1*) were enriched in dendritic structures regardless of gene expression levels. Additionally they were found to be enriched in hippocampal synaptosomes, suggesting active transport of circRNAs to synapses (Figure 4 (10))^{43,44}. In general, circRNAs were found to be highly enriched in synapses, both *in vitro* (in cell lines and primary neuronal cultures) and *in vivo* (synaptoneurosomes from the mouse brain)^{40,43}. Downregulation of circMbl in *Drosophila* heads caused abnormal synaptic function and it was reported that circGRIA1 regulates synaptic plasticity and synaptogenesis in the male macaque brain⁹⁰. Interestingly, increased spontaneous vesicle release was observed in the neurons of ciRS-7 knockout mice, suggesting that ciRS-7 might have a role in regulating synaptic transmission^{68,84}. Besides synaptic activity a growing body of experimental evidence indicates that circRNAs are involved in various cellular events, such as proliferation, differentiation and apoptosis⁴²⁻⁴⁴. For example, the knockdown of circSLC45A4 can induce spontaneous neuronal differentiation in human

neuroblastoma cells, while the pool of basal progenitors in the developing mouse cortex was reduced⁹¹. In all, these findings demonstrate a heterogeneous distribution of circRNAs within neurons and implicate a role for circRNAs in neuronal development and plasticity.

Circular RNAs may not only serve physiological functions in neurons, but have also been linked to brain disease. General insults to neurons, like neurotoxicity or injury, induce a stress response that involves changes in gene expression, splicing, and altered expression of ncRNAs, including circRNAs. Accumulating evidence suggests that circRNAs may be involved in a wide range of neuronal stress responses and that their aberrant expression or function may contribute to the development, progression and/or severity of various neurological disorders. CircRNAs have been implicated in several neurodegenerative diseases, including Alzheimer's and Parkinson's disease^{92,93}. Moreover, the RNA-binding protein FUS has been recognized as an important modulator of circRNA expression in ALS, and a subset of circRNAs, including a synaptically expressed circRNA from the *HOMER1* gene, showed significant differential expression in temporal lobe epilepsy (TLE) patient samples compared to healthy controls^{94,95}. Nonetheless, the relationships between circRNAs and various neurological disorders is currently still poorly understood. Understanding the relationship between circRNAs and brain disease is important, as circRNAs could be targets for therapeutic approaches. For example, circRNAs are closely intertwined with RNA processing (like pre-RNA splicing and RNA editing), which are affected in neurological diseases such as ALS and spinal muscular atrophy (SMA)⁹⁶. The splicing of circRNAs could be modulated with antisense oligonucleotides and other small molecules leading to a reduction in disease-causing circularized products^{74,97}. Interestingly, circRNAs have been also shown to accumulate during aging which could link them to various age-related neurodegenerative diseases⁴². Apart from acting as therapeutic targets, circRNAs might serve as biomarkers for disease, given their stability and secretion in extracellular vesicles (Figure 4 (11))⁹⁸. The biological role of this secretion is unknown but may be linked to communication between different cell types (e.g., neuron-glia) or different tissue compartments (including, for example, CSF and blood)^{77,99}.

Methodological difficulties to detect and manipulate circRNAs

Advances in RNA sequencing and bioinformatics tools have provided new opportunities in understanding the expression and function of circRNAs¹⁰⁰. However, the tools that

exist for the prediction and identification of circRNAs are often modified from traditional mRNA detection tools and are therefore not optimal in the specific detection of circRNAs¹⁰¹. For instance, for circRNAs sensitive to RNase R, a library preparation method based on RNase R treated samples will lead to a relatively low abundance of the circRNA resulting in poor detection or misinterpreted detection rates. The further development of bioinformatic and statistical approaches to identify circRNAs are important to not only reduce false-positive detection or improve splice-site detection, but also because they have an impact on other computational approaches that could be used to, for instance, characterize the potential functions of circRNAs. For example, circRNAs are suggested to have translational potential, but no tools are available for specifically predicting their translational capabilities¹⁰². Besides methodological obstacles to identify circRNAs *in silico*, the detection and visualization of circRNAs *in vitro* and *in vivo* using molecular and cellular approaches also remains challenging. Several techniques have been developed to detect and visualize RNA molecules by single-molecule *in situ* hybridization (smISH) approaches, but the detection of circRNAs by smISH is challenging due to their unique structural characteristics. circRNAs are often expressed at low levels and consequently ISH signals are weak relative to their linear mRNA counterparts. Moreover, as circRNA probes must include their unique back-splice junctions to avoid amplification of their linear counterparts, the combination of sequences available for probe design is limited and therefore often suboptimal^{40,74,103}. Different smISH techniques have been optimized to reduce these limitations in circRNA detection, but there is no golden standards in the circRNA field yet. Likewise, techniques for manipulating circRNA levels are emerging, but they still face many caveats. Essaying the function of circRNAs is not straightforward, as traditional molecular biology techniques for circRNA depletion may also alter the levels of their linear host transcript (and the vast majority circRNAs are derived from protein-coding genes). Moreover, it is also difficult to separate *cis* and *trans* functions of circRNAs, since the production of circular transcripts could compete with the splicing of linear transcripts. So far, one circRNA knockout mouse model has been reported. However, the development of this mouse model was only possible because the circle ciRS-7 does not have a linear transcript⁶⁸. *In vitro* studies have reported the inhibition of circRNAs using RNA interference (RNAi), a system that works with short interfering RNAs complementary to the sequence around the back-splice junction. Nonetheless, many circRNA manipulation tools need to be further developed and standardized.

AIM AND OUTLINE OF THE THESIS

Brain development and neural circuit formation are very complex processes, known to be controlled by a variety of molecules orchestrating the proper timing of many different cellular processes, including neuronal migration and differentiation. An interesting group of secreted and membrane-bound molecules, called axon guidance cues, play an important role in these neurodevelopmental processes by guiding axons to the appropriate targets. Although approximately 100 guidance proteins have been identified, very little is known about the role of circRNAs that are generated from these same axon guidance genes during the formation of complex neuronal architecture. Interestingly, a recent study revealed that circRNAs from axon guidance genes are specifically upregulated during the development of the porcine brain²⁸. Many of these axon guidance circRNAs were reported to be expressed in a tissue/developmental stage-specific manner and revealed a striking (up)regulation of circRNAs, not only during brain development but also during neuronal maturation and differentiation. These findings indicate that circRNAs from axon guidance genes may also play a role in neural circuit formation, but although the importance of the role of non-coding RNAs in neuronal development has started to emerge, no systematic investigation or studies on the specific expression or function of individual circRNAs from axon guidance genes have been reported up until now. Understanding the role of axon guidance circRNA in brain development is important as it may help to enhance our insight into the mechanisms of neuronal circuit formation and disease. Therefore, this thesis is aimed to investigate the expression and function of axon guidance circRNAs in the developing (mouse) brain. Hereto we used various new techniques to study the spatiotemporal expression of a selected group of axon guidance circRNAs (chapters 1, 2 and 4) and tested and adapted various manipulation tools to investigate their function *in vitro* and *in vivo* (chapter 3) (Figure 5).

Chapter 1: Axon guidance circRNAs are conserved in the human brain and dynamically expressed in the developing and adult mouse brain.

In this chapter, we first set out to identify axon guidance circRNAs expressed in the human brain using RNA sequencing. To determine which of the identified circRNAs are conserved and developmentally regulated in the mouse brain, we characterized the expression patterns of a large group of axon guidance circRNAs in the developing and adult mouse

brain using RT-qPCR, Nanostring and several other approaches, and made a further selection based on their spatiotemporal expression. We observed that axon guidance circRNAs are conserved between mammalian species, expressed independently of their linear host genes and noted that they exhibit a dynamic spatial and temporal expression pattern *in vivo* and *in vitro*. We identified an expression peak for axon guidance circRNAs in the developing mouse cortex just before birth and observed a trend in accumulation of circRNAs with age.

Chapter 2: Characterization of the spatiotemporal expression of axon guidance circRNAs in the developing mouse brain using *in situ* hybridization.

In chapter 2, we thoroughly evaluate the use of various *in situ* hybridization techniques (ISH) techniques to specifically label, detect and visualize circRNAs *in vitro* and *in vivo* in order to get a better understanding of axon guidance circRNA spatiotemporal expression in the developing mouse brain. Using single molecule fluorescent ISH (smFISH) we were able to create an overview of the spatiotemporal expression of selected axon guidance circRNAs in primary cortical neurons. This overview revealed that the expression levels and cellular localization of selected axon guidance circRNAs are dynamic and vary during neuronal maturation. Moreover, we observed that the axon guidance circRNAs investigated were predominantly expressed in excitatory neurons, with no expression in glial cells.

Chapter 3: Manipulation and functional assessment of axon guidance circRNA *in vitro* and *in vivo*.

Tools to manipulate circRNA levels are not well established yet. In chapter 3, we therefore describe and utilize various tools in a series of experiments to manipulate axon guidance circRNA levels *in vitro* and *in vivo*. CircRNAs were successfully overexpressed in neuronal cells and in the mouse retina. For circRNA knockdown, we implemented different manipulation strategies from which knockdown with siRNAs was most reproducible *in vitro*. Sholl analysis following knockdown of circRNAs in primary cortical neurons hinted at a possible role for certain axon guidance circRNAs in neurite branching. siRNA-mediated knockdown in the mouse cortex using *in utero* electroporation did not induce obvious defects. Lastly, we report that neuronal expression of axon guidance circRNAs is elevated as a result of cellular activation. We speculate on the function of axon guidance circRNAs

in light of our findings which pave the road for future experiments that can lead to insight into (axon guidance) circRNA function.

Chapter 4: CiRS-7 miRNA interactome and function in the healthy and epileptic brain.

CiRS-7 is the first characterized and most studied circRNA. This circRNA can sequester multiple miRNAs including miR-7, miR-671 and miR-135a, a process known as miRNA sponging. Previous research indicated that specifically miR-135a is associated with temporal lobe epilepsy (TLE). However, the exact role of the interaction between ciRS-7 and miR-135a in a disease context still remains unclear. In chapter 4, we explore the functional relationship between ciRS-7 and its binding miRNAs by studying their expression in temporal lobe epilepsy (TLE) patients and in mice using several molecular and cellular approaches. We analyzed ciRS-7 and miR-135a levels in TLE patient material (with and without hippocampal sclerosis) and found that ciRS-7 and miR-135a are significantly regulated in this tissue. An inverse expression correlation between ciRS-7 and miR-135a was observed *in vitro* after knockdown or overexpression of one of the two molecules, suggesting they have a biological interaction. The functional meaning of the relationship between ciRS-7 and miR-135a in TLE pathology remains to be further explored, but the presented data could serve as a meaningful starting point from which to conduct further studies.

Chapter 5: General discussion

In this last chapter, we summarize and critically discuss the results described in this thesis. In the light of what is currently known about circular RNAs in neuronal systems we review our findings and propose future studies to better comprehend (axon guidance) circRNA function.



Axon guidance circRNA

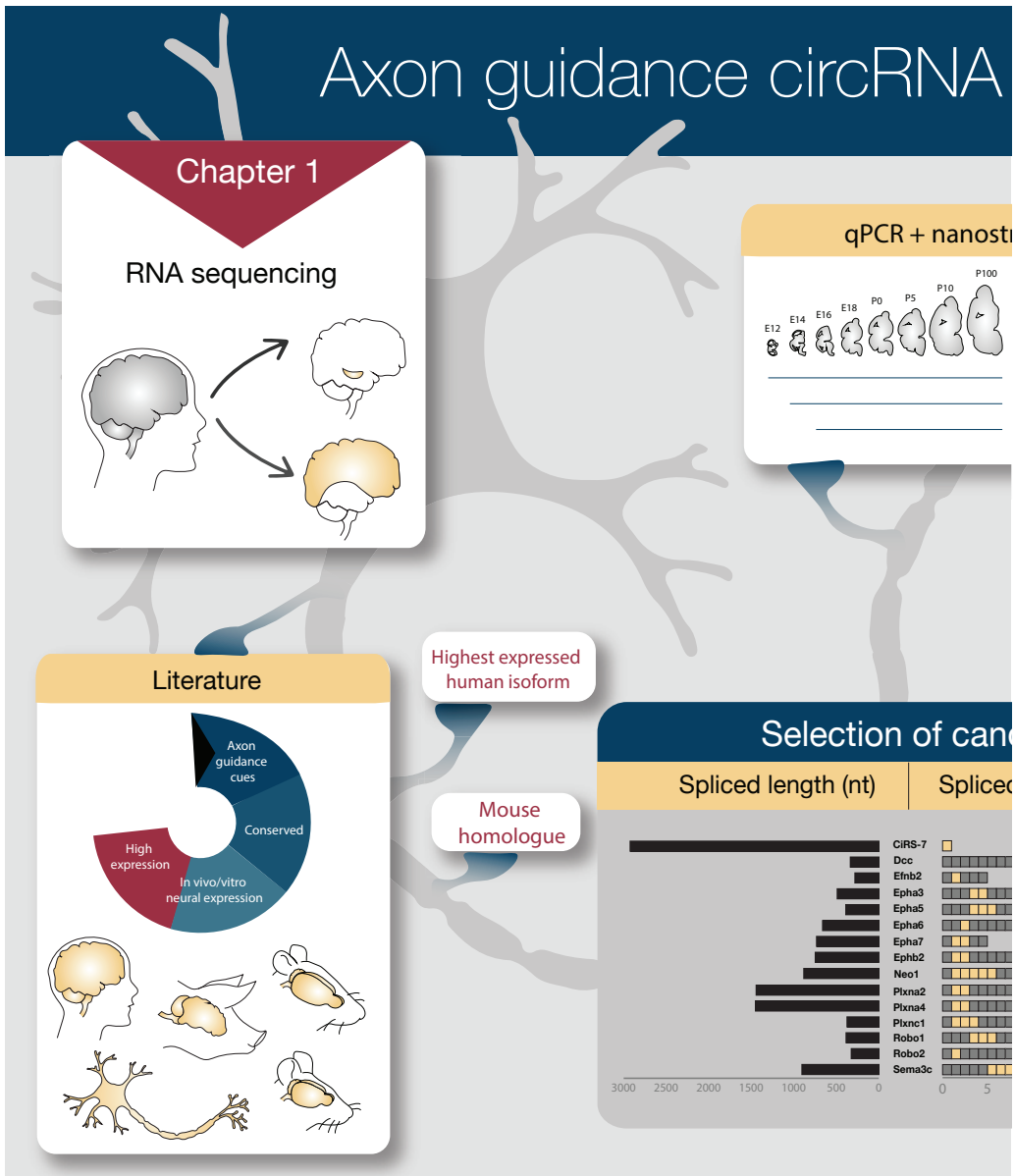
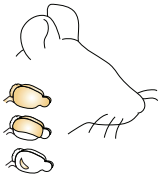


Figure 5 | Chapter flowchart: Axon guidance circRNA expression and function.

In chapter 1, we first set out to identify axon guidance circRNAs expressed in the human brain using RNA sequencing. To determine which of the identified circRNAs are interesting to investigate, we checked 1) whether the axon guidance circRNAs are neuronally conserved across species, 2) whether they are expressed in vitro and in vivo, and 3) whether they are generally highly expressed. Based on these criteria, we chose 14 axon guidance circRNAs (including cIRS-7 as a positive control), selected their most highly expressed human isoform and the corresponding mouse homologue. Next we investigated the developmental regulation of these circRNA in the developing and adult mouse brain using RT-qPCR and Nanostring. Based on their spatiotemporal expression, we made a further selection of a few axon guidance circRNAs and aimed

expression and function

ring



Selection criteria

From high to low during development

Dcc

Neo1

General high expression

Efnb2

Plxnc1

Epha3

Robo1

ciRS-7

Time specific regulation

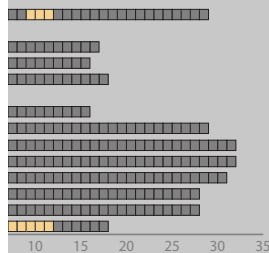
Robo2

Functional assays

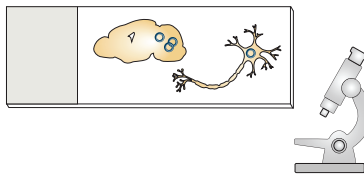
Chapter 3: circRNA manipulation tools

andidates

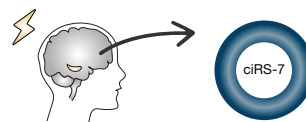
d exons from gene



Chapter 2: smFISH



Chapter 4: ciRS-7 in TLE



to further characterize the spatiotemporal expression in the developing mouse brain using in situ hybridization in chapter 2. In a series of experiments we describe and utilize various tools to manipulate axon guidance circRNA levels in vitro and in vivo in chapter 3. We speculate on the function of axon guidance circRNAs in light of our findings which pave the road for future experiments that can lead to insight into (axon guidance) circRNA function. In chapter 4, we explore the functional relationship between ciRS-7 and its binding miRNAs by studying their expression in temporal lobe epilepsy (TLE) patients and in mice using several molecular and cellular approaches. Based on our findings we discuss the potential role of ciRS-7 and miR-135a in the pathogenesis of TLE.

REFERENCES

1. Stoeckli, E. T. Understanding axon guidance: Are we nearly there yet? *Dev.* 145, (2018).
2. Chan, S. S. Y. et al. UNC-40, a *C. elegans* homolog of DCC (Deleted in Colorectal Cancer), is required in motile cells responding to UNC-6 netrin cues. *Cell* 87, 187–195 (1996).
3. Kolodkin, A. L. & Tessier-Lavigne, M. Mechanisms and molecules of neuronal wiring: A primer. *Cold Spring Harb. Perspect. Biol.* 3, 1–14 (2011).
4. Pasterkamp, R. J. Getting neural circuits into shape with semaphorins. *Nat. Rev. Neurosci.* 13, 605–618 (2012).
5. Colamarino, S. A. & Tessier-Lavigne, M. The axonal chemoattractant netrin-1 is also a chemorepellent for trochlear motor axons. *Cell* 81, 621–629 (1995).
6. Ly Alice et al. DSCAM is a netrin receptor that collaborates with DCC in mediating turning responses to netrin-1. *Cell* 133, 1241–1254 (2008).
7. Wilson, N. H. & Key, B. Neogenin interacts with RGMa and Netrin-1 to guide axons within the embryonic vertebrate forebrain. *Dev. Biol.* 296, 485–498 (2006).
8. Friocourt, F. et al. Recurrent DCC gene losses during bird evolution. *Sci. Rep.* 7, 1–11 (2017).
9. De Vries, M. & Cooper, H. M. Emerging roles for neogenin and its ligands in CNS development. *J. Neurochem.* 106, 1483–1492 (2008).
10. Brankatschk, M. & Dickson, B. J. Netrins guide *Drosophila* commissural axons at short range. *Nat. Neurosci.* 9, 188–194 (2006).
11. Kidd, T. et al. Roundabout controls axon crossing of the CNS midline and defines a novel subfamily of evolutionarily conserved guidance receptors. *Cell* 92, 205–215 (1998).
12. Zallen, J. A., Yi, B. A. & Bargmann, C. I. The conserved immunoglobulin superfamily member SAX-3/robo directs multiple aspects of axon guidance in *C. elegans*. *Cell* 92, 217–227 (1998).
13. Wong, K., Park, H. T., Wu, J. Y. & Rao, Y. Recent studies of molecular guidance cues including the Slit family of secreted proteins have provided new insights into the mechanisms of cell migration. Initially discovered in the nervous system, Slit functions through its receptor, Roundabout, and an. *Curr. Opin. Genet. Dev.* 12, 583–591 (2002).
14. Yazdani, U. & Terman, J. R. The semaphorins. *Genome Biol.* 7, (2006).
15. Verhagen, M. G. & Pasterkamp, R. J. Axon guidance : semaphorin / neuropilin / plexin signaling. 109–122 (2020).
16. Klein, R. Eph/ephrin signaling in morphogenesis, neural development and plasticity. *Curr. Opin. Cell Biol.* 16, 580–589 (2004).
17. Blits-Huizinga, C. T., Nelersa, C. M., Malhotra, A. & Liebl, D. J. Ephrins and their receptors: Binding versus biology. *IUBMB Life* 56, 257–265 (2004).
18. Flanagan, J. G. & Vanderhaeghen, P. The ephrins and Eph receptors in neural development. *Annu. Rev. Neurosci.* 21, 309–345 (1998).
19. Van Battum, E. Y., Brignani, S. & Pasterkamp, R. J. Axon guidance proteins in neurological disorders. *Lancet Neurol.* 14, 532–546 (2015).
20. Salvatori, B., Biscarini, S. & Morlando, M. Non-coding RNAs in Nervous System Development and Disease. *Front. Cell Dev. Biol.* 8, (2020).
21. Vangoor, V. R., Gomes-Duarte, A. & Pasterkamp, R. J. Long non-coding RNAs in motor neuron development and disease. *J. Neurochem.* 1–25 (2020). doi:10.1111/jnc.15198
22. Weyn-Vanhentenryck, S. M. et al. Precise temporal regulation of alternative splicing during neural development. *Nat. Commun.* 9, (2018).
23. Friedman, L. M. et al. MicroRNAs are essential for development and function of inner ear hair cells in vertebrates. *Proc. Natl. Acad. Sci. U. S. A.* 106, 7915–7920 (2009).
24. Iyer, A. N., Bellon, A. & Baudet, M. L. MicroRNAs in axon guidance. *Front. Cell. Neurosci.* 8, 1–14 (2014).

25. Zou, Y. Does Planar Cell Polarity Signaling Steer Growth Cones? *Current Topics in Developmental Biology* 101, (Elsevier Inc., 2012).
26. Bellon, A. et al. miR-182 Regulates Slit2-Mediated Axon Guidance by Modulating the Local Translation of a Specific mRNA. *Cell Rep.* 18, 1171–1186 (2017).
27. Tie, J. et al. MiR-218 inhibits invasion and metastasis of gastric cancer by targeting the robo1 receptor. *PLoS Genet.* 6, (2010).
28. Venø, M. T. et al. Spatio-temporal regulation of circular RNA expression during porcine embryonic brain development. *Genome Biol.* 16, 245 (2015).
29. Hsu, M. T. & Coca-Prados, M. Electron microscopic evidence for the circular form of RNA in the cytoplasm of eukaryotic cells. *Nature* 280, 339–340 (1979).
30. Sanger, H. L., Klotzt, G., Riesnert, D., Gross, H. J. & Albrecht, K. highly base-paired. *73*, 3852–3856 (1976).
31. Arnberg, A. C., Van Ommen, G. J. B., Grivell, L. A., Van Bruggen, E. F. J. & Borst, P. Some yeast mitochondrial RNAs are circular. *Cell* 19, 313–319 (1980).
32. Nigro, J. M. et al. Scrambled exons. *Cell* 64, 607–613 (1991).
33. Saad, F. A. et al. A 3' consensus splice mutation in the human dystrophin gene detected by a screening for intra-exonic deletions. *Hum. Mol. Genet.* 1, 345–346 (1992).
34. Zaphiropoulos, P. G. Exon skipping and circular RNA formation in transcripts of the human cytochrome P-450 2C18 gene in epidermis and of the rat androgen binding protein gene in testis. *Mol. Cell. Biol.* 17, 2985–2993 (1997).
35. Splicing with inverted order of exons occurs proximal to large introns. *Trends Genet.* 8, 157 (1992).
36. Bailleul, B. During in vivo maturation of eukaryotic nuclear mRNA, splicing yields excised exon circles. *Nucleic Acids Res.* 24, 1015–1019 (1996).
37. Jeck, W. R. et al. Circular RNAs are abundant, conserved, and associated with ALU repeats. *RNA* 19, 141–57 (2013).
38. Salzman, J., Chen, R. E., Olsen, M. N., Wang, P. L. & Brown, P. O. Cell-Type Specific Features of Circular RNA Expression. *PLoS Genet.* 9, (2013).
39. Salzman, J., Gawad, C., Wang, P. L., Lacayo, N. & Brown, P. O. Circular RNAs are the predominant transcript isoform from hundreds of human genes in diverse cell types. *PLoS One* 7, (2012).
40. Memczak, S. et al. Circular RNAs are a large class of animal RNAs with regulatory potency. *TL - 495. Nature* 495 VN-, 333–338 (2013).
41. Guo, J. U., Agarwal, V., Guo, H. & Bartel, D. P. Expanded identification and characterization of mammalian circular RNAs. *Genome Biol.* 15, 409 (2014).
42. Westholm, J. O. et al. Genome-wide Analysis of Drosophila Circular RNAs Reveals Their Structural and Sequence Properties and Age-Dependent Neural Accumulation. *Cell Rep.* 9, 1966–1981 (2014).
43. Rybak-Wolf, A. et al. Circular RNAs in the Mammalian Brain Are Highly Abundant, Conserved, and Dynamically Expressed. *Mol. Cell* 870–885 (2014). doi:10.1016/j.molcel.2015.03.027
44. You, X. et al. Neural circular RNAs are derived from synaptic genes and regulated by development and plasticity. *Nat. Neurosci. advance on*, 603–610 (2015).
45. Starke, S. et al. Exon circularization requires canonical splice signals. *Cell Rep.* 10, 103–111 (2015).
46. Ashwal-Fluss, R. et al. CircRNA Biogenesis competes with Pre-mRNA splicing. *Mol. Cell* 56, 55–66 (2014).
47. Zhang, Y. et al. Circular Intronic Long Non-coding RNAs. *Mol. Cell* 51, 792–806 (2013).
48. Li, Z. et al. Exon-intron circular RNAs regulate transcription in the nucleus. *Nat. Struct. Mol. Biol.* 22, 256–264 (2015).

49. Chen, Y., Li, C., Tan, C. & Liu, X. Circular RNAs: a new frontier in the study of human diseases. *J. Med. Genet.* jmedgenet-2016-103758 (2016). doi:10.1136/jmedgenet-2016-103758
50. Ebbesen, K. K., Kjems, J. & Hansen, T. B. Circular RNAs: Identification, biogenesis and function. *Biochim. Biophys. Acta - Gene Regul. Mech.* 1859, 163–168 (2016).
51. Chen, L. L. & Yang, L. Regulation of circRNA biogenesis. *RNA Biol.* 12, 381–388 (2015).
52. Liang, D. & Wilusz, J. E. Short intronic repeat sequences facilitate circular RNA production. *Genes Dev.* 28, 2233–2247 (2014).
53. Ivanov, A. et al. Analysis of intron sequences reveals hallmarks of circular RNA biogenesis in animals. *Cell Rep.* 10, 170–177 (2015).
54. Dubin, R. A., Kazmi, M. A. & Ostrer, H. Inverted repeats are necessary for circularization of the mouse testis *Sry* transcript. *Gene* 167, 245–248 (1995).
55. Åberg, K. et al. Human QKI, a new candidate gene for schizophrenia involved in myelination. *Am. J. Med. Genet. - Neuropsychiatr. Genet.* 141 B, 84–90 (2006).
56. Mulholland, P. J. et al. Genomic Profiling Identifies Discrete Deletions Associated Report ES INTRODUCTION RIB. *Cell Cycle* 783–791 (2006).
57. Conn, S. J. et al. The RNA binding protein quaking regulates formation of circRNAs. *Cell* 160, 1125–1134 (2015).
58. Chen, L. L. & Carmichael, G. G. Altered Nuclear Retention of mRNAs Containing Inverted Repeats in Human Embryonic Stem Cells: Functional Role of a Nuclear Noncoding RNA. *Mol. Cell* 35, 467–478 (2009).
59. Wahlstedt, H. et al. Large-scale mRNA sequencing determines global regulation of RNA editing during brain development Large-scale mRNA sequencing determines global regulation of RNA editing during brain development. 978–986 (2009). doi:10.1101/gr.089409.108
60. Osenberg, S. et al. Alu sequences in undifferentiated human embryonic stem cells display high levels of A-to-I RNA editing. *PLoS One* 5, (2010).
61. Shtrichman, R. et al. Altered A-to-I RNA editing in human embryogenesis. *PLoS One* 7, (2012).
62. Hansen, T. B., Kjems, J. & Damgaard, C. K. Circular RNA and miR-7 in Cancer. *Cancer Res.* 73, 5609–5612 (2013).
63. Zheng, Q. et al. Circular RNA profiling reveals an abundant circHIPK3 that regulates cell growth by sponging multiple miRNAs. *Nat. Commun.* 7, 11215 (2016).
64. Kefas, B. et al. microRNA-7 inhibits the epidermal growth factor receptor and the akt pathway and is down-regulated in glioblastoma. *Cancer Res.* 68, 3566–3572 (2008).
65. Junn, E. et al. Repression of alpha-synuclein expression and toxicity by microRNA-7. *Proc. Natl. Acad. Sci. U. S. A.* 106, 13052–7 (2009).
66. Choi, S. Y. et al. Post-transcriptional regulation of SHANK3 expression by microRNAs related to multiple neuropsychiatric disorders. *Mol. Brain* 8, 1–12 (2015).
67. Zhang, J., Sun, X. Y. & Zhang, L. Y. MicroRNA-7/Shank3 axis involved in schizophrenia pathogenesis. *J. Clin. Neurosci.* 22, 1254–1257 (2015).
68. Piwecka, M. et al. Loss of a mammalian circular RNA locus causes miRNA deregulation and affects brain function. *Sci.* 8526, 1–14 (2017).
69. Kleaveland, B., Shi, C. Y., Stefano, J. & Bartel, D. P. A Network of Noncoding Regulatory RNAs Acts in the Mammalian Brain. *Cell* 174, 350–362. e17 (2018).
70. Hansen, T. B. et al. miRNA-dependent gene silencing involving Ago2-mediated cleavage of a circular antisense RNA. *Embo J* 30, 4414–4422 (2011).
71. Hentze, M. W. & Preiss, T. Circular RNAs: splicing's enigma variations. *EMBO J.* 32, 923–925 (2013).

72. Wilusz, J. E. & Sharp, P. a. A Circuitous Route to Are Gold Clusters in RF Fields. *Science* (80-.). 6–8 (2013). doi:10.1126/science.1238522
73. Du, W. W. et al. Foxo3 circular RNA retards cell cycle progression via forming ternary complexes with p21 and CDK2. *Nucleic Acids Res.* 44, 2846–2858 (2016).
74. Jeck, W. R. & Sharpless, N. E. Detecting and characterizing circular RNAs. *Nat. Biotechnol.* 32, 453–61 (2014).
75. Lasda, E. & Parker, R. Circular RNAs: diversity of form and function. *RNA* 20, 1829–42 (2014).
76. Hansen, T. B. et al. Natural RNA circles function as efficient microRNA sponges. *TL - 495. Nature* 495 VN-, 384–388 (2013).
77. Li, P. et al. Using circular RNA as a novel type of biomarker in the screening of gastric cancer. *Clin. Chim. Acta* 444, 132–136 (2015).
78. Khoutorsky, A. et al. Control of synaptic plasticity and memory via suppression of poly(A)-Binding protein. *Neuron* 78, 298–311 (2013).
79. Enuka, Y. et al. Circular RNAs are long-lived and display only minimal early alterations in response to a growth factor. *Nucleic Acids Res. gkv1367-* (2015). doi:10.1093/nar/gkv1367
80. Chen, C. Y. & Sarnow, P. Initiation of protein synthesis by the eukaryotic translational apparatus on circular RNAs. *Science* (80-.). 268, 415–417 (1995).
81. Perriman, R. & Ares, M. Circular mRNA can direct translation of extremely long repeating-sequence proteins in vivo. *RNA* 4, 1047–1054 (1998).
82. Wang, G., Wu, J. & Song, H. LRIG2 expression and prognosis in non-small cell lung cancer. *Oncol. Lett.* (2014). doi:10.3892/ol.2014.2157
83. Legnini, I. et al. Circ-ZNF609 Is a Circular RNA that Can Be Translated and Functions in Myogenesis. *Mol. Cell* 66, 22–37.e9 (2017).
84. Pamudurti, N. R. et al. Translation of Circular RNAs. *Mol. Cell* 66, 9–21.e7 (2017).
85. Yang, Y. et al. Extensive translation of circular RNAs driven by N⁶-methyladenosine. *Cell Res.* 27, 626–641 (2017).
86. Shigeoka, T. et al. Dynamic Axonal Translation in Developing and Mature Visual Circuits. *Cell* 166, 181–192 (2016).
87. Chen, W. & Schuman, E. Circular RNAs in Brain and Other Tissues: A Functional Enigma. *Trends Neurosci.* 39, 597–604 (2016).
88. Chen, B. J., Huang, S. & Janitz, M. Changes in circular RNA expression patterns during human foetal brain development. *Genomics* 111, 753–758 (2019).
89. Zhang, X. O. et al. Diverse alternative back-splicing and alternative splicing landscape of circular RNAs. *Genome Res.* 26, 1277–1287 (2016).
90. Xu, K. et al. CircGRIA1 shows an age-related increase in male macaque brain and regulates synaptic plasticity and synaptogenesis. *Nat. Commun.* 11, 1–15 (2020).
91. Suenkel, C., Cavalli, D., Massalini, S., Calegari, F. & Rajewsky, N. A Highly Conserved Circular RNA Is Required to Keep Neural Cells in a Progenitor State in the Mammalian Brain. *Cell Rep.* 30, 2170–2179.e5 (2020).
92. Shao, Y. & Chen, Y. Roles of Circular RNAs in Neurologic Disease. *Front. Mol. Neurosci.* 9, 1–5 (2016).
93. Zhao, Y., Alexandrov, P. N., Jaber, V. & Lukiw, W. J. Deficiency in the ubiquitin conjugating enzyme UBE2A in Alzheimer's Disease (AD) is linked to deficits in a natural circular miRNA-7 sponge (circRNA; ciRS-7). *Genes (Basel).* 7, (2016).
94. Errichelli, L. et al. FUS affects circular RNA expression in murine embryonic stem cell-derived motor neurons. *Nat. Commun.* 8, 1–11 (2017).
95. Gray, L. G. et al. Identification of Specific Circular RNA Expression Patterns and MicroRNA Interaction Networks in Mesial Temporal Lobe Epilepsy. *Front. Genet.* 11, 1–9 (2020).
96. Scotti, M. M. & Swanson, M. S. RNA mis-splicing in disease. *Nat. Rev. Genet.* 17, 19–32 (2015).

97. Havens, M. A., Duelli, D. M. & Hastings, M. L. Targeting RNA splicing for disease therapy. *Wiley Interdiscip. Rev. RNA* 4, 247–266 (2013).
98. Lu, D. & Xu, A. D. Mini Review: Circular RNAs as potential clinical biomarkers for disorders in the central nervous system. *Front. Genet.* 7, 1–5 (2016).
99. Lasda, E. & Parker, R. Circular RNAs Co-Precipitate with Extracellular Vesicles: A Possible Mechanism for circRNA Clearance. *PLoS One* 11, 1–11 (2016).
100. Zhang, G. et al. Identifying Circular RNA and Predicting Its Regulatory Interactions by Machine Learning. *Front. Genet.* 11, 1–16 (2020).
101. Szabo, L. & Salzman, J. Detecting circular RNAs: Bioinformatic and experimental challenges. *Nat. Rev. Genet.* 17, 679–692 (2016).
102. Jakobi, T. & Dieterich, C. Computational approaches for circular RNA analysis. *Wiley Interdiscip. Rev. RNA* 10, 1–14 (2019).
103. Hansen, T. B. et al. Natural RNA circles function as efficient microRNA sponges. *Nature* 495, 384–388 (2013).





250 ml

APPROX. VOL

Made in Germany

Axon guidance circRNAs are conserved in the human brain and dynamically expressed in the developing and adult mouse brain

Daniëlle van Rossum¹ and R. Jeroen Pasterkamp¹

¹ Department of Translational Neuroscience, UMC Utrecht Brain Center, University Medical Center Utrecht, Utrecht University, Utrecht 3584 CG, the Netherlands

Working in the lab: "There's more to be seen than can ever be seen, more to do than can ever be done" (The circle of life)

ABSTRACT

Circular RNAs (circRNAs) are highly stable, circularized non-coding RNAs which are enriched in the nervous system. Recent studies show that many circRNAs are expressed in a tissue/developmental stage-specific manner and reveal a striking (up)regulation of circRNAs during brain development, neuronal maturation and differentiation. Interestingly, many circRNAs expressed in neural tissues derive from genes with prominent roles in early neural development, e.g. genes implicated in Wnt signaling and axon guidance. In this study, we investigate circRNAs generated from genes implicated in axon guidance. We characterize their expression patterns in the human adult brain using RNA-seq and in the developing and adult mouse brain using RT-qPCR, Nanostring and several other approaches. We observed that axon guidance circRNAs are conserved, expressed independently of linear host genes and that they exhibit a dynamic spatial and temporal expression pattern *in vivo* and *in vitro*. We identified an expression peak for axon guidance circRNAs in the developing mouse cortex just before birth and observed a trend in accumulation of circRNAs with age. In short, our data present an extensive profiling of the expression the axon guidance circRNAs in the human and mouse brain, and provide a beginning framework to examine the roles of axon guidance circRNAs. This is of interest as recent studies show that circRNA molecules substantially contribute to regulation of gene expression and that they may be involved in the development and progression of various neurological disorders.

INTRODUCTION

Brain development and neural circuit formation are very complex processes, known to be controlled by a variety of molecules orchestrating the proper timing of neuronal migration and differentiation. Non-coding RNAs such as miRNAs and long non-coding RNAs (lncRNAs) have emerged as key players in regulating these developmental processes, but very little is known about the role of the more recently identified circular RNAs (circRNAs) in the formation of complex neuronal architecture. CircRNAs are highly stable, circularized lncRNAs which are abundantly expressed in the brain compared to other mammalian tissues. They are upregulated during brain development and neuronal differentiation, but their precise roles in neuronal maturation, neurite outgrowth and synaptogenesis remain to be explored^{1,2}.

CircRNAs are often expressed independently and at lower levels than their respective linear host transcripts in the brain ². However, for some genes it is known that they generate more circular as compared to linear transcripts, in extreme cases by a factor $10^{1.3.4}$. These data suggest that circRNAs are not just transcriptional noise and more importantly, that the major function of some protein-coding genes may be to generate circular RNAs which have a specific role in brain development. Moreover, circRNAs have been shown to accumulate in the aging brain of flies, mice, rat and worms, which is not a general phenomenon of linear transcripts⁵⁻⁷. The enhanced stability of circRNAs may be the reason for their specific accumulation in the nervous system, which consists mostly of non-proliferating cells, but alterations of splicing patterns during brain development, maturation and aging have also been proposed to affect circRNA levels⁸.

As a whole circRNAs are highly expressed in the brain, but between brain structures and neuronal cell types the expression of individual circRNAs can vary substantially. Sequencing data from the developing porcine brain showed that circRNA expression is highest in the cortex and cerebellum and lowest in the brain stem⁹. Not only between brain structures, but also between cell types the expression of specific circRNAs can vary. The fly muscleblind circRNA is by far the most abundant RNA expressed from the muscleblind gene in fly heads, while in cell culture the normal linear muscleblind mRNA is expressed much higher than the circular isoform ¹⁰. Within neurons circRNAs also appear to be spatially regulated, as they for instance have been shown to be enriched in synaptosome fractions².

Interestingly, certain groups of circRNAs show specific spatial-temporal expression. Pathway analyses on highly expressed circRNAs in the developing porcine brain revealed specific upregulation of the axon guidance (e.g., from the Eph and Robo gene families) and Wnt signaling pathways⁹. Generally, axon guidance genes are significantly longer and have a slightly larger proportion of intronic sequence than most other genes, which has been reported to facilitate back-splicing and the formation of circRNAs^{3.9}. Differential expression analysis of circRNAs expressed during human late versus early prenatal brain development, also revealed a large association of circular axon guidance transcripts (e.g. circROBO2, circEPHA3, circPLXNA2, circNEO1), while this was not the case for linear transcripts¹¹. Furthermore, specific individual axon guidance circRNAs have been reported to be differentially regulated in the brain. A circRNA from the Ephb2 gene



could be detected at 10-fold higher levels than its linear form in neurites and circRNAs generated from the Epha3 gene have been reported to be upregulated in brains from patients with bipolar disorder^{12,13}. Together, these findings implicate that the specific spatial-temporal expression of axon guidance circRNAs is important for proper brain development and functioning.

Thus far no systematic study has been performed on the expression of axon guidance circRNAs at specific stages of pre- and postnatal (mouse) brain development. Here we report the identification of axon guidance circRNA expressed in the nucleus and cytosol of the human cortex and hippocampus using RNA sequencing (RNA-seq). We selected the highest human expressed axon guidance circRNA isoforms and validated their expression in the whole brain, cortex and hippocampus of the developing mouse using RT-qPCR and Nanostring. We mapped their spatial and temporal expression and observed that axon guidance circRNAs are conserved and generally expressed independently of their host gene *in vivo* and *in vitro*. We identified peak expression of axon guidance circRNAs in the developing mouse cortex just before birth and observed a trend in accumulation of axon guidance circular transcripts with age. Based on their observed spatial and temporal expression pattern we address the potential functional role of axon guidance circRNAs in brain development. Altogether, our data provides an overview of axon guidance circRNA expression in the human and developing mouse brain. Understanding the role of axon guidance circRNA in brain development may help to enhance our insight into the mechanisms of neuronal circuit formation and disease.

RESULTS

Axon guidance circRNAs are abundantly expressed in the human cortex and hippocampus

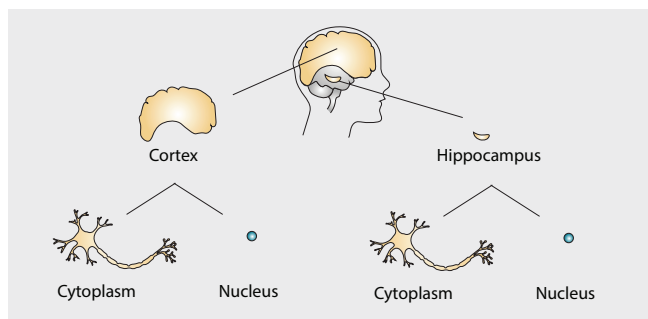
To determine which circRNAs from axon guidance genes are specifically expressed in the human brain, we collected human brain cortical and hippocampal tissue. This tissue was processed to generate nuclear and cytoplasmic fractions to obtain insight into the spatial expression of the circRNAs (Figure 1A). Next, we extracted total RNA and performed Ribominus RNA sequencing (RNA-seq) on all samples. We used a pipeline for the specific detection of circRNAs and identified circRNAs from fifty-five axon guidance genes (Figure

1B). Interestingly, most of these genes generated multiple different circRNA isoforms (Supplementary Figure 1). We observed that axon guidance circRNAs are expressed in both the nuclear and cytoplasmic compartments of the cells in the human cortex and hippocampus. Interestingly, a number of circRNAs were highly expressed across all samples, while others were only expressed in a specific brain structures or cellular compartment. More circRNAs from different genes were expressed in cortical samples compared to the hippocampal samples, while in both the cortex and the hippocampus nuclear expression was especially high compared to the cytoplasm. In all, this data supports a dynamic spatial expression of axon guidance circRNAs in the human brain.

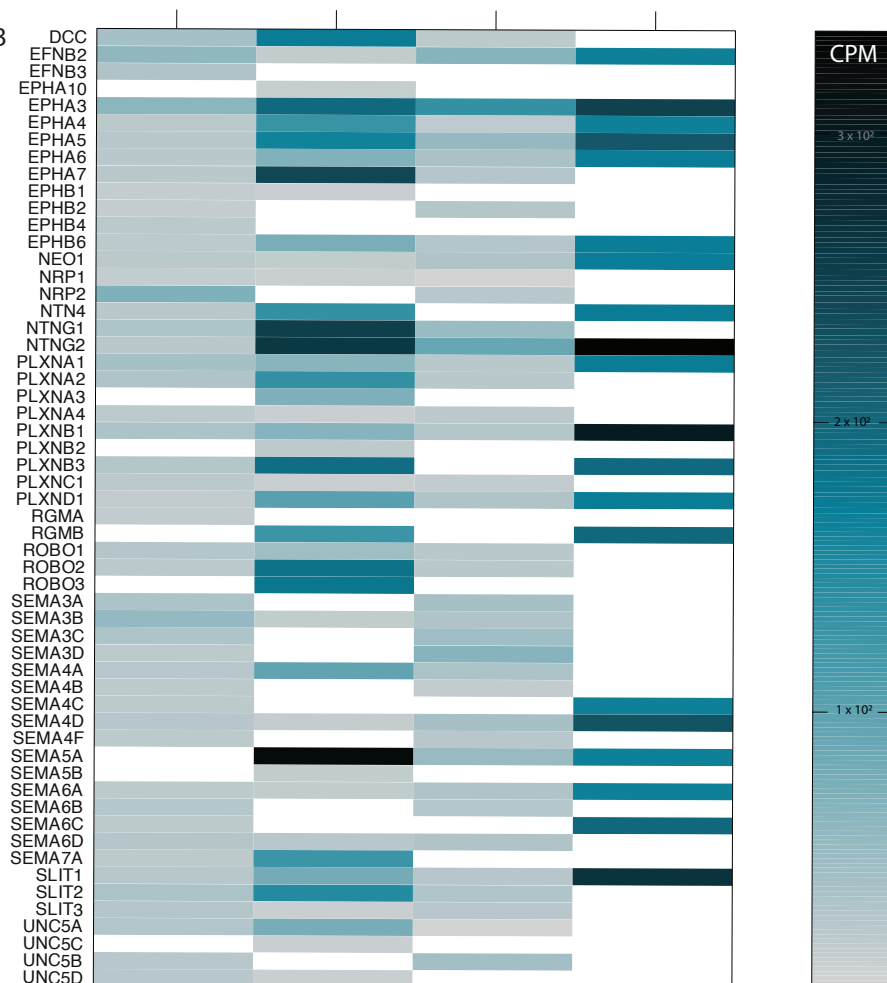
Axon guidance circRNA can be selected based on high expression and their degree of conservation

Based on the human RNA-seq data and previous reports on circRNA expression, we made a general overview of axon guidance circRNA expression in neuronal cells and tissues (Table 1) (Figures 1C and 1D). Axon guidance circRNAs are conserved between different species (human, mouse, rat, pig) and can be detected in mouse and human *in vitro* and *in vivo* systems. We noted that some gene families are detected at high levels in both the RNA-seq data as well as in published RNA-seq datasets (e.g. the EphA, Plxn and Robo gene families). A handful of circRNAs were not detected in the RNA-seq of the human samples, but are conserved across other species (e.g. the EphrinA and Netrin gene families). Some circRNA families are highly expressed in the human RNA-seq and highly conserved across species but less reported to be expressed *in vitro* (e.g. the Sema gene family). Based on the collected sequencing data and four selection criteria; (I) High general expression in the human RNA-seq dataset; (II) high expression in published RNA-seq datasets; (III) high degree of evolutionary conservation, and (IV) whether the circRNA was detected in mouse and human *in vitro* and *in vivo* systems, we selected candidate axon guidance genes for further investigation. From each of these circRNA producing axon guidance genes, we selected the most highly expressed human circRNA isoform and its corresponding mouse homologue for further analysis 1 (Table 2).

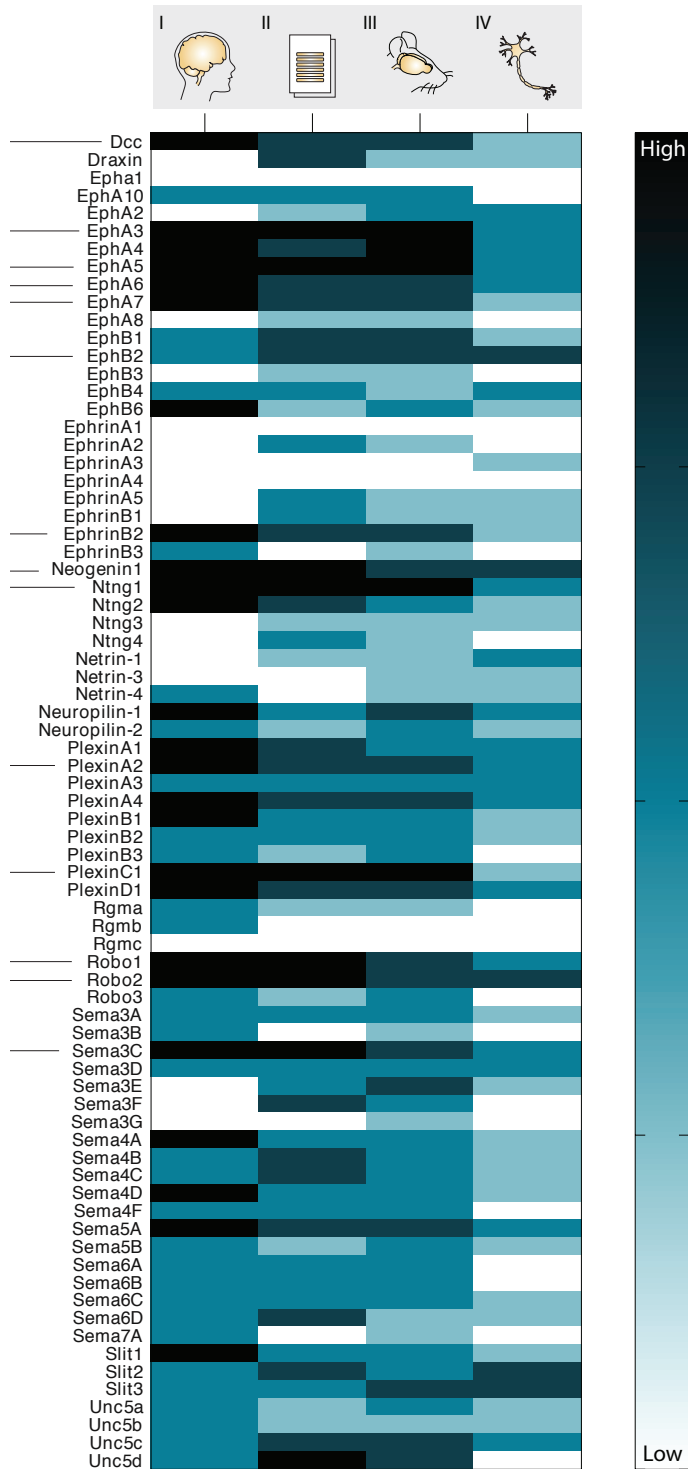
A



B



C



1

D

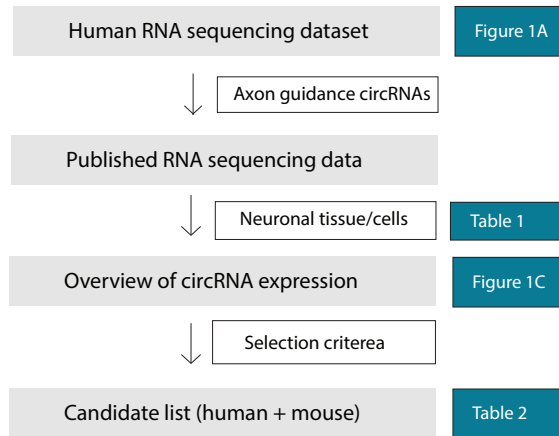


Figure 1 | RNA-sequencing guided axon guidance circRNA candidate selection.

(A) Schematic overview of human sample collection for RNA-sequencing. (B) CircRNAs from axon guidance genes detected with RNA-sequencing in human samples. CircRNA expression levels are expressed in counts per million (CPM). White = not detected. (C) Overview of axon guidance circRNA expression data. Axon guidance circRNA candidates were selected based on; (I) a high general expression level in the human RNA-seq dataset; (II) a high general level of expression in published RNA-seq datasets; (III) a high degree of evolutionary conservation; (IV) circRNA expression in mouse and human in vitro and in vivo systems. Black = high expression/level; white = low/no expression/level. The selected candidates are marked by a black dash. (D) Schematic overview of the sequence of circRNA candidate selection.

The selected axon guidance circRNA candidates are stable bona fide circRNAs

We validated the selected axon guidance circRNAs using several independent approaches. First, we designed divergent primers to amplify the back-splice junction of our axon guidance circRNAs of interest by RT-PCR. We also designed primers for a well-studied and highly expressed circRNA, CiRS-7, as a positive control. In contrast to conventional convergent primers that are used for the detection of linear RNA, divergent primers can be utilized to specifically detect circular RNA transcripts (Figure 2A). Using divergent primers in a RT-PCR assay we confirmed that axon guidance circRNAs are stably expressed in different parts of the adult mouse brain (Figure 2B).

Table 1 | Overview of published circRNA sequencing datasets on neuronal samples (until 2016) used for candidate selection

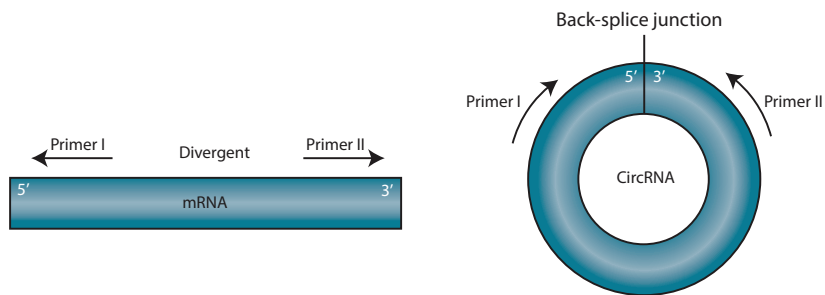
Study	Organism	Tissue/cell line	Age
Rybak-Wolf et al., Molecular Cell 2015	<i>Homo sapiens</i>	Cerebellum	Fetal week 37, 19
		Diencephalon	Fetal week 20, 22
		Frontal cortex	Fetal week 20, 22
		Occipital lobe	Fetal week 20, 22
		Parietal lobe	Fetal week 22, 24
		Temporal lobe	Fetal week 20, 24
		SH-SY5Y	NA
	<i>Mus musculus</i>	Forebrain	P0
		Midbrain	P0
		Hindbrain	P0
Cerebellum		P0	
Prefrontal cortex		P0	
Hippocampus		P0	
Olfactory bulb		P0	
Primary cortical neurons		E17.5 – E18.5	
Synaptoneurosome	Adult		
Salzman et al., Plos One 2013	<i>Homo sapiens</i>	SK-N-SH RA Neuroblastoma	NA
Memczak et al., Nature 2013	<i>Mus musculus</i>	Whole brain	Adult
		Head	E14.5
Veno et al., Genome Biology 2015	<i>Sus scrofa</i>	Forebrain	E23
		Cortex	E42, E60, E80, E100, E115
		Basal ganglia	E60, E115
		Brainstem	E60, E115
		Cerebellum	E60, E115
		Hippocampus	E60, E115
You et al., Nature Neuroscience 2015	<i>Mus musculus</i>	Brain	20 weeks old
		Hippocampus	E18, P1, P10, P30
		Hippocampal somata	4-5 weeks old
		Hippocampal neuropil	4-5 weeks old
	<i>Rattus Norvegicus</i>	Primary hippocampal neurons	DIV21
Memczak et al., Plos One 2015	<i>Homo sapiens</i>	Cerebellum	Fetal week 37, 19
Song et al., Nucleic Acids Research 2016	<i>Homo sapiens</i>	Glioblastoma multiforme	Age 50-80
		Oligodendroglioma	Age 50-81
		Cortical brain controls	Age 50-82
		Cerebellum	Age 50-83



Table 2 | *CircRNA candidates highest expressed human isoform and corresponding mouse homologue*

Human		Mouse	
Gene	circRNA ID Isoform	Gene	circRNA ID Isoform
CDR1AS	hsa_circ_0001946	Cdr1as	mmu_circ_0001878
DCC	hsa_circ_0108606	Dcc	mmu_circ_0007486
EFNB2	hsa_circ_0099818	Efnb2	mmu_circ_0015034
EPHA3	hsa_circ_0066598	Epha3	mmu_circ_0000696
EPHA5	hsa_circ_0126808	Epha5	mmu_circ_0012825
EPHA6	hsa_circ_0124806	Epha6	mmu_circ_0000694
EPHA7	hsa_circ_0132690	Epha7	mmu_circ_0011549
EPHB2	hsa_circ_0004085	Ephb2	mmu_circ_0001284
NEO1	hsa_circ_0036249	Neo1	mmu_circ_0001779
PLXNA2	hsa_circ_0002472	Plxna2	mmu_circ_0008579
PLXNC1	hsa_circ_0099504	Plxnc1	mmu_circ_0002595
ROBO1	hsa_circ_0066568	Robo1	mmu_circ_0000698
ROBO2	hsa_circ_0066556	Robo2	mmu_circ_0000700
SEMA3C	hsa_circ_0004365	Sema3c	mmu_circ_0012389

A



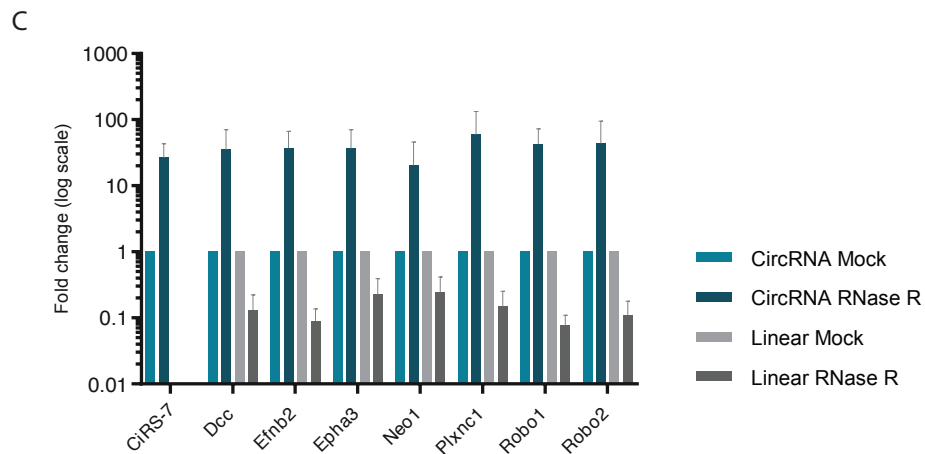
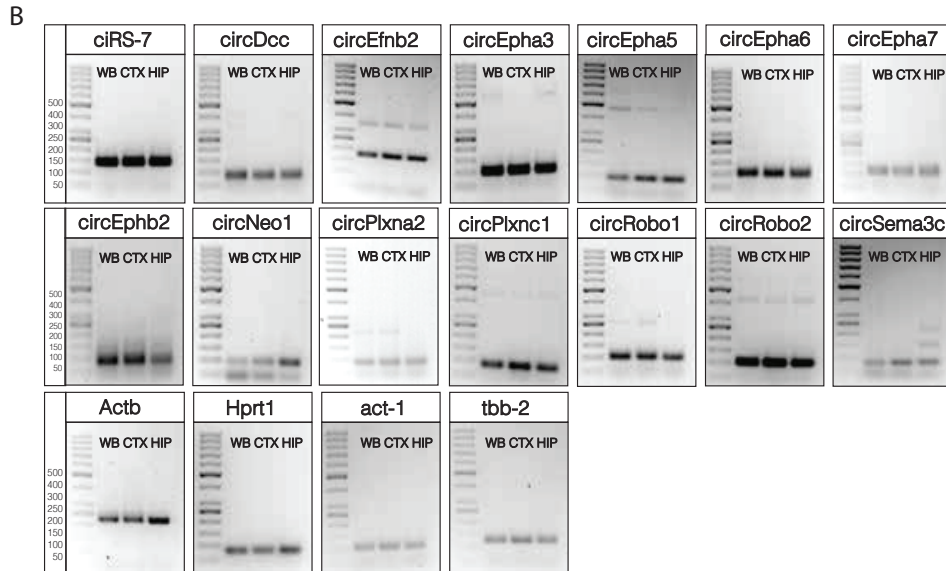


Figure 2 | Experimental validation of mouse axon guidance circRNAs.

(A) Schematic of the design of divergent primers over the back-splice junction used for the detection of circRNAs specifically (Left: linear RNA; Right: circular RNA). (B) Amplified RT-qPCR products resolved on an agarose gel (2,5%) show that circRNA candidates are detected in mouse postnatal day 100 (P100) whole brain (WB), cortex (CTX) and hippocampal (HIP) tissue. (C) Axon guidance circRNAs are resistant to RNase R treatment. Note the enrichment of circRNAs with RNase R treatment, whereas linear mRNAs are not enriched and largely degraded after enzyme treatment. Equal amounts of mock-treated and RNase R treated RNA were used for cDNA preparation prior to RT-qPCR. Mouse cortex (n = 3).



RNase R treatment has emerged as a reliable method for validation of the circular nature of circRNAs. This enzyme is a 3'-5' exoribonuclease that degrades linear RNA, but is much less efficient in targeting circular RNA. Although using RNase R a reliable method for circRNA validation, it needs to be considered that RNase R resistance depends on the tendency to form secondary structures and that larger circRNAs are more susceptible to RNase R^{5,14}. We treated our samples with RNase R which, as expected, resulted in decreased level of the expression of the linear transcripts (Figure 2C). In addition we observed an enrichment for circular transcripts in these samples, providing evidence of their non-linearity. Lastly, we aimed to use Northern blotting as a well-validated method for the detection of our circRNA candidates. However, Northern blotting was very insensitive and, in our hands, only the highly expressed ciRS-7 could be detected (Supplementary Figure 2B). Nevertheless our data confirmed that the amplified PCR transcripts are from bona fide circRNAs.

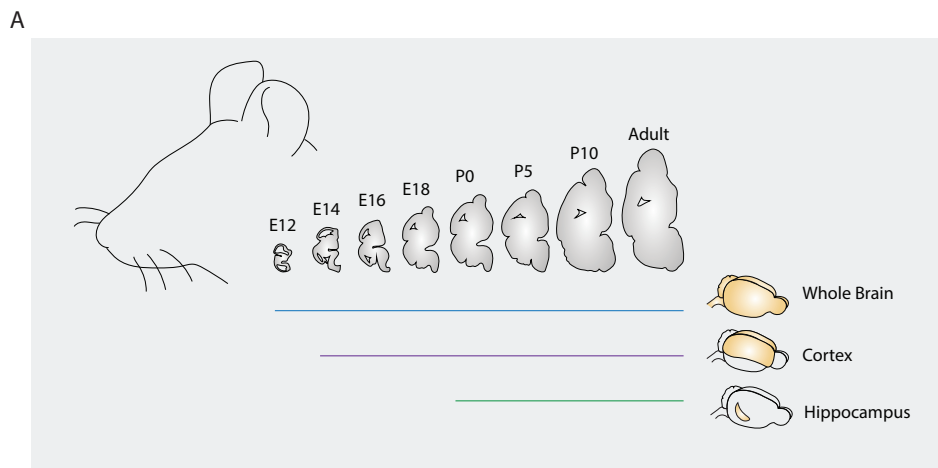
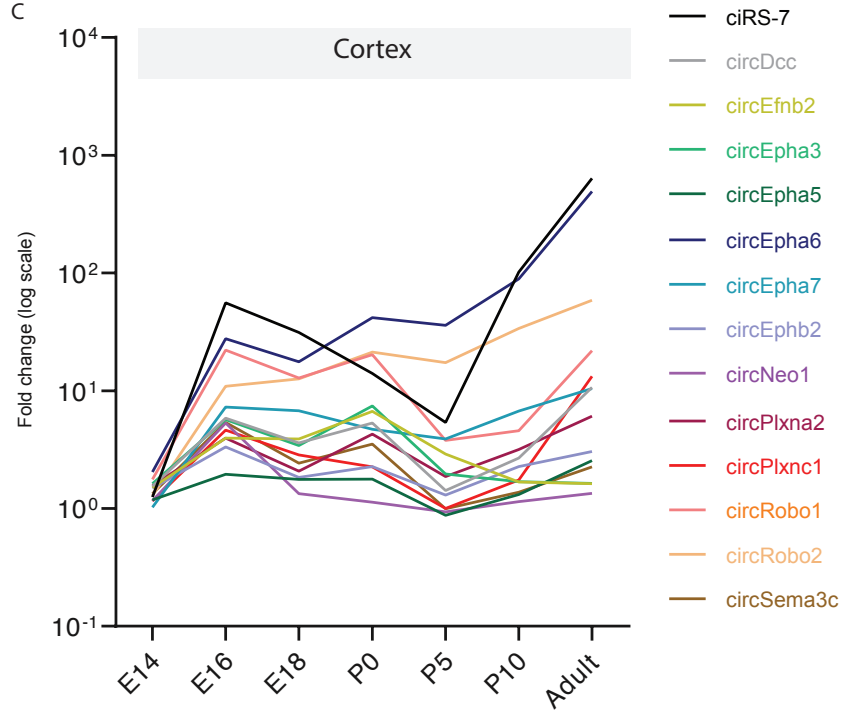
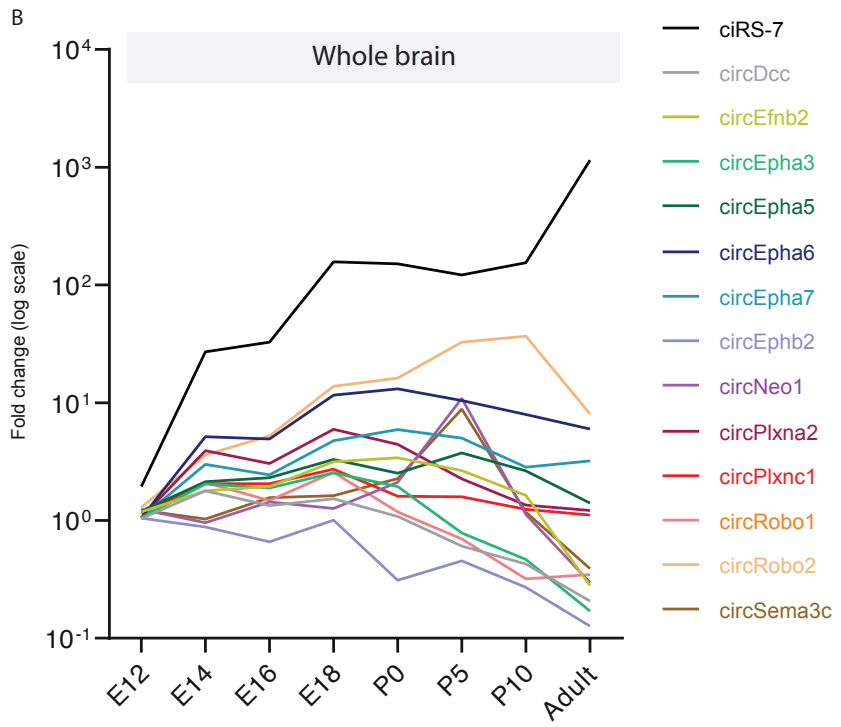
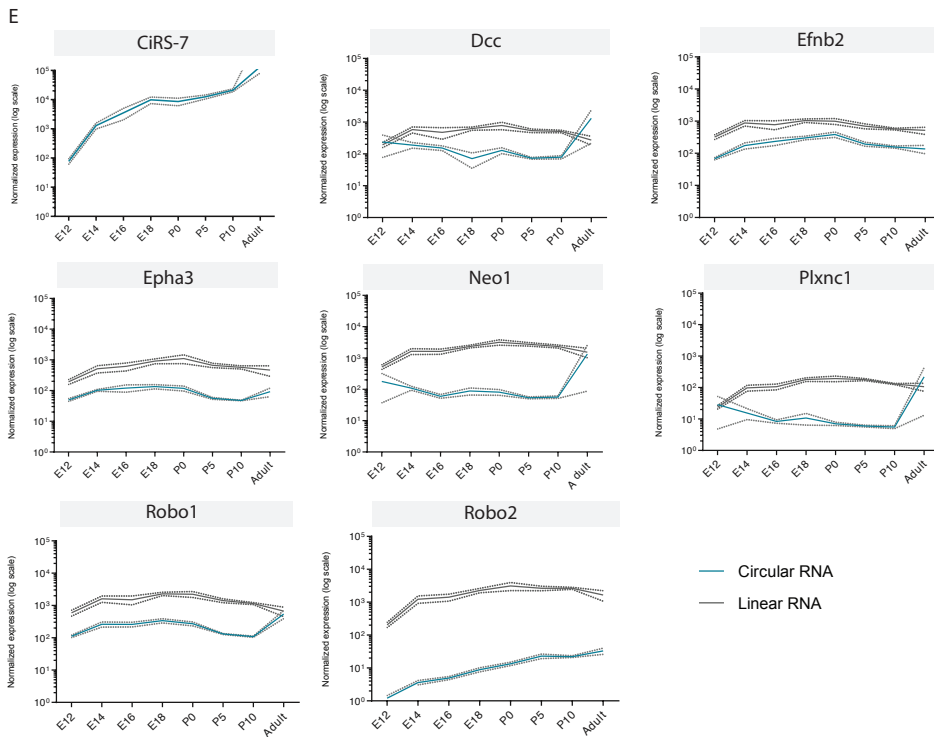
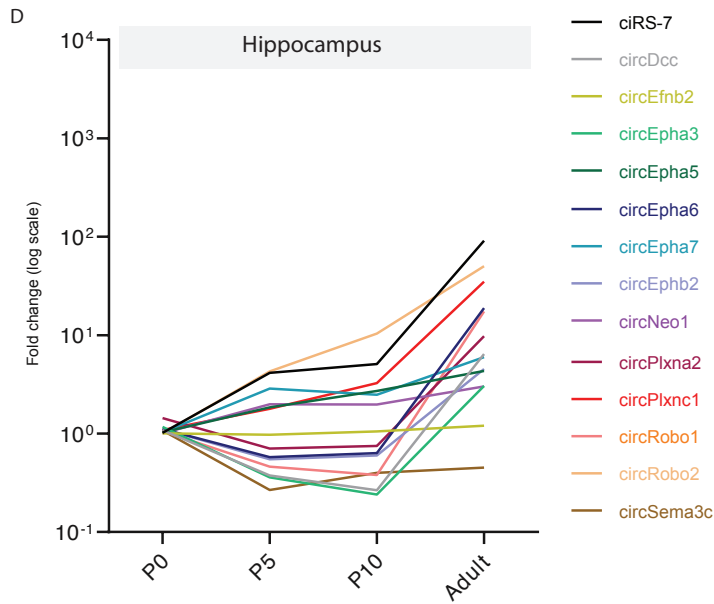


Figure 3 | Axon guidance circRNA expression in the developing mouse brain using RT-qPCR. (A) Schematic of tissue collected for axon guidance circRNA expression analysis with RT-qPCR and Nanos-tring. Embryonic day 12 (E12); embryonic day 14 (E14); Embryonic day 16 (E16); embryonic day 18 (E18); postnatal day 0 (P0); postnatal day 5 (P5); postnatal day 10 (P10); ± postnatal day 100 (Adult) (n = 3). The relative level of circRNA expression was assessed with RT-qPCR during mouse brain development in (B) whole brain (WB), (C) cortex (CTX) and (D) hippocampal (HIP) samples (n = 3). The expression of the axon guidance circRNAs in the developing brain is largely independent of the host gene expression in (E) whole brain (WB), (F) cortex (CTX) (G) and hippocampus (HIP).

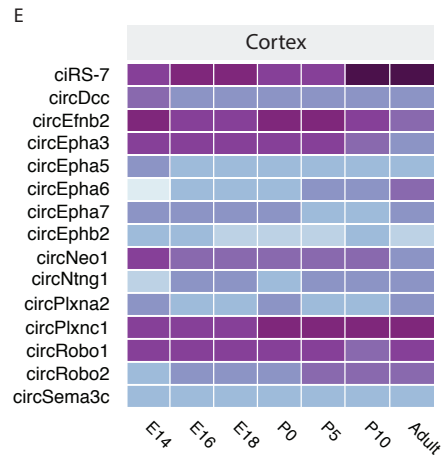
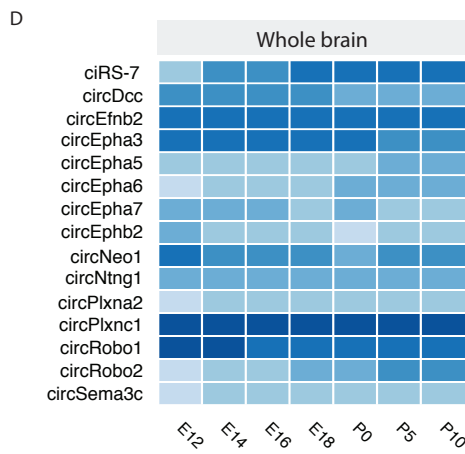
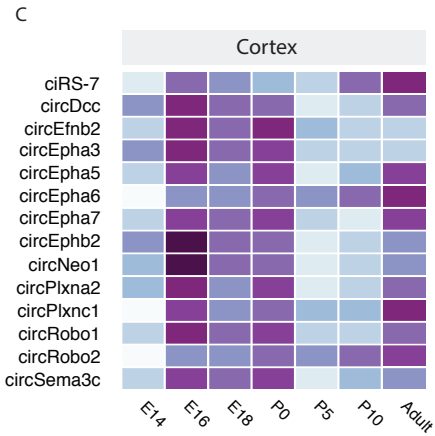
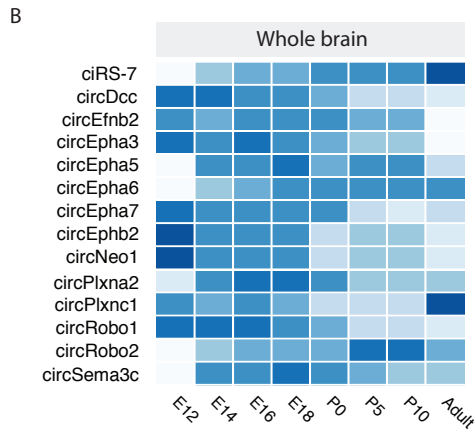
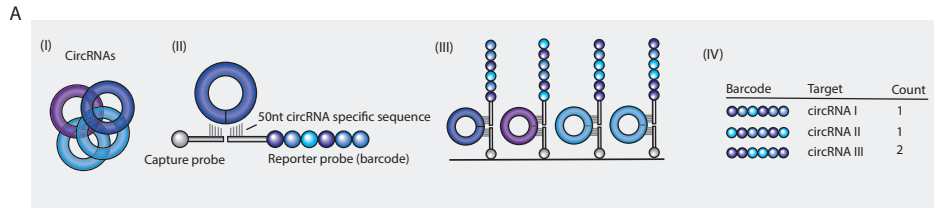




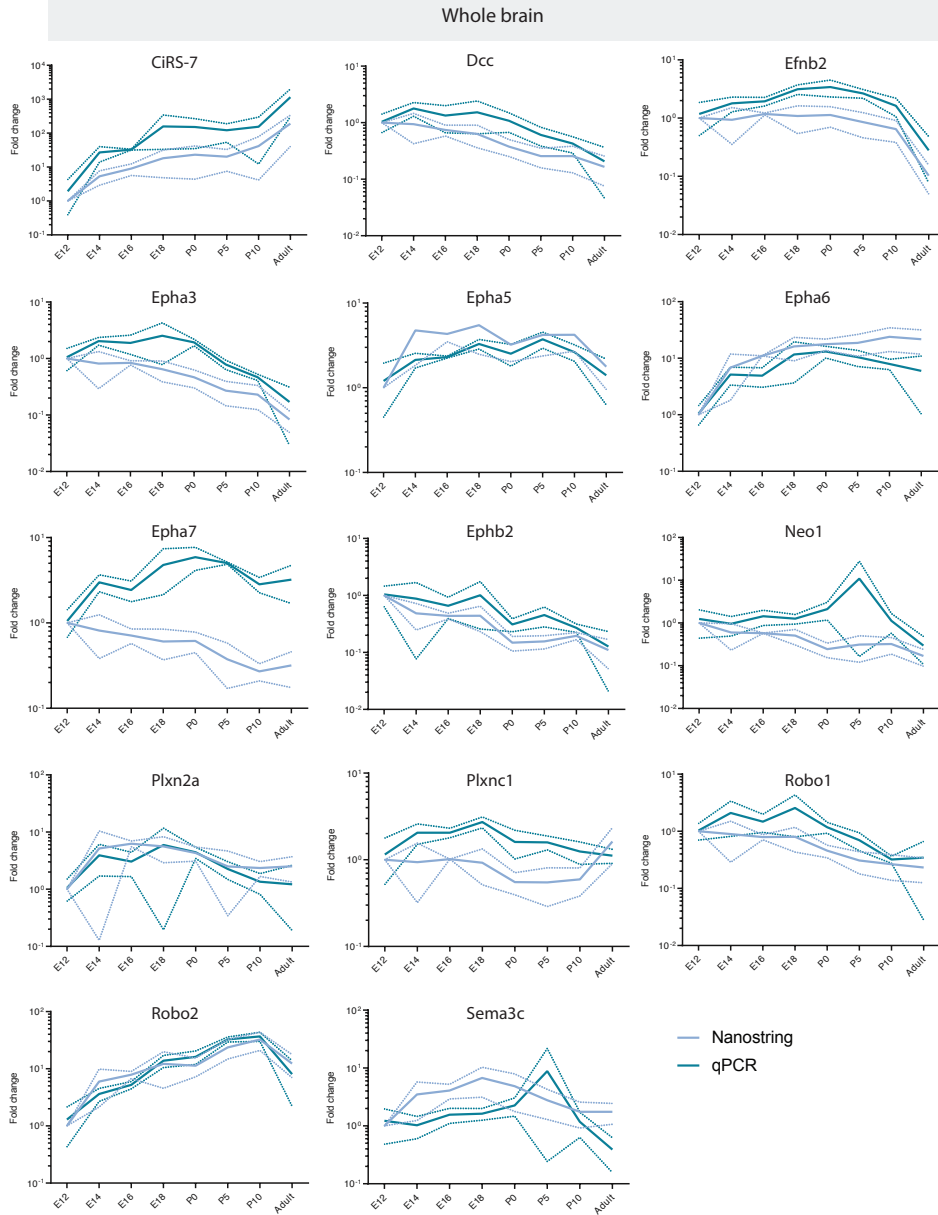
Axon guidance circRNAs are dynamically expressed during mouse brain development

To determine whether the expression of axon guidance circRNAs is developmentally regulated in the mouse brain we profiled the selected axon guidance circRNAs using RT-qPCR. We isolated RNA from mouse whole brain and of cortical and hippocampal tissue at different stages of brain development. We selected specific stages during development to capture the full developmental window from neuron formation and maturation (embryonic; E12, E14, E16, E18), synapse development (early postnatal; P0, P5, P10) until mature neural circuit formation and ageing (adult; \pm P100) (Figure 3A). This RT-qPCR analysis revealed that axon guidance circRNAs are dynamically expressed throughout the brain during development. Interestingly, most circRNAs peak in their expression in the cortex, but not in whole brain or hippocampus, around embryonic day 16 (E16). Moreover, we noted a gradual increase in the expression of circRNAs during maturation in the adult cortex and hippocampus, but not in the brain as a whole (Figure 3B-D). Lastly, we observed that the expression of circRNAs is largely independent of their linear host genes, while linear transcripts are often expressed at higher levels as compared to their circRNA counterparts (Figure 3E-G).

Because amplification bias during PCR can have an impact on RT-qPCR results and because RT-qPCR data is relative, we subjected the same RNA samples as used for RT-qPCR analysis to a NanoString analysis^{14,15}. Using NanoString technology, circRNA levels can be accurately quantified without the use of enzymes, but by employing color-coded probes and digital counting (Figure 4A). We observed the same peak in circRNA expression in the cortex around E16 and the accumulation of circRNAs during aging in the mouse brain in our NanoString data, suggesting that the circRNA expression profiles we observed with RT-qPCR could be validated with NanoString and that both techniques are suitable for circRNA detection (Figure 4B-G). Using NanoString, we were able to quantify the expression levels of the individual circRNAs which allowed us to get insight in the absolute expression levels of the axon guidance circRNAs. Interestingly, these data revealed that some circRNAs have substantially higher levels of expression than other circRNAs in whole brain samples as well as in the developing cortex specifically (Figure 4D, E). Taken together, the data from RNA-seq, RT-qPCR and Nanostring provide evidence that the expression of axon guidance circRNAs is developmentally regulated in the brain and that the expression of many circRNAs is changed independent of their host linear transcripts.



F



G

Cortex

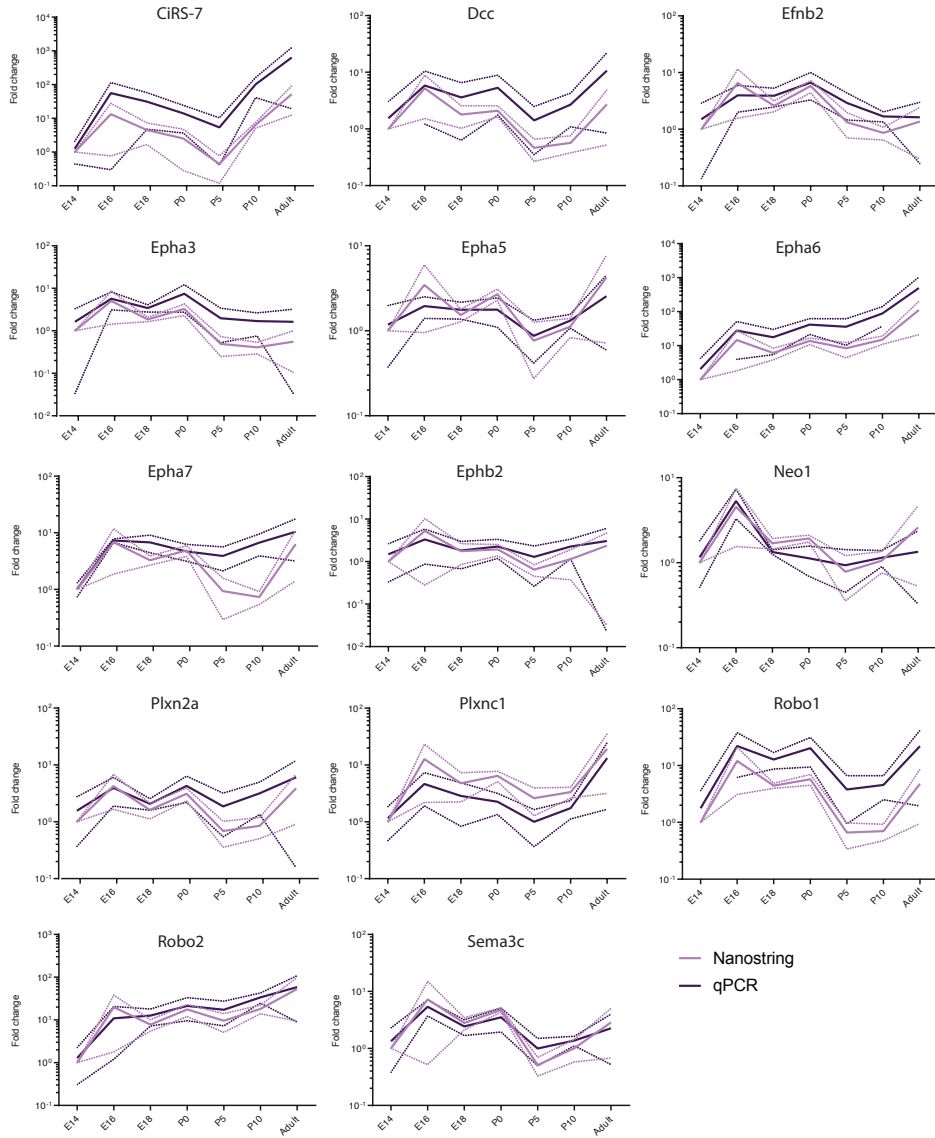


Figure 4 | Axon guidance circRNA expression in the developing mouse brain using Nanostring.

(A) Schematic of quantitative measurement of circRNA molecules in a sample using Nanostring technology. (I) RNA samples are mixed with (II) biotinylated capture probes and color-coded reporter probes. A combination of fluorophores on the reporter probes provides a unique barcode for each circRNA target. The probes contain sequences that specifically bind 50nt on both sides of the back-splice junction of the circRNAs of interest. After hybridization, (III) capture probes attach to a cartridge surface and (IV) the aligned unique barcodes can be counted. The axon guidance circRNAs read count was measured during mouse brain development using Nanostring analysis in (B,D) whole brain (WB) and (C,E) cortex (CTX). Heatmaps show the relative expression of the circRNA over time compared to its own expression (B-C) and compared to other circRNAs (D-E). Log₁₀ transformed. N = 3. (D) Axon guidance circRNA expression patterns are generally comparable between Nanostring and RT-qPCR data in (F) whole brain (WB) and (G) cortex (CTX). Data normalized to embryonic day 12 (E12) (WB) and embryonic day 14 (E14) (CTX). Embryonic day 16 (E16); Embryonic day 18 (E18); Postnatal day 0 (P0); Postnatal day 5 (P5); Postnatal day 10 (P10); ± Postnatal day 100 (Adult).

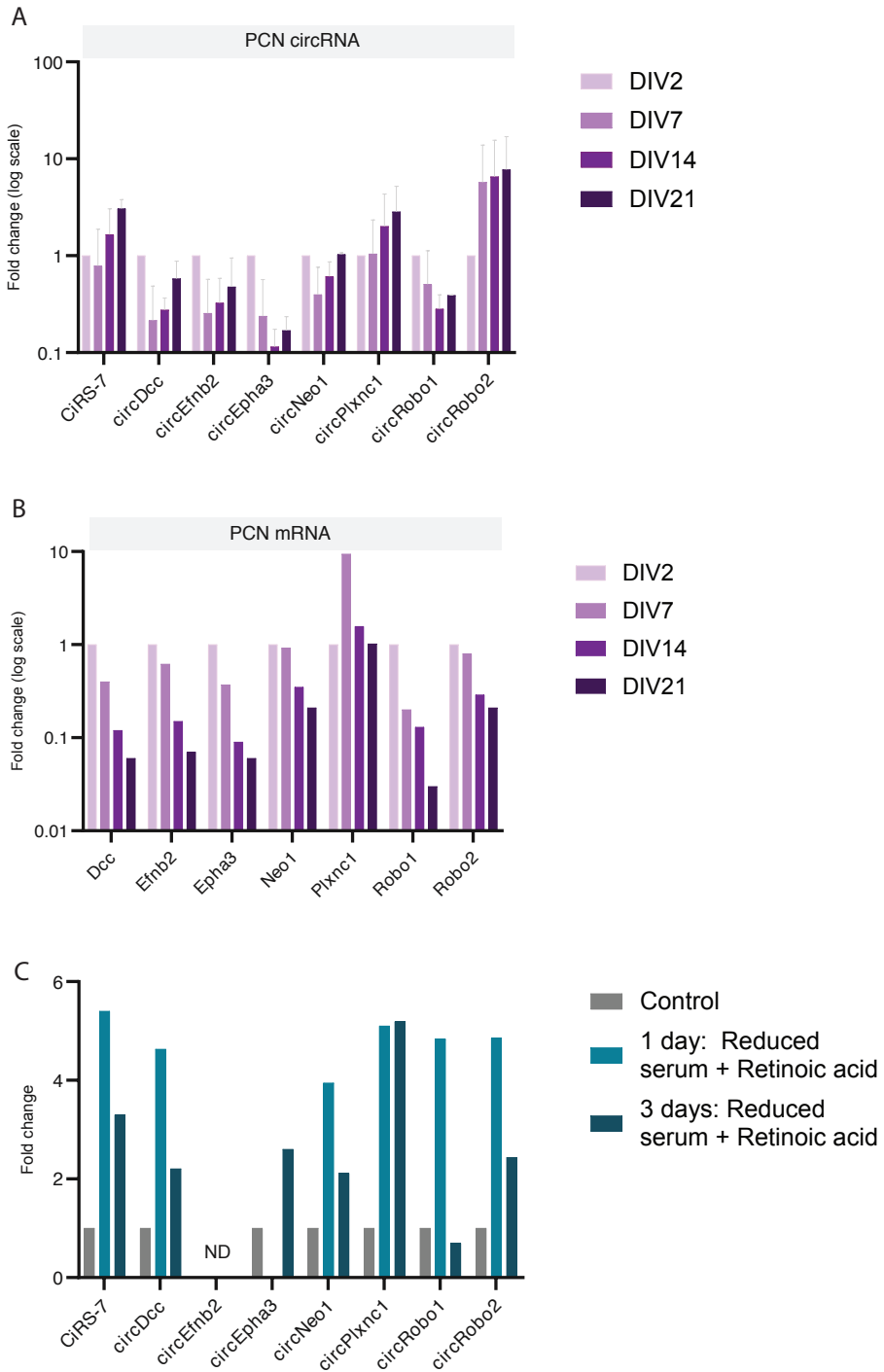
.....

Besides investigating axon guidance circRNA expression *in vivo*, we observed that circRNAs are also dynamically expressed in cell culture. In primary cortical neurons (PCNs) circRNAs have a slight tendency to accumulate during maturation of the neuron (Figure 5A), whereas the expression of the linear transcript generally decreases over time (Figure 5B). However, we did note that axon guidance circRNAs are relatively lowly expressed *in vitro*. Especially in the stable cell lines Neuro2a (N2a), N1E-115 and C2C12 the detection of circRNAs by RT-qPCR was difficult (Supplemental Figures 4A and 4B). Seeing that circRNA levels increase during maturation of PCNs, we speculated whether differentiating stable cell lines express higher levels of axon guidance circRNA than in their conventional state. Interestingly we could confirm that axon guidance circRNA levels were elevated in N2a cells after we serum starved and stimulated them using retinoid acid (RA), indicating that their expression is linked to neuronal differentiation and maturation (Figure 5C). These findings also suggest that axon guidance circRNAs may play a role in stress homeostasis, a process that is induced by serum starvation¹.

.....

Figure 5 | Axon guidance circRNA expression *in vitro*.

(A) CircRNA and (B) mRNA expression in primary cortical neurons (PCN) during neuronal maturation (circRNA n = 2; mRNA n = 1). Normalized to DIV2. (C) Axon guidance circRNAs levels are elevated in differentiating N2a cells after serum starvation and retinoic acid stimulation compared to non-treated control cells (n = 1). ND = Not detected with RT-qPCR. DIV = Days in vitro.



DISCUSSION

The complex anatomical organization of neurons during brain development requires very precise spatial-temporal regulation of gene expression. The recently identified circRNAs are abundant and widespread in the mammalian brain, but their role during neural circuit development is largely unknown¹. In the present study we provide an overview of the expression of axon guidance circRNAs in the human brain using RNA-seq and in the mouse brain using RT-qPCR and Nanostring. We observed that axon guidance circRNAs are highly conserved between species. This is interesting as only 4- to 20% of protein-coding genes produce circRNAs, presenting evidence for the developmental regulation of axon guidance circRNAs in neurons^{1,2,16}. Furthermore the presented RNA-seq data indicate that only a limited subset of axon guidance genes produces circRNAs in the adult human brain (Supplementary Table 4). However, no clear discrepancy between the expression of circRNAs produced by different groups of axon guidance genes (e.g. specifically from the *Eph* or *Robo* gene families) could be observed. We did find differential expression of individual axon guidance circRNAs on the basis of expression level and cellular localization. Our data shows that levels of axon guidance circRNAs are higher in cortical and hippocampal nuclear fractions compared to cytoplasmic fractions. This is interesting in light of reports that indicate that circRNAs as a whole have a preferential cytoplasmic localization¹⁷.

Cellular RNAs can exist in both linear and circular forms. Using RT-qPCR we observed a relative higher level of linear transcripts compared to circular transcripts in our samples, which is in line with previous findings. However, it can be speculated that because we only investigated one circRNA isoform per axon guidance gene, while most genes generate multiple circRNAs, the total level of circRNAs is underestimated in our study. Moreover, we clearly noted that axon guidance circRNA expression is often uncoupled from their host gene expression. This supports the idea that the circularization process is tightly controlled and argues for an axon guidance circRNA-specific function.

Evaluating our RT-qPCR and NanoString data, we noted a peak in the expression of circRNAs in the embryonic cortex starting around E15 and dropping around birth. These data are largely in line with the expression peak that was observed in the developing porcine brain 9. Interestingly, this is the time window in which neurogenesis and the first

wave of synaptogenesis occur (Supplementary Figure 5A). The prenatal peak expression is not observed very clearly in the overall brain in mice. This hints at the possibility that axon guidance circRNAs are specifically important for cortical development during processes like thalamocortical wiring and the formation of the complex cortical layering, which are taking place at late embryonic stages 18. However, when examining (highly expressed) circRNAs produced by genes apart from axon guidance genes, they reveal an expression peak in the cortex in the same time window, arguing against axon guidance circRNA specific functions in the developing cortex (Supplementary Figure 3A-D). Moreover, the prenatal expression peak in the developing mouse cortex does not seem specific for circRNA expression. Also linear transcripts from axon guidance genes show a peak in their expression in the cortex and in the whole brain around this time window (Supplementary Figures 5B and 5C). However, for linear transcripts the expression peak in the cortex is slightly later around embryonic day 18 (E18). Just before birth and in the first two postnatal weeks there are major waves of splicing switches that occur in the mouse brain 8. It was reported that around E16 in the mouse embryonic cortex a switch occurs that results in the splicing of exons linked to functions in synaptic transmission. Around postnatal day 2 (P2) another switch occurs that includes exons involved in general synapse biology. Interestingly these switches occur around the times that the general axon guidance circRNA expression is highest. We could therefore speculate that these splicing switches occur to retain a balance between the expression of the circular and linear transcripts, which affects the regulation of specific neuronal processes. The drop in circRNA expression around birth could also be linked to the slowing down of neurogenesis and the start of glial development during that time window (Supplementary Figure 5A). Astrocytes and oligodendrocytes have been reported to not express circRNAs. Because our analyzed samples are a mix of cell populations, circRNA levels around birth could be diluted due to increased numbers of glial cells². Taken together, our findings indicate a particular need for circRNAs at different time-points spanning developmental periods of the pre- and postnatal brain suggesting that axon guidance circRNA are key players in neuronal development.

The presented data uncover furthermore a trend for age-upregulation of axon guidance circRNAs. Age accumulation has been reported as a general feature for circRNAs. However, a study in mice showed that only 5% of circRNAs were significantly increased in aged brain tissue and that circRNA upregulation was tissue-specific¹⁹. This could explain why we do not see a general accumulation in the whole brain but only in the cortex

and hippocampus of our RT-qPCR and NanoString data. It was also reported that age-upregulated circRNAs in the cortex reveal enrichment in the terms synapse and protein binding, which hints at possible circRNA functions in these domains. Studies showed that the accumulation of circRNAs in the aging brain might also be protective¹⁹. This is interesting as we observed an increased expression of axon guidance circRNA in N2a cells after serum starvation, a treatment that creates a stressful environment for cells. This link between stress and axon guidance circRNA expression was also noted by other researchers that reported that axon guidance circRNAs are upregulated in the rat brain after traumatic brain injury²⁰.

Here, for the first time axon guidance circRNA expression has been systematically examined in the developing embryonic and adult mouse brain. We show that the abundance of several circRNAs changes at developmental stages and independently of the host linear transcript, suggesting a circRNA specific regulation. In all, the data suggest that axon guidance circRNAs are important players in brain and neuron development but the exact function and mechanism of action of these specific circRNAs needs further investigation. This is relevant since understanding the role of axon guidance circRNA during brain development is crucial as proper neural circuit formation is the basis of neuronal functioning in health and disease.

MATERIALS AND METHODS

Nuclear-cytoplasmic fractionations of human hippocampi and cortexes

Autopsy material from control human cortex (n = 6) and hippocampus (n = 5) was obtained. Before fractionation, brain samples were powdered in dry ice using a mortar pestle. Approximately 500 mg of powdered tissue was resuspended in Hypotonic Lysis Buffer (HLB)(10 mM Tris (pH 7.4), 3 mM CaCl₂, 2 mM MgCl₂, 1% Nonidet P-40, Protease inhibitor, 60 U Superase-In/mL) for 10 minutes on ice to lyse): homogenization and lysis were enhanced with the help of 30-80 strokes in a tightly fitting glass Douncer. The cytoplasmic fraction was collected following a gentle centrifugation (500g) for 5 minutes at 4 °C, and frozen in Trizol until RNA purification. The semi-pure nuclei (pellet) were resuspended in 2 mL Sucrose Buffer I (0,32 M Sucrose, 5 mM CaCl₂, 3 mM Mg(CH₃COO)₂,

0,1 mM EDTA, 10 mM Tris (pH 8.0), 0,5% Nonidet P-40, 1 mM DTT, 25 U Superase-In/mL) and placed on top of two thicker sucrose cushions: Sucrose Buffer II (1.6 M Sucrose, 3 mM Mg(CH₃COO)₂, 0,1 mM EDTA, 10mM Tris (pH 8.0), 1 mM DTT, Protease Inhibitor, 35 U Superase-In/mL), and a Sucrose Buffer III (2.0 M Sucrose, 3 mM Mg(CH₃COO)₂, 0,1 mM EDTA, 10 mM Tris (pH 8.0), 1 mM DTT, 35 U Superase-In/mL, Protease Inhibitor), respectively. Samples were centrifuged using an SW41.4 rotor at 30000g at 4 °C for 45 minutes. Pure nuclei were collected and stored in Trizol, prior to RNA isolation.

CircRNA-Seq library preparation and sequencing.

A pipeline for the specific detection of circRNAs was applied. Heatmaps were generated by taking the geomean from each sample (from all biological replicates per isoform) (Figure 1B). Next, these geomeans were averaged to all isoforms per gene to obtain a mean circRNA counts per million (CPM) per axon guidance gene. Cytoplasmic samples n = 6, hippocampal samples n = 5.

Literature selection

CircRNA candidate selection was based on the human RNA-seq dataset and published RNA-seq datasets on circRNA expression in neuronal tissue (Table 1). The following criteria were considered for the selection of circRNA candidates; (I) High general expression level in the human RNA-seq dataset; (II) High general level of expression in published RNA-seq datasets; (III) High level of conservedness (between species; human, mouse, rat, pig); (IV) CircRNA expression in mouse and human *in vitro* and *in vivo* systems. The selected candidates are marked by a black dash.

Ethics statement

All animal experiments were performed in accordance to and approved by the CCD (Centra Committee for animal research, The Netherlands), the University Medical Center Utrecht, the Dutch Law (Wet op Dierproeven 1996) and European regulation (Guideline 86/609/EEC). Mice were housed under standard conditions and were provided food and water *at libitum*.

Tissue sample collection

Tissue samples (whole brain, n = 3; cerebral cortex, n = 3; hippocampus, n = 3) were collected from C57BL/6 mice at 7 time points (E12, E14, E16, E18, P0, P5, P10, P100) and meninges were removed. Samples were directly homogenized using a T10 basic ultraturrax (IKA) in Trizol (Qiagen) and stored at -80 °C until further processing.

Nanostring

For Nanostring analysis, a custom CodeSet of capture and reporter probes was designed. The capture probes target regions of 100 nucleotides overlaying the back-splice junction of 30 unique circRNAs, each probe with a target sequence of exactly 50 nucleotides (Supplementary Table 3). In addition, 5 linear reference genes were included for normalization. RNase R treated mouse cortex and whole brain samples (50 ng/ μ l) were sent to Århus, Denmark, where 200 ng of the sample was analyzed on an nCounter SPRINT (NanoString Technologies) according to manufactures instructions. Using nSOLVER 3.0 software (NanoString Technologies) background subtraction using the mean of negative controls was performed. The geometric mean of the linear reference genes was used for normalization.

RNA isolation and RNase R treatment

Total RNA was isolated from tissue samples and cultured cells using Qiazol reagent (Qiagen) and miRNeasy Mini Kit (Qiagen) following the manufacturer's instructions with minor modifications. RNA concentration was determined using a Nanodrop 2000 (Thermo Scientific) and RIN values were determined using a Bioanalyzer (Agilent). RNase R treatment was performed on 10 μ g of total RNA per 20 μ l reaction using 10 U of RNase R (Epicentre) for 15 mins at 37 °C including 0,5 μ l RiboLock RNase Inhibitor (40 U/ μ L) in the reaction. Mock treatments in which the enzyme was omitted were carried out in parallel in order to assess the efficiency of digestion.

Reverse transcription

Complementary DNA (cDNA) was generated from RNase R- or mock-treated RNA using Superscript IV reverse transcriptase (RT) (Invitrogen) with random (hexamer) primers (Thermo Fisher Scientific) following the manufacturer's instructions. Per 20 μ l reaction, 1 μ g RNA was used. To normalize for technical variation between samples, 1 μ l *c.elegans*

was spiked-in in each sample.

PCR (RT-PCR)

Polymerase chain reaction (PCR) was performed using BIOTAQ DNA Polymerase (GC Biotech) following the manufacturer's instructions (2 minutes at 95 °C; 30 seconds at 95 °C, 30 seconds at 51 °C and 10 seconds at 72 °C for 35 cycles; and 10 minutes at 72 °C). For circRNA amplification, primers followed a divergent amplification design, in which the 5' primer was placed at the 3' end of the exon of interest and the 3' primer was placed at the 5' end. For linear RNA amplification, primers followed a standard convergent design. Primer sequences are listed in Supplementary Table 1. PCR products were separated on 1,5% agarose gels and visualized with SYBR Safe DNA Gel Stain (Invitrogen). After completion of electrophoresis, gels were scanned using an E-Gel Imager System with Blue Light Base (Life Technologies).

Quantitative Real-time RT-PCR (RT-qPCR)

Complementary DNA was diluted 10-fold with RNase-free water. In a 10 µl PCR reaction using FastStart Universal SYBR Green Master ([ROX]; Roche) 4 µl cDNA was used. The reaction mix was added to a 96 or 384 well plate and amplification of the product was measured after incubation steps at 50 °C for 2 minutes and 95 °C for 10 minutes during 40 PCR cycles (95 °C for 15 seconds and 60 °C for 1 minute) using a QuantStudio 6-flex Real-Time PCR system (Life Technologies). A melting curve was generated afterwards by ramping the temperature from 60 °C to 95 °C (Supplementary Figure 2). Amplification curves were analyzed using QuantStudio 6 and 7 Flex Real-Time PCR System Software (v1.0). Ct values were normalized to the geomean of the *c.elegans* spike-in reference genes *act-1* and *tbb-1* and to the housekeeping genes *Hprt1*, *Actb*, *Pgk* and *Tbp*. Expression values were analyzed using the $2^{-\Delta\Delta Ct}$ method. If the fluorescent threshold was not reached after 40 PCR cycles, a value of 40 was used in the analysis. All qPCR reactions were conducted in technical triplicates. Primer sequences (Integrated DNA Technologies) are listed in Supplementary Table 1.

Cell culture

All cell lines were maintained at 37 °C in a humidified incubator with 5% CO₂.

Coating

Neurons were cultured on coverslips (VWR, 18Ø) in 12-well plates (Costar 3513/3524). Coverslips were etched in 1 N HCl (Emsure) for 1 hour at 65 °C and washed and stored in 100% EtOH (Emsure). At the start of the experiment coverslips were coated with 20 µg/ml Poly-D-Lysine-ornithine (Sigma Aldrich) solution for 30 minutes at RT, washed with sterile PBS [1x] (Gibco), coated with 40 µg/ml Laminin (Gibco) for 1 hour at 37 °C, again washed with sterile PBS [1x] (Gibco) and used immediately to plate cells.

Primary cortical neurons (PCN)

Primary cortical neurons (PCNs) were prepared from 14 days old C57/BL6 mouse embryos (E14). The embryos were removed from the uterus and collected in Leibovitz's L-15 medium (Gibco). Cortices were separated and the meninges were removed. The tissue was dissociated in 2.5% trypsin for 15 minutes at 37 °C. Following trypsinization, the supernatant was removed and dissociation medium added, consisting of 10% Fetal Bovine Serum (FBS) (Gibco), 0.2% DNase (2 mg/ml, Roche) in Leibovitz's L-15 medium (Gibco). The cells were triturated in the dissociation medium with a 200 µl pipette before being spun down for 1 minute at RT (IKA miniG). The supernatant was removed and the cells were resuspended in 1 ml Neurobasal Culture Medium (NB+) (Gibco) supplemented with 2% B27 [50x] (Gibco); 0.1% Pen/Strep (10 kU/ml Pen; 10 mg/ml Strep, Gibco); 0.1% Glutamine (Gibco); 5% 400 nM D-Glucose (Sigma Aldrich). Cells were plated on coated coverslips placed in 12-well plates. Cells were cultured for 2, 7, 14 and 21 days *in vitro* (DIV) with half the medium changed every week.

Primary hippocampal neurons (PHN)

Primary hippocampal cultures were prepared from post-natal day 0 (P0) C57BL/6 mice. Mice were euthanized by decapitation and brains were dissected out in ice-cold L-15 medium (Gibco) with 7 mM HEPES (Gibco). Hippocampi were separated and the meninges removed in dissection medium containing 4.5 ml L-15 medium (Gibco) with 7mM HEPES (Gibco). The tissue was incubated in 0.5 ml trypsin [10x] at 37 °C for 20 minutes. Following trypsinization, the supernatant was removed and cells were washed

with a L-15 (Gibco), 7 mM HEPES (Gibco) mixture 3 times, removing as much supernatant as possible between washes. The cells were then exposed to 4 μ l DNase (0.012 mg/ml, Roche) diluted in 1 ml NB+ medium (Gibco) supplemented with 18 μ l HEPES 1M (Gibco), 2.5 μ l L-glutamine (Gibco), 1.8 μ l 14.3 mM β -mercapto, and 20 μ l B-27 (Gibco). Cells were triturated with a 200 μ l pipette and filtered through a 70 μ m nylon cell strainer (Falcon). A 1:10 dilution was made using 90 μ l NB+ medium and 10 μ l of the cell sample for cell counting. Hippocampal cultures were grown on coated coverslips in Neurobasal medium (NB) supplemented with B27, 14.3 mM β -mercapto, L-Glutamine and 1 M HEPES.

Stable cell lines

N2a cells were cultured in DMEM high glucose containing 10% fetal calf serum, L-glutamine and penicillin /streptomycin. On day 2 after plating 1 μ M or 10 μ M all trans-retinoic acid (Sigma) was added to the cell culture medium. After 1 or 3 days, the cells were washed with PBS [1x] and lysed in Qiazol (Qiagen). N1E-115 and C2C12 cells were grown in DMEM high glucose containing 10% fetal calf serum and penicillin/streptomycin.

Microscopes

All immunofluorescent images were acquired using an Axioscope epifluorescent microscope (Zeiss) and a LSM 880 confocal microscope (Zeiss). Brightfield images were acquired using a ZEISS Axio Scan Z1 (Zeiss).

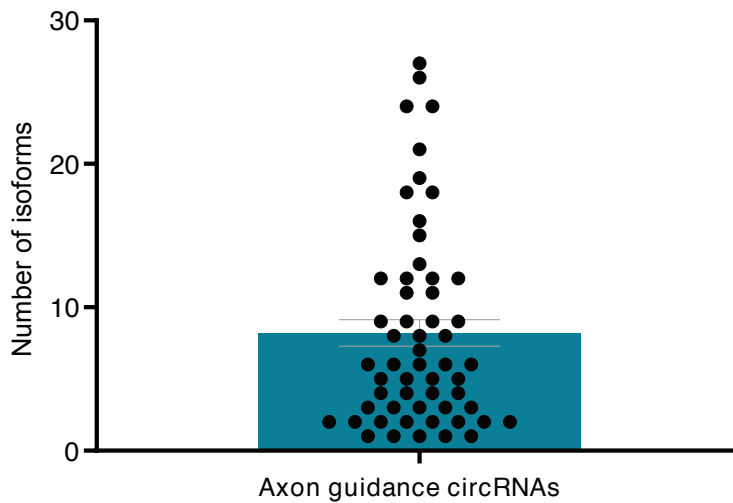
Northern blotting

For Northern blotting 20 μ g of RNA was loaded on an 1,2% agarose gel. The gel was run for 2.5 hours and RNA was transferred to an Amersham Hybond-N+membrane (GE Healthcare). After transfer, the membrane was hybridized with [³²P] labeled probes at 55 °C in ULTRAhyb Ultrasensitive Hybridization Buffer (ThermoFisher Scientific). The membranes were exposed to a phosphoscreen for 1 hour and imaged on a FLA phosphoimager. Probe sequence is listed in Supplementary figure 1.

Acknowledgements

We thank Lasse Sommer Kristensen for running the NanoString samples. This project has received funding from the Netherlands Organization of Scientific Research NWO (Personal grant DvR, part of Graduate Programme project (022.003.003) and NWO VICI to RJP) and the European Union's Horizon 2020 research and innovation programme under the Marie Skłodowska-Curie grant agreement No 721890 (circRTain).

SUPPLEMENTARY DATA



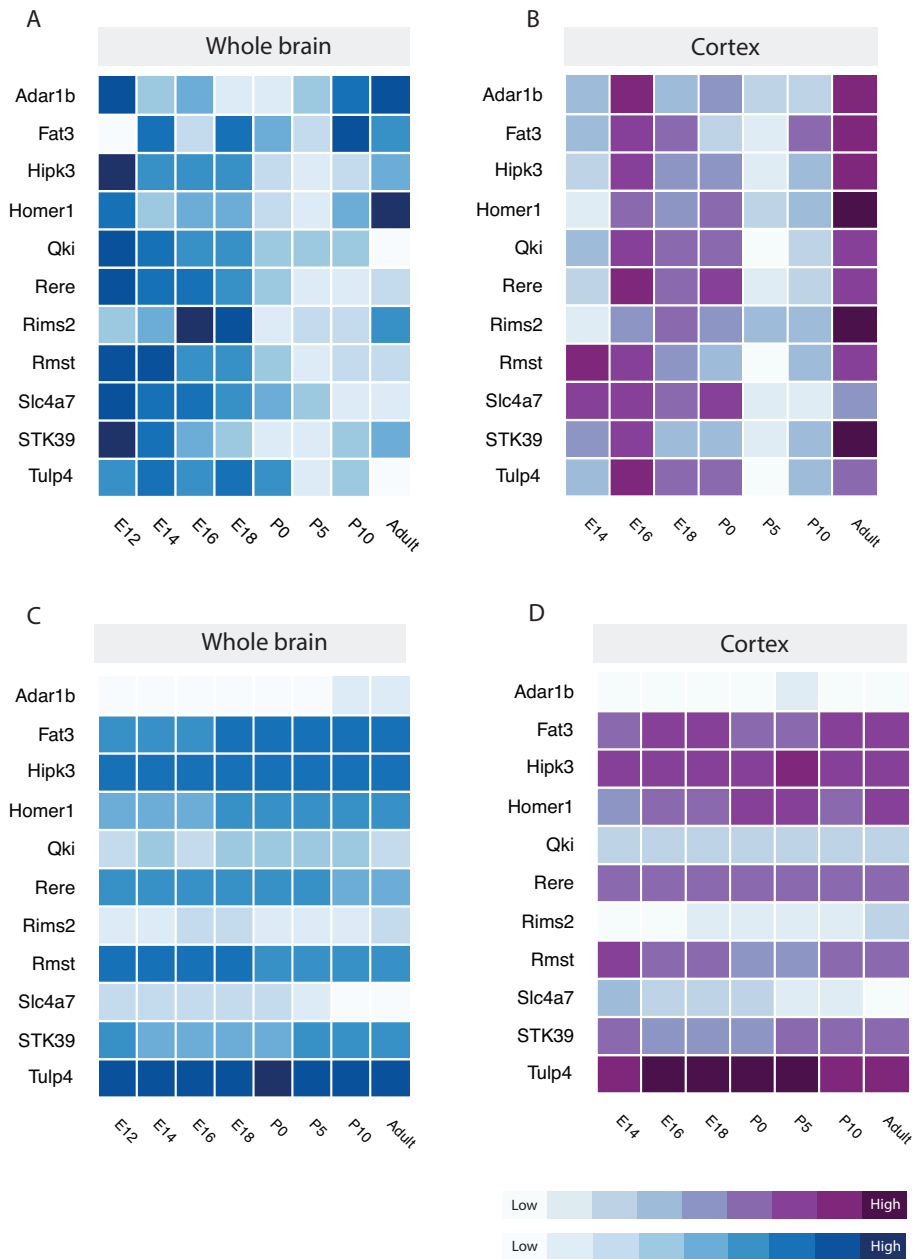
Supplementary figure 1 | Axon guidance circRNA isoforms.

The number of axon guidance circRNA isoforms detected per axon guidance gene in human samples with RNA-sequencing. Each dot represents an axon guidance gene.



Supplementary figure 2 | Axon guidance circRNA validation.

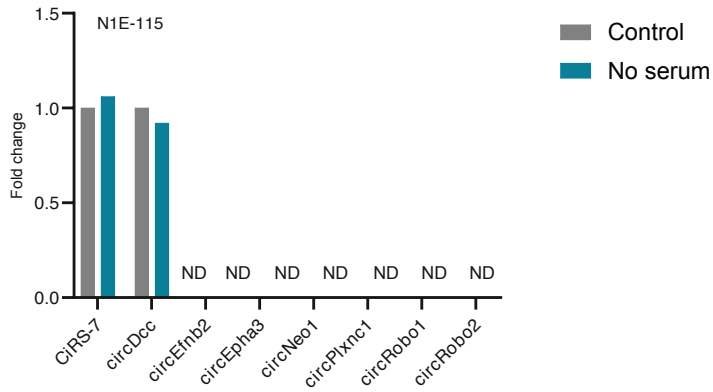
(A) RT-qPCR melt curves confirming that the divergent primers specifically amplify the back-splice sequence of the circRNAs. (B) Bands corresponding to CiRS-7 in a mock and RNase R treated sample can be detected using Northern Blotting, confirming the circular nature of the amplified sequence.



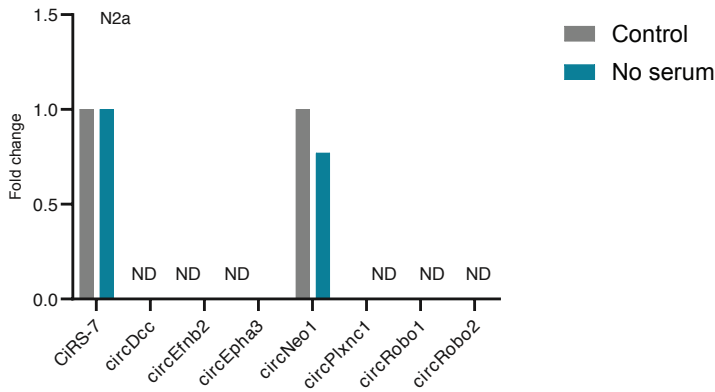
Supplementary figure 3 | Nanostring data of non-axon guidance circRNAs.

Heatmaps show the relative expression of the circRNA over time compared to its own expression (B-C) and compared to other circRNAs (D-E). Log₁₀ transformed. N = 3.

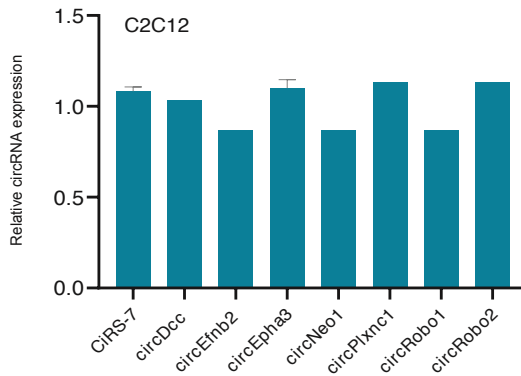
A



B



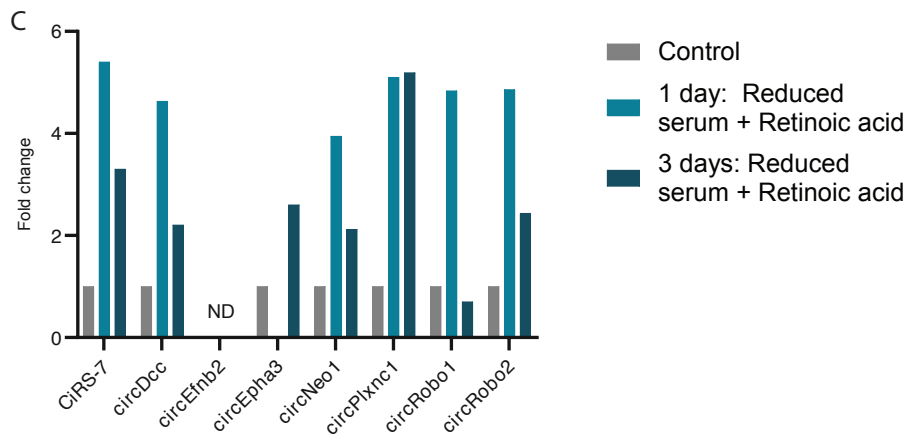
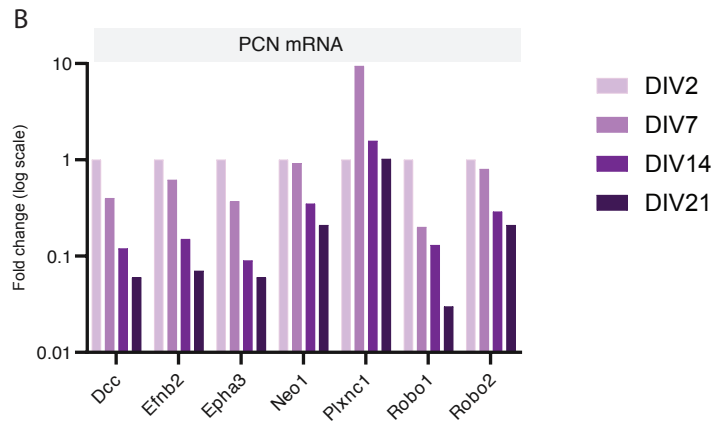
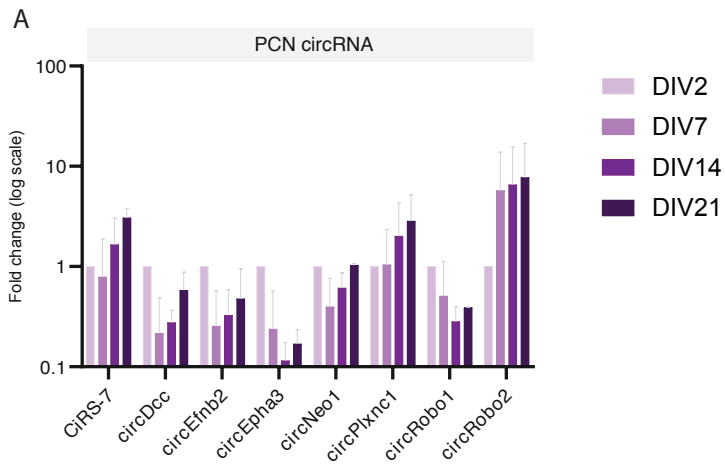
C



Supplementary figure 4 | Axon guidance circRNA are very lowly expressed in stable cell lines.

Axon guidance circRNAs are very lowly expressed in (A) N1E-115 and (B) N2a cells, also after serum starvation. ND = Not detected with RT-qPCR. (C) Axon guidance circRNAs are lowly expressed in C2C12 cells.





Supplementary figure 5 | Developmental processes in the developing mouse brain.

(A) Schematic of the onset and peaks of key processes in the developing mouse brain over time (Adapted from Reemst et al., 2016). (B) Linear host gene expression in the rostral secondary prosencephalon during brain development. Adapted from the Allen brain atlas. (C) The absolute level of circRNA expression was assessed with RT-qPCR during mouse brain development in whole brain and cortical samples (n = 3). E = embryonic; P = postnatal.

Supplementary table 1 | Primers used for RT-qPCR analysis

Target	Species	Primer sequence FW (5'-3')	Primer sequence RV (5'-3')
ciRS-7	mmu	GGCGTTTTGACATTAGGTT	GGAAGATCACGATTGTCTGGA
circDcc	mmu	TTTTCTACTGGCCCTGGAAC	CCTTTCAGTGCCAAAGTGCTC
circEfnb2	mmu	CAGACCAGACCAAGATGTGAAA	GTCCACTTTGGGGCAAATAA
circEpha3	mmu	GGTGGGCACTAGCACACTT	GAGACAGTATGCCGAGTCA
circEpha5	mmu	CAAAGCCAGATCCCATCAT	GAGAAGGAGCTGCCACTGAG
circEpha6	mmu	TGGGCCTATTGTGTTATCC	CCTCTTGAAGGTGTATCTGC
circEpha7	mmu	AGGCTCTTCGCTGCTGTAG	TTGGACAACGAGAACACTGG
circEphb2	mmu	GTACCATCCAGCCAGCTC	GCTTCGAGGCTGTGGAGA
circNeo1	mmu	CTGAGGATGATGCTGGGACT	ACACTGGCTCCTGCACAGT
circPlxna2	mmu	TGGGGACTAAGAGTGGCAAG	GGGGGACAGCTCCTCTATGT
circPlxnc1	mmu	GTGCCTCCCATTACAAGAA	CGTCAGGTGAGAGTGATCA
circRobo1	mmu	TATGGTCGGGAAAGCTGAAG	ACTTGCCAGCATCGCTTTTA
circRobo2	mmu	TGGAAGTGGCATGATCTCGT	GTTGAGAGTGGTGGGCTCTC
circSema3c	mmu	CACAAAGATTGCTGTGGACCG	TGAATACCTGGTCTGTGCC
Dcc	mmu	CCCTTACACCCGTTTTGTC	CCCAAGGGAGGCCGTTTTTA
Efnb2	mmu	GGTTTTGTGCAGAACTGCGAT	GGCCTGTCCGGGTAGAAAT
Epha3	mmu	CAGCCTTCCAACGAAGTAATCT	TGCACACCTGGTAAGTCTGA
Neo1	mmu	TTGCTCGGCATATTCTGAGCC	TGGCGTCGATCATCTGATTCTAA
Plxnc1	mmu	GTGTGGCGATCTGAGCAAG	GTATAGCGGAGAGAGCCTGTT
Robo1	mmu	TGGTCATCCCCTCTCTGGTT	ACGGGGTTCCGTGAGAATC
Robo2	mmu	TGATGGATCTCGTCTTCTGCA	GTCGGCCCTCTGCTTTACAG
Hprt1	mmu	ATGGGAGGCCATCACATTGT	ATGTAATCCAGCAGGTGAGCAA
Actb	mmu	AGCCATGTACGTAGCCATCC	CTCTCAGCTGTGGTGGTAA
act-1	cel	ACGACGAGTCCGGCCATCC	GAAAGCTGGTGGTACGATGGTT
tbb-2	cel	CAAATTCTGGGAGGTCATCT	CATACTTCCGTTGTTGGC

circ ID	Sequence (sense strand 5'-3')
mnuu_circ_0001878	TAATGCTTCGAACACTGGCAGAGTGCTCAGAGTGTATGGGGTTTTCGATTCAGAGTTTCTGCGTATCCAGGGTTTCAGTGGTCCAGTACGAAGGTTCCGACGATCTCCAGAGTCTCCGAAKCTCCGAAKCTGCAG
mnuu_circ_0007486	ACTGTAATGATCTTATTCCTTGAGTGGCCGAGTGCTCCACTCAAGCACTCGATCGAGGTTGTACTACGGTGGTTACTACGGTGGAGTCCAGGGCCAGTAGAAKCTGGATCGTATGATCTCCANTCTTATTAATAGGGGAACCCCTT
mnuu_circ_0015034	ATTCACATCAAGTTCCAGAAATTGAGGCTACCTCTGGGCTCTAGATTACAGTATGAAAGGAAATGATTAATTTCTACCCGAAKAGGCTGGTACTATAATCCACAGATAGGAGAGAAATGGAAATATATTGGCCCAAGGTGGACTCTA
mnuu_circ_0000696	CGATGCTTTAATGGGGTTCAGAGCTGAGCTGCGCACGACAGATGATGCCGAGTCAAGTACAAKTAATAGCTGCTTCGACAGGCTCTACAAAGGCTCTACAAAGGCTCTGATGGTGGTCTGTCTTAAAGTGTCTGTAAGTGCCTCAACGACGACAAAGGAA
mnuu_circ_0012825	CGATTTCCCATGATGGAGTCTAGTGAAGTGGGATCATTTGTGGCAGATGATGCTGGCTCTCTGATGGAGCTCTTCCTCATGACCAATTGGAAGGGGGAATGGACAGAGCATTTCTTTGGTTCGCGAGAGCGAGATCGCC
mnuu_circ_0000694	AGCTGATGGGGATTGGCTTCTCTTGGAAGGTGATCTGCAGTA CAGGSGTATGAAGAATTGGAAGGGTTCTTCGCAATGSGGATGCATTA CTGAATTGATGAAKCAATAGSGCCCATATACTACACAGATATGCATGTCATGGAACCAAAKCA
mnuu_circ_0011549	TGGAGAGAGAGATGGCTAGTACCTCGAAGGAGGCTATCGAAGGAGGCTATCGAAGAAAGGAGCACTTGCAACTACTACTGGAACTGAAAGCCACAAKAAAGATGGAAATGGATTTCTCTCAKCCAGTGGGGTAGTAGCAKCTC
mnuu_circ_0001284	CGGCGAATGGCTGGTCCATAGGCTGCCATGTCGAGGCGGGCTCGAGGCTGTGAGAGGCGGACCTCTGCGCGAAGAACCTGATGCACTACGACACAGCGCGTGGCTGGATGGTAACTCCCATGAGGGGTGAGTCTGCTCCC
mnuu_circ_0013627	TAAAGGTACTAAAGCAATGAGCTGACAGCTATCAKCAKCTATGAGGCTGCTTCTCATAGGAGTGTCTCTCTTTTTAAKCTGAATATAAAGACTCTCCGAGATGACTCTGCTGTTTTGAGGACTTGAAKGAATCTGGAGGAAGTGTGAGTGT
mnuu_circ_0010322	AGCAGAGAGAGAGGCGGGCTTTCGACCAKCPATGAGAGATGACTGAGAACTCTCTCTCTCATAGAGGAGAGGTGGGATTTGAGTGAATMCCGGTCTCTACTGGAAKAAKCTTGGAAKAAKCTTGGAAKAAKCTTGAAGTGTAAAGTATTTTAA
mnuu_circ_0001779	GGATGATGCTGGGACTATTTTGGATGACTGATGGAAATAGAAKCTTGAAGCTCAGGGGAGCTTCTGAGGCGAGCTTACGAGTGGAAAGCCAGTGTTCGAAKACTACTCCGTTTATTTTCTGGGCGAGCTAGAAKAAKCTCTCTGTT
mnuu_circ_0010373	GCCGTTGGGAAATATTTTGGAAKTAATTTGGCAKCTTTAATGCACTCGAGACTAAAGGTTGCGAGGAGGGCGAACCTTCAKATGTGCMAATAGAGTGTGATGGAGTAAKCCCTCAKCTGCGAAKAAKCTCCCTGACTGATGTTGATTT
mnuu_circ_0008579	GCCTGACTCTGTGGCTCTCATGTTAAKAGTGCATAGGTTTGGGGACTAAAGTGGGAAGCTGAAGAGCAATGAGGACTGATGAGGACTGATCTTGAAMAGTGGAATAKTAGAGAGGCTGTTCCCAGCCTCAKCCCTTAGGGATGGAG
mnuu_circ_0013291	GCATGACTCTGCTATCCTAIGCTCAAGAAKCACTCTGGCTTCTGGCGCAKCAAAAGTGGGAAGCTGAAAGGGGGAGACAGCCCTGCTGAGTCCGCCCCGAAAGGGAGATGTTGGTGGAGTGGCTGTGGAGTGGCTGTGTT
mnuu_circ_0002595	AACTGCAGTAAACGGAAATCTCTGTTCAAGAGTCTTACGACAGCCCACTGTGGCTGCCTCCGTTAAGAAAGAAAGAGGGGATGGGCTGAAKCCGGTCCAGCGGGTCCAGTCTAGACTCATCAGCTCAKCTGATCTGTTAATGG
mnuu_circ_0000698	TGGCGAKATGGGATCATACACTGTGGCAGAAATAATGTTGGGAACCTGAMGCTCCGCTACTTGTGAGTCTAAGATACGAGAGGAAACTCATGATCACTATACCCGTAAMGGGATGCTGGGAATGTATTGGCTGGACCAKCAKATGGT
mnuu_circ_0000700	GGACGAAGGGGATTTACTGTTGTGAAAGGACATCTTGGTGGAGAGTAGTGAAGTGCATCTGGAAGTGGGATGATCTTCGCAAGGAGCAGGAGCAGAGGAAKCTTCCCTGTGATGATGATGTCTCCAGGGGAGAGGCC
mnuu_circ_0012389	TGAKTAAAGTACAAAGATGCTGTGGACCGTGTAAAGTCTGATGGGAGGATACAGTCTGTTTCTGGCGAGGACAGAGGTATGATGCTGACTCATAGTGGTGAATGATGCTGGCAAGGAGGATGCTTTCCAAKCCGAAATGTGAAKCACTGTGTC
mnuu_circ_0000723	CTTTCAKCTCGATGCTGTGGAGAGTAGGATACACAGAGAAATACTTCAACTCCGAGGGCAKAAAGTAGGAGTGTAGAGTCACTCAAGACTTCACTGATGATGAATACTGATGAGTCTCTGATTAATCCGGGAAKAAAGATACA
mnuu_circ_0000411	AGTACAGATGCTTTTCCACTTTGGCCCAKCTGMAAGCTCCCGAGCAATGAGAGAGTACAGAGTTCGATCTCGAGAGTACAGAGTTCGATCTCGAGAGTACAGAGTTCGATCTCGAAGATTTATCCGAAKCATCAGGAACAGAT
mnuu_circ_0000595	ATCTAGATGGGGCCCAAAATGGTAGTATGTTGTTCTCACGAAAAGTCCGAGTCTCTCACTAAGCCAAKCCGGTGTAGGATAGAGGGAGAAATGGCCAAATGAAKTAAGAGGAGGATCCGGATGAAKAGCCGACCCTGACGCTG
mnuu_circ_0000491	GATGAGAGAAACACCCGATGTGAAKCAKAGAACTGAGAGCCAAAGGGCTGAGCAATGCAGATTGCCATTTCCAAAGTCAATGGGAGCAKCTTACTCCAGCACTCGAGCTCATGTTCTCGAGATGACCTCGAAGCAAAAGAAAGAACTGGATACCACAGCA

mmu_circ_0001052	GTAAAGTATAGACTTGGATGGCCAGTCATGATGAAAGCTGTTGTCACGATCTTCACTCGCTACACAGGATGGCTCGAAGCTTGGTCTACCCAGCTGATGTTTATCAACTCAGTCAAGTGCCTTTTGTAGTGTGAGAAACTC
mmu_circ_0001746	TCTGGTAGGGATGGAGAGATCCAGTACTCTAAGAGATGGGAGTGGTCTTGGGAGGTTCAATATGATGATGAGAGTGGACGGAGATGATGATGATGTGTGACTATGGGACACTGATGGCAAAAGCCTCCTCTTGCATCATCTCTCTGCTC
mmu_circ_0000205	CAGAAATGAGAAAGTAGAAGATGTGCTCGAATATTCGAGCGAGTGCMAAGGGGCTAGTTGAGGAATGGCTTCATGAGATACTCAGTGGAGTCAAGGCAAGGTCGCTTATCAACAAACAGAGGATGTCTGCAGGGAAACAGAACTTATCAAGC
mmu_circ_0005070	TAGATCAAGTACTGTTCTTCCAGGAGAGTGGGATCCTTCATACGGATAGAGCCTCCAAAAGTGTCTTCCAGGCTTCAGATGAAAGAGCTTGTGGACTTGGCAAACTAGCTGACACCCAGTTTGAAGAGAAAGATTAGAGC
mmu_circ_0001027	AATCTTTTGGCAACAGAGAGTACTGTATCGAAGAGCTGTGCAAAAGAACCTCCAGACATAGCCCAAGAGCCAAAGAGCCAGCGAGAACTCGCGGTTCAGGGACCTTATGCAACTCAGCGCAAGAAAGGCTAGCTAAAGCGGATCAACTTG
mmu_circ_0006533	TACAGCTAAACACTTGAGCAGAAACGGGATGTAAATATGTCCGAGGCAAGGCTCATGTAGGATAAAGAAAGAAATTAGCAAGATGACATGACAGTGGAAAGACATGTACATGACAGTAAATGGGCAATACAGAAAGAAAGAAAGTGCAGAAATGGCTGAC
mmu_circ_0002430	CTGCTCAATTGCACTGGACCAACACATCTGGCAGCCTGCTCGATGAGGGTCTCATGTTGATTGCCACAGGGTGAAGTATGACTCTCTCTCGAAGTGGGAGAGCCACCCAGAGCTTCTGATGCTCGTGGTGTAGATGGCCAG
mmu_circ_0001298	TCTGACAAATTTGCTCTCGAGAGTTTAAAGCCCGAGTGGACTATTTCTACAAATTAGGATACAACTTCCAGAGTCCAGAGTCCAGAGGCTTGTGAGATCTTCAGCTCCTGCTTGTGACCCCTCCAGATGCTCTCTGCGGTGGCACT



Supplementary table 3 | Primer efficiency test

Primer	R-sq	Efficiency
ciRS-7	1.00	99.89
circDcc	0.96	166.78
circEfnb2	1.00	100.48
circEpha3	1.00	101.74
circNeo1	1.00	102.14
circPlxnc1	1.00	114.97
circRobo1	1.00	96.10
linDcc	1.00	96.39
linEfnb2	0.99	118.92
linEpha3	1.00	99.55
linNeo1	1.00	99.79
linNtng1	1.00	102.95
linPlxnc1	0.97	91.26
linRobo1	1.00	109.21
Actb	1.00	101.53
Hprt1	1.00	95.02
act-1	1.00	124.33
tbb-2	1.00	96.15

Supplementary table 4 | Identified circRNA isoforms from (canonical) axon guidance genes in human and mouse (neuronal) tissue (adapted from CircBase)

Gene	CircRNA isoforms	Gene	CircRNA isoforms
DCC	hsa_circ_0108613, hsa_circ_0108613, hsa_circ_0108594, hsa_circ_0108599, hsa_circ_0108597, hsa_circ_0108595, hsa_circ_0108600, hsa_circ_0108596, hsa_circ_0108607, hsa_circ_0108608, hsa_circ_0108601, hsa_circ_0108605, hsa_circ_0108603, hsa_circ_0108606, hsa_circ_0108602, hsa_circ_0108609, hsa_circ_0108611, hsa_circ_0108612, hsa_circ_0108604, hsa_circ_0108610	Dcc	mmu_circ_0000893, mmu_circ_0000893, mmu_circ_0007485, mmu_circ_0007489, mmu_circ_0007486, mmu_circ_0007484, mmu_circ_0007488, mmu_circ_0007490, mmu_circ_0007483, mmu_circ_0007487
DRAXIN	hsa_circ_0110596, hsa_circ_0110596, hsa_circ_0110589, hsa_circ_0110593, hsa_circ_0110591, hsa_circ_0110590, hsa_circ_0110588, hsa_circ_0110595, hsa_circ_0110594		
EPHA2	hsa_circ_0005240, hsa_circ_0005240, hsa_circ_0111020, hsa_circ_0010130, hsa_circ_0010128, hsa_circ_0010126, hsa_circ_0010131, hsa_circ_0010132, hsa_circ_0010124, hsa_circ_0010121, hsa_circ_0010122, hsa_circ_0010129, hsa_circ_0010127, hsa_circ_0010125, hsa_circ_0010123	Epha2	mmu_circ_0001290
EPHA3	hsa_circ_0124749, hsa_circ_0124749, hsa_circ_0124744, hsa_circ_0124762, hsa_circ_0124764, hsa_circ_0124757, hsa_circ_0124754, hsa_circ_0124763, hsa_circ_0124758, hsa_circ_0124750, hsa_circ_0124741, hsa_circ_0124755, hsa_circ_0124751, hsa_circ_0124760, hsa_circ_0124761, hsa_circ_0124756, hsa_circ_0124747, hsa_circ_0124752, hsa_circ_0124748, hsa_circ_0124759, hsa_circ_0124746, hsa_circ_0124742, hsa_circ_0124745, hsa_circ_0124753, hsa_circ_0066598, hsa_circ_0066596, hsa_circ_0066601, hsa_circ_0066600, hsa_circ_0066597	Epha3	mmu_circ_0000696, mmu_circ_0000696, mmu_circ_0000697, mmu_circ_0006368, mmu_circ_0006369
EPHA4	hsa_circ_0119195, hsa_circ_0119195, hsa_circ_0119197, hsa_circ_0119198, hsa_circ_0119196, hsa_circ_0058423, hsa_circ_0058424, hsa_circ_0058425	Epha4	mmu_circ_0008968, mmu_circ_0008968, mmu_circ_0008970, mmu_circ_0008971
EPHA5	hsa_circ_0126806, hsa_circ_0126806, hsa_circ_0126815, hsa_circ_0126797, hsa_circ_0126812, hsa_circ_0126817, hsa_circ_0126808, hsa_circ_0126807, hsa_circ_0126818, hsa_circ_0126813, hsa_circ_0126824, hsa_circ_0126810, hsa_circ_0126825, hsa_circ_0126814, hsa_circ_0126802, hsa_circ_0126803, hsa_circ_0126811, hsa_circ_0126805, hsa_circ_0126800, hsa_circ_0126804, hsa_circ_0126801, hsa_circ_0126798, hsa_circ_0126816, hsa_circ_0126799, hsa_circ_0126819, hsa_circ_0126809	Epha5	mmu_circ_0001362, mmu_circ_0001362, mmu_circ_0001361, mmu_circ_0012824, mmu_circ_0012825, mmu_circ_0012822, mmu_circ_0012832, mmu_circ_0012827, mmu_circ_0012823, mmu_circ_0012826, mmu_circ_0012820, mmu_circ_0012821, mmu_circ_0012830, mmu_circ_0012831, mmu_circ_0012829
EPHA6	hsa_circ_0124807, hsa_circ_0124807, hsa_circ_0124820, hsa_circ_0124812, hsa_circ_0124819, hsa_circ_0124810, hsa_circ_0124821, hsa_circ_0124816, hsa_circ_0124808, hsa_circ_0124817, hsa_circ_0124814, hsa_circ_0124806, hsa_circ_0124818, hsa_circ_0124815, hsa_circ_0124805, hsa_circ_0124804, hsa_circ_0124811, hsa_circ_0124809	Epha6	mmu_circ_0000694, mmu_circ_0000694, mmu_circ_0006355



EPHA7	hsa_circ_0132683, hsa_circ_0132683, hsa_circ_0132684, hsa_circ_0132689, hsa_circ_0132690, hsa_circ_0132685, hsa_circ_0132686, hsa_circ_0132688, hsa_circ_0132687, hsa_circ_0077398	Epha7	mmu_circ_0011554, mmu_circ_0011554, mmu_circ_0011553, mmu_circ_0011552, mmu_circ_0011551, mmu_circ_0011549
EPHA8	hsa_circ_0010794	Epha8	mmu_circ_0011317, mmu_circ_0011317
EPHB1	hsa_circ_0122032, hsa_circ_0122032, hsa_circ_0122026, hsa_circ_0122030, hsa_circ_0122034, hsa_circ_0122028, hsa_circ_0122035, hsa_circ_0122033, hsa_circ_0122027, hsa_circ_0122031, hsa_circ_0122029, hsa_circ_0122025, hsa_circ_0067449, hsa_circ_0067445, hsa_circ_0067448, hsa_circ_0067446	Ephb1	mmu_circ_0015178, mmu_circ_0015178, mmu_circ_0015179, mmu_circ_0015180, mmu_circ_0015177, mmu_circ_0015176, mmu_circ_0015181
EPHB2	hsa_circ_0002720, hsa_circ_0002720, hsa_circ_0004085, hsa_circ_0112387, hsa_circ_0010796, hsa_circ_0010797, hsa_circ_0010795	Ephb2	mmu_circ_0001284, mmu_circ_0001284, mmu_circ_0011316, mmu_circ_0011315
EPHB3	hsa_circ_0122998		
EPHB4	hsa_circ_0001730, hsa_circ_0001730, hsa_circ_0081527, hsa_circ_0081522, hsa_circ_0081523, hsa_circ_0081534, hsa_circ_0081524, hsa_circ_0081521, hsa_circ_0081533, hsa_circ_0081532, hsa_circ_0081525, hsa_circ_0081520, hsa_circ_0081530, hsa_circ_0081528, hsa_circ_0081531, hsa_circ_0081529, hsa_circ_0081518, hsa_circ_0081519		
EPHB6	hsa_circ_0001765, hsa_circ_0001765, hsa_circ_0133599	Ephb6	mmu_circ_0013388
NRP1	hsa_circ_0008235, hsa_circ_0008235, hsa_circ_0002169, hsa_circ_0018161, hsa_circ_0018157, hsa_circ_0018164, hsa_circ_0018163, hsa_circ_0018158, hsa_circ_0018159, hsa_circ_0018162		
NRP2	hsa_circ_0057895		
NTN1	hsa_circ_0042061		
NTN4	hsa_circ_0006419, hsa_circ_0006419, hsa_circ_0007199, hsa_circ_0099579, hsa_circ_0099577, hsa_circ_0099578, hsa_circ_0027786, hsa_circ_0027785, hsa_circ_0027794, hsa_circ_0027792, hsa_circ_0027787, hsa_circ_0027793, hsa_circ_0027788, hsa_circ_0027789, hsa_circ_0027790, hsa_circ_0027795, hsa_circ_0027783, hsa_circ_0027791		
NTN5	hsa_circ_0051767		
NTNG1	hsa_circ_0002286, hsa_circ_0002286, hsa_circ_0013366		
RGMA	hsa_circ_0104934		
RGMB	hsa_circ_0073484, hsa_circ_0073484		

ROBO1	hsa_circ_0004788, hsa_circ_0004788, hsa_circ_0066568, hsa_circ_0124693, hsa_circ_0124701, hsa_circ_0124709, hsa_circ_0124710, hsa_circ_0124687, hsa_circ_0124690, hsa_circ_0124708, hsa_circ_0124707, hsa_circ_0124696, hsa_circ_0124685, hsa_circ_0124691, hsa_circ_0124698, hsa_circ_0124699, hsa_circ_0124695, hsa_circ_0124692, hsa_circ_0124694, hsa_circ_0124711, hsa_circ_0124688, hsa_circ_0124686, hsa_circ_0124689, hsa_circ_0124684, hsa_circ_0124703, hsa_circ_0124702, hsa_circ_0124697, hsa_circ_0124713, hsa_circ_0124704, hsa_circ_0124705, hsa_circ_0124700, hsa_circ_0124706, hsa_circ_0066566, hsa_circ_0066567, hsa_circ_0066569, hsa_circ_0066570, hsa_circ_0066565, hsa_circ_0066562, hsa_circ_0066564, hsa_circ_0066563	Robo1	mmu_circ_0000698, mmu_circ_0000698, mmu_circ_0006390, mmu_circ_0006388, mmu_circ_0006382, mmu_circ_0006381, mmu_circ_0006385
ROBO2	hsa_circ_0124639, hsa_circ_0124639, hsa_circ_0124619, hsa_circ_0124647, hsa_circ_0124660, hsa_circ_0124682, hsa_circ_0124648, hsa_circ_0124646, hsa_circ_0124632, hsa_circ_0124652, hsa_circ_0124623, hsa_circ_0124649, hsa_circ_0124624, hsa_circ_0124628, hsa_circ_0124641, hsa_circ_0124617, hsa_circ_0124677, hsa_circ_0124655, hsa_circ_0124659, hsa_circ_0124661, hsa_circ_0124616, hsa_circ_0124656, hsa_circ_0124640, hsa_circ_0124635, hsa_circ_0124618, hsa_circ_0124679, hsa_circ_0124667, hsa_circ_0124680, hsa_circ_0124668, hsa_circ_0124683, hsa_circ_0124669, hsa_circ_0124681, hsa_circ_0124627, hsa_circ_0124657, hsa_circ_0124662, hsa_circ_0124622, hsa_circ_0124621, hsa_circ_0124644, hsa_circ_0124645, hsa_circ_0124670, hsa_circ_0124626, hsa_circ_0124671, hsa_circ_0124674, hsa_circ_0124654, hsa_circ_0124663, hsa_circ_0124678, hsa_circ_0124664, hsa_circ_0124672, hsa_circ_0124675, hsa_circ_0124665, hsa_circ_0124673, hsa_circ_0124636, hsa_circ_0124666, hsa_circ_0124631, hsa_circ_0124658, hsa_circ_0124630, hsa_circ_0124653, hsa_circ_0124643, hsa_circ_0124642, hsa_circ_0124650, hsa_circ_0124637, hsa_circ_0124629, hsa_circ_0124625, hsa_circ_0124651, hsa_circ_0124638, hsa_circ_0124633, hsa_circ_0066557, hsa_circ_0066556, hsa_circ_0066560, hsa_circ_0066559	Robo2	mmu_circ_0000700, mmu_circ_0000700, mmu_circ_0000699, mmu_circ_0006396, mmu_circ_0006394, mmu_circ_0006397, mmu_circ_0006398, mmu_circ_0006395
SEMA3A	hsa_circ_0004363, hsa_circ_0004363, hsa_circ_0134887, hsa_circ_0134886, hsa_circ_0134889, hsa_circ_0134882, hsa_circ_0134885, hsa_circ_0134888, hsa_circ_0134891, hsa_circ_0134883, hsa_circ_0134884, hsa_circ_0134890, hsa_circ_0080945	Sema3a	mmu_circ_0012193, mmu_circ_0012193
SEMA3B	hsa_circ_0065848		



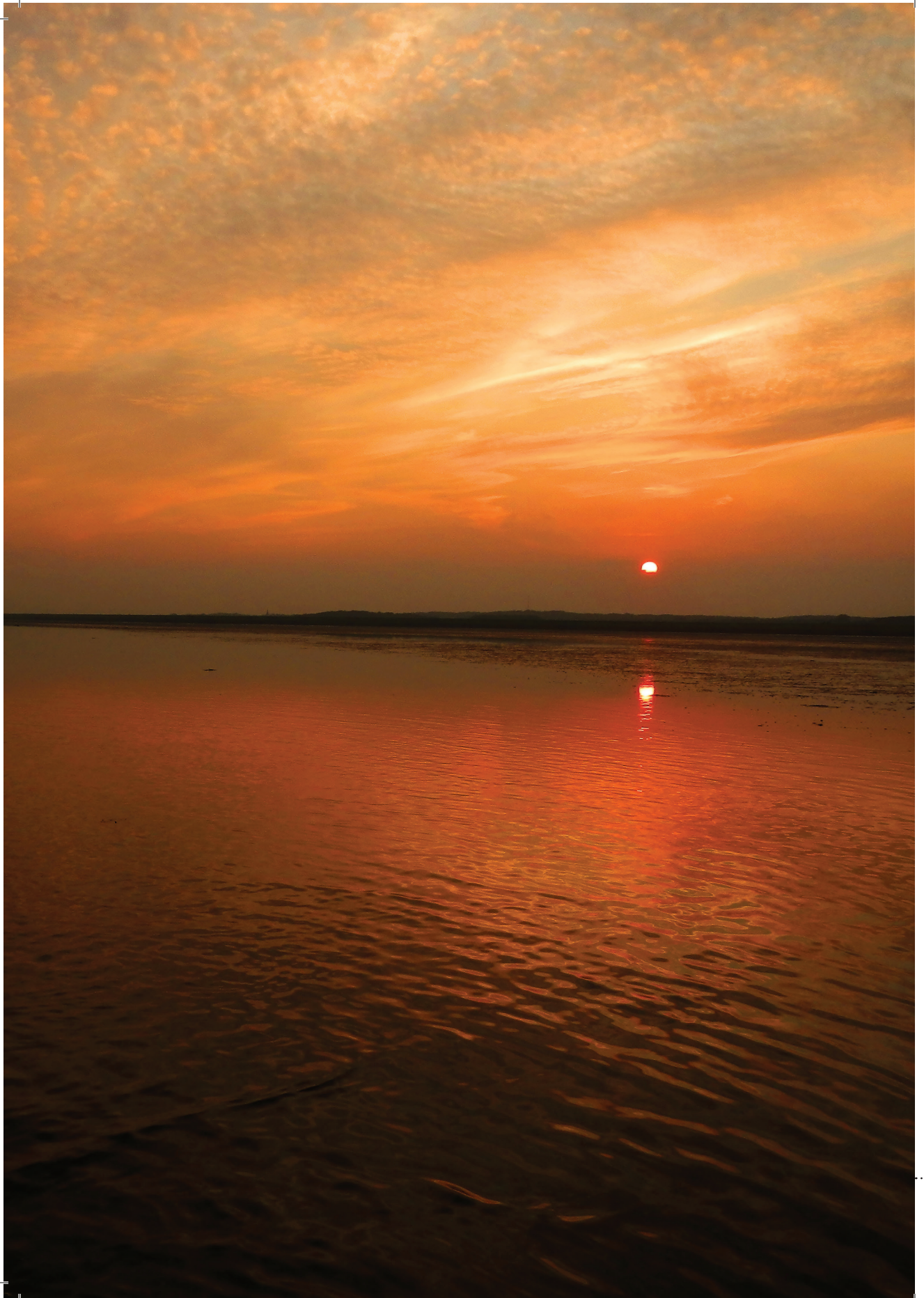
SEMA3C	hsa_circ_0002714, hsa_circ_0002714, hsa_circ_0004365, hsa_circ_0003634, hsa_circ_0134781, hsa_circ_0134768, hsa_circ_0134772, hsa_circ_0134767, hsa_circ_0134773, hsa_circ_0134770, hsa_circ_0134769, hsa_circ_0134780, hsa_circ_0134771, hsa_circ_0080896, hsa_circ_0080911, hsa_circ_0080910, hsa_circ_0080890, hsa_circ_0080909, hsa_circ_0080897, hsa_circ_0080906, hsa_circ_0080903, hsa_circ_0080904, hsa_circ_0080894, hsa_circ_0080895, hsa_circ_0080899, hsa_circ_0080905, hsa_circ_0080907, hsa_circ_0080891, hsa_circ_0080912, hsa_circ_0080898, hsa_circ_0080908, hsa_circ_0080888, hsa_circ_0080892, hsa_circ_0080900, hsa_circ_0080889, hsa_circ_0080887, hsa_circ_0080893, hsa_circ_0080901, hsa_circ_0080885, hsa_circ_0080886, hsa_circ_0080882, hsa_circ_0080883, hsa_circ_0080884	Sema3c	mmu_circ_0012391, mmu_circ_0012391, mmu_circ_0012390, mmu_circ_0012389
SEMA3D	hsa_circ_0134894, hsa_circ_0134894, hsa_circ_0134892, hsa_circ_0134893, hsa_circ_0080946, hsa_circ_0080948		
SEMA3E	hsa_circ_0134881, hsa_circ_0134881	Sema3e	mmu_circ_0012255, mmu_circ_0012255, mmu_circ_0012254
SEMA3F	hsa_circ_0005441, hsa_circ_0005441, hsa_circ_0124081, hsa_circ_0065839, hsa_circ_0065833, hsa_circ_0065829, hsa_circ_0065834, hsa_circ_0065835, hsa_circ_0065832, hsa_circ_0065828, hsa_circ_0065836, hsa_circ_0065830, hsa_circ_0065837, hsa_circ_0065838, hsa_circ_0065831	Sema3f	mmu_circ_0001840
SEMA3G	hsa_circ_0066032, hsa_circ_0066032, hsa_circ_0066033, hsa_circ_0066034		
SEMA4A	hsa_circ_0014682, hsa_circ_0014682, hsa_circ_0014681	Sema4a	mmu_circ_0010856, mmu_circ_0010856
SEMA4B	hsa_circ_0000650, hsa_circ_0000650, hsa_circ_0036763, hsa_circ_0036771, hsa_circ_0036768, hsa_circ_0036774, hsa_circ_0036772, hsa_circ_0036762, hsa_circ_0036770, hsa_circ_0036764, hsa_circ_0036765, hsa_circ_0036761, hsa_circ_0036766, hsa_circ_0036769, hsa_circ_0036767, hsa_circ_0036773	Sema4b	mmu_circ_0014420
SEMA4C	hsa_circ_0121237, hsa_circ_0121237, hsa_circ_0055694, hsa_circ_0055699, hsa_circ_0055697, hsa_circ_0055695, hsa_circ_0055698, hsa_circ_0055700, hsa_circ_0055696		
SEMA4D	hsa_circ_0142618, hsa_circ_0142618, hsa_circ_0142617, hsa_circ_0001872, hsa_circ_0139316, hsa_circ_0139315, hsa_circ_0087449, hsa_circ_0087451, hsa_circ_0087450, hsa_circ_0087444, hsa_circ_0087445, hsa_circ_0087446, hsa_circ_0087447		
SEMA4F	hsa_circ_0120997, hsa_circ_0120997, hsa_circ_0120999, hsa_circ_0120998		

SEMA5A	hsa_circ_0006634, hsa_circ_0006634, hsa_circ_0004707, hsa_circ_0002099, hsa_circ_0008329, hsa_circ_0008875, hsa_circ_0003918, hsa_circ_0002734, hsa_circ_0006397, hsa_circ_0007413, hsa_circ_0006329, hsa_circ_0004307, hsa_circ_0130031, hsa_circ_0130002, hsa_circ_0071820, hsa_circ_0071818, hsa_circ_0071819, hsa_circ_0071813, hsa_circ_0071817, hsa_circ_0071814, hsa_circ_0071815, hsa_circ_0071807, hsa_circ_0071816, hsa_circ_0071810, hsa_circ_0071806, hsa_circ_0071812, hsa_circ_0071801, hsa_circ_0071808, hsa_circ_0071811, hsa_circ_0071809, hsa_circ_0071802, hsa_circ_0071798, hsa_circ_0071805, hsa_circ_0071804, hsa_circ_0071799, hsa_circ_0071800, hsa_circ_0071803	Sema5a	mmu_circ_0005593, mmu_circ_0005593, mmu_circ_0005592, mmu_circ_0005589, mmu_circ_0005590
SEMA5B	hsa_circ_0121650, hsa_circ_0121650	Sema5b	mmu_circ_0006238
SEMA6A	hsa_circ_0127704, hsa_circ_0127704, hsa_circ_0127703, hsa_circ_0073647, hsa_circ_0073646, hsa_circ_0073648	Sema6a	mmu_circ_0007372, mmu_circ_0007372
SEMA6B	hsa_circ_0109714, hsa_circ_0109714, hsa_circ_0048650, hsa_circ_0048649, hsa_circ_0048640, hsa_circ_0048648, hsa_circ_0048647, hsa_circ_0048646, hsa_circ_0048635, hsa_circ_0048636, hsa_circ_0048637, hsa_circ_0048638, hsa_circ_0048641, hsa_circ_0048642, hsa_circ_0048643, hsa_circ_0048644, hsa_circ_0048639	Sema6b	mmu_circ_0006860
SEMA6C	hsa_circ_0110800, hsa_circ_0110800, hsa_circ_0110799, hsa_circ_0014103, hsa_circ_0014101	Sema6c	mmu_circ_0010943
SEMA6D	hsa_circ_0103691, hsa_circ_0103691, hsa_circ_0103698, hsa_circ_0103701, hsa_circ_0103695, hsa_circ_0103697, hsa_circ_0103696, hsa_circ_0103700, hsa_circ_0103699, hsa_circ_0035125		
SEMA7A	hsa_circ_0036269		
		Slit1	mmu_circ_0000951, mmu_circ_0000951
SLIT2	hsa_circ_0008907, hsa_circ_0008907, hsa_circ_0007369, hsa_circ_0004638, hsa_circ_0008127, hsa_circ_0008864, hsa_circ_0008689, hsa_circ_0009113, hsa_circ_0002700, hsa_circ_0008407, hsa_circ_0069298, hsa_circ_0125983, hsa_circ_0125981, hsa_circ_0125982, hsa_circ_0125985, hsa_circ_0125984, hsa_circ_0069288, hsa_circ_0069295, hsa_circ_0069305, hsa_circ_0069312, hsa_circ_0069307, hsa_circ_0069296, hsa_circ_0069306, hsa_circ_0069308, hsa_circ_0069310, hsa_circ_0069290, hsa_circ_0069309, hsa_circ_0069311, hsa_circ_0069297, hsa_circ_0069286, hsa_circ_0069299, hsa_circ_0069300, hsa_circ_0069301, hsa_circ_0069293, hsa_circ_0069291, hsa_circ_0069302, hsa_circ_0069303, hsa_circ_0069304, hsa_circ_0069292, hsa_circ_0069294, hsa_circ_0069289	Slit2	mmu_circ_0012662, mmu_circ_0012662, mmu_circ_0012661, mmu_circ_0012664



SLIT3	hsa_circ_0128566, hsa_circ_0128566, hsa_circ_0128569, hsa_circ_0128567, hsa_circ_0128568, hsa_circ_0074932, hsa_circ_0074903, hsa_circ_0074928, hsa_circ_0074929, hsa_circ_0074931, hsa_circ_0074920, hsa_circ_0074917, hsa_circ_0074933, hsa_circ_0074915, hsa_circ_0074930, hsa_circ_0074921, hsa_circ_0074904, hsa_circ_0074922, hsa_circ_0074916, hsa_circ_0074905, hsa_circ_0074913, hsa_circ_0074906, hsa_circ_0074910, hsa_circ_0074927, hsa_circ_0074924, hsa_circ_0074914, hsa_circ_0074907, hsa_circ_0074918, hsa_circ_0074923, hsa_circ_0074925, hsa_circ_0074899, hsa_circ_0074919, hsa_circ_0074902, hsa_circ_0074926, hsa_circ_0074900, hsa_circ_0074911, hsa_circ_0074912, hsa_circ_0074908, hsa_circ_0074901	Slit3	mmu_circ_0002996, mmu_circ_0002996, mmu_circ_0002995, mmu_circ_0002994
UNC5A	hsa_circ_0128654, hsa_circ_0128654		
UNC5B	hsa_circ_0018682, hsa_circ_0018682		
UNC5C	hsa_circ_0127382, hsa_circ_0127382, hsa_circ_0127380, hsa_circ_0127383, hsa_circ_0127381, hsa_circ_0127379, hsa_circ_0127376, hsa_circ_0127366, hsa_circ_0127378, hsa_circ_0127377, hsa_circ_0127374, hsa_circ_0127367, hsa_circ_0127369, hsa_circ_0127368, hsa_circ_0127372, hsa_circ_0127375, hsa_circ_0127370, hsa_circ_0127371, hsa_circ_0070478	Unc5c	mmu_circ_0010496, mmu_circ_0010496, mmu_circ_0010497
UNC5D	hsa_circ_0136452, hsa_circ_0136452, hsa_circ_0136451, hsa_circ_0136436, hsa_circ_0136445, hsa_circ_0136444, hsa_circ_0136450, hsa_circ_0136443, hsa_circ_0136438, hsa_circ_0136446, hsa_circ_0136441, hsa_circ_0136448, hsa_circ_0136449, hsa_circ_0136440, hsa_circ_0136447, hsa_circ_0136431, hsa_circ_0136432, hsa_circ_0136442, hsa_circ_0136433, hsa_circ_0136437, hsa_circ_0136426, hsa_circ_0136434, hsa_circ_0136423, hsa_circ_0136428, hsa_circ_0136419, hsa_circ_0136435, hsa_circ_0136422, hsa_circ_0136420, hsa_circ_0136424, hsa_circ_0136427, hsa_circ_0136430, hsa_circ_0136425, hsa_circ_0136421, hsa_circ_0136429, hsa_circ_0083913, hsa_circ_0083914, hsa_circ_0083923, hsa_circ_0083915, hsa_circ_0083918, hsa_circ_0083916, hsa_circ_0083924, hsa_circ_0083925, hsa_circ_0083921, hsa_circ_0083919, hsa_circ_0083917, hsa_circ_0083922, hsa_circ_0083920	Unc5d	mmu_circ_0014765, mmu_circ_0014765, mmu_circ_0014766, mmu_circ_0014767





Characterization of the spatiotemporal expression of axon guidance circRNAs in the developing mouse brain using *in situ* hybridization

Daniëlle van Rossum¹, N. Solée Pop¹, Lance Fredrick Pahutan Bosch¹ and R. Jeroen Pasterkamp¹

¹ Department of Translational Neuroscience, UMC Utrecht Brain Center, University Medical Center Utrecht, Utrecht University, Utrecht 3584 CG, the Netherlands

'Single sun in situ' - Photo taken during a memorable labouting on Terschelling in 2017.

ABSTRACT

In situ hybridization (ISH) is a powerful technique that can be used to get a better understanding of the spatio-temporal expression of RNAs. Over the past years various ISH techniques have been developed to specifically label and detect circRNAs *in vitro* and *in vivo*. In this study, we discuss available ISH techniques for the detection of circRNAs, covering their advantages and disadvantages. Using ViewRNA we were able to create an overview of the spatiotemporal expression of selected axon guidance circRNAs in primary cortical neurons. This overview revealed that the expression levels and cellular localization of selected axon guidance circRNAs are dynamic and vary during neuronal maturation. Moreover, the axon guidance circRNAs investigated were predominantly expressed in excitatory neurons, with no expression in glial cells. These findings serve as a meaningful starting point from which to conduct further studies on the functionality of axon guidance circRNAs.

INTRODUCTION

Circular RNAs (circRNAs) are a novel type of non-coding RNA with a dynamic spatiotemporal expression in the mammalian brain. Although several techniques have been developed to detect RNA molecules by single-molecule *in situ* hybridization (smISH) approaches, the detection of circRNAs by smISH is often more challenging due to their unique structural characteristics. First, with few exceptions, circRNAs are expressed at low levels and consequently ISH signals are weak relative to their linear mRNA counterparts. Optimal signal-to-noise ratios are important for detecting circRNAs and can be achieved by reducing non-specific background staining. Second, as circRNA probes must include their unique back-splice junctions to avoid amplification of their linear counterparts, the combination of sequences available for probe design is limited¹⁻³. Different smISH techniques have been optimized to reduce these limitations in circRNA detection, including (a) employing a modified nucleic acid probe design with increased affinity and specificity, (b) using signal amplification through the application of enzymatic reactions or chemical amplification like branched DNA (bDNA) technology, (c) enzymatic pre-treatment of tissue including proteinase to better expose the back-splice sequence and (d) RNase R treatment to remove linear RNA. However, most protocols for the detection of circRNAs with smISH require extensive optimization.

The detection of single circRNA molecules with ISH can roughly be divided into two categories: (1) assays in which probes are directly coupled to fluorophores (e.g. Stellaris, labelled oligos) or (2) assays that rely on signal amplification and subsequent labeling of the probe (e.g. ViewRNA, BaseScope)⁴⁻⁸. The available single molecule (and fluorescent (F)) ISH approaches to detect circRNAs have specific advantages and limitations which must be considered in relation to a number of factors (Table 1). These factors include, but are not limited to: (a) the nature of the circRNA (e.g. circRNA expression levels, relative expression of linear RNA counterparts); (b) the nature of the study (e.g. chromogenic versus fluorescent; options for multiplexing); and (c) the pricing of different kits and probes. For example, Stellaris RNA FISH uses multiple short DNA oligonucleotide probes that hybridize with their complementary RNA molecules⁹. However, because of possible off-target effects, Stellaris probes can only be used for circRNAs that do not have linear counterparts and is therefore unsuitable for the detection of axon guidance circRNAs, which do have linear host gene expression.

Table 1 | Overview of different ISH techniques for the detection of circRNAs and their (dis)advantages

	Technique Advantage	Disadvantage
BaseScope	<ul style="list-style-type: none"> Single molecule detection Signal amplification with branched DNA technology Can be applied on a wide range of tissues following treatment with different fixatives Sensitive assay 	<ul style="list-style-type: none"> Chromogenic 1-plex assay Expensive probes
ViewRNA	<ul style="list-style-type: none"> Single molecule detection Signal amplification with branched DNA technology Multiplexing possible Possible to combine with immunostaining 	<ul style="list-style-type: none"> Unreliable on tissue Not clear which kit works best for which purpose Low sensitivity
Stellaris	<ul style="list-style-type: none"> High signal-to-noise ration Multiplexing possible Use of probesets 	<ul style="list-style-type: none"> Only for circRNAs that have no linear transcripts Needs very sensitive imaging techniques

So far, the expression of axon guidance circRNAs using ISH has not been described. In this study we report on the spatiotemporal expression of selected axon guidance circRNAs in primary cortical neuron using the ViewRNA assay. We observed that the expression levels and cellular localization of selected axon guidance circRNAs change throughout neuronal maturation. In line with previous reports on circRNA localization, we noted that axon guidance circRNAs are not expressed in glia and that they are predominantly expressed in excitatory neurons. The observed specific expression patterns serve as a foundation for possible future investigations on the functionality of axon guidance circRNAs.

RESULTS

CiRS-7 can be detected with BaseScope in mouse brain tissue

CiRS-7 (Cerebellar Degeneration-Related Protein 1 Anti-sense circular RNA sponge for microRNA-7) is stably expressed in the mouse brain, but in contrast to many other circRNAs, ciRS-7 is an antisense transcript that does not exist as a linear RNA form. Because of these characteristics we chose to use ciRS-7 to set up and test various smISH techniques and kits before continuing with our own selection of candidates. Using BaseScope technology, a robust ISH assay that allows for the detection of single circRNA molecules in a chromogenic assay, we confirmed the widespread expression of ciRS-7 in the adult mouse brain (Figures 1A-C). This finding is in line with previous reports on the expression of ciRS-7 (Piwecka et al., 2017).

Axon guidance circRNAs cannot be detected *in vivo* using ViewRNA

Given that BaseScope probes can only be used in a chromogenic assay, they do not allow multiplexing with other mRNAs and/or circRNAs, and are expensive, we decided to continue our analysis with a non-chromogenic assay, ViewRNA (Figure 1A). After performing ViewRNA on sections of the adult mouse brain, we observed that ciRS-7 is mainly expressed in the granule cell layer of the cerebellum of the mouse brain, while the mRNA *Actb* is observed mostly in the Purkinje cell layer. To determine whether the expression of ciRS-7 is developmentally regulated in the brain, we profiled the expression of ciRS-7 at several stages of mouse-brain development: embryonic day 15 (E15) (formation of cortex/hippocampus); embryonic day 18 (E18) (around birth); post-natal day 5 (P5)

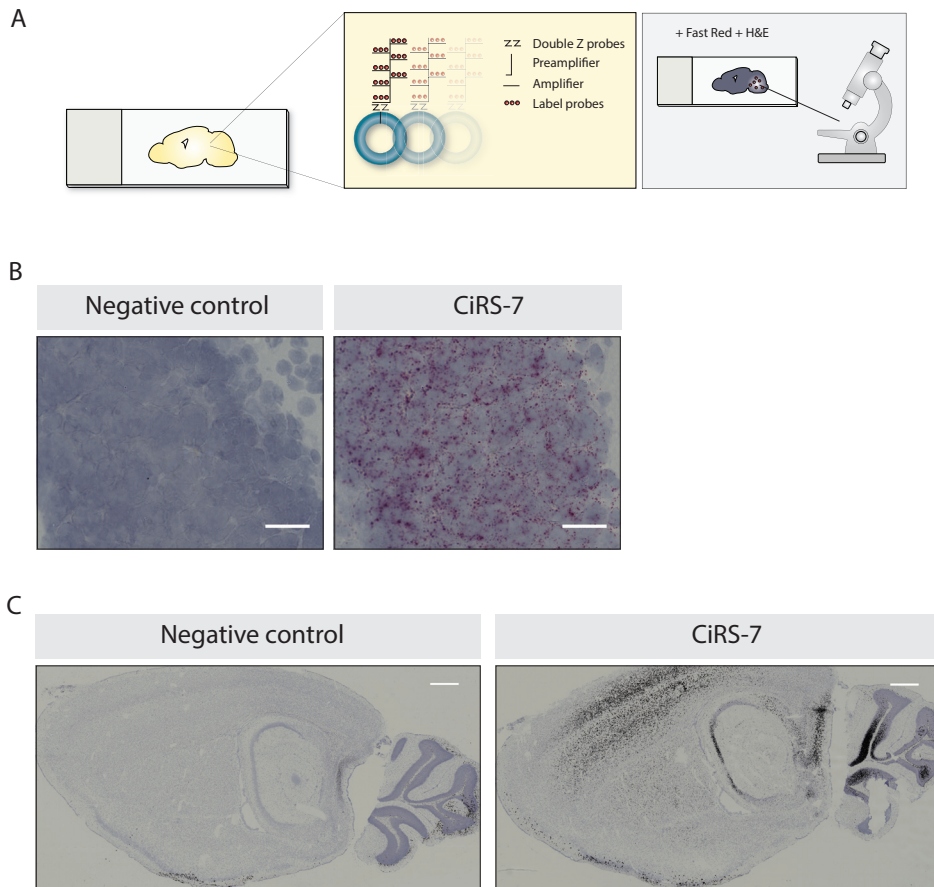
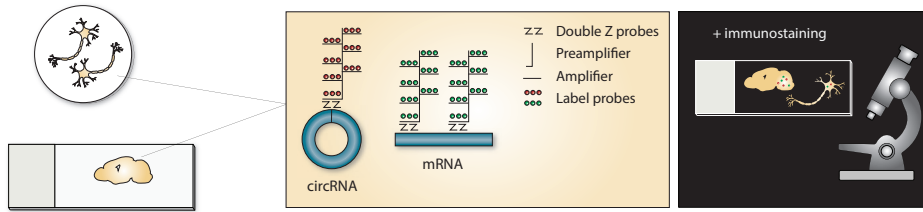


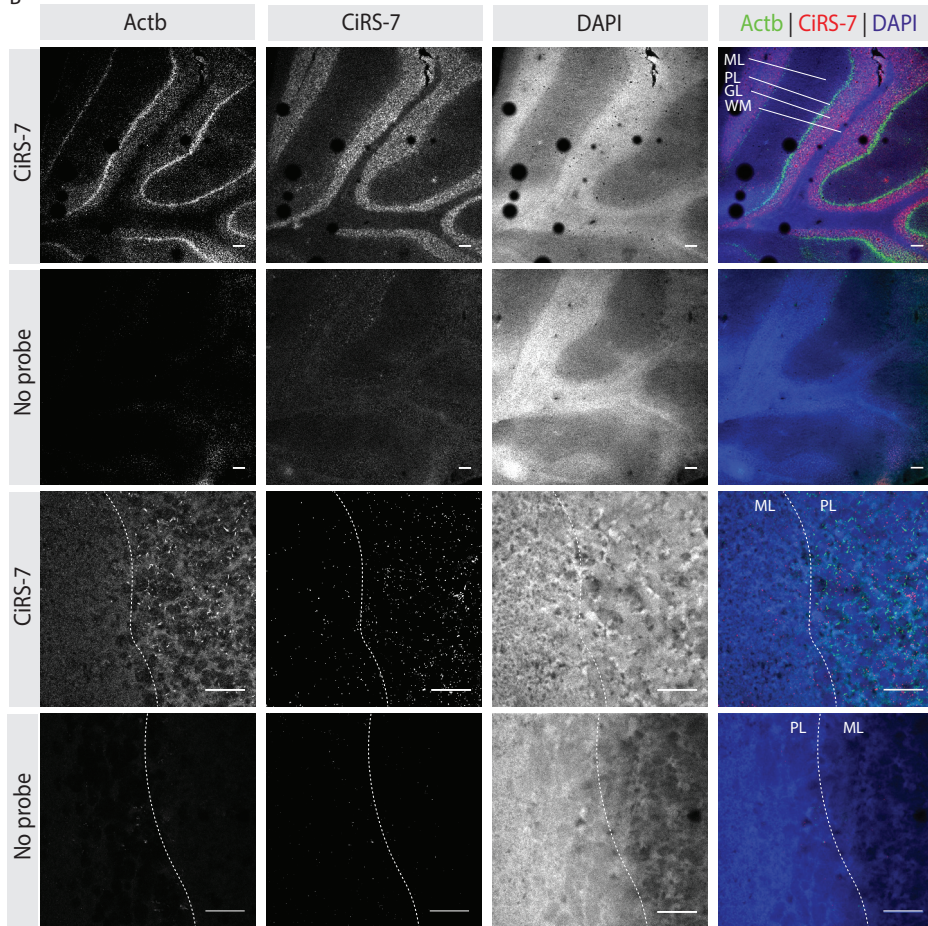
Figure 1 | BaseScope ISH assay for the detection of circRNAs.

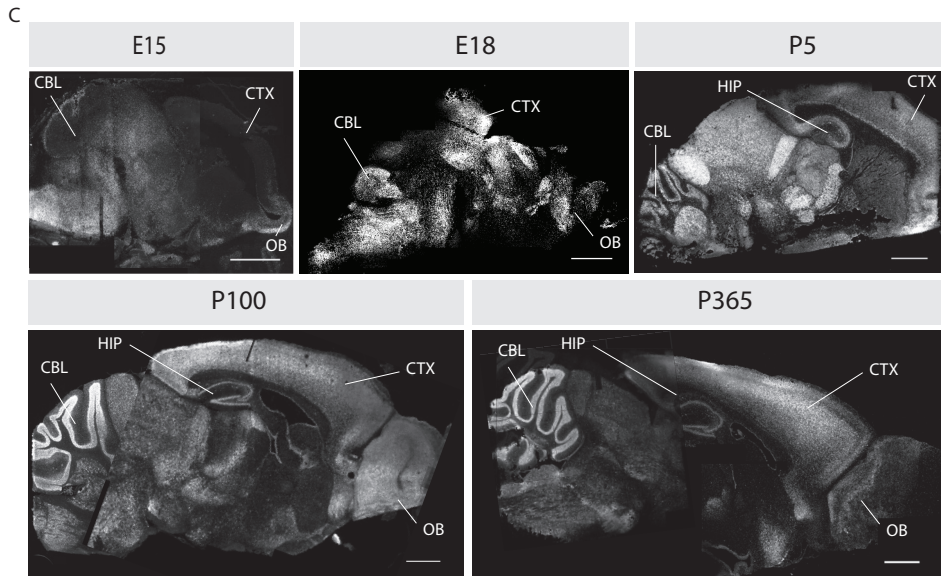
(A) Schematic representation of the BaseScope assay. BaseScope assays are (1-plex) chromogenic ISH assays that allow detection of single circRNA molecules. The assay uses two adjacent Z-probes with 18-23 nucleotides complementary sequence to the termini of the circularized exon(s). Following binding of the probes to the target sequence, branched DNA (bDNA) technology is used for signal amplification and for increasing the signal-to-noise ratio. In a subsequent step, an alkaline phosphatase-labeled probe binds the amplified molecules. Alkaline phosphatase converts Fast-Red into a precipitate that marks the spatial localization of the circRNA. Before imaging, the tissue is subjected to a Hematoxylin staining to facilitate anatomical/spatial orientation. (B) Using the BaseScope assay on sagittal mouse brain sections (P100) reveals the expression of ciRS-7 in the granular cell layer of the cerebellum. The negative control is a probe against the soil bacterium *Bacillus subtilis* gene *DapB*. Scale = 500 μm . (C) Using the BaseScope assay on sagittal mouse brain (P100) reveals the broad expression of ciRS-7 in the mouse brain. Scale = 2 mm. The Fast-Red precipitates are represented in a black color. Theoretically one dot = one circRNA.

A



B





2

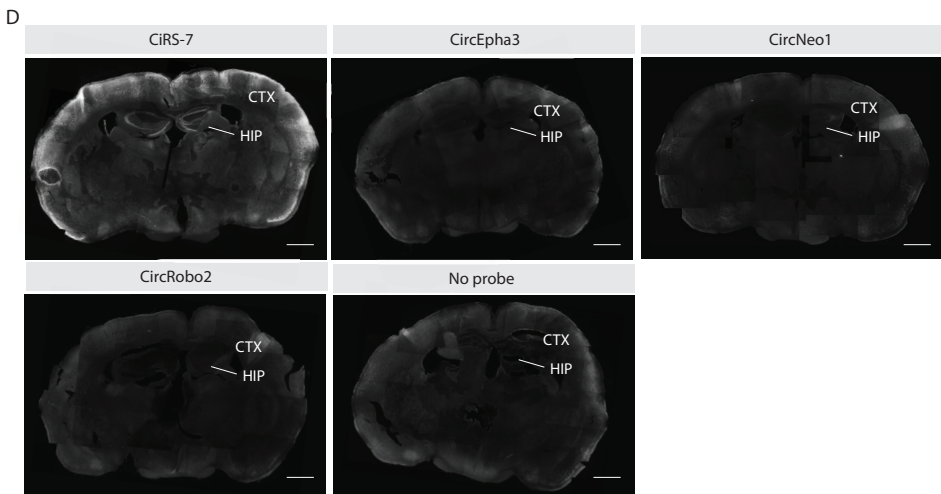


Figure 2 | ViewRNA FISH assay for the detection of circRNAs.

(A) Schematic representation of the ViewRNA assay. The ViewRNA assay relies on a 40-60 nucleotide probe targeting the unique back-splice junction of circRNAs. After sequential steps of hybridization, signal amplification can be achieved using bDNA technology. Label probes conjugated to alkaline phosphatase hybridize to the amplified molecules (containing 400 binding sites for this probe). Alkaline phosphatase converts Fast-Red into a precipitate that marks the spatial localization of the circRNA. Using ViewRNA, multiplexing with mRNAs is possible. The assay can be used in combination with an immunostaining protocol before imaging. (B) CircRNA- and mRNA probes can be multiplexed in tissue using the ViewRNA assay. *CIRS-7* is mainly expressed in the granular layers of the cerebellum, while the mRNA *Actb* is observed mostly in the purkinje layers. Sagittal sections. Scale upper two panels = 100 μ m; lower two panels = 25 μ m. (C) *CIRS-7* is abundantly and dynamically expressed in the developing mouse brain. Scale = 1 mm. (D) ViewRNA is a very sensitive assay, not all circRNAs can be easily detected in mouse brain tissue. Coronal sections (P414). Scale = 1 mm. ML = Molecular Layer; PL = Purkinje Layer; GL = Granular Layer; WM = White Matter; CTX = Cortex; HIP = Hippocampus; CBL = Cerebellum; OB = Olfactory bulb.

.....

(early postnatal); P100 (young adult) and P365 (adult). In line with previous reports, we observed that *ciRS-7* is expressed abundantly and broadly throughout the mouse brain (Figure 2C). At E15 the expression of *ciRS-7* is most abundant in the spinal cord, hindbrain and the olfactory bulb. As the brain develops embryonically, the hindbrain continues to highly express *ciRS-7*, especially in the cerebellum, but also more rostrally. From P5 onwards *ciRS-7* appears to be expressed globally throughout the brain. Although this widespread expression remains in adulthood, at P100 the *ciRS-7* expression is especially strong within the cerebral cortex, structures in the midbrain, the pyramidal cells in the hippocampus and the granular layers of the cerebellum.

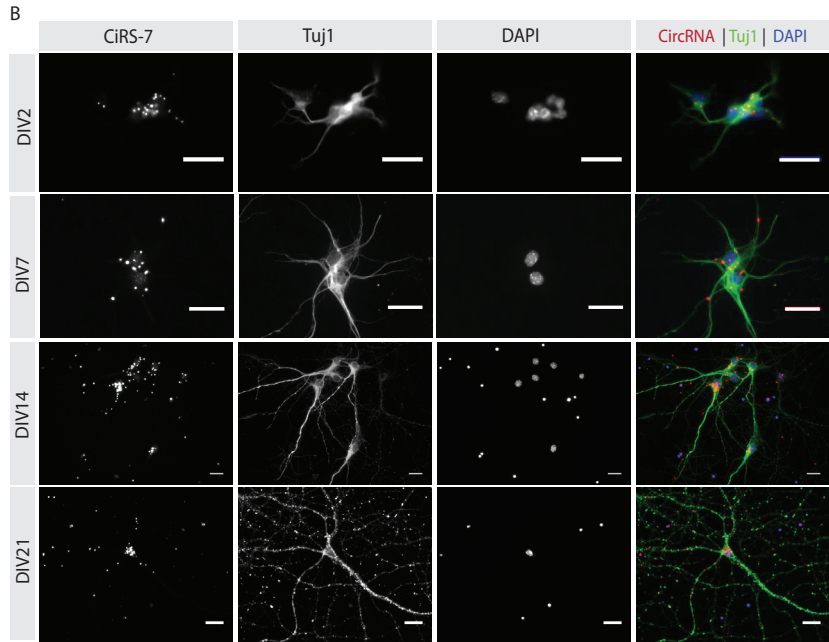
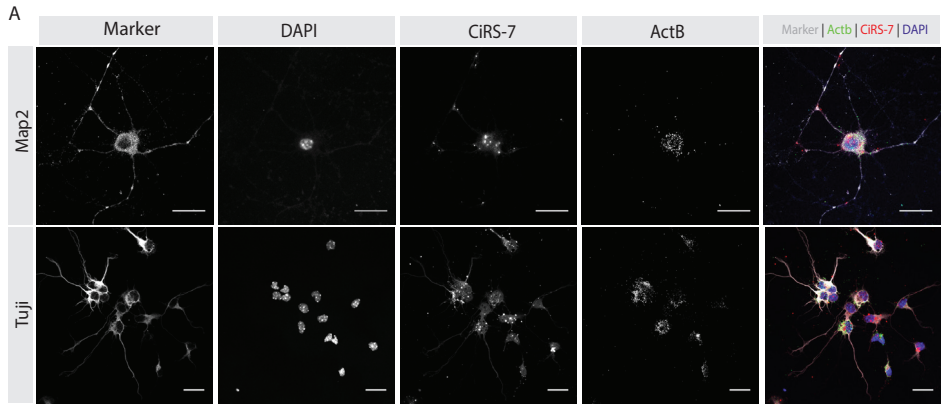
After we successfully examined expression of *ciRS-7* during mouse brain development, we attempted to perform a similar analysis for our axon guidance circRNAs of interest. These circRNAs were selected based on their conservation across species, high neuronal expression and dynamic spatiotemporal expression pattern (Chapter 1). Unfortunately, these axon guidance circRNAs could not be specifically detected using ViewRNA in mouse brain tissue in our hands despite an extensive optimization process (e.g. different tissue treatments (fresh frozen or fixed (different duration and fixation with various amounts of ((RNase-free) PFA/NBF)), cut with cryostat or vibratome, free-floating or on glass slides, different types and durations of permeabilizations), different kits (e.g. miRNA kit, Cell kit, CellPlus kit, Tissue kit)) different reagent and probe concentrations and various experimental conditions (different machines, incubation times, temperatures)) (Figure 2D).

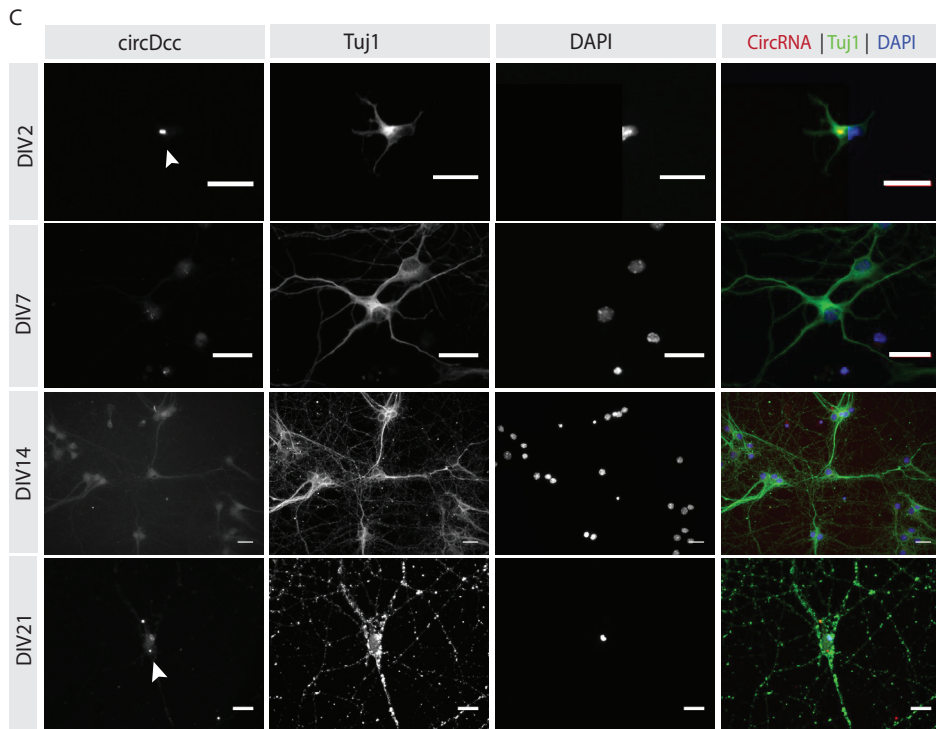
Axon guidance circRNAs are expressed in a specific spatio-temporal manner *in vitro*

Given that the ViewRNA assay allows the combination of immunocytochemistry and smFISH, we were able to clarify the spatial expression of ciRS-7 *in vitro* using certain antibodies. We confirmed that ciRS-7 can be detected *in vitro* and that ciRS-7 is expressed mostly in the cell body, and to a lesser extent in neurites of primary cortical neurons (PCNs) (Figures 3A and 3B). This is in line with previous studies that reported that, on average, circRNAs have a preferential cytoplasmic localization and are more enriched in synaptic processes^{6,11}.

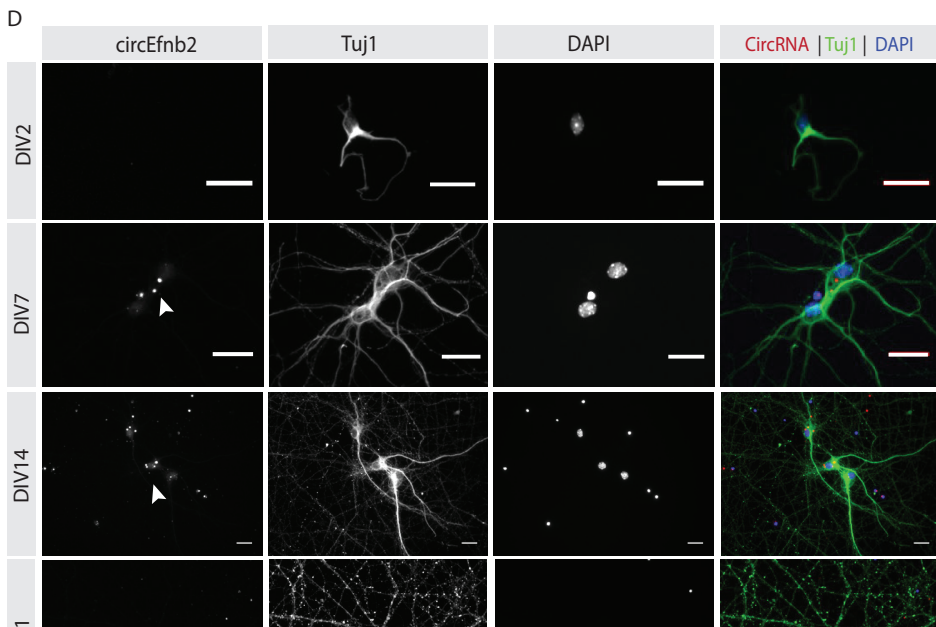
Next, we explored whether we could determine the level of expression and distribution of circular axon guidance transcripts in single cells using ViewRNA. To profile the expression of circDcc, circEfnb2, circEpha3, circNeo1, circPlxnc1, circRobo1 and circRobo2 at different stages of neuronal development and maturation, we chose the following timepoints: 2 days *in vitro* (DIV2; i.e. formation of neurites); DIV7 (i.e. branching); DIV14 (i.e. synapse maturation); DIV21 (i.e. neuronal maturation) (Figures 3 C-J). Notably, all axon guidance circRNAs were expressed at a substantially lower level than ciRS-7 at all timepoints (Figure 3K). The expression of circDcc and circRobo1 remained relatively constant during the maturation of the neurons. Other circRNAs, like circEfnb2 and circEpha3, were expressed more dynamically and slightly accumulated over time. CircPlxnc1 was barely detected, either due to its low expression or insensitivity of the assay. Off note, we also observed a lot of false positive signals in the samples, mainly in the nucleus of cells or in cell debris (indicated by the red arrows).

Interestingly, we observed that circRNA expression was not uniform between the PCNs (Figure 3L). It is known that circRNAs, and especially ciRS-7, are predominantly expressed in excitatory neurons^{10,6}. Therefore, we investigated whether our population of primary neurons consisted of different cell types that may express different levels of circRNA. We cultured PCNs (DIV5) and stained them for excitatory (PV; VGAT) and inhibitory (VGLUT1; VGLUT2) cell makers. The culture was found to consist of excitatory neurons exclusively; all neurons were positive for excitatory and not for inhibitory markers (Figure 3M). In line with existing literature, we also confirmed that the selected circRNAs are not expressed in glia because we could not detect signals in GFAP-positive astrocytes (Figure 3N)⁶. Lastly, to confirm the finding that circRNAs and their corresponding mRNAs often do not colocalize, we multiplexed Epha3 circular and linear probes in a ViewRNA assay but were unable to obtain specific results (Figure 3O)⁶.

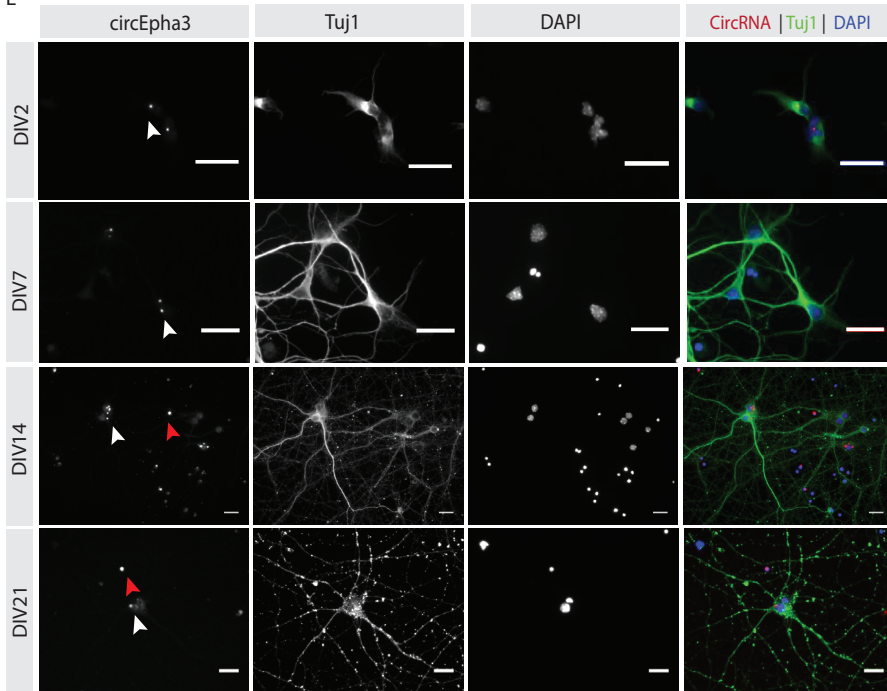




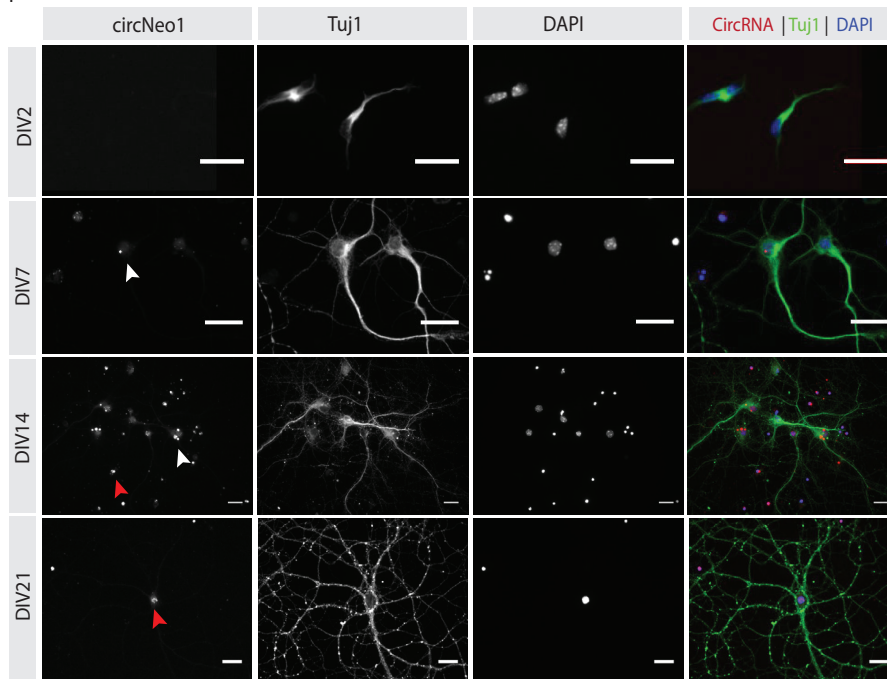
2

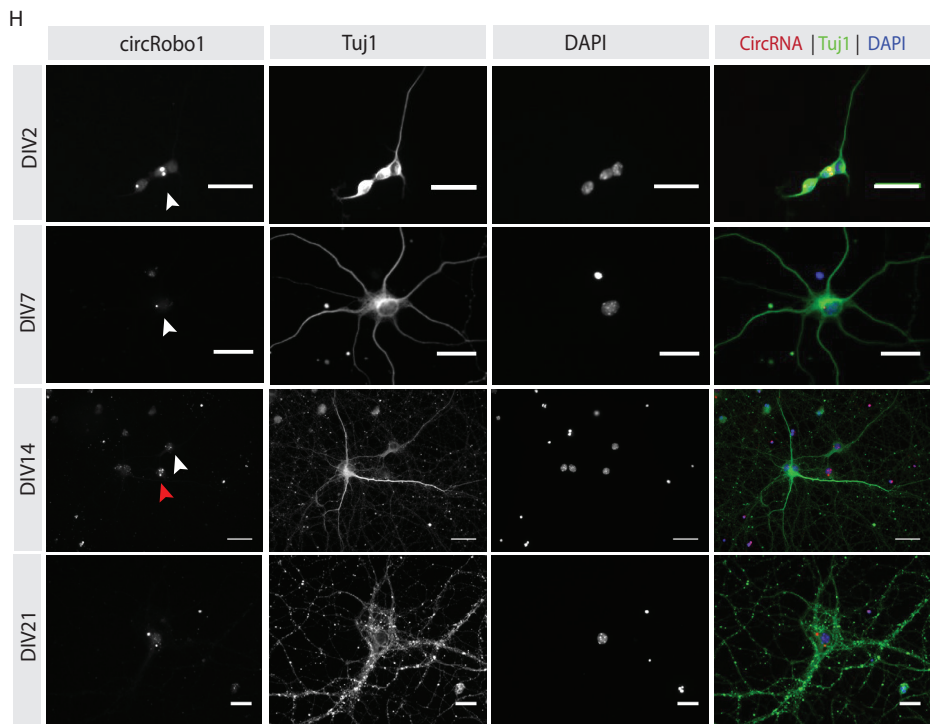
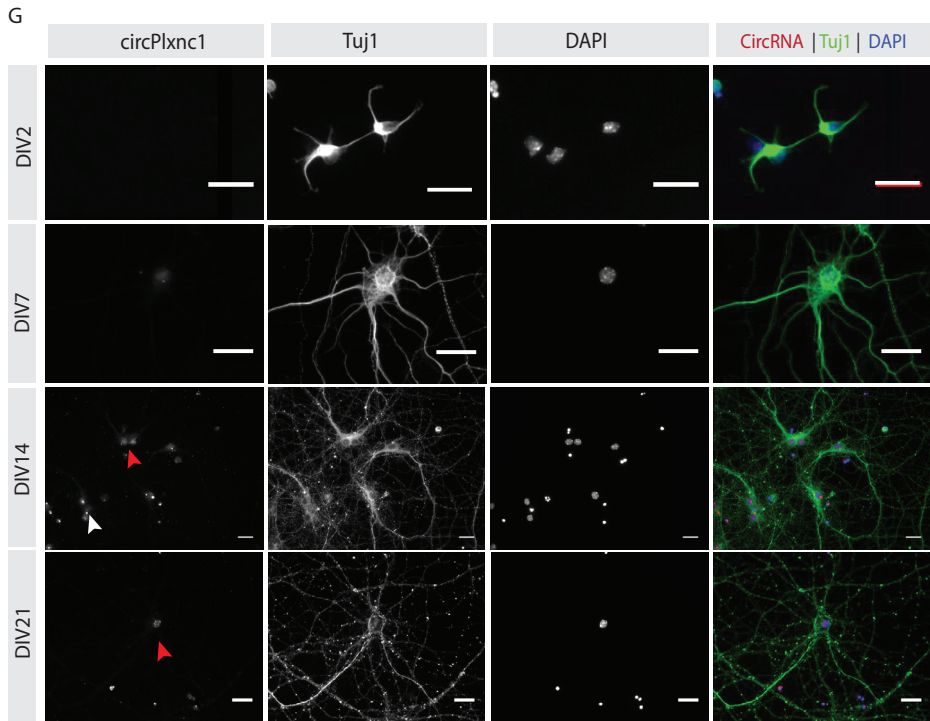


E

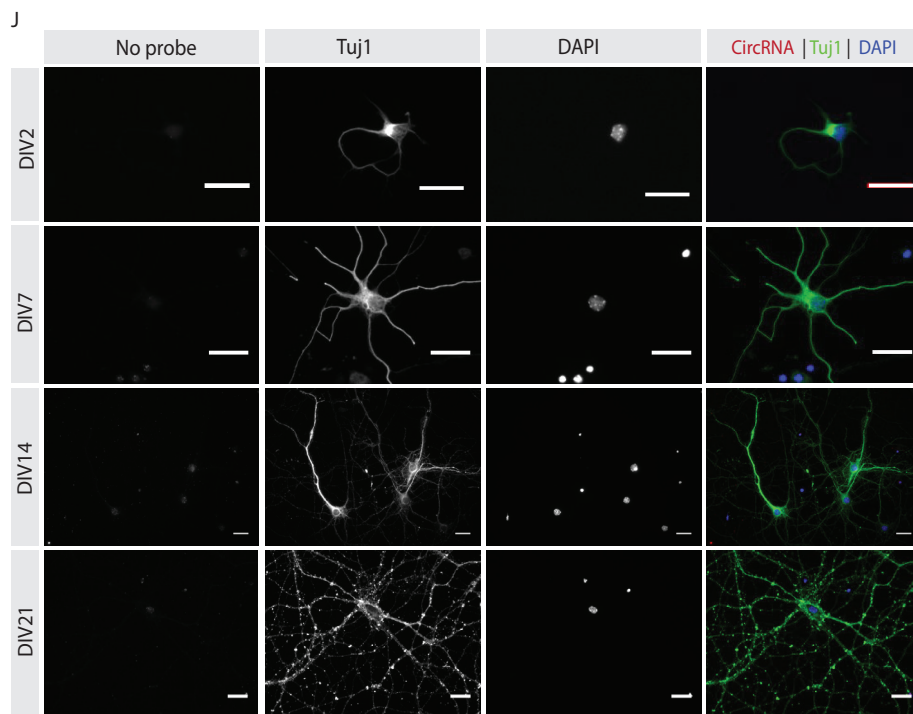
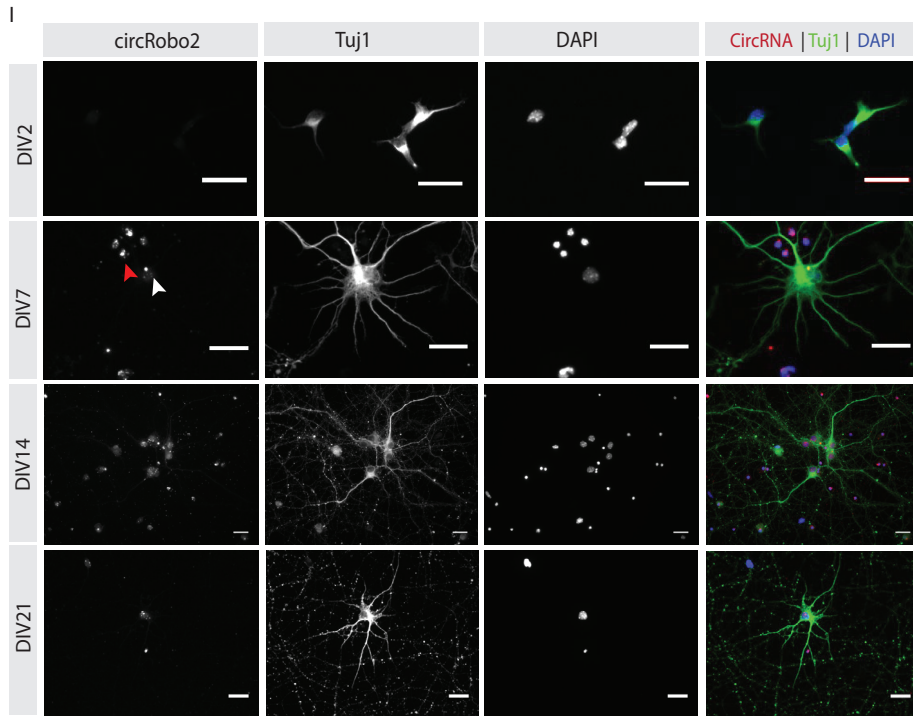


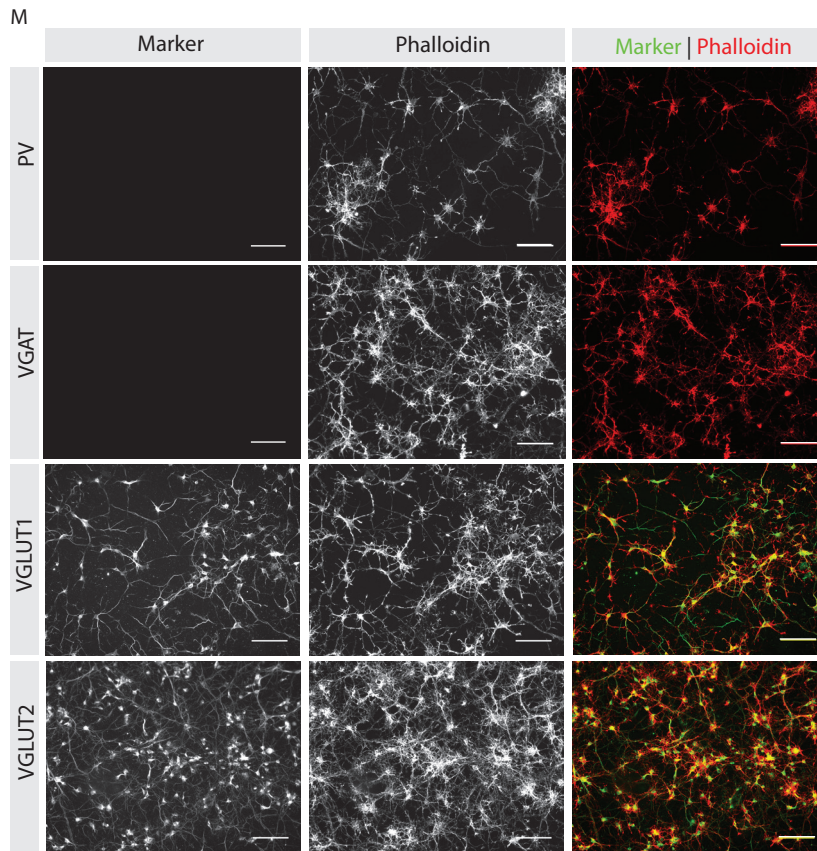
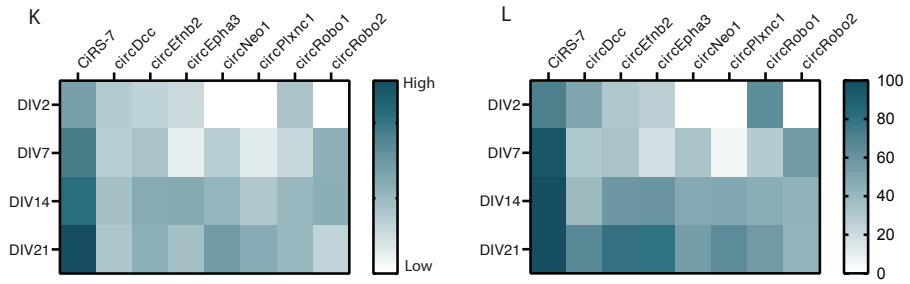
F





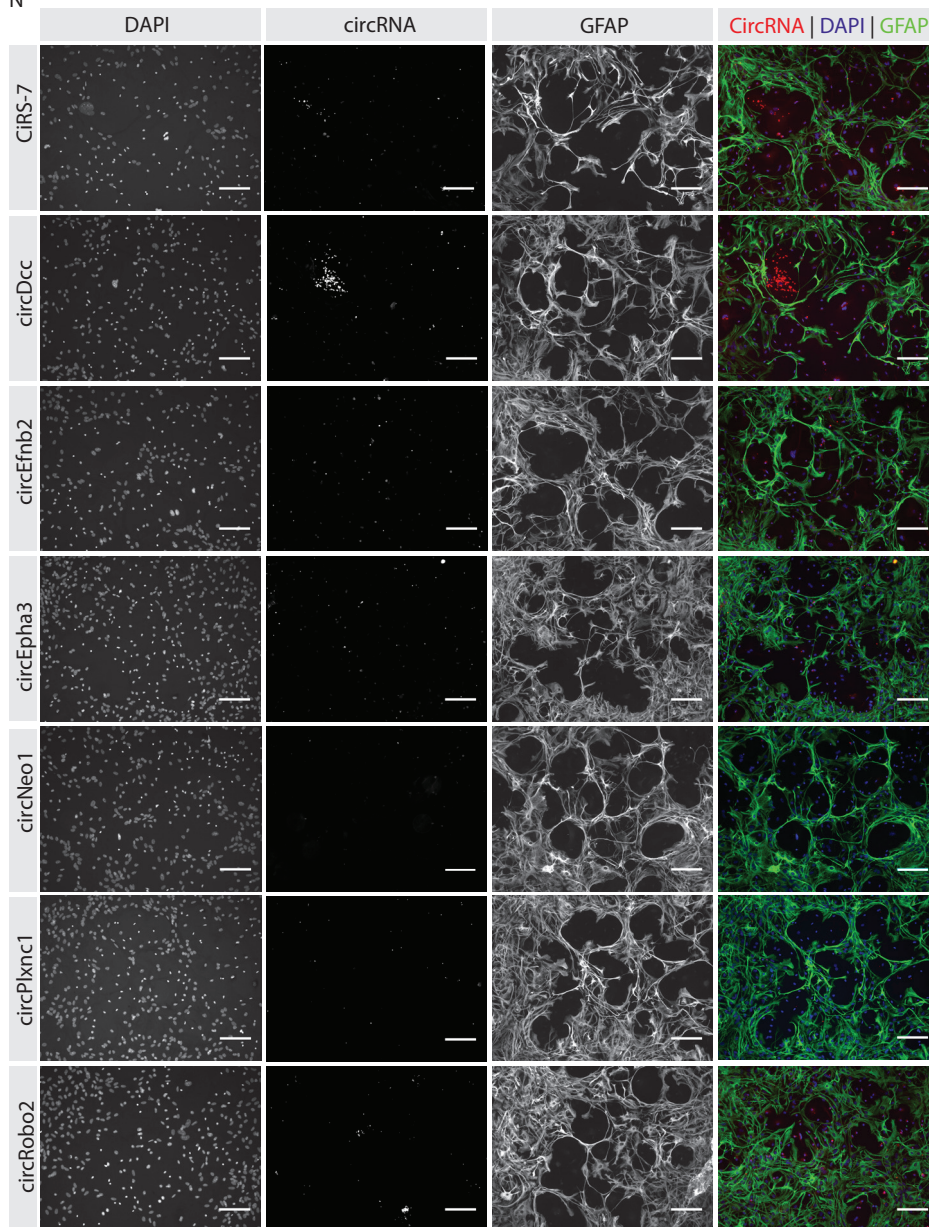
2





2

N



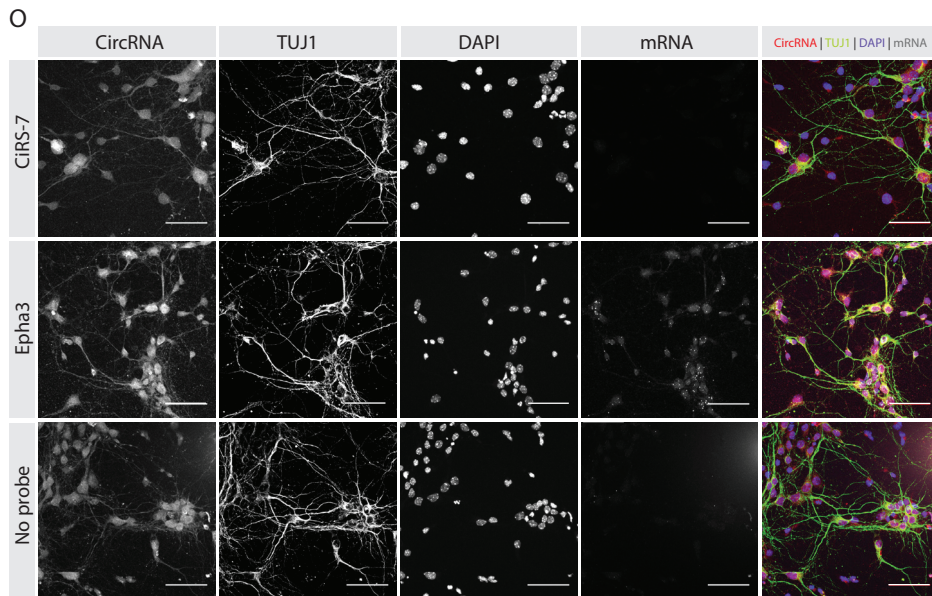


Figure 3 | Axon guidance circRNA expression during neuronal maturation using ViewRNA. (A) CircRNAs can be detected with ViewRNA in primary cortical neurons (upper panel DIV21, lower panel DIV7), multiplexed with a mRNA probe (*Actb*) and combined with immunostainings (*Map2*, *Tuj1*). Scale = 25 μm . Representative images of subcellular localization of axon guidance circRNAs was visualized using ViewRNA in primary cortical neurons (PCN) DIV2, DIV 7, DIV14 and DIV21 for *ciRS-7* (B), *circDcc* (C), *circEfnb2* (D), *circEpha3* (E), *circNeo1* (F), *circPlxnc1* (G), *circRobo1* (H), *circRobo2* (I) and no probe control (J). Scale = 25 μm . (K) Heatmap of the average expression of axon guidance circRNAs per neuron ($n = 30$). (L) Heatmap of the percentage of PCNs that contain circRNAs. (M) Primary cortical neurons (DIV5) are excitatory and not inhibitory. Scale = 100 μm . (N) Axon guidance circRNAs are not expressed in GFAP-positive astrocytes. Scale = 100 μm . (O) The co-expression of *Epha3* circRNA and *Epha3* mRNA with ViewRNA is not very efficient. Scale = 50 μm .

DISCUSSION

Successful ISH assays can provide a better understanding of the spatiotemporal expression of circRNAs. Over the years different ISH techniques and kits have been developed to label and detect circRNAs *in vitro* and *in vivo*. Unfortunately, there is no gold standard for sm(F)ISH circRNA detection yet and choosing the most suited assay is therefore essential. For example, in our experience the ViewRNA assay was less sensitive compared to BaseScope technology, especially for weakly expressed circRNAs. After

choosing a certain technique, protocols required extensive optimization depending on the specific circRNA target and type of tissue. This is illustrated by the finding that we were able to detect ciRS-7 adequately in mouse brain tissue, while other tested circRNAs did not reach a sufficient detection level *in vivo*, even though these circRNAs were detected *in vitro*. The observed variability between and within the various assays raises the question whether the observed signal is specific and whether single molecule quantification can be considered reliable. Increasing probe specificity and reducing background noise during the assay could improve reliability, while enhancing signal strength could improve signal detection sensitivity. Altogether, ISH can be seen as a valuable tool for circRNA localization purposes, but whether it is a reliable and quantitative tool for studying circRNA levels remains arguable.

The various sm(F)ISH assays all come with their own advantages and disadvantages. One of the interesting features of the ViewRNA assay is the possibility of combining immunochemistry with smFISH before ISH (using the ViewRNA cell plus kit) or after ISH (using the ViewRNA miRNA kit). Although the latter protocol worked best in our hands, we observed that not all antibodies are compatible with the stringent hybridization conditions that are required during the assay (e.g. immunostainings with Alexa-conjugated antibodies were not successful). A large advantage of the ViewRNA assay is that it allows multiplexing. CircRNAs can be detected with a probe type that corresponds to a certain fluorophore (e.g. type 1; AF568), while an mRNAs can have a probe type corresponding to a different fluorophore (e.g. type 4; AF488). This allows the detection and discrimination of the two different signals within one sample. However, probes for circRNAs and miRNAs are both only available in type 1 probes, meaning that they cannot be multiplexed within one sample. This could be a disadvantage, since circRNAs and miRNA have been reported to interact and are therefore interesting candidates for co-localization studies. Multiplexing between circRNA and mRNA should be possible with ViewRNA because of their different probe types. In our hands multiplexing of ciRS-7 and the mRNA *Actb* worked well, but multiplexing with relatively lowly expressed circRNAs and mRNAs (e.g. (circ)*Epha3*) was not possible. We conclude that ViewRNA is not sensitive enough for weakly expressed circRNAs, especially for detection in tissue.

Besides the nature of the assay, other factors could play a role in the detection limit of certain circRNAs. The back-splice junction is the only sequence that can be targeted for circRNA detection, which limits probe design and can result in suboptimal probe

specificity. Also, RNA degradation, secondary structure formation, RBP binding or packaging of circRNAs in RNA granules could prevent probe binding and reduce signal strength¹². Hence, not all circRNA molecules may be detected. Moreover, fixation is critical for successful sm(F)ISH. Fixatives will cross-link cellular structures and link sections/cells to the coverslips which is necessary to perform the ISH assay, while prolonged fixation could mask the circRNA probe site and increase background signal. In spite of using different ViewRNA kits (ViewRNA cell assay kit, ViewRNA cell PLUS assay kit, ViewRNA miRNA cell assay kit, ViewRNA cell TISSUE kit) and testing various optimization steps in the protocol in terms of fixation, cross-linking, permeabilization and incubation (e.g. type, temperature and duration), most of our efforts failed to facilitate proper circRNA detection in tissue sections. Whether these problems could be ascribed to the level of circRNA expression, test conditions or the quality of the kits remains unresolved.

BaseScope and ViewRNA are described as single molecule ISH techniques, but in practice these methods are not perfectly quantitative. For example, the efficiency of the BaseScope circRNA probe is stated to be around 15-20% compared to conventional mRNA probes, depending on how fresh the experimental tissue is. This means that circRNAs that are expressed at < 5-10 molecules per cell are difficult to detect. Another problem to consider is that the signal-to-noise ratio of each probe and each sample is different. For example, the use of FFPE tissue generally gives rise to more background signal as compared to freshly frozen tissue. Etching of glass coverslips will increase signal strength, but certain coatings are known to increase unspecific probe binding resulting in more background fluorescence. For labelled probes, signal-to-noise ratio should ideally be at least 2 while for ViewRNA the ratio should be >3 for mRNAs and > 8 for circRNAs¹³. Moreover, the most optimal method for interpreting and quantifying smFISH data is still a matter of debate. We decided to do our quantitative analysis by hand (Figures 3K and 3L), but for certain analyses software is available that can aid quantification, such as StarSearch and ImageM^{13,14}.

Using ViewRNA, we established that axon guidance circRNAs are expressed in excitatory primary cortical neurons. During neuronal maturation, we observed that the expression of axon guidance circRNA tends to increase. This is in line with previous studies that report the accumulation of circRNAs in time *in vitro* and *in vivo*¹⁵ (Chapter 1). Whether axon guidance circRNAs accumulate due to low turnover in these neurons (e.g. they are not degraded by cellular machinery) or because they have a specific function in neuronal

maturation remains to be elucidated. So far we only tested the different sm(F)ISH assays in mouse brain tissue. It would be interesting to also investigate the spatiotemporal expression of axon guidance circRNA in human (*post mortem*) tissue. Based on our expression analysis in PCNs, we can conclude that axon guidance circRNA expression is mainly cytoplasmic. This is not unexpected as most circRNAs have been reported to be located in the cytoplasm^{16,17}.

The notion that circRNAs are not expressed in glia supports a neuron-specific function of axon guidance circRNAs. However, it is difficult to speculate on axon guidance circRNA function based on their spatiotemporal expression because the detected axon guidance circRNA signal was relatively weak in most samples. Either axon guidance circRNAs were not very highly expressed in our samples, or the ViewRNA assay failed to detect them. Future investigations are needed to examine whether circRNA expression is affected by/dependent on glia-neuron interactions. Notably, in PCNs the expression of selected axon guidance circRNAs was higher in the soma than in dendrites, with a small increase in neurites during neuronal maturation. A clear localization of these circRNAs to growth cones or synapses, which could suggest a role in axon guidance, could not be observed. Because the expression of some circRNAs (e.g. circEfnb2 and circNeo1) increases during neuronal maturation and because they are expressed in excitatory cortical neurons, it is interesting to speculate that they play a role in neurite/synapse formation and/or cellular communication. For most circRNAs, age-dependent accumulation is not as clear as observed for ciRS-7.

In summary, sm(F)ISH techniques can be used to investigate the spatiotemporal expression of circRNAs in mice, but most of the assays require further optimization and/or improvement for robust and reliable detection of (axon guidance) circRNAs. Improved spatiotemporal expression data in different model systems, both *in vitro* or *in vivo*, will aid the quest of finding a functional role for axon guidance circRNAs.

MATERIALS AND METHODS

Ethics statement

All animal experiments were performed in accordance to and approved by the CCD (Central Committee for animal research, The Netherlands), the University Medical Center Utrecht, the Dutch Law (Wet op Dierproeven 1996) and European regulation (Guideline 86/609/EEC)

Cell culture

Primary cortical neurons

Primary cortical neurons (PCNs) were cultured on coverslips (VWR, 18Ø) in 12-well plates (Costar 3513/3524). Coverslips were etched in 1 N HCl (Emsure) for 1 hour at 65 °C and washed and stored in 100% EtOH (Emsure). The coverslips were coated with 20 µg/ml Poly-D-Lysine-ornithine (Sigma Aldrich) solution for 30 minutes at room temperature (RT), washed with sterile PBS [1x] (Gibco) and coated with 40 µg/ml Laminin (Gibco) for 1 hour at 37 °C. The wells/coverslips were washed with sterile PBS [1x] (Gibco) and used immediately to plate cells. PCNs were prepared from 14 days old C57/BL6 mouse embryos (E14). The embryos were removed from the uterus and collected in Leibovitz's L-15 medium (Gibco). Cortices were separated and the meninges were removed before. The tissue was dissociated in 2.5% trypsin for 15 minutes at 37 °C. Following trypsinization, the supernatant was removed and dissociation medium added, consisting of 10% Fetal Bovine Serum (FBS) (Gibco), 0.2% DNase (0.01 2 mg/ml, Roche) in Leibovitz's L-15 medium (Gibco). The cells were triturated in the dissociation medium with a 200 µl pipette before being spun down for 1 minute at RT (IKA miniG). The supernatant was removed and the cells were resuspended in 1 ml Neurobasal Culture Medium (NB+) (Gibco) supplemented with 2% B27 (50x) (Gibco); 0.1% Pen/Strep (10 kU/ml Pen; 10 mg/ml Strep, Gibco); 0.1% Glutamine (Gibco); 5% 400 nm D-Glucose (Sigma Aldrich). Cells were plated on coated coverslips placed in 12-well plates. Cells were cultured for 2, 5, 7, 14 or 21 days *in vitro* (DIV) at 37 °C in a humidified incubator with 5% CO₂ with half the medium changed every week.

2

Glia

Primary hippocampal glia were obtained from C57/BL6 pups (postnatal day 4). Four brains were isolated and kept in dissection medium, containing: HBSS (1x; [-] Ca²⁺, Mg²⁺; [+] Phenol red), D-Glucose [400 nM] (Gibco), HEPES [7 mM] (Gibco). Two hippocampi per brain were dissected out and transferred to a falcon with dissection medium. A 2.5% Trypsin (Gibco) solution was released in the falcon and incubated for 20-30 minutes at 37 °C. The hippocampi were washed three times with chilled dissection medium. Dissection medium containing 10% FBS (Gibco) and DNase I [40 µg/ml] (Qiagen) was added to the hippocampi. The cells were triturated with a flamed glass Pasteur pipette (VWR) about 5-6 times. The cells were stained through a 40 µm cell strainer (Corning) into a clean 50 ml tube (Greiner). The tube was centrifuged for 12 minutes, 165 g at 12 °C in a centrifuge (Rotina 420R, Hettich Zentrifugen). The supernatant was discarded and the cell pellet was resuspended in standard complete medium, containing: DMEM [1x; [+] D-glucose [400 nM] (Gibco), [+] L-glutamine 0.1% (Gibco)], 10% FBS (Gibco) and 1% Pen/Strep (10 kU/ml Pen; 10 mg/ml Strep, Gibco). The cells were transferred onto a T75 flask (Greiner). After one day, the medium was renewed in a ratio of 50:50. The medium was renewed every three days in a ratio of 50:50. At DIV20, the cells were fixed in ultra clean PFA [4%] (PFA, Electron Microscopy Sciences) for 10 minutes.

BaseScope

In Situ Hybridization was performed using the BaseScope™ Reagent Kit – RED (ACD) according to the manufacturer's protocol with adjustments; Adult whole brains were dissected out of C57BL/6 mice, immediately frozen in dry ice, and stored at -80 °C until further processing. Using a cryostat, 16 µm thick sagittal sections of the brains were cut and collected on Superfrost Plus object glasses (VWR). Hydrophobic barriers were created around each section using an ImmEdge hydrophobic barrier PAP pen (Vector Laboratories). The sagittal sections were dried for 10 minutes before fixation in 4% RNase free PFA (Electron Microscopy Sciences) for 30 minutes at 4 °C. The tissue was washed in PBS [1x] and dehydrated in sequential steps of EtOH (50%, 70%, 100%). Next, the tissue was incubated with RNAscope Hydrogen Peroxide (ACD) for 10 minutes at RT, washed with PBS [1x] and incubated in RNAscope Protease IV (ACD) for 30 minutes at RT. After PBS [1x] washes, probe solution was added to the tissue and the slides were incubated for 2 hours at 40 °C in a hybEZ II hybridization oven (ACD). In order to build the amplification tree, slides were washed in Wash Buffer (ACD) and incubated in AMPO

(ACD) for 30 minutes at 40 °C; Washed in Wash buffer and incubated in AMP1 (ACD) for 15 minutes at 40 °C; Washed in Wash buffer and incubated in AMP2 (ACD) for 30 minutes at 40 °C; Washed in Wash buffer and incubated in AMP3 (ACD) for 30 minutes at 40 °C; Washed in Wash buffer and incubated in AMP4 (ACD) for 15 minutes at 40 °C; Washed in Wash buffer and incubated in AMP5 (ACD) for 30 minutes at 40 °C; Washed in Wash buffer and incubated in AMP6 (ACD) for 15 minutes at 40 °C in a hybEZ II hybridization oven (ACD). Next, slides were incubated in a 1: 60 reaction mix of RED-B to RED-A (ACD) for 10 minutes at RT. Slides were rinsed in tap water and the tissues were counterstained with a 50% Gill's Hematoxylin (Thermo Fisher Scientific) staining for 2 minutes at RT. After washes with tap water, the slides were dipped in 0.02% ammonia water and rinsed again. Next, sections were dried in a 60 °C in a dry oven for 7 minutes and mounted in VectaMount (Vector Laboratories) before imaging. The following probes were used; CIRS-7 probe BA-Mm-Cdr1-as-circRNA-Junc; Negative Control Probe - DapB-1ZZ.

ViewRNA

Tissue

Fluorescent *In Situ* Hybridization was performed by the ViewRNA miRNA ISH Cell Assay Kit (Invitrogen), according to the manufacturer's protocol with adjustments; Whole brains were dissected out of C57BL/6 mice at 5 time points (embryonic day 15 (E15); embryonic day 18 (E18); postnatal day 5 (P5); postnatal day 100 (P100); postnatal day 365 (P365)), frozen immediately in dry ice, and stored at -80 °C until further processing. Using a cryostat 16 µm thick sagittal sections of mouse brains were cut. Hydrophobic barriers were created around each section using an ImmEdge hydrophobic barrier PAP pen (Vector Laboratories) in order to: (i) prevent drying out during hybridization steps; (ii) reduce the amount of solution required to fully submerge the sections throughout the experiment. The sagittal sections were dried for 10 minutes before fixation in 4% RNase free PFA (Electron Microscopy Sciences) for 30 minutes at RT. Sections were incubated twice in crosslinking buffer QM (Thermo Fisher Scientific) for 10 minutes at RT. Next, sections were incubated in 0.16 M N-(3-Dimethylaminopropyl)-N'-ethylcarbodiimide hydrochloride (EDC; Sigma Aldrich) crosslinking buffer for an hour at RT. To permeabilize the sections they were exposed to detergent solution QM (Thermo Fisher Scientific) for 10 minutes at RT. The probes (Thermo Fisher Scientific) were diluted in probe set solution (Thermo Fisher Scientific) at a ratio of 1:100 pipetted onto the sections, placed into a HybEZTM II Hybridization System and incubated for 3 hours at 40 °C. The sections were

washed in wash buffer (Thermo Fisher Scientific) and left overnight at 4 °C in storage buffer (Thermo Fisher Scientific). The following day, the sections were incubated in Preamplifier mix QM (Thermo Fisher Scientific) for 1 hour at 40 °C in the HybEZ™ II Hybridization System. The sections were washed in wash buffer (Thermo Fisher Scientific) and incubated in amplifier mix QM (Thermo Fisher Scientific) for 1 hour at 40 °C. Label Probe 1 Alkaline Phosphatase (LP1-AP; Thermo Fisher Scientific) was diluted to a 0.07% concentration in label probe diluent QF (Thermo Fisher Scientific) and added to the tissue sections. After incubation at 40 °C for 1 hour, the sections were washed in wash buffer (Thermo Fisher Scientific) and exposed to AP enhancer solution (Thermo Fisher Scientific) for 5 minutes at RT. Fast red (Thermo Fisher Scientific) was mixed with Naphthol buffer and added to the sections for 45 minutes at 40 °C. The sections were then washed in RNase free PBS [1x], refixed in RNase free 4% PFA (Electron Microscopy Sciences) for 10 minutes, and then washed again in RNase free PBS [1x]. Finally, samples were mounted in Fluorsave (Merck) and imaged.

Cells

Fluorescent *In Situ* Hybridization was performed by the ViewRNA miRNA ISH Cell Assay Kit (Invitrogen), according to the manufacturer's protocol with adjustments. A hybEZ II hybridization oven (ACD) was used for the incubation steps at 40 °C, N-(3-Dimethylaminopropyl)-N'-ethylcarbodiimide hydrochloride (EDC) was provided by SigmaAldrich. The probes (type I Alexa Fluor 568, type 4 Alexa Fluor 488) were designed to bind the back-splice junctions of the circRNAs. Primary cortical neurons were fixed in ultra clean PFA [4%] (PFA, Electron Microscopy Sciences) for 10 minutes and washed three times in PBS [1x]. The coverslips were blocked for 1 hour at RT with 5% Normal-Goat-Serum and 0.1% Triton-X in PBS [1x] (blocking buffer). Next, they were incubated in primary antibody in blocking buffer o/n at 4 °C. The coverslips were washed three times in PBS [1x] and cells were incubated in secondary antibody in PBS [1x] for 45 minutes at RT. The coverslips were washed three times in PBS [1x] followed by a 4',6-diamidino-2-phenylindole (DAPI) [1 µg/ml] (Sigma, D-9564-10MG) incubation for 10 minutes at RT. Coverslips were washed with PBS [1x] and mounted on Superfrost Plus object glasses (VWR) with Fluorsave (Calbiochem) mounting medium. Primary antibodies used; β -tubulin IgG (SAB4200732, 1:1000); GFAP (DAKO Z0334, 1:1000); Anti-Map2 (801801 Biolegend (Covance) 1:500). Secondary antibodies used; goat-anti-mouse Alexa Fluor 488 (Invitrogen A11029, 1:750); goat-anti-rabbit Alexa Fluor 488 (Abcam 150077, 1:750).

Microscopes

All immunofluorescent images were acquired using an Axioscope epifluorescent microscope (Zeiss) and a LSM 880 confocal microscope (Zeiss). Brightfield images were acquired using a ZEISS Axio Scan.Z1 (Zeiss).

Funding

This project has received funding from the Netherlands Organization of Scientific Research NWO (Personal grant DvR, part of Graduate Programme project (022.003.003) and NWO VICI to RJP) and the European Union's Horizon 2020 research and innovation programme under the Marie Skłodowska-Curie grant agreement No 721890 (circRTrain) (to RJP).



2

REFERENCES

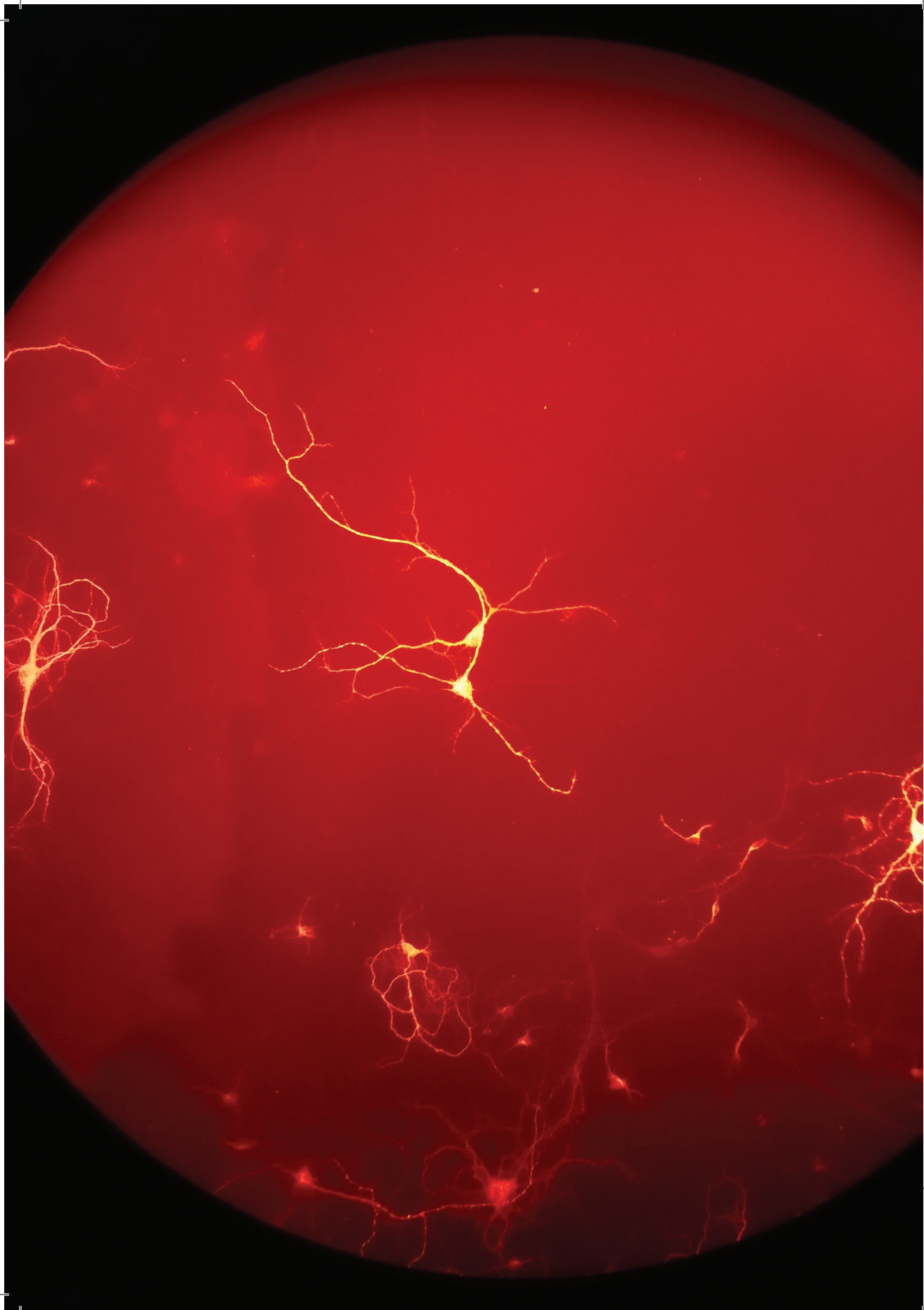
1. Hansen, T. B. et al. Natural RNA circles function as efficient microRNA sponges. *Nature* 495, 384–388 (2013).
2. Memczak, S. et al. Circular RNAs are a large class of animal RNAs with regulatory potency. *Nature* 495 VN-, 333–338 (2013).
3. Jeck, W. R. & Sharpless, N. E. Detecting and characterizing circular RNAs. *Nat. Biotechnol.* 32, 453–61 (2014).
4. Piwecka, M. et al. Loss of a mammalian circular RNA locus causes miRNA deregulation and affects brain function. *Science* (80-.). 357, (2017).
5. Venø, M. T. et al. Spatio-temporal regulation of circular RNA expression during porcine embryonic brain development. *Genome Biol.* 16, 245 (2015).
6. You, X. et al. Neural circular RNAs are derived from synaptic genes and regulated by development and plasticity. *Nat. Neurosci. advance on*, 603–610 (2015).
7. Zheng, Q. et al. Circular RNA profiling reveals an abundant circHIPK3 that regulates cell growth by sponging multiple miRNAs. *Nat. Commun.* 7, 11215 (2016).
8. Zirkel, A. & Papanonis, A. Detecting Circular RNAs by RNA Fluorescence In Situ Hybridization. in *Circular RNAs: Methods and Protocols* 1724, 69–75 (Elsevier, 2018).
9. Raj, A., van den Bogaard, P., Rifkin, S. A., van Oudenaarden, A. & Tyagi, S. Imaging individual mRNA molecules using multiple singly labeled probes. *Nat. Methods* 5, 877–879 (2008).
10. Piwecka, M. et al. Loss of a mammalian circular RNA locus causes miRNA deregulation and affects brain function. *Sci.* 8526, 1–14 (2017).
11. Huang, C., Liang, D., Tatomer, D. C. & Wilusz, J. E. RESEARCH COMMUNICATION A length-dependent evolutionarily conserved pathway controls nuclear export of circular RNAs. 639–644 (2018). doi:10.1101/gad.314856.118.GENES
12. Buxbaum, A. R., Yoon, Y. J., Singer, R. H. & Park, H. Y. Single-molecule insights into mRNA dynamics in neurons. *Trends Cell Biol.* 25, 468–475 (2015).
13. Itzkovitz, S. et al. Single-molecule mRNA detection and counting in mammalian tissue. *Nat. Protoc.* 8, 1743–1758 (2013).
14. Levesque, M. J. & Raj, A. Single-chromosome transcriptional profiling reveals chromosomal gene expression regulation. *Nat. Methods* 10, 246 (2013).
15. Westholm, J. O. et al. Genome-wide Analysis of Drosophila Circular RNAs Reveals Their Structural and Sequence Properties and Age-Dependent Neural Accumulation. *Cell Rep.* 9, 1966–1981 (2014).
16. Jeck, W. R. et al. Circular RNAs are abundant, conserved, and associated with ALU repeats. *RNA* 19, 141–57 (2013).
17. Salzman, J., Gawad, C., Wang, P. L., Lacayo, N. & Brown, P. O. Circular RNAs are the predominant transcript isoform from hundreds of human genes in diverse cell types. *PLoS One* 7, (2012).

SUPPLEMENTARY DATA

Supplementary Table 1 | ISH probe sequences.

Technique	Target	Species	Probes	Probe type
ViewRNA	CIRS-7	mmu	ttctgggtctgccttatccag // ggtttcagtggtgccagtac	1
ViewRNA	circDcc	mmu	cactggaagtggtaactcaagg // tgcaagttccaggccagtag	1
ViewRNA	circEfnb2	mmu	ttcagaagaacaagattactacattatat // atttctaccggacaaggc	1
ViewRNA	circEpha3	mmu	cagcatcacaaactcaggctg // ctgtcgaccaggcttctacaa	1
ViewRNA	circNeo1	mmu	gaggagcttactgtgcaag // gagccaggttcgaacattcactc	1
ViewRNA	circPlxnc1	mmu	gggtgcctcccgttacaag // aaagaaggggatcggcctg	1
ViewRNA	circRobo1	mmu	ttccgtaactttgacagttcaag // atacgaggaggaaaactcatgatc	1
ViewRNA	circRobo2	mmu	atgcatctctggaagtggcat // gatctcgtcttcgtaagaagact	1
ViewRNA	Epha3	mmu	VB1-3029635-VC	1
ViewRNA	ActB	mmu	VB4-10432-VCP	4
BaseScope	CIRS-7	mmu	Position 2896 and 12 of mmu_circ_0001878	NA
BaseScope	DapB	bsu	Position 414 and 862 of EF191515	NA

2



Manipulation and functional assessment of axon guidance circRNA *in vitro* and *in vivo*

Daniëlle van Rossum¹, N. Solée Pop¹, Mateja Rybiczka-Tesulov¹, Andreia Gomes Duarte¹, Lasse S. Kristensen², Ivano Legnini³, Nikolaus Rajewsky³, Jørgen Kjems² and R. Jeroen Pasterkamp¹

¹ Department of Translational Neuroscience, UMC Utrecht Brain Center, University Medical Center Utrecht, Utrecht University, Utrecht 3584 CG, the Netherlands

² Department of Molecular Biology and Genetics, Interdisciplinary Nanoscience Center (iNANO), Aarhus University, Aarhus, Denmark

³ Berlin Institute for Medical Systems Biology, Max-Delbrück Center for Molecular Medicine, 10115 Berlin, Germany

⁴ Department of Translational Neuroscience, UMC Utrecht Brain Center, University Medical Center Utrecht, Utrecht University, Utrecht 3584 CG, the Netherlands

Primary cortical neurons through the circular objective of an epifluorescent microscope.

ABSTRACT

Circular RNAs (circRNAs) are long non-coding RNAs characterized by high sequence conservation, enrichment in the brain and cell-type specific expression. Since their re-discovery in 2013, many studies have addressed the biogenesis of circRNAs and their involvement in gene regulation. Some putative functions have been assigned to (neuronal) circRNAs and their deregulation has been linked to altered cell proliferation and development. Although techniques for manipulating circRNA levels are emerging, they still face many caveats. In this chapter, we describe and utilize various recently developed techniques for the manipulation of circRNAs derived from axon guidance genes, specifically. CircRNAs were successfully overexpressed in neuronal cells and in the mouse retina. For circRNA knockdown, we implemented different manipulation strategies from which knockdown with siRNAs was most robust and specific *in vitro*. Sholl analysis following knockdown of circRNAs in primary cortical neurons hinted at a possible role for certain axon guidance circRNA in neurite branching. SiRNA-mediated knockdown in the mouse cortex using *in utero* electroporation did not induce obvious defects. Lastly, we report that neuronal expression of axon guidance circRNAs is elevated as a result of cellular activation. In all, this chapter provides an overview of different tools to manipulate circRNA levels *in vitro* and *in vivo* and paves the way for future experiments that can lead to better insight in (axon guidance) circRNA function.

INTRODUCTION

Conventionally, RNA molecules were attributed to the transfer of the genetic DNA code into specific proteins. Nowadays it has become clear that around 98% of all transcriptional output comes from the non-protein coding parts of the transcriptome, suggesting that RNA largely fulfills other functions¹. A recently re-discovered and highly conserved group of long non-coding RNAs called circular RNAs (circRNAs) can be considered as part of this group of molecules^{2,3}. CircRNAs are single-stranded RNA molecules that are formed by a back-splicing event where a 3' upstream donor splices to a 5' downstream acceptor⁴. After formation of the covalent bond, circRNAs are highly stable molecules that can be translocated to various cellular compartments. CircRNAs are specifically highly expressed in neuronal tissue, where their expression is spatiotemporally regulated⁵⁻⁷. Often circRNAs are expressed independently of their linear host gene, suggesting they have

specific functions rather than being splicing artifacts. Although thousands of circRNAs have been identified, so far only a few have been reported to have specific biological functions such as the sponging of microRNAs and proteins, modulation of transcription, interference with splicing, and translation of small peptides.

Most studies on circRNAs have been focused on their interactions with microRNAs (miRNAs) and RNA binding proteins (RBPs). Accumulating evidence indicates that certain circRNAs play a crucial role in gene expression regulation by inhibiting miRNA activity. MiRNAs are small non-coding RNA molecules that are known to have complementarity with specific mRNA targets through which they regulate their stability and/or translation. The well-studied ciRS-7 (cerebellar degeneration-related antisense circular RNA sponge for miR-7) was the first circRNA described to have complementarity to two miRNAs and to act as a microRNA 'sponge'. Human ciRS-7 possesses over 70 partially complementary binding sites for microRNA-7 (miR-7). By binding large numbers of miR-7, ciRS-7 prevents this miRNA from interacting with its targets²³. This interaction may be important in different diseases since Alzheimer's disease, diabetes and different types of cancers have been linked to both ciRS-7 and miR-7⁸⁻¹⁰. Over the years, additional circRNAs have been described that modulate the activity of specific miRNAs in a disease-related (often cancer) context. MiRNAs can have complementarity with both circRNAs and mRNAs, which in turn can also bind to, sequester and transport RBPs, resulting in complex circRNA-miRNA-mRNA-protein regulatory networks¹¹⁻¹³. Thus far, specific circRNA-miRNA-mRNA-protein regulatory networks have only been described for a few circRNAs. Most circRNAs are predicted to contain only few microRNA-binding sites¹⁴.

There is evidence that supports the translation of endogenous circRNAs, but this is most likely not the primary function of circRNAs¹⁴⁻¹⁸. Interestingly, a growing body of experimental evidence indicates that circRNAs are involved in various cellular events, such as proliferation, differentiation and apoptosis^{5,7,19}. For example, recent studies indicate that knockdown of circSLC45A4 can induce spontaneous neuronal differentiation in human neuroblastoma cells, while the pool of basal progenitors in the developing mouse cortex was reduced²⁰. In addition, circGRIA1 regulates synaptic plasticity and synaptogenesis in the male macaque brain²¹. It has, therefore, been proposed that circRNAs regulate neuronal functions.

Despite progress in understanding the biological functions of circRNAs, the field has to deal with one main obstacle. Essaying the function of circRNAs is not straightforward, as traditional molecular biology techniques for circRNA depletion may also alter the levels of their linear host transcript (the vast majority circRNAs are derived from protein-coding genes). Moreover, it is also difficult to separate *cis* and *trans* functions of circRNAs, since the production of circular transcripts could compete with the splicing of linear transcripts. So far, one circRNA knockout mouse model (ciRS-7) has been reported. However, the development of this mouse model was only possible because the circle ciRS-7 does not have a linear transcript²². *In vitro* studies have reported the inhibition of circRNAs using RNA interference (RNAi), a system that works with short interfering RNAs complementary to the sequence around the back-splice junction. Nonetheless, many circRNA manipulation tools need to be further developed and standardized.

In this study, we adapted the use of currently developed methodologies for circRNA knockdown or overexpression such as small interfering RNAs (siRNAs), short hairpin RNAs (shRNAs), AgoRNA and CRISPR-Cas13 to specifically target axon guidance circRNAs *in vitro* and *in vivo* in mice and assessed the perturbations caused by these modulations. CircRNAs were successfully overexpressed in Neuro2a cells and in the mouse retina, and in our hands the knockdown of axon guidance circRNAs was most reproducible *in vitro* using siRNAs. The results of sholl analysis following siRNA-mediated knockdown of circRNAs in primary cortical neurons hint at a possible role for certain axon guidance circRNAs in neurite branching, while an siRNA-mediated knockdown in the mouse cortex using *in utero* electroporation did not lead to observable morphological changes. In all, this chapter provides an overview of the tools available for circRNA manipulation and discusses the challenges that arise with each technique. These findings provide a framework for future experiments that can lead to better insight in (axon guidance) circRNA function.

RESULTS

Axon guidance circRNAs can be successfully overexpressed *in vitro*

To investigate the biological function of axon guidance circRNAs *in vitro*, we developed a number of tools for circRNA manipulation (Figure 1A)(Table 1). First, we overexpressed circRNAs using a previously reported laccase vector²³. This vector contains a circRNA sequence surrounded by *Drosophila* complementary intronic sequences that facilitate the circularization of the RNA. We cloned overexpression constructs for two axon guidance circRNAs (circEfnb2 and circRobo1) based on their high neuronal expression and dynamic spatiotemporal expression patterns during brain development (Chapters 1 & 2). After successful cloning, we expressed the circEfnb2 and circRobo1 overexpression constructs in mouse Neuro2a (N2a) cells. The overexpression resulted in a substantial increase in the expression of both circEfnb2 and circRobo1, but not of their linear counterparts, in N2a cells (Figure 1B). Although we found that circRNA levels can be successfully manipulated using an overexpression vector, overexpression is often not a physiological reflection of the behavior of a circRNA in a cell. For instance, the use of these vectors can result in the formation of concatemers and other undesired transcripts leading to off-target effects as a result of rolling circle transcription of the plasmid²⁴. Moreover, in our hands the overexpression constructs were less efficient in primary cortical neurons (PCNs) as compared to N2a cells (either due to low endogenous levels of the circRNAs or due to inefficient transfection) (Supplementary figure 1). Therefore, we continued developing tools for circRNA knockdown.

AgoshRNAs are not efficient in knocking down axon guidance circRNAs

To knockdown circRNAs in PCNs, we developed AgoshRNAs that were reported to efficiently knockdown mRNAs²⁵. These AgoshRNAs have a shorter stem length (17-19 base pairs) and a smaller loop (6 nucleotides) than conventional shRNAs (Figure 1A). They avoid Dicer recognition, which activates Ago2 to cleave only the guide strand of the siRNA. AgoshRNAs are predicted to have fewer off-target effects as compared to shRNAs and to establish more precise cleavage ends. However, in our hands, the use of AgoshRNAs for the knockdown of selected axon guidance circRNAs (circDcc, circEfnb2, circEpha3, circNeo1, circPlxnc1, circRobo1 and circRobo2, based on their high neuronal

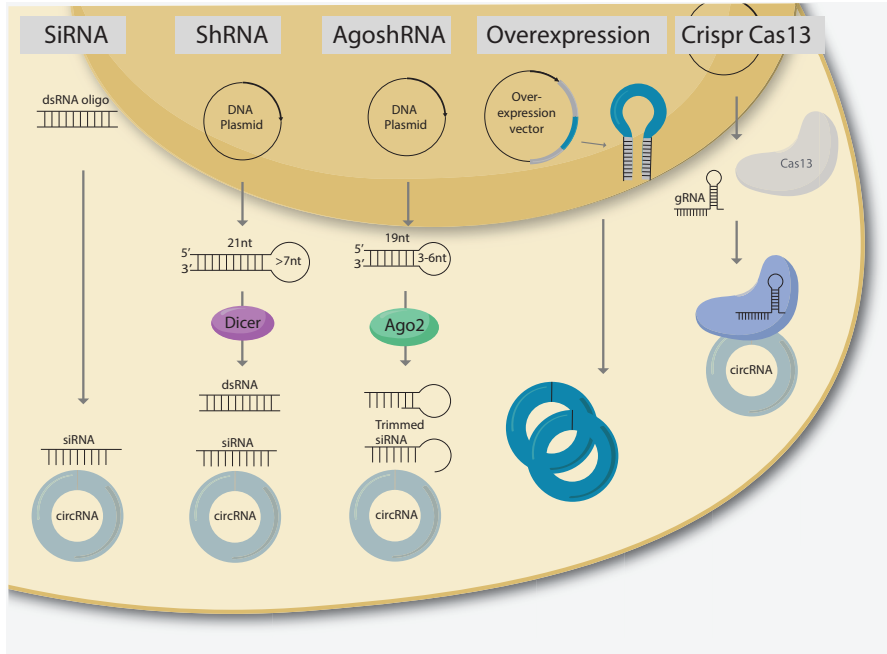
expression and dynamic spatiotemporal expression patterns during brain development) did not lead to their desired downregulation in PCNs. For the AgoshRNAs that induced a knockdown of the circular transcript, the level of the linear transcript was often also positively (circEfnb2) or negatively affected (circNeo1, circPlxnc1) despite specific circRNA primer design (Figure 1C). Although the data indicate that the use of most AgoshRNAs results in off-target effects, these negative findings can also be an artifact of the low expression of the circRNAs in PCNs and N2a cells. In a new experiment we therefore first increased circRNA expression levels in N2a cells using a circRobo1 overexpression construct prior to circRNA knockdown with circRobo1 AgoshRNAs. This approach also did not result in consistent knockdown of circRobo1, while the linear transcript was targeted (Figure 1D). Besides off-target effects, other factors have possibly contributed to the lack of circRNA knockdown with AgoshRNAs. We observed that the transfection of the AgoshRNA plasmids was inefficient in PCNs and developed therefore AgoshRNA lentiviruses. Using a pCAG-GFP reporter, we confirmed that the AgoshRNA lentiviruses efficiently transduced PCNs (data not shown). Nonetheless, this method did not result in knockdown of circNeo1 and circEpha3 *in vitro* (Figure 1E). Therefore, we continued investigating other circRNA knockdown tools.

ShRNAs and CRISPR-Cas13 are promising tools for specific circRNA knockdown

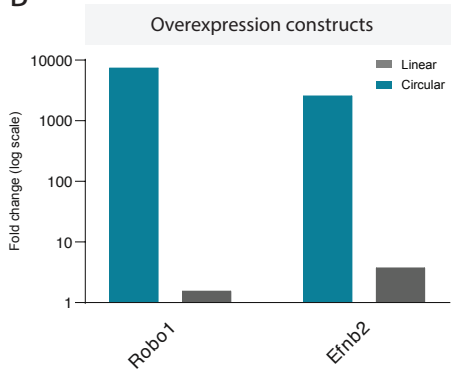
Compared to AgoshRNAs, conventional shRNAs were more successful in the specific knockdown of circular transcripts of the *Rmst* gene (Figure 1F). For two of three different designs (sequences targeting the back-splice junction with each 3 nucleotides upstream or downstream of the back-splice junction) *Rmst* circRNAs were significantly reduced, while the linear transcript was unchanged. One design did not lead to knockdown, indicating that probe design is very important for successful circRNA manipulation.

The recently developed CRISPR-Cas13 system is proposed to knockdown RNAs with high efficiency and specificity. This system makes use of an engineered CRISPR-Cas13 effector and an associated guide RNA²⁶. We tested a CRISPR-Cas13-mediated knockdown for a circRNA from the *SATB1* gene (circSatb1) and observed that a successful circRNA knockdown was achieved in N2a cells (Figure 1G). However, while the latter two techniques were still further validated in our lab, we continued investigating the use of siRNAs for the knockdown of axon guidance circRNA.

A



B



C

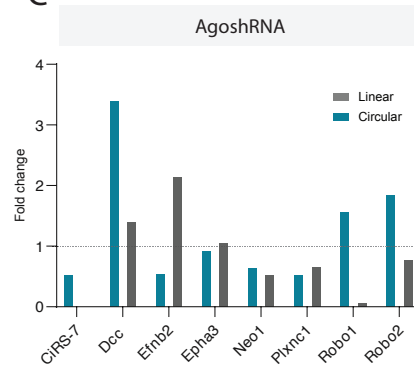
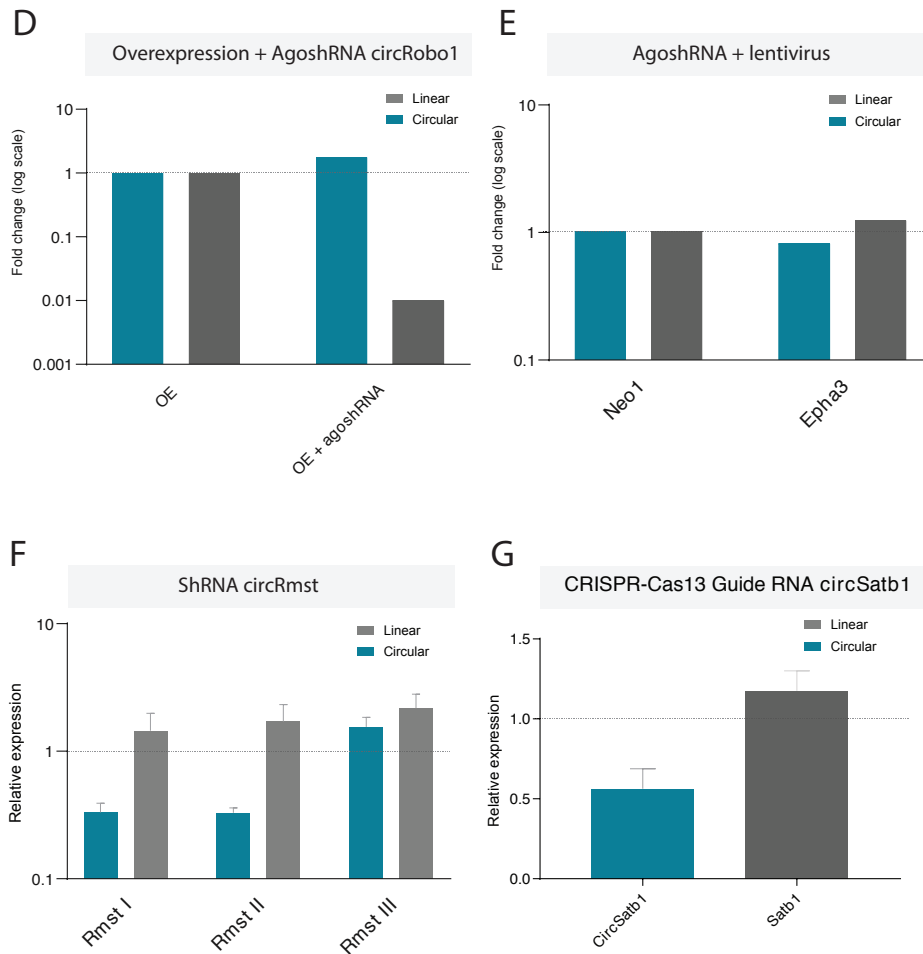


Figure 1 | CircRNA manipulation tools.

(A) Schematic of circRNA manipulation tools. Small interfering RNAs (siRNAs) form a class of double-stranded RNA molecules (20-25 base pairs in length) that operate within the RNA interference (RNAi) pathway. After processing into a single stranded siRNAs, they interfere with the expression of circRNAs by binding to complementary nucleotide sequences followed by degradation. Expression of shRNA in cells is accomplished by delivery of plasmids. Once the vector has integrated into the host genome, the shRNA is transcribed in the nucleus. After further processing, the shRNA is exported from the nucleus, processed by Dicer and loaded into the RNA-induced silencing complex (RISC). The sense (passenger) strand is degraded. The antisense (guide) strand directs RISC to a circRNA that has a complementary sequence and the RISC



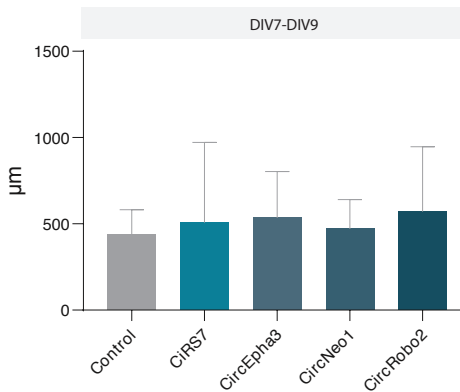
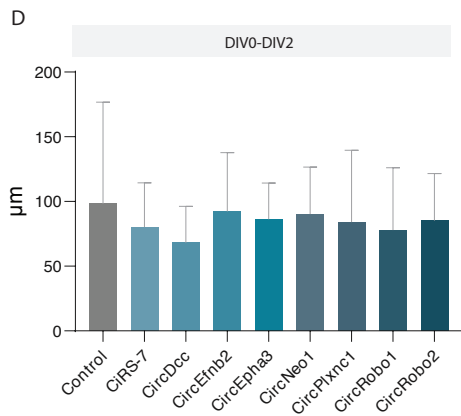
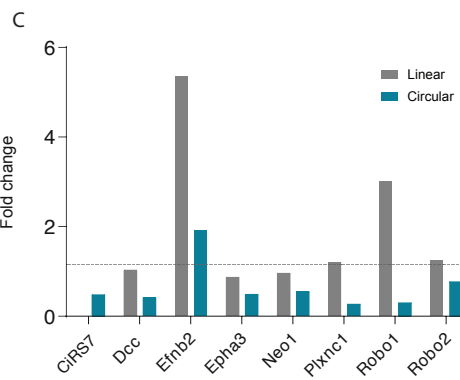
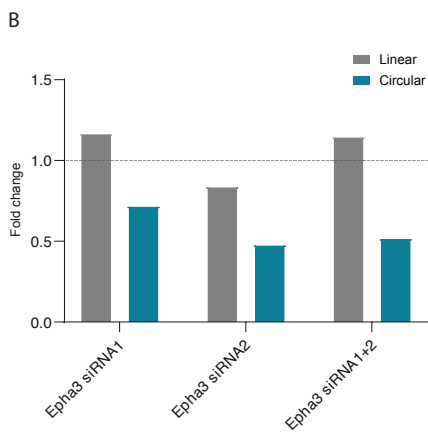
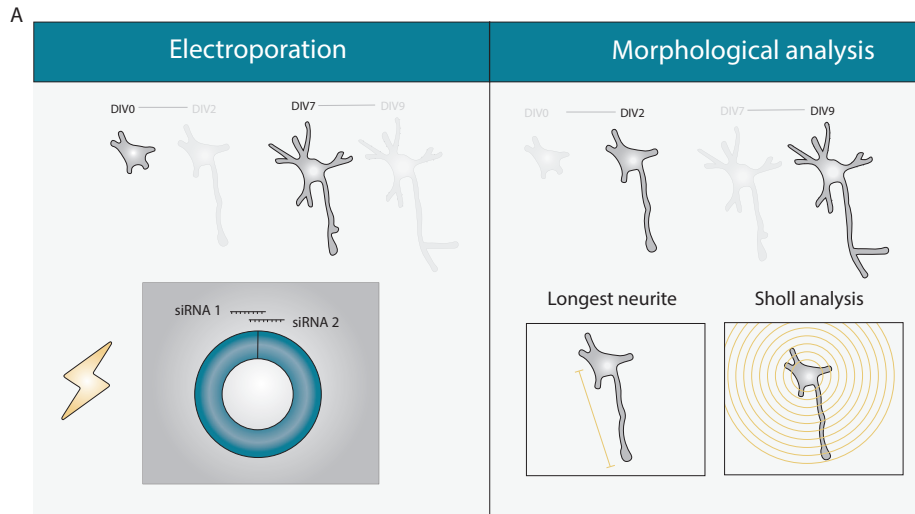
cleaves the circRNA leading to degradation. AgosRNAs are a type of shRNAs, but have a shorter stem length (approx. 19 base pairs) and a smaller loop (approx. 3-6 nucleotides) compared to shRNAs. They avoid Dicer recognition, which activates Ago2 to cleave only the guide strand of the siRNA. After further trimming, the AgoshRNA can bind to circRNA and induce cleavage. Cas13 is the only member of the CRISPR-Cas systems that specifically targets and cleaves RNA using a guide RNA that is specific for each circRNA. CircRNA overexpression can be achieved using a mini vector. This vector contains the circRNA sequence flanked by highly complementary intronic sequences. Once the vector has integrated into the host genome, the overexpression vector is transcribed in the nucleus. After further processing, where the flanking introns facilitate the back-splicing process, the circRNA is transported to the cytoplasm. (B) CircRobo1 and circEfnb2 can be specifically overexpressed in N2a cells. (C) AgoshRNAs do not efficiently knock down circRNAs in primary cortical neurons (PCN) (DIV0 - DIV5). (D) AgoshRNAs do not knockdown circRobo1 in N2a cells after overexpression of circRobo1. (E) Transduction of lentivirus AgoshRNAs in PCNs does not result in circ-Neo1 and circEpha3 knockdown (DIV0 - DIV4). (F) Circular transcripts of the Rmst gene can be specifically knocked down using shRNAs with two out of three different designs (Rmst I and II). (G) CircSatb1 transcripts are reduced after 48 hours in N2a cells using guideRNAs of the CRISPR-Cas13 system (n = 3 independent experiments with 1/2 replicates each).

Table 1 | Overview of circRNA manipulation tools

Manipulation strategy	Mechanism	Advantage(s)	Disadvantage(s)	Reference	Figure(s)
Overexpression	Minigene	Stable over expression of circRNA	Possibility of concatamer formation; non physiological levels	Kramer et al., 2018	1B, 2D, 4F-G, S3B
ShRNA knockdown	RNA interference	Stable, long term knockdown	Difficult to transfect in primary cultures; Off-target NA effects		1F
AgoRNA knockdown	RNA interference	Supposedly less off-target effects	Difficult to transfect in primary cultures; No stable circRNA knockdown	Berkhout and Liu, 2014	1C, 1E
Lentiviral knockdown	RNA interference	Efficient infection of primary cultures	Batch to batch variation	Rubinson et al., 2003	1E-F
siRNA knockdown	RNA interference	No cloning; Transfection/electroporation efficient	Short term effect	Legnini et al., 2016	2B-F, 3B, 3D, S3A
CRISPR-Cas13	RNA editing	Does not affect linear transcripts; Stable knockdown	Time-consuming	Konermann et al., 2018	1G

SiRNAs can efficiently and specifically knockdown circRNAs in PCNs

Previous reports confirmed the successful use of siRNAs for circRNA knockdown¹⁷. To test siRNA knockdown efficiency in our lab, we selected a group of circRNAs from axon guidance genes with differential expression patterns during brain development (circDcc, circEfnb2, circEpha3, circNeo1, circPlxnc1, circRobo1, circRobo2 and ciRS-7 as a positive control) (Chapter 1-2). First, we designed two siRNAs targeting the back-splice junction of circEpha3 (Figure 2A, left panel). We electroporated these siRNAs individually or the combination of the two siRNAs in separate PCN cultures, collected the cells after two days and evaluated circEpha3 expression levels using RT-qPCR. Although both siRNA strategies resulted in a stable and specific knockdown for circEpha3, the knockdown was more efficient with two different siRNAs targeting the back-splice junction simultaneously (Figure 2B). We then continued testing the knockdown of other axon guidance circRNAs using two siRNAs per target and established a reproducible siRNA-mediated circRNA knockdown in PCNs for ciRS-7, circDcc, circNeo1, circPlxnc1 and circRobo2. CircRNA levels were approximately reduced 50% after knockdown, while levels of the linear transcripts from the same host genes remained mostly unchanged (Figure 2C). These findings



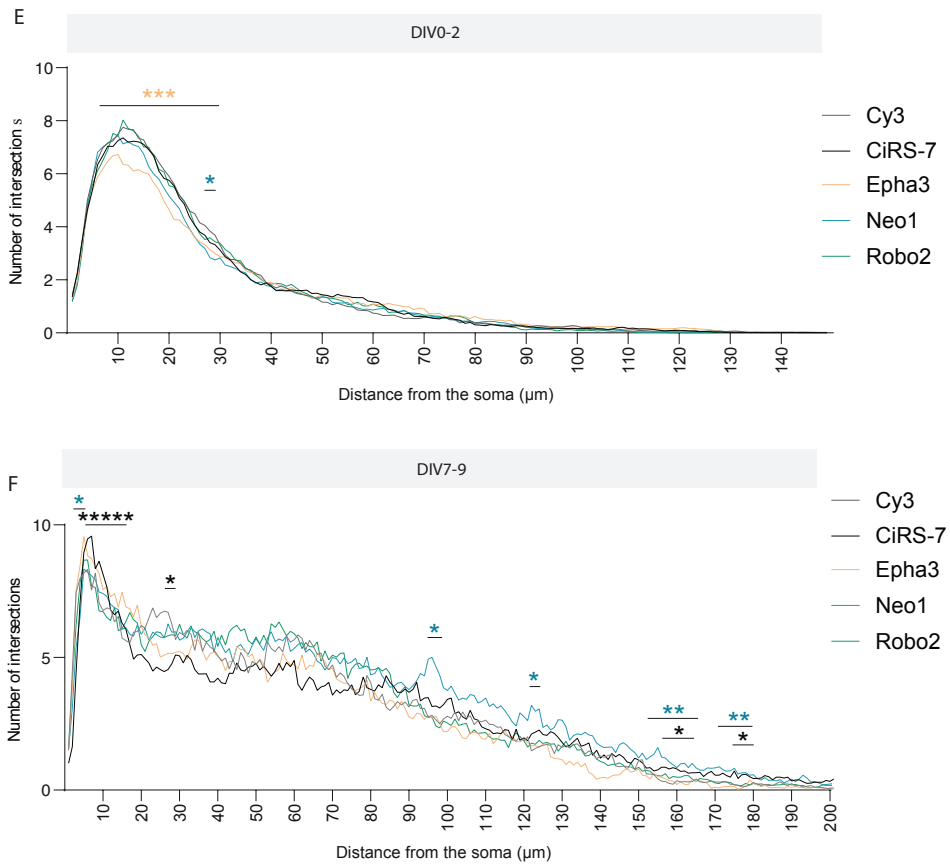


Figure 2 | SiRNA-mediated knockdown of circRNA.

(A) Schematic of siRNA electroporation on DIV0 and DIV7 PCNs for circRNA knockdown (left panel) and morphological analysis; longest neurite- and Sholl analysis on DIV2 and DIV9 (right panel). (B) SiRNA knockdown of circRNAs is more efficient using two siRNAs to target the back-splice junction than one, indicated by reduced off-target effects in PCNs (DIV0 – DIV2) (C). SiRNAs specifically knockdown axon guidance circRNAs. Linear host gene transcripts are not targeted (some are enriched). (D) Longest neurite length analyses of PCNs after siRNA knockdown is not significant ($n = 20$ cells measured per condition) (DIV7 - DIV9). Sholl analysis on (E) DIV2 and (F) DIV9 after 48 hours of siRNA knockdown in PCNs (DIV2; Step size = $1 \mu\text{m}$; Four independent experiments with $n = \pm 60$ cells per condition per experiment; Statistical significance determined with a Students t-test using the post hoc Holm-Sidak method, with $\alpha = 0.05$; * $p < 0.05$, *** $p < 0.001$) (DIV9; Step size = $5 \mu\text{m}$; Four independent experiments with $n = \pm 20$ cells per condition per experiment; Statistical significance determined with a Students t-test using the post hoc Holm-Sidak method, with $\alpha = 0.05$; * $p < 0.05$, ** $p < 0.01$, ***** $p < 0.00001$).

indicate that siRNAs are suitable tools to manipulate axon guidance circRNA levels *in vitro*. After circEfnb2 siRNA-mediated knockdown in PCN no circEfnb2 knockdown was observed. Similar to circEfnb2, siRNA-mediated knockdown of circRobo1 resulted in the upregulation of the linear transcript, indicating that these specific siRNAs are not circRNA specific (Figure 2C).

SiRNA-mediated knockdown of circEpha3 suggests a reduced proximal branching in primary cortical neurons

To study the function of axon guidance circRNAs *in vitro*, we investigated neuronal morphology after siRNA-mediated circRNA knockdown in PCNs (Figure 2A, right panel). First, we electroporated PCNs with siRNAs against the selected axon guidance circRNAs (2 siRNAs per target circRNA) and a GFP-expressing construct at two different timepoints during neuronal maturation: DIV0 (0 days *in vitro*) to capture the effect of the knockdown on the neurite outgrowth in immature neurons and DIV7 to observe branching of more mature neurons. Chosen as the optimal window for siRNA activity (data not shown), we continued to culture the PCNs for 48 hours post-electroporation (from DIV0 until DIV2 and DIV7 until DIV9) before fixing the cells. After processing and imaging of siRNA-electroporated PCNs, we were able to identify successfully electroporated neurons based on their GFP signal. To determine whether the knockdown of axon guidance circRNAs has an effect on neuronal morphology we measured the longest neurite of electroporated cells (Figure 2D). No significant difference in the length of neurites was detected between knockdown and control conditions. Next, we performed Sholl analysis, a quantitative analysis that can be used to measure dendritic arborization, on the siRNA electroporated cells (Figure 2E and 2F). Interestingly, after knockdown of circEpha3 in immature PCNs neurons (DIV2) we noticed a reduction in the branching of dendrites close to the soma of the neuron, indicated by a reduced number of intersections as compared to control conditions. In mature neurons (DIV9), we did not observe this effect for circEpha3, but noted an increase in proximal branching after ciRS-7 knockdown and in distal branching after circNeo1 knockdown (Figure 2F). Although these findings are significant ($p < 0.05$), it is important to mention that we observed a lot of branching heterogeneity between neurons in the same experiment at DIV9 (Supplemental Figures 2A and 2B). With the aim to investigate processes such as synapse formation, we also electroporated more mature neurons (DIV14 and DIV21). However, at this stage of maturation electroporation was not successful.

***In utero* electroporation of siRNAs targeting axon guidance circRNAs in the mouse motor cortex does not lead to morphological changes**

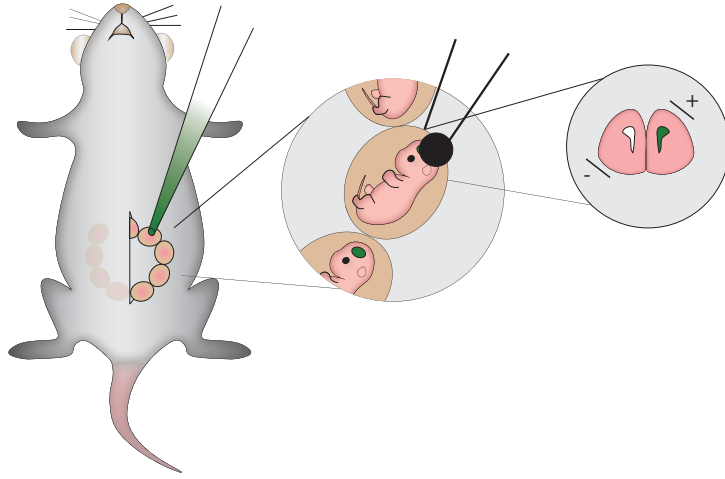
The developing mouse cortex is a widely used model system to study the mechanisms of nervous system formation. In the cortex many different processes must be coordinated to establish correct neuronal development and layering. To understand the function of axon guidance circRNAs in the developing brain, we electroporated the cortex of mouse embryo's *in utero* with siRNAs. We targeted the motor cortex at embryonic day 15 (E15; selected based on the results described in chapter 1 where we report that axon guidance circRNAs have an expression peak in the cortex around E16) with circEpha3 siRNAs ((pCAG-GFP constructs were co-electroporated with the siRNAs) and analyzed the brains two days later at E17 (Figure 3A). We collected the embryonic mouse brains, processed them into coronal sections and analyzed the GFP signal. We found that neurons in the ventricular and subventricular zones of the cortex were GFP positive, indicating that the siRNA-mediated knockdown was successful in these cells (Figure 3B). Then we studied the position and layering of the targeted cells in the cortex and did not observe obvious morphological changes as compared to the control brains. To determine whether

3

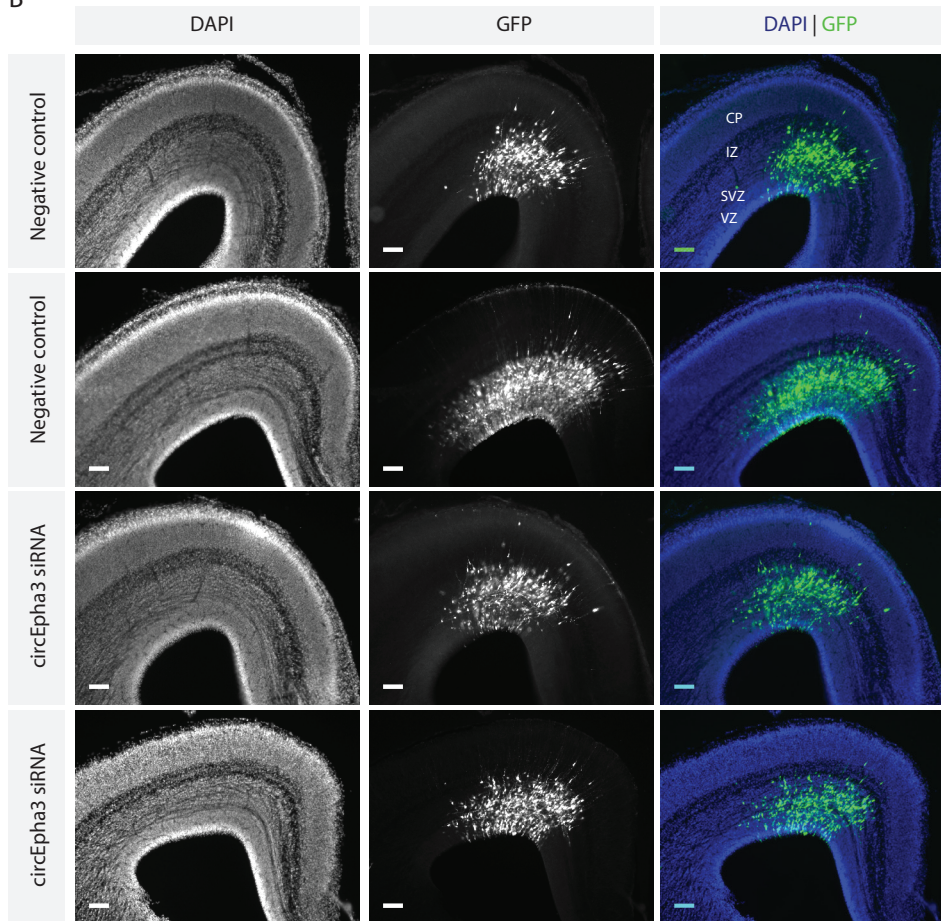
Figure 3 | Axon guidance circRNAs can be manipulated *in vivo*.

(A) Schematic of an *in utero* electroporation procedure. The uterus of a mouse containing E15 mouse embryos was exposed under anesthetics and embryos were injected in their lateral ventricles with a fast-green/siRNA/DNA mix. Next, siRNA/DNA was targeted to the motor cortex with electrodes. Embryos were placed back in the uterus and processed for analysis at E17. (B) Representative images of *in utero* electroporated motor cortices of mouse embryos (E15 - E17) with either control (Cy3) or circEpha3 siRNAs (and pCAG-GFP). Coronal view. Scale bar = 200 μ m. (C) Schematic of neonatal surface electroporation procedure. Anaesthetized P2 pups were injected just under the skull with a mouth pipet with fast-green/siRNA/DNA mix. Next, siRNA/DNA was targeted to cortical layer II from the outside using electroporation. Brains were harvested and processed for further analysis on P5. (D) Neonatal surface electroporation of P2 - P5 mice pups does not result in efficient electroporation of layer II cortical neurons. Representative images show electroporated pyramidal neurons and glial cells. Scale bar = 100 μ m. Coronal view. (E) Schematic of neonatal mouse (P1) retinal electroporation. The retina is the innermost layer of the wall of the eye. The vitreal cavity is in immediate contact with the retina. After injection of the construct in the vitreous, the retina can be electroporated. (F) Representative images of neonatal mouse retinas (P1) electroporated with circEfnb2 overexpression (and pCAG-GFP) constructs and analyzed at postnatal day 8 (P8). Scale bar = 500 μ m. (G) Representative images of neonatal mouse retinas (P1) electroporated with circEfnb2 overexpression (and pCAG-GFP) construct and analyzed at P8. Electroporated cells can be identified in the outer nuclear layer (ONL) and the inner nuclear layer (INL) of the retina. IPL = inner plexiform layer, INL = inner nuclear layer, OPL = outer plexiform layer, ONL = outer nuclear layer, IS/OS = outer-/inner segments of photoreceptors, RPE = retinal pigment epithelium. Scale bar = 50 μ m.

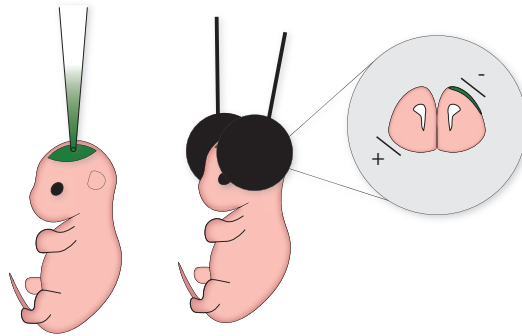
A



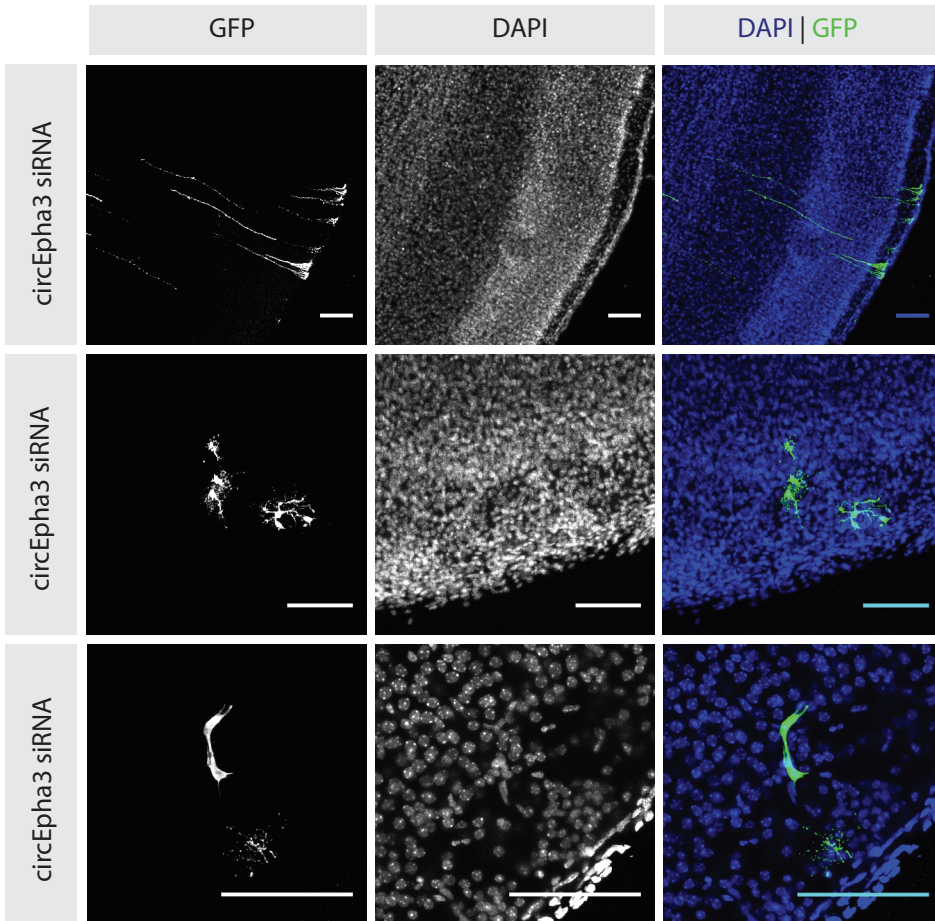
B



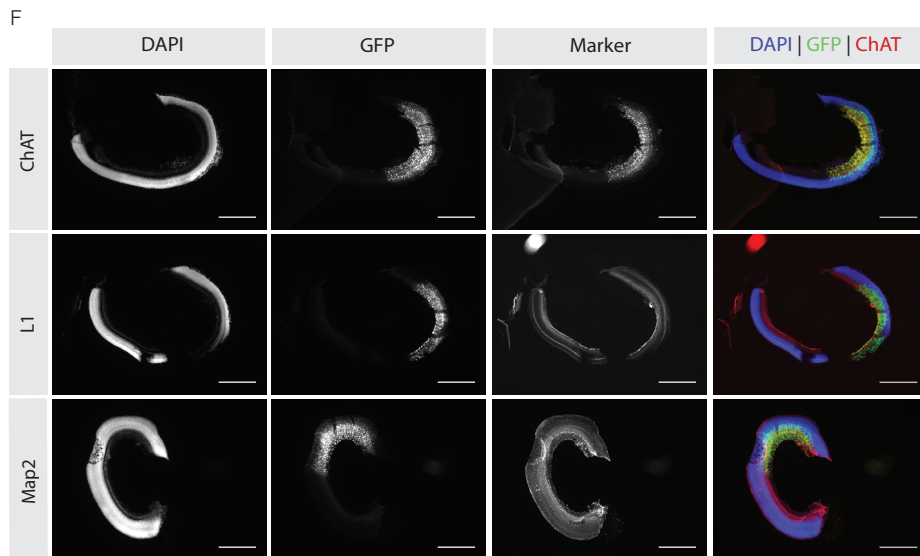
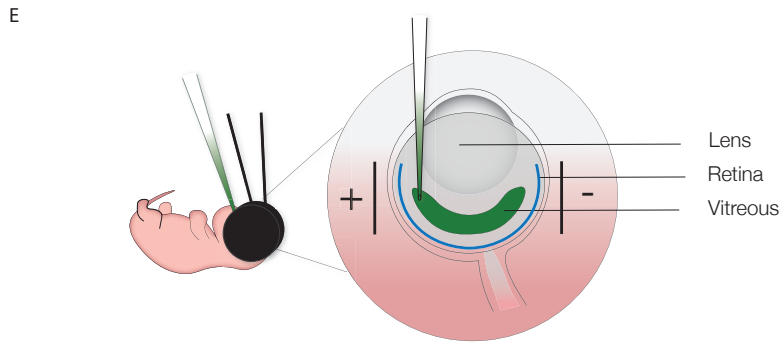
C



D

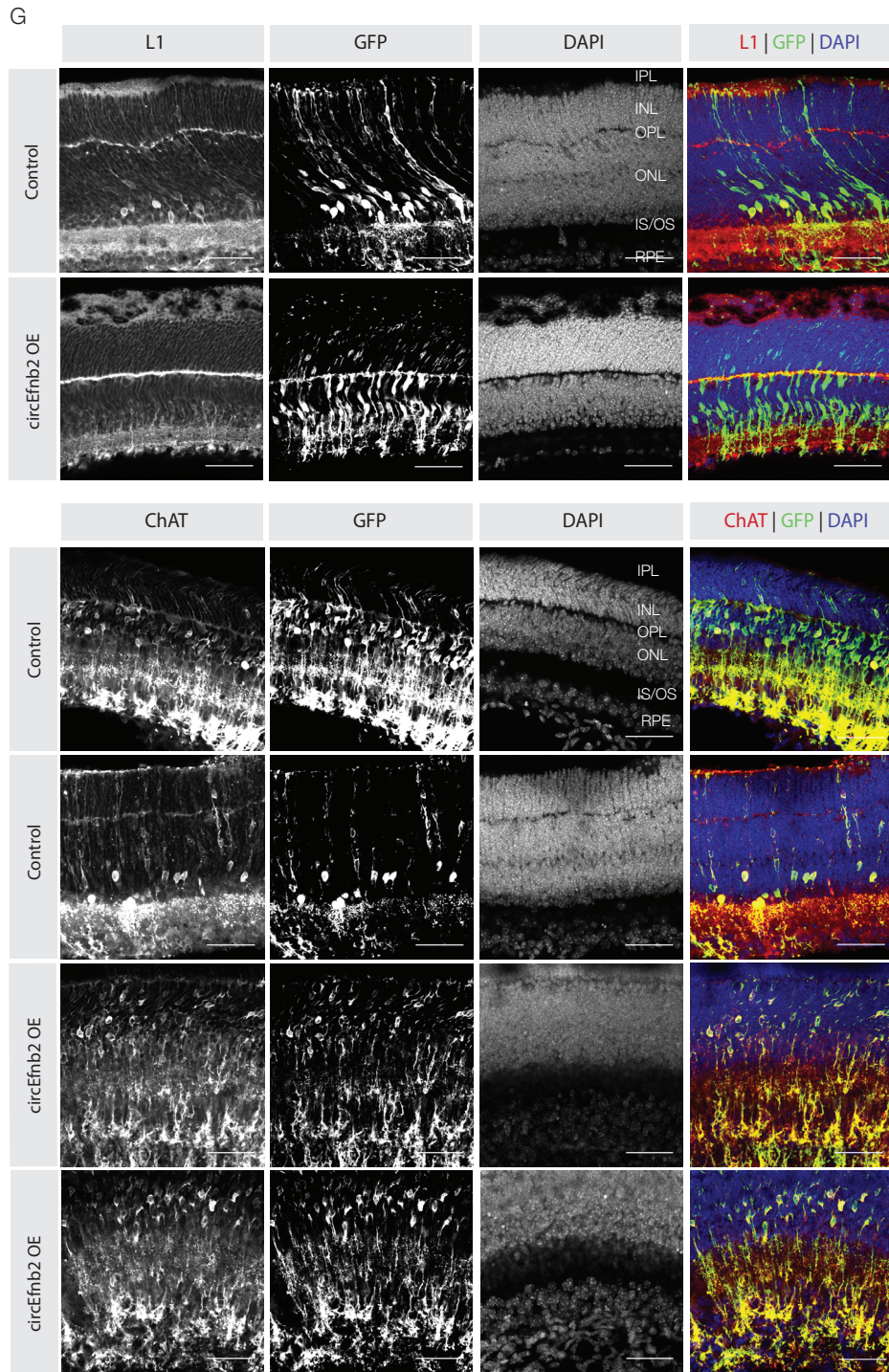


3



.....

axon guidance circRNAs act together and thus may compensate each other following knockdown, we combined multiple siRNAs against different axon guidance circRNAs roughly based on their axon guidance gene function (group 1 siRNAs (circNeo1, circDcc, circNtng1), group 2 siRNAs (circRobo1, circRobo2, ciRS-7) and group 3 siRNAs (circEfnb2, circEpha3, circPlxnc1)) and electroporated these groups of siRNAs in the mouse motor cortex *in utero*. However, no clear aberrant morphological phenotypes were found (Supplementary Figure 3A). Also, overexpression of a ciRS-7 using *in utero* electroporation in the embryonic mouse cortex did not reveal any noticeable morphological changes (Supplementary Figure 3B).



3

Postnatal electroporation of siRNAs targeting axon guidance circRNAs in the mouse motor cortex does not lead to morphological changes

To determine whether branching of cortical neurons is also decreased *in vivo* after siRNA-mediated circEpha3 knockdown, it would be interesting to target them using IUE. However, layer II cells in the cortex only start branching at postnatal day 2 (P2), making it impossible to target them embryonically with IUE using siRNAs due to their short-term effect. Instead, we attempted to target cortical layer II cells via the pial membrane of the cortex (from just below the skull) at postnatal day 1 (P1) in mouse pups, as previously reported²⁷ (Figure 3C). Although a few neuronal cells were hit in the cortex, most of the targeted cells were glial cells and no neuronal analysis could be performed (Figure 3D). Therefore, we continued exploring other *in vivo* circRNA manipulation tools.

CircEfnb2 can be successfully overexpressed in the mouse retina

Like the cerebral cortex, the (mouse) retina is highly structured. It contains 8 cellular layers that can be anatomically distinguished, making it an interesting region to study cellular development. Recently it was reported that circEfnb2 was significantly downregulated between P3 and P7 in the rat retina²⁸. Another study reported that AAV vectors encoding circRNAs injected in the eye of mice could lead to robust transgene expression across multiple retinal cell layers²⁹. We electroporated a circEfnb2 overexpression construct (plus a pCAG-GFP construct) in the mouse retina at P1 and analyzed the electroporated retinas at P8 (Figure 3E). Although we observed GFP signal across multiple retinal layers, no morphological changes were observed in the targeted cells (Figures 3F-G). In summary, we did not observe any morphological phenotypes *in vivo* after siRNA knockdown or overexpression of axon guidance circRNAs, but our findings do highlight the potential of circRNA expression tools for studying circRNA function and tissue-specific regulation in animal models.

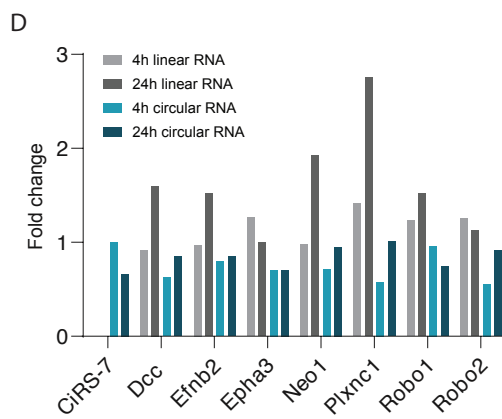
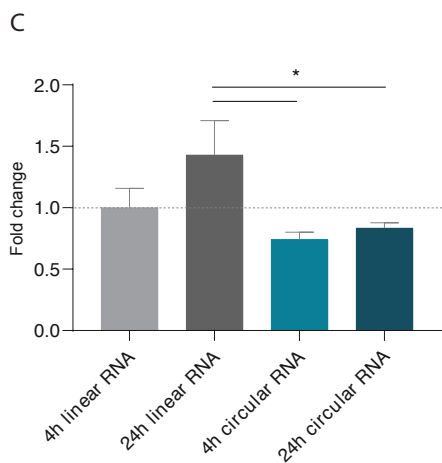
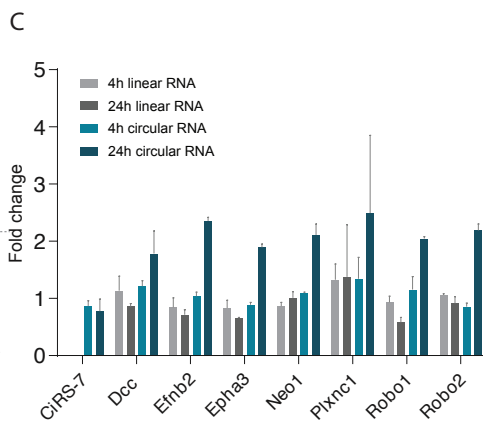
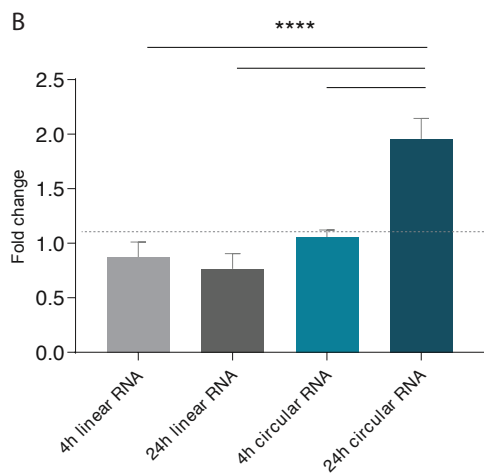
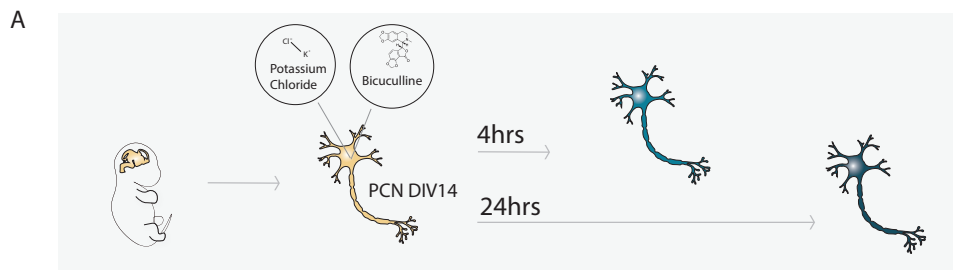
Neuronal activity is linked to axon guidance circRNA expression

Given that circRNAs generated from genes required for synaptic functions are enriched in synaptosome and neuropil samples (some of which were found to be upregulated in response to altered neuronal activity), we speculated that if axon guidance circRNAs

also regulate synaptic function, then their expression levels might be modulated by alterations in neuronal activity¹⁹. To test this hypothesis, we induced synaptic plasticity in PCNs by interfering with neuronal activity using 1) potassium chloride (KCl), enhancing neuronal activity due to Ca²⁺ influx after depolarization of the cells, and 2) bicuculline, a GABA receptor antagonist that enhances excitatory neuronal network activity (Figure 4A). First, we cultured PCNs for 14 days to allow them to mature, form synapses and start network connections with surrounding neurons. Then we added either KCL or bicuculline to the cell culture media for 4 hours, refreshed the media and collected the cells after an additional 4 or 24 hours. These timepoints were selected to observe short- and long-term effects of the chemically-induced change in neuronal activity. After harvesting the cells, their RNA was isolated and the expression of seven circRNAs (circDcc, circEfnb2, circEpha3, circNeo1, circPlxnc1, circRobo1, circRobo2 and ciRS-7 as a positive control) was analyzed using RT-qPCR. Interestingly, we found that the expression of all axon guidance circRNAs is upregulated in PCNs that were cultured for 24 hours after incubation with KCl (Figures 4B and 4C). The expression of ciRS-7 and the linear host gene transcripts were generally not altered. Together, these findings suggest that neuronal expression of axon guidance circRNAs is activity-dependent. However, bicuculline treatment in PCNs did not lead to an increase, but slight decrease in circRNA expression, while linear transcript expression was increased for most genes (Figures 4D and 4E). The difference between the effect of KCL and bicuculline may suggest that axon guidance circRNAs play a role in the activation, but not inhibition of neurons, which is in line with the finding that circRNAs are predominantly expressed in excitatory neurons²² (Chapter 2).

Figure 4 | Elevated levels of axon guidance circRNA expression after neuronal activation.

(A) Schematic of the neuronal activity assay. Mouse primary cortical neurons (PCN) were cultured for 14 days (DIV14) in vitro and potassium chloride (KCl) or bicuculline was added to the cells for 4 hours. The cells were analyzed with RT-qPCR for their circRNA (and linear host transcript) expression an additional 4 or 24 hours after treatment. CircRNAs are specifically upregulated in PCNs after stimulation with KCL as a group (B) and on an individual level (C) ($n = 2$ independent experiments; Two-way ANOVA with Tukey's multiple comparison post hoc test; **** $p < 0.0001$). Bicuculline treatment of PCN does not lead to altered circRNA expression as a group (D) and on an individual level (E) ($n = 1$; Two-way ANOVA with Tukey's multiple comparison post hoc test; * $p < 0.05$; $p = 0.017$ (24 hours linear vs. 4 hours circular); $p = 0.046$ (24 hours linear vs. 24 hours circular)).



DISCUSSION

CircRNAs are very abundant in neural tissue, but little is known about their general biology and function in neuronal cells. In order to investigate the role of axon guidance circRNAs in the developing mouse brain, we adapted the use of various tools for circRNA overexpression or knockdown. Targeting a select group of axon guidance circRNAs with overexpression vectors, siRNAs, shRNAs, AgoshRNAs and CRISPR-Cas13 resulted in altered expression levels of the circRNA molecules and their linear host gene transcripts *in vitro* and *in vivo*. In our hands, the knockdown of axon guidance circRNAs was most robust and specific *in vitro* using siRNAs. Analysis following knockdown of circRNAs in PCNs at different stages of maturation hinted at a possible role for certain axon guidance circRNA in neurite branching, albeit not convincing in mature cells (DIV9) due to large variability between the targeted neurons. Axon guidance circRNA siRNA-mediated knockdown in the mouse cortex *in utero* and overexpression in the retina, did not lead to clear aberrant morphological phenotypes. Lastly, we report that neuronal expression of axon guidance circRNAs is elevated as a result of neuronal activation.

The lack of efficient methods for the specific manipulation of circRNA levels has limited the ability to perform functional experiments and to define their function. Traditional molecular biology techniques for circRNA depletion tend to also alter the levels of their linear host gene transcripts. To overcome this, RNAi tools have been developed that specifically target the back-splice junction of circRNAs. This back-splice junction is nonetheless a very specific and limited sequence, which challenges the design of an optimal circRNA-specific siRNA without off-target effects. We observed this limitation in the efficiency of our siRNAs, shRNAs and AgoshRNAs. When the target sequence was shifted a few nucleotides upstream/downstream of the back-splice junction, either the linear transcript was degraded (we did not investigate this, but limited complementarity to an mRNA can also inhibit protein production) or circRNA knockdown was not efficient (in spite of specific siRNA design and modifications) (Figures 1C and 1F). Although AgoshRNAs are, according to literature, more efficient and specific compared to conventional shRNAs, we did not find support for this in our studies²⁵. Initially, *in vitro* experiments were hampered by suboptimal transfection and electroporation techniques, but also after successful lentivirus production, we found that shRNAs are more efficient in knocking down circRNAs than AgoshRNAs. Besides the manipulation tools described

in this study, the use of gapmers (antisense oligonucleotides that anneal to the back-splice junction of specific circRNAs and trigger degradation via a RNase H-mediated process) to knockdown specific circRNAs has been reported, but limited probe design may also hamper the efficiency of these molecules³¹. Other strategies to interfere with circRNA expression could include the deletion of flanking inverted RNA repeats or RNA binding proteins by CRISPR. However, this type of manipulation might also alter the levels of the linear host transcripts, which makes deletion experiments sub-optimal. The CRISPR-Cas13 system only targets specific RNA sequences using a guide RNA and our preliminary results indicate that it is an efficient strategy for future circRNA manipulation experiments (Figure 1G).

Using siRNAs we established a reproducible and specific knockdown for a select group of axon guidance circRNAs in PCNs. The downside of an siRNA-mediated knockdown is that the effect of an siRNA is generally short lasting, which limits their long-term use *in vivo*. An siRNA-mediated knockdown of 48 hours in the mouse cortex using *in utero* electroporation did not lead to clear morphological changes. Besides the short time window, other factors may have contributed to a lack of clear phenotype; siRNA concentrations were not optimal, functional redundancy occurred (via other circRNA isoforms from the same or from different genes), we did not target the right cell type or within the right time window, or changes that occurred were not detectable using the described techniques.

Interestingly, we demonstrated that neuronal activation using KCL increases axon guidance circRNA levels *in vitro*. This finding indicates that the neuronal expression of axon guidance circRNAs is activity-dependent. Neuronal activity is known to affect gene expression in multiple ways, and one potential novel way may thus be by interfering with circRNA levels. Using bicuculline no increased circRNA expression in PCNs was observed, which was described for certain circRNAs in a previous study¹⁹. However, the results of this study are difficult to compare to our findings, as the experiments of You et al. were conducted in rat neurons (compared to mouse), hippocampal slices (compared to cortical cells) and it involved circRNAs from a different gene family. It is interesting to speculate that our findings confirm that the observed effect is axon guidance circRNA-specific and that the expression of circRNAs is spatially regulated. Many circRNAs are enriched in synaptosomes, which might indicate active transport of circRNAs to synapses. Perhaps circRNAs interfere with local translation of mRNAs in the synapse in an activity-dependent

fashion which is important for synaptic plasticity³². Yet, not all circRNAs localize to the synapse and we have no direct proof that axon guidance circRNA specifically do so too¹⁹ (Chapter 2). For future experiments it would be interesting to monitor cell activation after circRNA manipulation *in vitro* and *in vivo* by using a multi electrode array (MEA) system which would allow us to investigate neuronal activity at a network level.

The question remains how we can extrapolate our current findings to speculate on the specific function of axon guidance circRNAs. First, we can systematically evaluate the characteristics of our selected circRNAs. All selected axon guidance circRNA isoforms are relatively small in size (around 400 nucleotides (nt)), compared to other circRNAs (e.g. ciRS-7 is around 3000 nts) (Supplementary Table 1). From the seven selected circRNAs (circDcc, circEfnb2, circEpha3, circNeo1, circPlxnc1, circRobo1 and circRobo2) only four contain exon 2 from the linear host transcript. It has been previously reported that exon 2 is often spliced into circRNAs, and therefore this appears not to be an axon guidance circRNA-specific feature. The majority of the selected circRNAs consist of multiple predicted exons, while circEfnb2 and circRobo2 only consist of one exon. Among the spliced exons, no general inclusion of similar protein-coding domains was observed (data not shown). Interestingly, the DCC gene can be considered a 'circRNA hotspot' as it produces 10 different circRNA isoforms in mice (Supplementary Table 4). Using the online Circinteractome and MIRDB tools, we predicted miRNA binding sites on the human homologues of the selected circRNAs^{33,34}. Although we noted that they are predicted to have binding sites for 10 to 30 miRNAs, depending on the specific circRNA, they were predicted to have only 1-2 binding sites for each miRNA (in contrast to ciRS-7 that has 70 binding sites for miR-7)^{2,3}. MiRNA sponging does not seem to be a general feature for circRNAs (including axon guidance circRNAs), but we could speculate that by sponging miRNAs, axon guidance circRNAs could contribute to enhanced protein synthesis in the growth cone or in synapses. This is interesting as axon guidance requires very specific timing, and transporting proteins along the axon takes time, while sponging can occur quick and locally. Looking at our axon guidance circRNA selection (that was based on specific high expression of axon guidance circRNAs during neuronal development) and on the function of the axon guidance genes from which these circRNA derive, we cannot see a clear pattern based on attraction/repulsion and/or ligand/receptor function. Whether proteins and circRNAs from the same host gene locus have similar functions is unknown, but studies indicate that circRNAs and mRNAs do not seem to co-localize¹⁹. Nonetheless there is a large cooperation and crosstalk between the different axon guidance molecules

needed for axonal navigation. In view of this complexity it is not entirely unlikely that circular axon guidance molecules are involved in some of these processes.

Although the Epha3 protein (a membrane-bound receptor that binds Ephrin family ligands present on neighboring cells, resulting in bidirectional signaling) is widely studied, nothing has been reported on the Epha3 circRNA, besides its differential expression during human fetal brain development and its upregulation in brains from patients with bipolar disorder^{35,36}. We observed that knockdown of circEpha3 in PCNs in immature neurons (DIV2) leads to less proximal branching, while this is not observed in mature neurons (DIV9). Although we did not observe morphological changes *in vivo*, these data suggest that the specific timing of circEpha3 expression in neurons is crucial for its potential role in neurite branching. Interestingly, these data also indicate that the Epha3 circRNA can fulfill diverse roles depending on the timing and context, which is something that is commonly observed in axon guidance (e.g. switching between attraction and repulsion or bidirectional signaling). However, additional experiments are necessary to dissect the precise role of circRNAs in neuronal development (Supplementary Figure 4) (Supplementary Table 5).

In summary, the findings in this chapter are interesting in the light of a recent debate in the field concerning circRNA function. However, understanding the exact role of axon guidance circRNA in neural circuit development remains a challenge. The ongoing development of tools to manipulate circRNA expression will aid us in obtaining better insight in the molecular mechanisms of action of axon guidance circRNAs in the near future.

MATERIALS & METHODS

Ethics statement

All animal experiments were performed in accordance to and approved by the CCD (Central Committee for animal research, The Netherlands), the University Medical Center Utrecht, the Dutch Law (Wet op Dierproeven 1996) and European regulation (Guideline 86/609/EEC).

Cell culture

Primary cortical neuron culture

Primary cortical neurons (PCNs) were cultured on coverslips (VWR, 18Ø) in 12-well plates (Costar 3513/3524). Coverslips were etched in 1 N HCl (Emsure) for 1 hour at 65 °C, washed and stored in 100% EtOH (Emsure). At the start of the experiment the coverslips were coated with 20 µg/ml Poly-D-Lysine-ornithine (Sigma Aldrich) solution for 30 minutes at room temperature (RT), washed with sterile PBS [1x] (Gibco) and coated with 40 µg/ml Laminin (Gibco) for 1 hour at 37 °C. The coverslips were washed with sterile PBS [1x] (Gibco) and used immediately to plate cells. PCNs were prepared from 14 days old C57/BL6 mouse embryos (E14). The embryos were removed from the uterus and collected in Leibovitz's L-15 medium (Gibco). Cortices were separated and the meninges were removed. The tissue was dissociated in 2.5% trypsin for 15 minutes at 37 °C. Following trypsinization, the cells were triturated in dissociation medium (10% Fetal Bovine Serum (FBS) (Gibco), 0.2% DNase (2 mg/ml, Roche) in Leibovitz's L-15 medium (Gibco)) with a 200 µl pipette. Dissociated cells were spun down for 1 minute at room temperature (IKA miniG), the supernatant was removed and the cells were resuspended in 1 ml Neurobasal Culture Medium (NB+) (Gibco) supplemented with 2% B27 [50x] (Gibco); 0.1% Pen/Strep (10 kU/ml Pen; 10 mg/ml Strep, Gibco); 0.1% Glutamine (Gibco); 5% 400 nm D-Glucose (Sigma Aldrich). Cells were plated on coated coverslips placed in 12-well plates. Cell were maintained at 37 °C in a humidified incubator with 5% CO₂ with half the medium changed every week. At the appropriate DIV cells were washed with PBS [1x] fixed in 4% PFA or lysed in Qiazol (Qiagen).

Ventral midbrain primary culture

Ventral midbrain primary cultures were prepared as described by Doucet-Beaupré et al. with the following modifications^{37,38}. In brief, ventral midbrains of E14 mouse embryos were micro dissected in dissection medium containing [1x] HBSS (Thermofisher), 0.7% D-Trehalose (AlfaAesar), and 16 mM Hepes (Thermofisher) and incubated for 15 minutes in 20 U/ml Papain and DNase (Worthington). After trituration in a BSA-containing trituration solution with fire-polished glass pipettes, dissociated cells were purified on a BSA column for 4 minutes at 200 x g at room temperature. The cell pellet of brains from one litter was resuspended in 1 ml full growth medium consisting of [1x] B27 PLUS Supplement (Thermofisher), [0.27x] Glutamax (Thermofisher), [1x] Penicillin/Streptomycin/Amphotericin (Thermofisher), and 7.3 mM D-Glucose in Neurobasal Plus medium (Thermofisher) and filtered through a 70 µm cell strainer to remove remaining debris. The cell count was determined with the Countess II FL Automated Cell Counter (ThermoFisher). 200 000 cells were plated in a drop in the center of a precoated (50 µg/ml Poly-L-Ornithine hydrobromide (Sigma) and 10 µg/ml Laminine (Sigma)) glass coverslip. Approximately 60 minutes after plating, wells were filled with warm medium. Half of the medium was refreshed every 2-3 days unless otherwise specified.

N2a culture

Neuro2a cells (N2a) were cultured in DMEM high glucose containing 10% fetal calf serum, L-glutamine and penicillin/streptomycin. Cell lines were maintained at 37 °C in a humidified incubator with 5% CO₂.

RNA isolation & reverse transcription

Total RNA was isolated from tissue samples and cultured cells using Qiazol reagent (Qiagen) and miRNeasy Mini Kit (Qiagen) following the manufacturer's instructions with minor modifications. RNA concentration was determined using a Nanodrop 2000 (Thermo Scientific). Complementary DNA (cDNA) was generated from RNA using Superscript IV reverse transcriptase (RT) (Invitrogen) with random (hexamer) primers (Thermo Fisher Scientific) following the manufacturer's instructions. Unless stated otherwise, per 20 µl reaction, 1 µg RNA was used.

Quantitative Real-time RT-PCR (qPCR)

Complementary DNA was diluted 10-fold with RNase-free water. In a 10 μ l PCR reaction using FastStart Universal SYBR Green Master ([ROX]; Roche) 4 μ l cDNA was used. For circRNA amplification, primers followed a divergent amplification design, in which the 5' primer was placed at the 3' end of the exon of interest and the 3' primer was placed at the 5' end. For linear RNA amplification, primers followed a standard convergent design. The reaction mix was added to a 96 or 384 well plate and amplification of the product was measured after incubation steps at 50 °C for 2 minutes and 95 °C for 10 minutes during 40 PCR cycles (95 °C for 15 seconds and 60 °C for 1 minute) using a QuantStudio 6-flex Real-Time PCR system (Life Technologies). A melting curve was generated afterwards by ramping the temperature from 60 °C to 95 °C. Amplification curves were analyzed using QuantStudio 6 and 7 Flex Real-Time PCR System Software (v1.0). Ct values were normalized to the geomean of the reference genes (Hprt1, Actb, Pgk, Tbp unless otherwise stated). Expression values were analyzed using the $2^{-\Delta\Delta Ct}$ method. If the fluorescent threshold was not reached after 40 PCR cycles, a value of 40 was used in the analysis. All qPCR reactions were conducted in technical triplicates. Primer (Integrated DNA Technologies) sequences are listed in Supplementary Table 3.

Activity assay

PCNs were prepared as described above. NB+ medium containing 40 mM KCl/NaCl (VRW chemicals/EMSURE) or 40 μ M bicuculline was added to the cells and incubated for at 37 °C with 5% CO₂. After 4 hours the medium was respired and replaced with normal NB+ medium. After an additional 4 hours/24 hours of incubation at 37 °C with 5% CO₂, the cells were lysed and collected in Qiazol (Qiagen).

CircRNA manipulation tools

Overexpression plasmid generation

Using primers specifically binding each side of the back-splice junction of the circRNA of interest, circRNA sequences were generated by RT-PCR (2 μ g cDNA (mouse whole brain), 10 pmol/ μ l forward and reverse primer, PFU buffer, PFU polymerase and 10 mM dNTPs. Annealing at 57 °C, elongation for 2 minutes at 72 °C, 30 cycles). Products were separated using gel electrophoreses on a 1% agarose gel and correct size products were isolated using a gel extraction kit PureLink DNA kit (Invitrogen) according to the manufacturer's

protocol. The DNA was polished and ligated into a pGEM®-T Easy Vector in a 3:1 insert : vector ratio following manufactures instructions. Next, the DNA was transformed in Dh5a competent cells. After blue/white colony selection on indicator plates colonies were propagated and plasmids were purified using the QIAprep Spin Miniprep Kit (Qiagen) following the manufactures instructions. Plasmid concentration was measured on a Nanodrop 2000 (Thermo Fisher Scientific) and 2 µg DNA was restricted during a sequential restriction with PaeI and SacII (1 µl enzyme in 50 µl volume for 4 hours at 37 °C with PaeI and overnight at 37 °C with SacII). The digested products were run on a 2% agarose gel, bands of the correct size were cut out and purified with the PureLink DNA kit (Invitrogen) following the manufactures instructions. Next, inserts were ligated into a pcDNA3.1(+)-Laccase2 MCS-ciRS7 Exon (Addgene) vector (with the ciRS-7 sequence digested out) with T4 DNA ligase (Roche) in a 3:1 insert : vector ratio O/N at 16 °C. The ligated plasmid was transformed in Dh5a competent cells. After blue/white colony selection on indicator plates colonies were propagated and plasmids were purified using QIAGEN plasmid Maxi kit (Qiagen). Plasmid concentration was measured on a Nanodrop 2000 (Thermo Fisher Scientific) and 2 µg DNA was restricted during a sequential restriction with PaeI (NEB) and SacII (NEB) (1 µl enzyme in 50 µl volume for 1 hour at 37 °C). The digested products were run on a 1% agarose gel, bands of the correct size were cut out and purified with the PureLink kit following the manufactures instructions. The correct sequence was verified by sanger sequencing with T7 and BGH primers (Macrogen).

SiRNA generation

SiRNAs were designed to target the back-splice junction of circRNAs of interest. Two siRNAs of approx. 21 nucleotides spanning the back-splice junction that had the highest score on the following criteria were selected; Moderate to low (30% - 52%) GC Content, at least 3 A/Us at positions 15-19 (sense), minimal internal repeats, A at position 19 (sense), A at position 3 (sense), U at position 10 (sense), no G/C at position 19 (sense), no G at position 13 (sense). SiRNAs were ordered with [dT][dT] overhangs and desalted (10 nM) (Sigma-Aldrich). Target sequences of siRNAs are listed in (Supplementary Table 2).

AgoshRNA generation

AgoshRNAs were designed as 21 nucleotide sequences with 100% complement to the back-splice junction, where 10 nucleotides align upstream of the back-splice junction of the circRNAs (downstream in linear counterpart) and 11 nucleotides align at the start of the sequence. In addition, AgoshRNA oligos contain overhangs matching to BbsI (Bpil)

restriction sites, a poly-T stretch and partially complementary sequences for hairpin formation, resulting in a total of 43 nt. The oligos were inserted downstream of a U6 promoter. The lentiviral backbone was a kind gift from Jørgen Kjems (iNano, University Aarhus, Denmark, unpublished). For cloning, 600 ng of the backbone was linearized for 1 hour at 37 °C in with 10 U BbsI (Thermofisher), [1x] restriction Buffer G (Thermofisher) and dH₂O to a total amount of 20 µl, and subsequently purified from a 1% Agarose gel with a Genomic DNA isolation kit (PureLink, Thermofisher). To anneal oligos prior to insertion into the vector, 1 µl (100 µM) of each oligo (forward and reverse) was mixed with [1x] T4 Ligase Buffer (Thermofisher) and dH₂O to a total of 100 µl, was heated for 5 minutes at 95 °C and let to be cooled off to room temperature. A ligation mix containing 50 ng of purified plasmid, 9 µl of annealed oligos, 1 µl 10 mM ATP, 10 U T4 Polynucleotide kinase (Thermofisher), 2 µl [10x] T4 Ligase Buffer (Thermofisher) and dH₂O up to 19 µl, was incubated for 30 minutes at 37 °C, followed by addition of 10 U T4 DNA ligase (Thermofisher) and incubation at 16 °C overnight. Ligation mix was transformed into Stbl3 competent E.coli according to manufacturer's protocol and plated on Ampicillin containing LB/Agar plates. Colonies were purified with a Qiagen MiniPrep Kit and sent for Sequencing (Macrogen). Positive clones were used for 2nd generation Lentivirus synthesis.

ShRNA generation

ShRNAs were designed to target the back-splice junction of circRmst. Three different shRNAs were designed – targeting directly the back-splice junction (last 11 nucleotides of the last downstream exon, 10 nucleotides of the first exon around the back-splice junction), shifted three nucleotides upstream or shifted three nucleotides downstream of the back-splice junction. The pLentiLox3.7 (pLL3.7), was a gift from Luk Parijs (Addgene plasmid # 11795; RRID:Addgene_11795) and was used as a third generation Lentivirus backbone which expresses the cloned shRNA under a U6 promoter in infected cells³⁹. A poly-A tail and matching restriction sites were added to the single-strand oligo encoding a 21-nucleotides sense target sequence, a 10-nucleotides loop sequence (TTGGATCCAA, biosettia.com) and the 21-nucleotides antisense target sequence (Supplementary Table 2). Annealed oligos were cloned into the previously with Xho1 and Hpa1 restricted pLL3.7 plasmid. Annealing of the two complementary oligos was obtained by incubation of 1 µM shRNA_FW, 1µM shRNA_REV with [1x] T4 Ligase Buffer (Roche) in dH₂O for 5 minutes at 95 °C. Subsequently, samples were left to cool down to room temperature. For linearization, 600 ng of the pLL3.7 plasmid was digested with 2.5 U HpaI (NEB), 20 U

XhoI (NEB) and [1x] Cut Smart Buffer (NEB) in H₂O for 2 hours at 37 °C. The linearized vector was purified by gel electrophoresis on a 1% agarose gel, followed by DNA isolation using the PureLink Quick Gel Extraction kit (Invitrogen). To ligate both components, 50-100 ng purified vector were incubated with different molecular ratios (1:1, 1:3) of oligos, 0.5 nM ATP, 10 U T4 Polynucleotide Kinase, [1x] T4 ligase buffer (Roche) and H₂O up to a total volume of 19 µl. After 30 min at 37 °C, 1 U T4 Ligase (Roche) was added for a following overnight incubation at 16 °C. To amplify and screen the plasmids, 5 µl of the ligation mix was transformed into 50 µl Stbl3 competent E.coli according to manufacturer's protocol and plated on Ampicillin containing LB/Agar plates. Colonies were tested for positive clones by DNA sequencing (Macrogen) after purification with QIAprepSpin Miniprep Kit (Qiagen). Positive clones were further amplified and used for third generation lentivirus synthesis.

Lentivirus generation

Both, second and third generation lentiviruses carrying AgoshRNA constructs were synthesized in HEK293T cells. Prior to transfection of the lentivirus generating plasmids, the medium was changed into low serum containing medium (DMEM high glucose, 2% FBS, 1% P/S). Envelope plasmid pMD2.G (Addgene ID 12259) and packaging plasmids for second generation (psPax2, Addgene ID 12260) or third generation (pRSV-Rev and pMDLg/pRRE, Addgene ID 12253 and 12251, respectively) were co-transfected with the Lentivirus transfer plasmid by incubation with the transfection agent PEI overnight. Per 15 cm dish, the transfection mix for second generation lentivirus (27.5 µg transfer plasmid, 9.6 µg pMD2.G and 17.8 µg psPax2) or third generation lentivirus (22.5 µg transfer plasmid, 7.9 µg pMD2.G, 15.6 pMDLg/PRRE, 5.6 µg pRSV-Rev) were incubated with 4 µl/µg DNA PEI in DMEM high glucose for 15 minutes prior to addition to the medium. The envelope and packaging plasmids were a gift from Didier Trono. Next day, fresh medium was added to the cells. The virus was harvested and concentrated from sterile filtered medium by ultracentrifugation (Beckman Coulter, 70Ti rotor) for 2,75 hours at an avg. of 32450 x g and 16 °C, 48 hours after transfection. The virus pellet was dissolved in 150 µl 0.5% BSA in PBS, aliquoted and stored at -80 °C until use. Titer determination of the concentrated viruses were evaluated by quantitative analysis of GFP expressing cells after infection of HEK293T in a dilution series, 48 hours post infection.

CRISPR-Cas13 generation

We generated CRISPR-Cas13 constructs as described in Konermann et al., 2018. In short, guide RNAs (gRNAs) targeting the circRNA and a non-specific control, were annealed and cloned into Addgene #51026 plasmid using the BbsI restriction enzyme; the sequence coding for CasRX protein is inserted in the Addgene #51026 plasmid.

Overexpression and knockdown assays

Transfection overexpression plasmid in N2a cells

N2a cells were transfected with overexpression constructs [1 µg] using Lipofectamine 2000 (Thermo Fischer Scientific) following manufactures instructions. Cell lines were maintained at 37 °C in a humidified incubator with 5% CO₂. After 2 days, cells were washed with PBS [1x], lysed in Qiazol (Qiagen) and processed for further analysis.

SiRNA electroporation in PCNs

Cells were electroporated in OptiMem medium (Gibco) with siRNAs [100 nM each] in combination with a pCx-GFP construct [1 µg/µl]. MISSION® siRNA Fluorescent Universal Negative Control #1, Cyanine 3 (Sigma-Aldrich) scrambled siRNA was used as a negative control. PCNs were electroporated at DIV0 in suspension in pre-chilled electroporation cuvettes (Nepagene) in the NEPA21 electroporator (electroporation settings: Poring pulse 175 V, duration 5 milliseconds, interval 50 milliseconds, 2 pulses, decay 10%, one direction. Transfer pulse 20 V, duration 50 milliseconds, interval 50 milliseconds, 5 pulses, decay 40%, two directions). After electroporation, the cells were plated in NB+ medium. Adherent PCNs (> DIV0) were electroporated with a Napagene Culture Electrode in pre-warmed OptiMem (electroporation settings: Poring pulse 200 V, duration 5 milliseconds, interval 50 milliseconds, 2 pulses, decay 10%, two directions. Transfer pulse 30 V, duration 50 milliseconds, interval 50 milliseconds, 5 pulses, decay 40%, two directions.) After electroporation, fresh medium was added to the cells. At 48 hours post electroporation, supernatant was removed, cells were lysed immediately in Qiazol reagent (Qiagen) and processed for further analysis.

AgoshRNA electroporation in PCNs

PCNs [1.000.000 cells] were electroporated at DIV0 in OptiMem medium (Gibco) with AgoshRNAs [10 ug plasmid] as described under siRNA electroporation. At DIV5 the supernatant was removed and cells were lysed immediately in Qiazol reagent (Qiagen) and processed for further analysis.

Sequential transfection overexpression vector and AgoshRNA in N2a cells

N2a cells were transfected with overexpression plasmid [1 µg] (+ 1 µg Td-Tomato plasmid) using Lipofectamine 2000 (Thermo Fisher Scientific) following manufactures instructions, 2 days prior to transfection with AgoshRNA [1 ug] (+ 1 µg pCAG-GFP). Cell lines were maintained at 37 °C in a humidified incubator with 5% CO₂. After 2 days, the cells were washed with PBS [1x], lysed in Qiazol (Qiagen) and processed for further analysis.

Lentivirus shRNA transduction ventral midbrain neurons

Cultured primary ventral midbrain neurons were transduced with shRNA lentivirus at DIV1. One hour prior to infection, half of the medium was removed from the cultured cells, sterile filtered and stored at 4 °C until the next day. Concentrated experimental Lentiviruses carrying the shRNA encoding plasmid or control viruses with only pII3.7 ("empty") were thawed to ca. 37 °C and added dropwise to each well to a multiplicity of infection (MOI) of five. Next day, virus containing medium was replaced by medium consisting of 50% fresh medium and 50% pre-conditioned medium from the day before. Seventy-two hours post infection, the medium was discarded and cells were collected in Qiazol (Qiagen). RNA isolation, cDNA synthesis and RT-qPCR were performed as described under 'RNA isolation & reverse transcription' and 'Quantitative Real-time RT-PCR (qPCR)' with minor modifications; *C.elegans* RNA was added to experimental RNA prior to cDNA synthesis as a spike-in control. Ct values corresponding to the expression levels were normalized to normalization genes (PI13a and Tbp) and to samples infected with the control virus.

Lentivirus AgoshRNA transduction PCNs

Cultured PCNs were transduced with AgoshRNA lentivirus to a multiplicity of infection (MOI) of 2 at DIV1. Concentrated experimental Lentiviruses carrying the AgoshRNA encoding plasmid or scrambled control viruses were thawed to ca. 37 °C and added dropwise to each well to MOI2. Next day, virus containing medium was replaced by medium consisting of 50% fresh medium and 50% pre-conditioned medium from the day before. At DIV6 medium was discarded and cells were collected in Qiazol (Qiagen).

CRISPR-Cas13 transfection N2a cells

CRISPR-Cas13 constructs were transfected in N2a cells (24 well plate with 50 000 cells/well in 500 µl medium) in a 1:1 ratio [250 ng gRNA vector: 250 ng CasRx vector]. After 24 hours the medium was replaced. After 2 days, the cells were washed with PBS [1x], lysed in Qiazol (Qiagen) and processed for further analysis. RNA isolation, cDNA synthesis and RT-qPCR were performed as described under 'RNA isolation & reverse transcription' and 'Quantitative Real-time RT-PCR (qPCR)' with minor modifications; 500 ng RNA was used for cDNA synthesis and Ct values were normalized to the Hprt1 reference gene.

Morphological analysis

Coverslips with PCNs subjected to siRNA knockdown were washed three times with pre-warmed PBS [1x] and fixed in paraformaldehyde (PFA) / sucrose [4%] for 10 minutes at room temperature 48 hours after electroporation. After fixation the coverslips were washed three times with PBS [1x] and blocked in 2.5% Bovine Serum Albumin, 0.5% Triton-X and 5% Normal-Goat-Serum (blocking buffer) for 1 hour at room temperature. The coverslips were incubated overnight at 4 °C in rabbit-anti-GFP primary antibody (Invitrogen A11122, 1:1000), washed three times with PBS [1x] and incubated in goat-anti-rabbit IgG Alexa Fluor 488 (Abcam 150077, 1:750) for 1 hour at room temperature. Coverslips were washed two times with PBS [1x] followed by a 4',6-diamidino-2-phenylindole (DAPI) [1 µg/ml] (Sigma, D-9564-10MG) staining for 10 minutes at RT. Coverslips were washed once more with PBS [1x] and mounted on Superfrost Plus object glasses (VWR) with FluorSave Mounting Medium Reagent (Calbiochem). Cells were imaged and neurite branching data was acquired in Fiji (v.1.0) using the Sholl Plugin. DIV0-2; 1 µm radius. DIV7-9; 5 µm radius. Longest neurite length was determined with Fiji (v.1.0) using the Simple Neurite Tracer Plugin.

***In utero* electroporation**

Pregnant C57Bl/6 mice at E14/E15 were deeply anaesthetized with Isoflurane (induction: 3 - 4%, surgery 1.5 - 2%) and the abdominal cavity was opened under sterile surgical conditions. The uterus was partially lifted out of the abdominal cavity and a siRNA/DNA/FastGreen mix (25 μ M siRNA (each) (cy3 negative control); 0,4 μ g/ μ l pCAG-GFP, FastGreen FCF (Sigma)) was injected in the lateral ventricles of the embryos using pulled glass capillary pipettes and a PL1-100 Pico injector (Harvard Apparatus). The brains of the embryos were electroporated using an ECM 830 Electro-Square-Porator (Harvard Apparatus) set to five unipolar pulses at 30 V (50 milliseconds interval and 950 milliseconds pulse length). The motor cortices were targeted by covering both sides of the brain with a platinum tweezer electrode while a third gold-plated Genepaddle (Thermo Fisher Scientific) was placed on top of the head. Embryos were placed back in the abdomen and abdominal muscles and skin sutured separately. The mother was awakened by release of the isoflurane. Embryos were collected at E16/E17 after cervical dislocation of the mother. The brains were dissected out and fixed in 4% PFA o/n at 4 °C. Brains were washed in PBS [1x] and 60 μ m vibratome sections were cut. Next, sections were blocked for 1 hour at room temperature in 10% FCS + 1% Triton-X in PBS. After three PBS [1x] washes, the sections were incubated in primary antibodies in PBS [1x] o/n at 4 °C. After three PBS [1x] washes, the sections were incubated in secondary antibodies in PBS [1x] for 1,5 hours at room temperature. Thereafter sections were washed two times with PBS [1x] followed by a 4',6-diamidino-2-phenylindole (DAPI) [1 μ g/ml] (Sigma, D-9564-10MG) staining for 30 minutes at room temperature. Sections were washed once more with PBS [1x] and mounted on Superfrost Plus object glasses (VWR) with FluorSave Mounting Medium Reagent (Calbiochem). Primary antibody used; Anti-green fluorescent protein (A11122 Life Technologies 1:1000) Secondary antibody used; Goat-anti-rabbit Alexa Fluor 488 (Abcam ab150077 1:750). Control and test conditions were distributed equally among the embryos in the uterus. Analysis images are based on coronal slices around the completion of the corpus callosum.

Postnatal surface electroporation

Postnatal day 2 (P2) C57Bl/6 mice were anaesthetized in a 4,5% Isoflurane chamber for 1 minute. An siRNA/DNA/FastGreen mix (25 μ M siRNA (each)(cy3 negative control), 0,4 μ g/ μ l pCAG-GFP, FastGreen FCF (Sigma)) was injected below the skull with a pulled glass capillary pipette and a mouth piece. The pipette tip was stopped from further penetration after first clearing the skull, which was indicated by the lack of further resistance felt just after piercing the skull. The capillary pipette was used to penetrate the skin and skull. Care was taken to avoid the cerebral arteries. After injection, brains were electroporated using an ECM 830 Electro-Square-Porator electroporator (Harvard Apparatus) set to five unipolar pulses at 90 Volt into the cortex. The cortices were targeted by covering both sides of the brain with a platinum tweezer electrode while a third gold-plated Genepaddle (Thermo Fisher Scientific) was placed on top of the head. After electroporation mice were placed on a heating pad prior to being returned to their mother. Brains were collected on postnatal day 5 (P5) and fixed in 4% PFA o/n at 4 °C. Brains were washed in PBS and 60 μ m vibratome sections were cut. Sections were subjected to immunohistochemistry as described under '*In utero* electroporation'.

Postnatal retinal electroporation

Postnatal day 1 (P1) C57Bl/6 mice were anesthetized on ice for several minutes. The eye epithelium was cut carefully with a sharp knife. Slowly siRNA/DNA/FastGreen mix (0,05 μ g/ μ l circEfnb2 overexpression vector/empty control, 0,4 μ g/ μ l pCAG-GFP, FastGreen FCF (Sigma)) was injected in the subretinal space/viscous space using a thin needle. The head of the injected pup was held between a platinum tweezer electrode with the injected eye adjacent to the positive pole electrode and the non-injected eye adjacent to the negative pole electrode. After injection, the retinas were electroporated using an ECM 830 Electro-Square-Porator electroporator (Harvard Apparatus) set to five unipolar pulses at 60 Volt. After electroporation the mice were placed on a heating pad prior to being returned to their mother 40. At postnatal day 8 (P8) the electroporated eyes were removed and fixed in 4% paraformaldehyde at 4 °C overnight. After the retinas were dissected away from the sclera, cornea, lens, choroid and retinal pigmented epithelium, they were embedded in 4% agarose and cut in 60 μ m section on the cryostat in PBS [1x]. Next, sections were blocked for 1,5 hours at room temperature in 5% BSA + 0,1% Triton-X in PBS. After three PBS [1x] + 0,1% Triton-X washes, the sections were incubated in primary antibodies in 2,5% BSA + 0,1% Triton-X in PBS [1x] o/n at 4 °C. After three

PBS [1x] + 0,1% Triton-X washes, the sections were incubated in secondary antibodies in 2,5% BSA + 0,1% Triton-X in PBS for 1,5 hours at room temperature. Thereafter sections were washed two times with PBS [1x] followed by a 4',6-diamidino2-phenylindole (DAPI) [1 µg/ml] (Sigma, D-9564-10MG) staining for 30 minutes at room temperature. Sections were washed once more with PBS [1x] and mounted on Superfrost Plus object glasses (VWR) with FluorSave Mounting Medium Reagent (Calbiochem). Primary antibodies used; Anti-Choline Acetyltransferase (ChAT) (AB144P Merck Millipore 1:200); Anti-Neural Cell Adhesion Molecule L1 (MAB5272 Merck Milipore 1:500), Anti-Map2 (801801 Biolegend (Covance) 1:500). Secondary antibodies used; Donkey-anti-mouse Alexa Fluor 568 (A10037 Life Technologies 1:750); Donkey-anti-rat Alexa Fluor 568 (A11077 Life Technologies 1:750); Donkey-anti-goat Alexa Fluor 568 (Abcam ab175474 1:750).

Microscopes

All immunofluorescent images were acquired using an Axioscope epifluorescent microscope (Zeiss) and a LSM 880 confocal microscope (Zeiss).

Statistical analysis

Statistical analyses were performed in GraphPad Prism version 8 (GraphPad Software). The number of experiments performed with independent cultures or mice, (n) unless otherwise stated, is indicated in the figure text. All data are represented as means and error bars represent as standard error of the mean (SEM). The significance is defined as * $p < 0.05$, ** $p < 0.01$, *** $p < 0.001$, **** $p < 0.0001$.

Acknowledgements

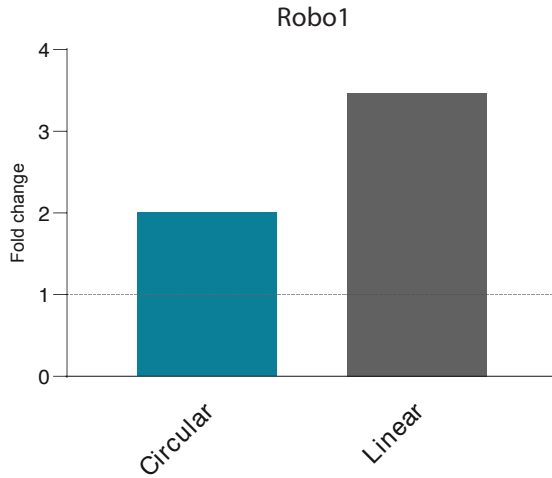
We would like to thank Christiaan van der Meer, Youri Adolfs, Marieke Verhagen and Eljo van Battum for their help with the *in utero*-, retinal and postnatal electroporations. This project has received funding from the Netherlands Organization of Scientific Research NWO (Personal grant DvR, part of Graduate Programme project (022.003.003) and NWO VICI to RJP) and the European Union's Horizon 2020 research and innovation programme under the Marie Skłodowska-Curie grant agreement No 721890 (circRTrain to RJP).

REFERENCES

1. Mattick, J. S. Non-coding RNAs : the architects of eukaryotic complexity. *2*, 986–991 (2001).
2. Memczak, S. et al. Circular RNAs are a large class of animal RNAs with regulatory potency. *TL - 495. Nature 495 VN-*, 333–338 (2013).
3. Hansen, T. B. et al. Natural RNA circles function as efficient microRNA sponges. *Nature 495*, 384–388 (2013).
4. Jeck, W. R. & Sharpless, N. E. Detecting and characterizing circular RNAs. *Nat. Biotechnol.* *32*, 453–61 (2014).
5. Rybak-Wolf, A. et al. Circular RNAs in the Mammalian Brain Are Highly Abundant, Conserved, and Dynamically Expressed. *Mol. Cell 870–885* (2014). doi:10.1016/j.molcel.2015.03.027
6. Salzman, J., Chen, R. E., Olsen, M. N., Wang, P. L. & Brown, P. O. Cell-Type Specific Features of Circular RNA Expression. *PLoS Genet.* *9*, (2013).
7. Westholm, J. O. et al. Genome-wide Analysis of Drosophila Circular RNAs Reveals Their Structural and Sequence Properties and Age-Dependent Neural Accumulation. *Cell Rep.* *9*, 1966–1981 (2014).
8. Zhao, Y., Alexandrov, P. N., Jaber, V. & Lukiw, W. J. Deficiency in the ubiquitin conjugating enzyme UBE2A in Alzheimer's Disease (AD) is linked to deficits in a natural circular miRNA-7 sponge (circRNA; ciRS-7). *Genes (Basel).* *7*, (2016).
9. Xu, H., Guo, S., Li, W. & Yu, P. The circular RNA Cdr1as, via miR-7 and its targets, regulates insulin transcription and secretion in islet cells. *Sci. Rep.* *5*, 1–12 (2015).
10. Zhang, Z. et al. Circular RNA: New star, new hope in cancer. *BMC Cancer* *18*, 1–10 (2018).
11. Hentze, M. W. & Preiss, T. Circular RNAs: splicing's enigma variations. *EMBO J.* *32*, 923–925 (2013).
12. Salzman, J., Gawad, C., Wang, P. L., Lacayo, N. & Brown, P. O. Circular RNAs are the predominant transcript isoform from hundreds of human genes in diverse cell types. *PLoS One* *7*, (2012).
13. Wilusz, J. E. & Sharp, P. a. A Circuitous Route to Are Gold Clusters in RF Fields. *Science (80-.).* *6–8* (2013). doi:10.1126/science.1238522
14. Guo, J. U., Agarwal, V., Guo, H. & Bartel, D. P. Expanded identification and characterization of mammalian circular RNAs. *Genome Biol.* *15*, 409 (2014).
15. Chen, C. Y. & Sarnow, P. Initiation of protein synthesis by the eukaryotic translational apparatus on circular RNAs. *Science (80-.).* *268*, 415–417 (1995).
16. Wang, Y. & Wang, Z. Efficient backsplicing produces translatable circular mRNAs. *Rna* *21*, 172–179 (2015).
17. Legnini, I. et al. Circ-ZNF609 Is a Circular RNA that Can Be Translated and Functions in Myogenesis. *Mol. Cell* *66*, 22–37.e9 (2017).
18. Pamudurti, N. R. et al. Translation of CircRNAs Article Translation of CircRNAs. *Mol. Cell* *1–13* (2017). doi:10.1016/j.molcel.2017.02.021
19. You, X. et al. Neural circular RNAs are derived from synaptic genes and regulated by development and plasticity. *Nat. Neurosci. advance on*, 603–610 (2015).
20. Suenkel, C., Cavalli, D., Massalini, S., Calegari, F. & Rajewsky, N. A Highly Conserved Circular RNA Is Required to Keep Neural Cells in a Progenitor State in the Mammalian Brain. *Cell Rep.* *30*, 2170–2179.e5 (2020).
21. Xu, K. et al. CircGRIA1 shows an age-related increase in male macaque brain and regulates synaptic plasticity and synaptogenesis. *Nat. Commun.* *11*, 1–15 (2020).
22. Piwecka, M. et al. Loss of a mammalian circular RNA locus causes miRNA deregulation and affects brain function. *Science (80-.).* *357*, (2017).
23. Kramer, M. C. et al. Combinatorial control of Drosophila circular RNA expression by intronic repeats , hnRNPs , and SR proteins. *2168–2182* (2015). doi:10.1101/gad.270421.115.3

24. Barrett, S. P. & Salzman, J. Circular RNAs: analysis, expression and potential functions. *Development* 143, 1838–1847 (2016).
25. Liu, Y. P., Karg, M., Herrera-Carrillo, E. & Berkhout, B. Towards antiviral shRNAs based on the AgoshRNA design. *PLoS One* 10, 1–20 (2015).
26. Konermann, S. et al. Transcriptome Engineering with RNA-Targeting Type VI-D CRISPR Effectors. *Cell* 173, 665–676.e14 (2018).
27. Breunig, J. J. et al. Rapid genetic targeting of pial surface neural progenitors and immature neurons by neonatal electroporation. *Neural Dev.* 7, 1 (2012).
28. Han, J. et al. The expression profile of developmental stage-dependent circular RNA in the immature rat retina. *Mol. Vis.* 23, 457–469 (2017).
29. Meganck, R. M. et al. Tissue-Dependent Expression and Translation of Circular RNAs with Recombinant AAV Vectors In Vivo. *Mol. Ther. - Nucleic Acids* 13, 89–98 (2018).
30. Piwecka, M. et al. Loss of a mammalian circular RNA locus causes miRNA deregulation and affects brain function. *Sci.* 8526, 1–14 (2017).
31. Ottesen, E. W., Luo, D., Seo, J., Singh, N. N. & Singh, R. N. Human survival motor neuron genes generate a vast repertoire of circular RNAs. *Nucleic Acids Res.* 47, 2884–2905 (2019).
32. Bramham, C. R. & Wells, D. G. Dendritic mRNA: Transport, translation and function. *Nat. Rev. Neurosci.* 8, 776–789 (2007).
33. Dudekula, D. B. et al. Circinteractome: A web tool for exploring circular RNAs and their interacting proteins and microRNAs. *RNA Biol.* 13, 34–42 (2016).
34. Chen, Y. & Wang, X. miRDB: an online database for prediction of functional microRNA targets. *Nucleic Acids Res.* 48, D127–D131 (2020).
35. Chen, B. J., Huang, S. & Janitz, M. Changes in circular RNA expression patterns during human foetal brain development. *Genomics* 111, 753–758 (2019).
36. Luykx, J. J., Giuliani, F., Giuliani, G. & Veldink, J. Coding and non-coding RNA abnormalities in bipolar disorder. *Genes (Basel)*. 10, 1–14 (2019).
37. Doucet-Beaupré, H. et al. Lmx1a and Lmx1b regulate mitochondrial functions and survival of adult midbrain dopaminergic neurons. *Proc. Natl. Acad. Sci. U. S. A.* 113, E4387–E4396 (2016).
38. Saxena, A. et al. Trehalose-enhanced isolation of neuronal sub-types from adult mouse brain. *Biotechniques* 52, 381–385 (2012).
39. Rubinson, D. A. et al. A lentivirus-based system to functionally silence genes in primary mammalian cells, stem cells and transgenic mice by RNA interference. *Nat. Genet.* 33, 401–406 (2003).
40. de Melo, J. & Blackshaw, S. In vivo electroporation of developing mouse retina. *J. Vis. Exp.* 1–7 (2011). doi:10.3791/2847
41. Constance, W. D. et al. Neurexin and neuroligin-based adhesion complexes drive axonal arborisation growth independent of synaptic activity. *Elife* 7, 1–33 (2018).

SUPPLEMENTARY DATA

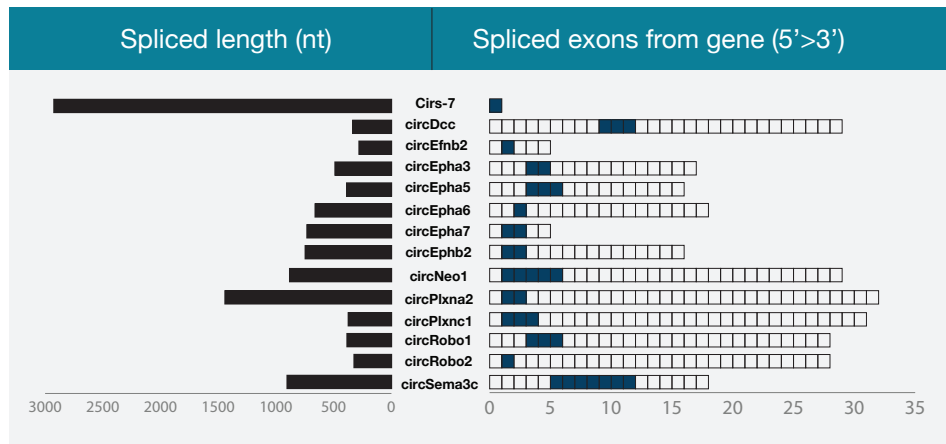


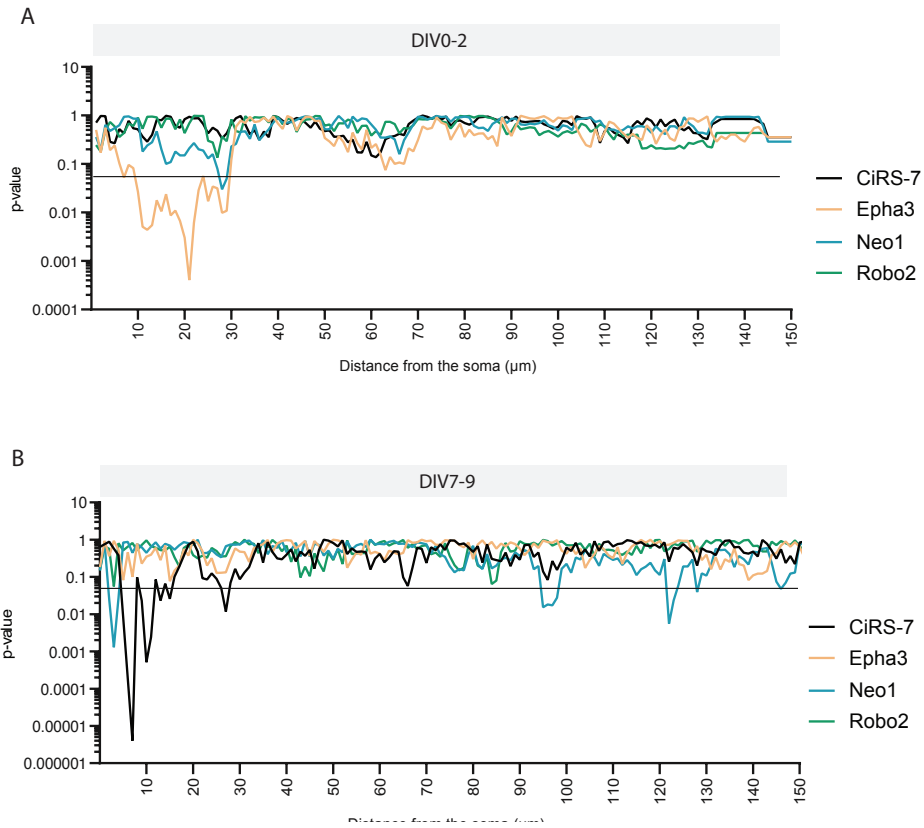
Supplementary Figure 1 | CircRobo1 overexpression in PCNs.

CircRobo1 overexpression is not efficient in primary cortical neurons (PCNs) (DIV0 - DIV5), N = 1.



Supplementary Table 1 | Characteristics of a selection of axon guidance circRNA isoforms



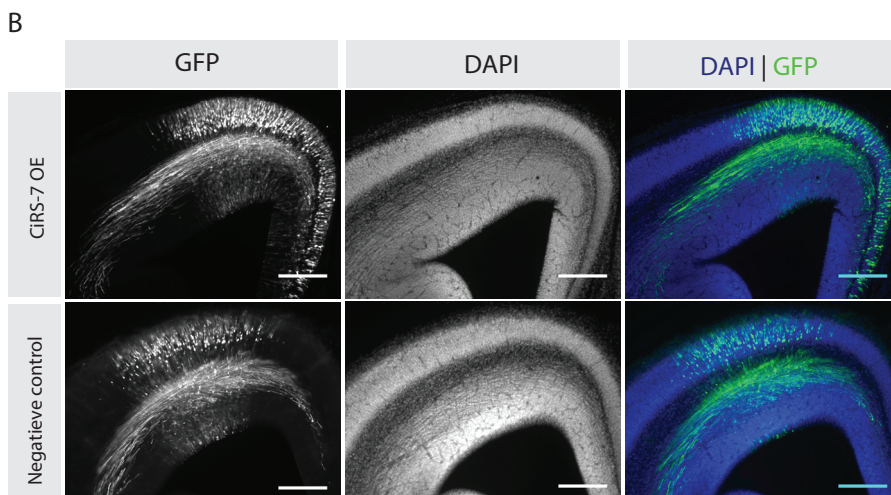
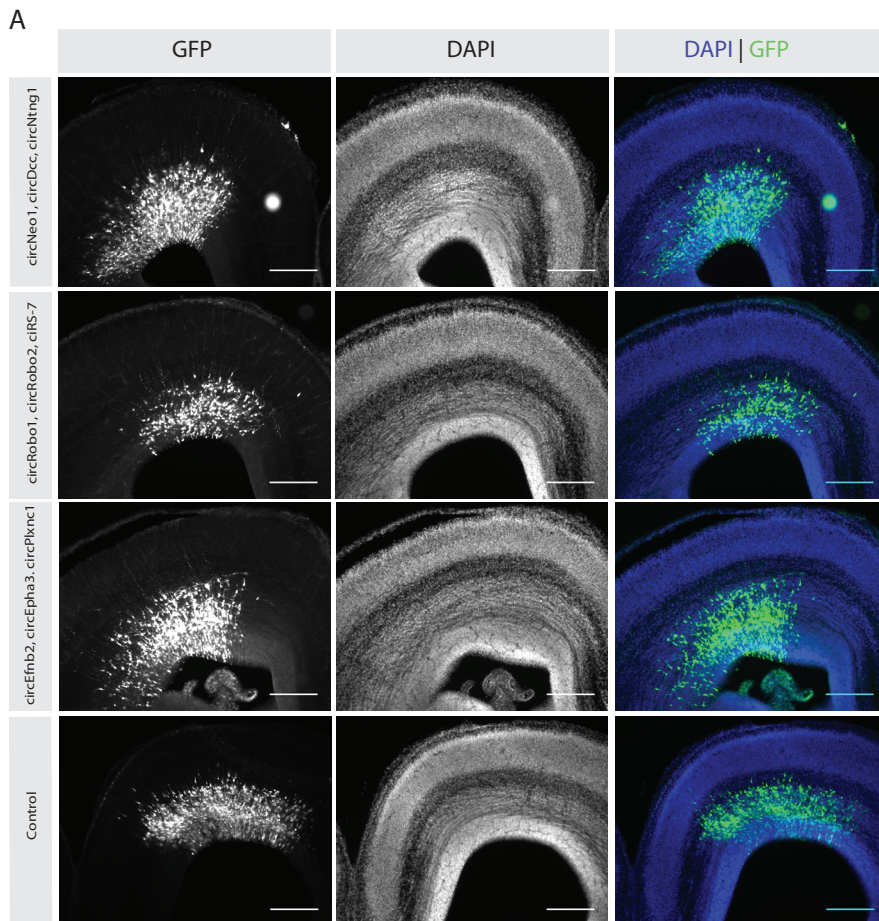


Supplementary Figure 2 | Statistics of Sholl analyses. (left)

Statistical significance determined of the Sholl-analyses was tested using a two-way ANOVA, and the Holm-Sidak test for post hoc comparisons with $\alpha = 0.05$. Indicated are the P-values of the Sholl analyses on PCN after siRNA knockdown on DIV2 (A) and DIV9 (B).

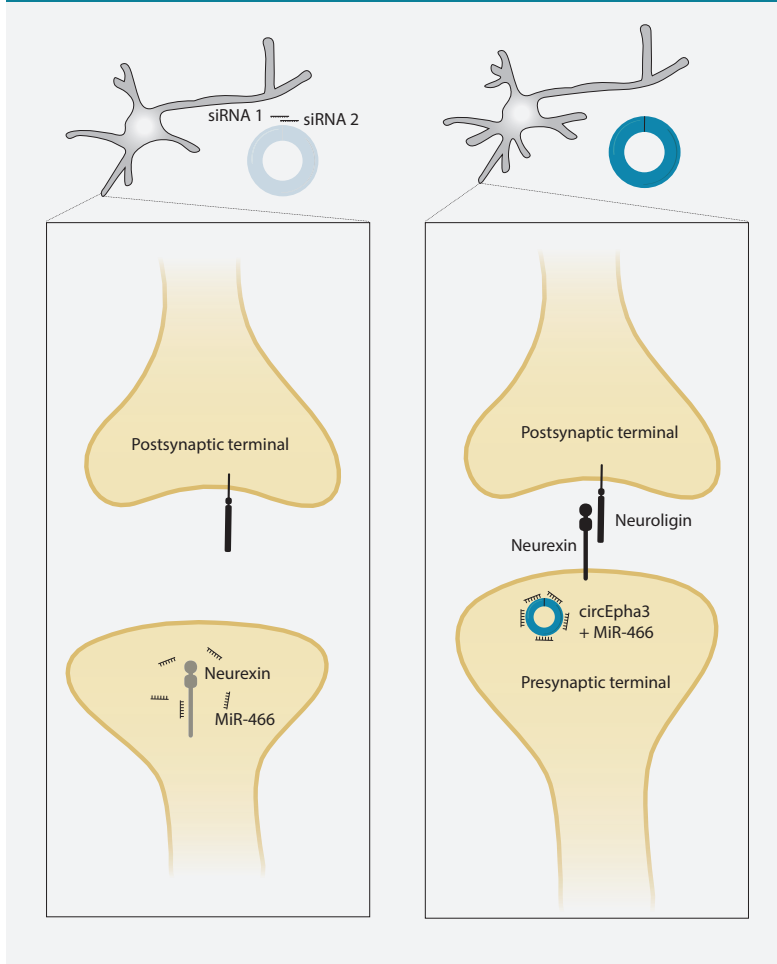
Supplementary Figure 3 | CircRNA manipulation using *in utero* electroporation.

(A) Representative images of *in utero* electroporated motor cortices of mouse embryos (E15 - E17) with either control (GFP) or group 1 siRNAs (*circNeo1*, *circDcc*, *circNtng1*), group 2 siRNAs (*circRobo1*, *circRobo2*, *ciRS-7*) or group 3 siRNAs (*circEfnb2*, *circEpha3*, *circPlxnc1*). Coronal view. Scale bar = 250 μm . (B) Representative images of *in utero* electroporated motor cortices of mouse embryos (E14 - E16) with either control (GFP) or *ciRS-7* overexpression construct. Coronal view. Scale bar = 250 μm .



3

Speculation on circEpha3 function in the synapse (DIV0-2)



Supplementary Figure 4 | Speculation on circEpha3 function in the synapse.

There are multiple miRNAs predicted to bind to circEpha3, of which miR-466 with high confidence (Supplementary Table 5). This miRNA is also predicted to bind the protein Neurexin 1 (Nrxn1), which is a presynaptic cell adhesion protein that connects neurons at the synapse via Neuroligin at the postsynaptic cell. It is interesting to speculate that when circEpha3 is normally expressed in the neuron (right panel), there is sponging of miR-466 by circEpha3 in the pre-synaptic terminal, resulting in a normal expression of Nrxn1 and accurate synaptic communication. Downregulation of circEpha3 (left panel) results in upregulation of free miR-466 in the pre-synapse due to a lowered sponging capacity. Next, miR-466 degrades Nrxn1, impairing communication of the protein via neuroligin on the membrane of the post-synapse. The altered dynamics between Nrxn1 and Neuroligin has an effect on neurite branch growth, resulting in decreased branching in immature PCNs (Constance et al., 2018). In more mature neurons circEpha3 is higher expressed as a result of increased synaptic activity and neuronal communication (circEpha3 is upregulated in activated PCN neurons after stimulation with KCL) and stabilization of branch formation has occurred as this timepoint. Therefore, the effects of a circEpha3 knockdown are less severe in matured neurons.

Supplementary Table 2 | List of probe sequences for circRNA manipulation tools

Tool	Probe	Sequence FW	Sequence RV
Overexpression	circRobo1	TTAATTAATACGAGGAGGAAAATCATG	CCGCGGCTTGAACGTCAAGTAGCG
Overexpression	circEfnb2	TTAATTAATTTCTACCCGGACAAGGCC	CCGCGGATATAATGTAGTAATCTTTG
AgoshRNA	circDcc	caccATGGAACTTGACACCTTGAGTTATCAAGGTG- CAAGTCCA	aaagTGGAACTTGACACCTTGATACTCAAGGTG- CAAGTCCAT
AgoshRNA	circEfnb2	caccACGGGTAGAAATATATAATGTATTATATATTT- TACCCG	aaagCGGGTAGAAATATATAATACATTATATATTTCTAC- CCGT
AgoshRNA	circEpha3	caccATGGTCGACAAGCAGCCTGATTAGGCT- GCTTGTCGACCA	aaagTGGTCGACAAGCAGCCTAATCAGGCTGCTTGTC- GACCAT
AgoshRNA	circNeo1	caccAAACTGGCTCCTTGACAGTTGCAAGGAG- CCAGTGTT	aaagAACTGGCTCCTTGCAACTGTGCAAGGAGC- CAGTGTTT
AgoshRNA	circPlxn1	caccATCCCTCTTTCTTTGTAACGA- CAAAGAAAGAGGGGA	aaagTCCCTCTTTCTTTGCTTAAAGAAAGAAAG- GGGAT
AgoshRNA	circRobo1	caccACCTCCTCGTATCTTGAAGTGTTCAGAGATC- GAGGAGG	aaagCCTCCTCGTATCTTGAACAGTTCAGATACGAG- GAGGT
AgoshRNA	circRobo2	caccAAAGACGAGATCATGCCACTCTGGCAT- GATCTCGTCTT	aaagAAGACGAGATCATGCCAGAAGTGGCATGATCTC- GTCTTT
ShRNA	circRmst I	TGGCTTCATGAGATACTCAGGTTTGATC- CAACCTGAGTATCTCATGAAGCCTTTTTCC	TCGAGGAAAA GGCTTCATGAGATACTCAGGTTTG- GATCCAACCTGAGTATCTCATGAAGCCA
ShRNA	circRmst II	TAATGGCTTCATGAGATACTCATTGGATCCAAT- GAGTATCTCATGAAGCCTTTTTTCC	TCGAGGAAAA AATGGCTTCATGAGATACTCATTG- GATCCAATGAGTATCTCATGAAGCCATTA
ShRNA	circRmst III	TTTCATGAGATACTCAGGTTGATTGGATCCAAT- CAACCTGAGTATCTCATGAATTTTTCC	TCGAGGAAAA TTCATGAGATACTCAGGTTGATTG- GATCCAATCAACCTGAGTATCTCATGAAA
Crispr-CasRx	gRNA circSATB1	aaacACAGATCACCTGCCAGAAGTGGCTT	aaaAAGCCAGTTCGGCAGGTGATCTGT
siRNA	ciRS-7	UCUGCCGUUCCAGGGUUU	CGUAUCCAGGGUUUCCAGU
siRNA	circDcc	UAACUCAAGGUGCAAGUUC	ACUCAAGGUGCAAGUCCA
siRNA	circEfnb2	ACUACAUUUAUUAUUUCUA	AUAUUAUUUACCCGGACA
siRNA	circEpha3	UAUCAGGCUUCUUGUCGA	UCAGGCUUCUUGUCACCA
siRNA	circNeo1	GCAAGGAGCCAGUUGUCA	CAAGGAGCCAGUUGUCGAA
siRNA	circPlxn1	CUCCGUUACAAGAAAGA	UCCCGUUACAAGAAAGAA
siRNA	circRobo1	ACAGUUCAAGAUACGAGGA	UCAAGAUACGAGGAGGAA
siRNA	circRobo2	GAGUGGCAUGAUCUCGUC	AGUGGCAUGAUCUCUCUU

Supplementary Table 3 | List of RT-qPCR probes (5' - 3')

Target	Species	Primer sequence forward	Primer sequence reverse
ciRS-7	mmu	GGCGTTTTGACATTGAGTT	GGAAGATCACGATTGCTGGA
circDcc	mmu	TTTTCTACTGGCCCTGGAAC	CCTTCAGTGCCAAGTGCTC
corcEfnb2	mmu	CAGACCAGACCAAGATGTGAAA	GTCCACTTTGGGGCAAATAA
circEpha3	mmu	GGTGGGCACTTAGCACACTT	GAGACAGTATGCCGCAGTCA
circNeo1	mmu	CTGAGGATGATGCTGGGACT	ACACTGGCTCTTGACAGT
circPlxnc1	mmu	GTGCCTCCCGTTACAAGAA	CGTCAGGTGAGAGTGATCA
circRobo1	mmu	TATGGTCGGGAAAGCTGAAG	ACTTCCAGCATCGCTTTTA
circRobo2	mmu	TGGAAGTGGCATGATCTCGT	GTTCAGAGTGGTGGGCTCTC
circSatb1	mmu	GCCAGTTCTGGCAGGTGATC	CCCTTCGGATCACTCACATTG
circRmst1	mmu	GAATGGCTTCATGAGATACTCA	CAGACAATCTGGCCATGTCTG
Dcc	mmu	CCCTTACACCCGCTTTTGTC	CCCAGGGAGGCCGTTTTA
Efnb2	mmu	GGTTTTGTGAGAAGTGCAT	GGCCTTGTCCGGGTAGAAT
Eha3	mmu	CAGCCTTCCAACGAAGTTAATCT	TGCACACCTGGTAAGTCTGA
Neo1	mmu	TTGCTCGGCATATTCTGAGCC	TGGCGTCGATCATCTGATTCTAA
Plxnc1	mmu	GTGTGGCGATCTGAGCAAG	GTATAGGCGAGAGAGCCTGTT
Robo1	mmu	TGGTCATCCCCTCTCTGGTT	ACGGGGTTCCGTGAGAATC
Robo2	mmu	TGATGGATCTGCTTCTGTC	GTCGGCCCTCTGCTTACAG
Satb1	mmu	CATGTTACCAGTTTTCTGCGTG	GTGAATAGCCTAGAGACAGCAA
Rmst1	mmu	TTGAGAGCTCGGCCAATT	CTCAGGATCGGGTGACAAT
Hprt1	mmu	ATGGGAGGCCATCACATTGT	ATGTAATCCAGCAGGTCAGCAA
Actb	mmu	AGCCATGTACGTAGCCATCC	CTCTCAGCTGTGGTGGTGAA
Pgk	mmu	GATGGTGTCCCATGCCTGA	AGGCATTCTCGACTTCTGGG
Tbp	mmu	CCACAGCTCTTCCACTCACA	GCCGTACAATCCCAGAAGTCT
Rpl13a	mmu	GGGGTTGGTATTATCCGCT	TGTGGCCAAGCAGGTAAGTCT
Tbb-2	cel	CAAACTCTGGGAGGTCATCT	CATACTTCCGTTGTTGGC

Supplementary Table 4 | *CircRNA isoforms of axon guidance circRNAs in mice*

Gene name	Position	Strand	circRNA ID	Genomic length	Spliced length
Cdr1	chrX:58436422-58439349	+	mmu_circ_0001878	2927	2927
Dcc	chr18:71968713-71985941	-	mmu_circ_0007490	17228	573
Dcc	chr18:71707073-71708762	+	mmu_circ_0007487	1689	1689
Dcc	chr18:71701898-71708805	-	mmu_circ_0007486	6907	338
Dcc	chr18:71480684-71502431	-	mmu_circ_0000893	21747	573
Dcc	chr18:72114407-72129124	-	mmu_circ_0007491	14717	14717
Dcc	chr18:71838471-71838946	-	mmu_circ_0007488	475	475
Dcc	chr18:71605990-71616666	-	mmu_circ_0007485	10676	253
Dcc	chr18:71480684-71538481	-	mmu_circ_0007483	57797	1221
Dcc	chr18:71839114-71841970	-	mmu_circ_0007489	2856	276
Dcc	chr18:71487052-71502431	-	mmu_circ_0007484	15379	456
Efnb2	chr8:8620313-8639489	-	mmu_circ_0015032	19176	1154
Efnb2	chr8:8639205-8639489	-	mmu_circ_0015034	284	284
Efnb2	chr8:8639205-8641256	-	mmu_circ_0015035	2051	2051
Epha3	chr16:63566404-63603459	-	mmu_circ_0006367	37055	1099
Epha3	chr16:63598015-63652376	-	mmu_circ_0006369	54361	921
Epha3	chr16:63772735-63773396	-	mmu_circ_0000697	661	661
Epha3	chr16:63583213-63603459	-	mmu_circ_0006368	20246	755
Epha3	chr16:63652040-63653404	-	mmu_circ_0000696	1364	492
Neo1	chr9:58724402-58728449	+	mmu_circ_0015726	4047	4047
Neo1	chr9:58837997-58838315	-	mmu_circ_0015732	318	318
Neo1	chr9:58723577-58723708	-	mmu_circ_0015725	131	131
Neo1	chr9:58750720-58752358	-	mmu_circ_0015729	1638	303
Neo1	chr9:58760954-58778922	-	mmu_circ_0015730	17968	1107
Neo1	chr9:58803765-58838315	-	mmu_circ_0015731	34550	1161
Neo1	chr9:58741681-58778922	-	mmu_circ_0015728	37241	2119
Neo1	chr9:58736207-58741829	-	mmu_circ_0015727	5622	480
Neo1	chr9:58826431-58838315	-	mmu_circ_0001779	11884	885
Plxnc1	chr10:94289915-94315362	-	mmu_circ_0002592	25447	1629
Plxnc1	chr10:94369098-94385404	-	mmu_circ_0002595	16306	377
Plxnc1	chr10:94304209-94315362	-	mmu_circ_0002593	11153	913
Plxnc1	chr10:94273409-94276045	-	mmu_circ_0002591	2636	282
Plxnc1	chr10:94327564-94329632	-	mmu_circ_0002594	2068	191
Robo1	chr16:72744618-72744922	-	mmu_circ_0006382	304	304
Robo1	chr16:72933457-72962570	+	mmu_circ_0006389	29113	685

3

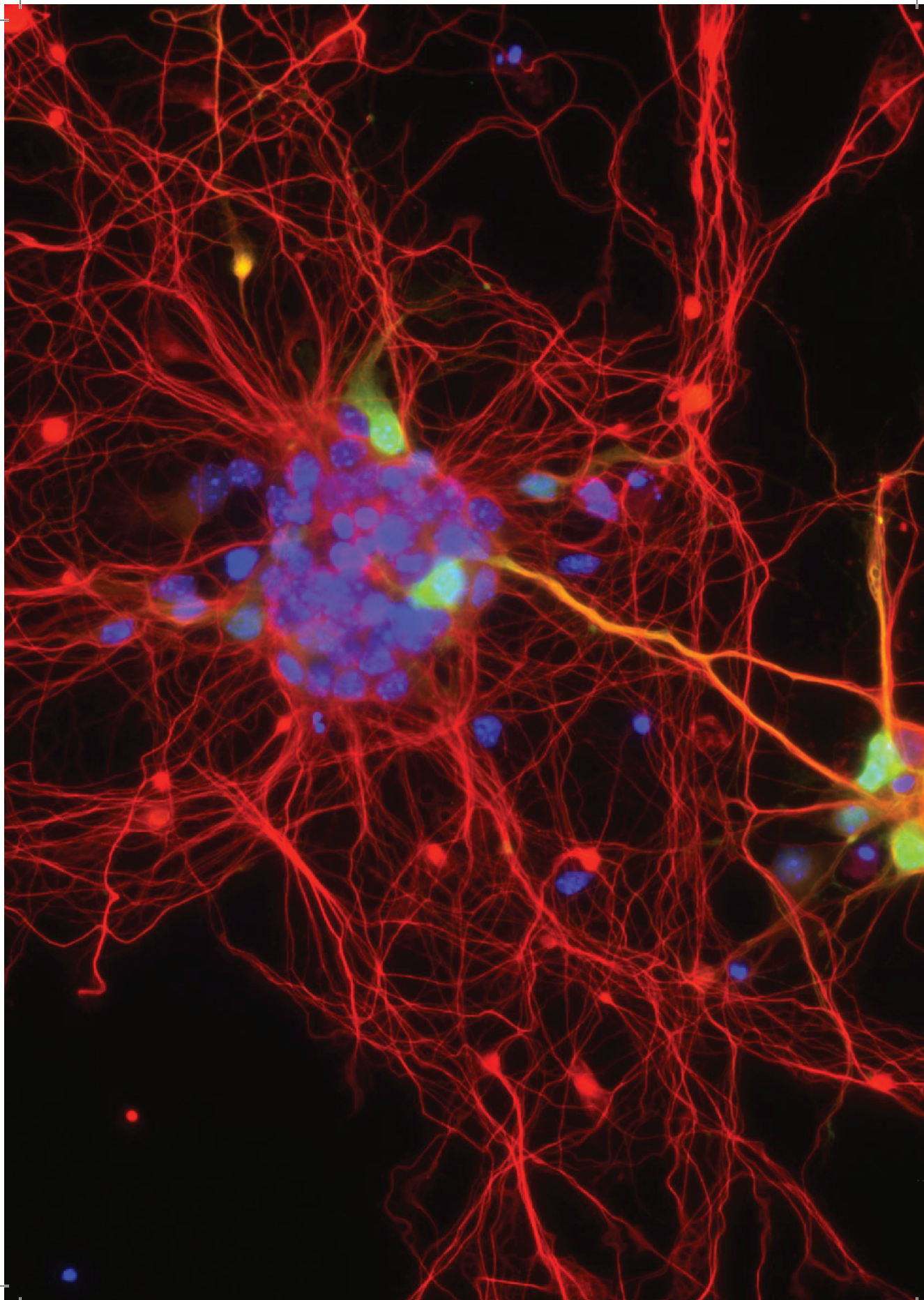
Robo1	chr16:73044815-73045022	-	mmu_circ_0006390	207	207
Robo1	chr16:72933457-72934057	+	mmu_circ_0006388	600	260
Robo1	chr16:72904874-72936031	+	mmu_circ_0006385	31157	546
Robo1	chr16:72933457-72936031	+	mmu_circ_0000698	2574	388
Robo1	chr16:72742370-72742697	+	mmu_circ_0006381	327	327
Robo2	chr16:73916342-73985957	-	mmu_circ_0006393	69615	2949
Robo2	chr16:74352795-74353122	-	mmu_circ_0000700	327	327
Robo2	chr16:73928268-73948630	-	mmu_circ_0006394	20362	916
Robo2	chr16:73956732-73985957	-	mmu_circ_0000699	29225	1566
Robo2	chr16:73948447-73985957	-	mmu_circ_0006395	37510	1749
Robo2	chr16:74240914-74242562	+	mmu_circ_0006398	1648	1648
Robo2	chr16:73982293-73982394	+	mmu_circ_0006396	101	101
Robo2	chr16:74191921-74193407	+	mmu_circ_0006397	1486	1486

Supplementary Table 5 | MiRNAs predicted to bind to circEpha3

miRNA Name	Gene	Gene description
mmu-miR-466i-5p	Nrxn1	neurexin I
	Asb13	ankyrin repeat and SOCS box-containing 13
	Lrrc32	leucine rich repeat containing 32
	Unc5d	unc-5 netrin receptor D
	Tmem236	transmembrane protein 236
mmu-miR-466k	Nrxn1	neurexin I
	Asb13	ankyrin repeat and SOCS box-containing 13
	Lrrc32	leucine rich repeat containing 32
	Unc5d	unc-5 netrin receptor D
	Tmem236	transmembrane protein 236
mmu-miR-466d-5p	Nrxn1	neurexin I
	Ttc4	tetratricopeptide repeat domain 4
	Cplx2	complexin 2
	Asb13	ankyrin repeat and SOCS box-containing 13
	Lrrc32	leucine rich repeat containing 32
mmu-miR-466l-5p	Nrxn1	neurexin I
	Asb13	ankyrin repeat and SOCS box-containing 13
	Lrrc32	leucine rich repeat containing 32

	Unc5d	unc-5 netrin receptor D
	Tmem236	transmembrane protein 236
mmu-miR-6903-3p	Nrxn1	neurexin I
	Calcoco1	calcium binding and coiled coil domain 1
	Tmem236	transmembrane protein 236
	Dmd	dystrophin, muscular dystrophy
	Zfp248	zinc finger protein 248
mmu-miR-293-5p	Plagl1	pleiomorphic adenoma gene-like 1





CiRS-7 miRNA interactome and function in the healthy and epileptic brain

Daniëlle van Rossum¹, Andreia Gomes Duarte¹, Lance Fredrick Pahutan Bosch¹, Vamshidhar R. Vangoor¹, and R. Jeroen Pasterkamp¹

¹ Department of Translational Neuroscience, UMC Utrecht Brain Center, University Medical Center Utrecht, Utrecht University, Utrecht 3584 CG, the Netherlands

*A 'neuronal galaxy' of primary cortical neurons - Winner of the Bioimaging Utrecht Image contest 2017
(Image taken with a Zeiss LSM 880 confocal microscope)*

ABSTRACT

CiRS-7 is the first characterized and most studied circular RNA (circRNA). It is highly conserved across species and can sequester multiple microRNAs (miRNAs) including miR-7, miR-671 and miR-135a, a process known as miRNA sponging. Importantly, these miRNAs have been associated with various diseases. Recent reports from our lab indicate that miR-135a is associated with temporal lobe epilepsy (TLE). However, the exact role of the interaction between ciRS-7 and miR-135a in a disease context remains unclear. In this study, we systematically investigated the expression patterns of miR-7, miR-671 and ciRS-7 in the developing mouse brain. Furthermore, we analyzed ciRS-7 and miR-135a levels in TLE patient material (with and without hippocampal sclerosis) and found that ciRS-7 and miR-135a are both significantly downregulated in this tissue. The inverse expression correlation between ciRS-7 and miR-135a was observed *in vitro* after knockdown or overexpression of one of the two molecules, suggesting a biological interaction. The functional meaning of the relationship between ciRS-7 and miR-135a in TLE pathology remains to be further explored, but the presented data could serve as a meaningful starting point from which to conduct further studies.

INTRODUCTION

Circular RNAs (circRNAs) are long non-coding RNAs that are dynamically expressed in various tissues in a spatial and temporal manner¹⁻³. Amongst the many circRNAs enriched in the brain, Cerebellar Degeneration-Related Protein 1 Anti-sense circular RNA sponge for microRNA-7 (ciRS-7) has stood out to the research community due to various reasons. Firstly, ciRS-7 expression is highly conserved across species, dynamically expressed in the brain and is not detectable as a linear transcript. Next, human ciRS-7 has a large number of microRNA (miRNA) binding sites^{4,5}. MiRNAs are small non-coding RNAs that are processed by Drosha and Dicer in the nucleus and the cytoplasm, respectively. These small molecules can bind with their seed area to the 3' untranslated region of target RNAs, including circRNAs, and affect gene regulation. Interestingly, the sequence of human ciRS-7 (1485 nucleotides in size) contains over 70 partially complementary binding sites for microRNA-7 (miR-7(-5p)), 1 fully complementary binding site for microRNA-671 (miR-671(-5p)), 6 partially complementary binding sites for microRNA-135a (miR-135a(-5p)) and has been predicted to bind a few other miRNAs with lower affinity, thereby far outnumbering

other circles (e.g. the Sry circRNA contains 16 binding sites for miR-138, but most circRNA have single to none predicted miRNA binding sites 6) (Figure 1A)^{4,5,7,8}.

The extent to which ciRS-7's binding sites are complementary to miR-7, miR-671, and miR-135a has led to speculations about ciRS-7's possible functions. The full complementarity of miR-671 to ciRS-7 can induce AGO2-mediated cleavage of ciRS-7 upon binding, whereas ciRS-7 may bind large quantities of miR-7 without resulting in ciRS-7 cleavage (Piwecka et al., 2017). By binding large numbers of miR-7, ciRS-7 could prevent the miRNA from interacting with its targets, thereby inhibiting its activity, a process also known as miRNA sponging¹¹⁻¹³. Experimental evidence has provided further insight into this interaction. In ciRS-7 knock-out mice the expression of miR-7 and miR-135a is downregulated in various brain regions (e.g. cerebellum, cortex, hippocampus), while miR-671 is upregulated^{10,14}. Moreover, in cell lines depleted of ciRS-7, miR-7 target mRNAs are down-regulated, fueling speculations on a functional interaction between the molecules¹⁴.

Recent studies have provided evidence for the deregulation of ciRS-7 and its binding miRNAs as an important regulatory factor in the pathogenesis and progression of different types of cancers and neurological diseases. CiRS-7 overexpression (or miR-7 knockdown) was reported to decrease the size of the midbrain in zebrafish embryos, while miR-7 is able to downregulate important players involved in the clearance of amyloid peptides in Alzheimer's disease affected tissues (e.g. UBE2A) and thereby contribute to neuronal degeneration^{15,16}. Vice versa, miR-7 protects cells against oxidative stress in Parkinson's disease by downregulating α -synuclein¹⁷. Furthermore, overexpression of ciRS-7 in the bladder inhibits the proliferation of bladder cancer cells by sponging miR-135a specifically, providing further evidence for their functional relationship¹⁸.

Various miRNAs have been associated with the pathogenesis of epilepsy, a chronic neurological disease characterized by recurrent seizures. Temporal lobe epilepsy (TLE) is a subclass of adult epilepsy that often subsides with cases of hippocampal sclerosis. Interestingly, a large number of miRNAs are dysregulated in human hippocampal tissue resected from TLE patients compared to healthy controls¹⁹. Of those dysregulated miRNAs, miR-135a is of particular interest as it has been reported to be involved in the function of the synapse and in establishing neuronal morphology (e.g. promoting axon growth and branching and cortical neuronal migration)²⁰. A recent study revealed that miR-135a is highly upregulated in both experimental and human TLE and that silencing

of miR-135a reduces seizure activity at the spontaneous recurrent seizure stage²¹. In all, these findings indicate that a complex of various cellular and molecular network processes contribute to epilepsy pathogenesis, but how the interaction between ciRS-7 and miR-135a contributes to the disease is not understood.

The wide array of processes that ciRS-7 and miR-7, miR-671 and miR-135a are proposed to be involved in indicate how vital these RNAs are in regulating neural systems. A systematic overview of the expression of these molecules could give insight in their function. Although ciRS-7 is the most intensively studied circRNA molecule, only its expression at the adult stages has previously been explored^{10,11}. In this study we provide an overview of ciRS-7, miR-7 and miR-671 expression throughout mouse brain development and in primary neurons using RT-qPCR. Moreover, we report on the spatial expression of ciRS-7, miR-7, miR-671 and miR-135a using single molecule fluorescent *in situ* hybridization (smFISH). Next, we show that ciRS-7 and miR-135a significantly downregulated in WO TLE patient material, and note that ciRS-7 and miR-135a display an inverse correlation in various *in vitro* systems after manipulation of one of the molecules, whereas we observe a positive correlation between ciRS-7 and miR-135a expression mouse *in vivo* systems (e.g. the ciRS-7 knockout mouse). With these data, we speculate how an interplay and disbalance between ciRS-7 and miR-135a could contribute to epileptogenesis. This is of interest, as a focused investigation on the relationship between these molecules could begin to unravel their role in health and disease.

RESULTS

CiRS-7, miRNA-7 and miRNA-671 expression in the developing mouse brain

Although expression of ciRS-7 has been reported in the adult human and the adult mouse brain, no systematic study on the expression of this molecule, and of miR-7 and miR-671, has been performed throughout brain development. Because an overview of the expression of these molecules may provide insight into their possible function, we investigated the expression of the three molecules in the whole mouse brain, and in two major brain regions where ciRS-7 is expressed, the cortex and hippocampus. Using RT-qPCR we analyzed the level of expression of ciRS-7, miR-7 and miR-671 at different

developmental timepoints from early embryonic stages until adulthood, examining a wide window of brain development (E12, E15, E18, P5, P25, P100 and P365) (Figure 1B). We observed that ciRS-7, miR-7 and miR-671 exhibit similar expression patterns in the developing mouse hippocampus, and miR-7 and miR-671 in the cortex. The maturation of primary hippocampal neurons (PHN) *in vitro* mimics the expression changes (i.e. decrease over time) seen in the *in vivo* samples (Figure 1C). Interestingly, while miR-7 and miR-671 expression steadily increases in the hippocampus, their expression specifically decreases in the brain as a whole. During primary cortical neuron (PCN) maturation miR-7 and miR-671 expression levels steadily decrease and unlike the miRNAs, ciRS-7 expression in primary culture diverges from the *in vivo* data, as it only slightly accumulates over time.

CiRS-7 is downregulated in TLE W0 and W4 patient material

We next investigated the expression and possible regulatory miRNA network of the ciRS-7 in TLE patient material as certain circRNAs and miRNAs are reported to be dysregulated in TLE. Hippocampal W0 and W4 TLE tissue that was surgically removed from epilepsy patients was processed for RT-qPCR analysis (Figure 2A). We observed that ciRS-7 is significantly downregulated in both W0 and W4 material compared to healthy control tissue (Figures 2B and 2C). In W4 patient material, ciRS-7 expression is significantly lower as compared to W0 material (Supplementary Figure 2A).

MiRNA-135a binds to ciRS-7 and is regulated in TLE W0 and W4 patient material

Next, we performed high-throughput sequencing of RNA isolated by crosslinking immunoprecipitation (HITS-CLIP) from W0 TLE patients and healthy controls (Figure 2D). Subsequent analysis showed that in W0 tissue dysregulated ciRS-7 is specifically bound by miR-135a (Supplementary Table 2). Using RT-qPCR we show that miR-135a is downregulated in TLE W0 tissue compared to healthy controls (Figure 2E)(similar to miR-7, miR-671 and ciRS-7 (Supplementary Figures 2C and 2D)). These findings are in line with previous studies reporting that miR-135a is downregulated in W0 tissue (and upregulated in W4 material)^{19,21}. Interestingly, not all detected miRNAs are expressed significantly different in W0 patient tissue, suggesting a functional relationship between ciRS-7 and miRNA-135a in the TLE brain (Supplementary Figure 2B).



Figure 1 | CiRS-7 interacts with miR-7, miR-671 and miR-135a.

(A) Schematic of (human) ciRS-7 and miRNA interaction. miR-7 and miR-135a have partial complementary binding sites to ciRS-7 and miR-671 has full complementary binding sites to ciRS-7. (B) CiRS-7, miR-7 and miR-671 are expressed in different regions (whole brain, cortex and hippocampus) and at different ages (embryonic day 12 (E12); embryonic day 15 (E15); embryonic day 18 (E18); postnatal day 5 (P5); postnatal day 25 (P25); postnatal day 100 (P100); postnatal day 365 (P365)) in the mouse brain. (C) CiRS-7, miR-7 and miR-671 are dynamically expressed during mouse primary hippocampal neuron (PHN) and primary cortical neuron (PCN) maturation *in vitro*. DIV = Days *in vitro*.

CiRS-7 and miR-135a have a positive *in vivo* and a negative *in vitro* expression correlation in mice

In order to understand the role of ciRS-7 and miR-135a in TLE pathogenesis, we investigated their expression *in vivo* and *in vitro*. Since most circRNAs and miRNAs are expressed in a very specific spatial and temporal manner, we hypothesized that if ciRS-7 and miR-

135a demonstrate similar (sub)cellular localization patterns, this could lend support to the idea that these molecules have a functional relationship with each other. Therefore we looked at the expression of ciRS-7 and miR-135a during mouse brain development and observed for both molecules decreased expression at early postnatal stages and an accumulation during aging (Figure 3A). Moreover, we made efforts to perform systematic co-localization in sections of the adult mouse brain using single molecule fluorescent *in situ* hybridizations (smFISH) (Chapter 2). Although the results are not conclusive, our data suggest that ciRS-7 and miR-135a are both highly expressed in the adult mouse cortex and hippocampus (Figure 3B). Next, we investigated the expression levels of ciRS-7 and miR-135a in the recently developed ciRS-7 knockout mouse¹⁰. We confirmed that this mouse indeed lacks the ciRS-7 genomic locus (located on the X chromosome), indicated by the (almost) undetectable levels of ciRS-7 in the whole brain, cortex and cerebellum of adult female and male knockout mice (Figure 3C). We found miR-135a levels decreased in the ciRS-7 knockout mice (Figure 3D), which is in accordance with literature (Piwecka et al., 2017). Next, we investigated the expression of ciRS-7 and miR-135a *in vitro* using smFISH. In PCNs that were cultured for 7 days, we observed that ciRS-7 and miR-135a are expressed in both the nucleus and the cytoplasm. MiR-135a has a predominant nuclear expression, whereas ciRS-7 is expressed mainly cytosolic (Figure 4A). The miRNAs miR-7 and miR-671 are also mainly expressed in the nucleus (Supplementary Figure 1B). The cytoplasmic expression of miR-135a is mostly localized around the nucleus, while ciRS-7 expression is more widespread in axons and dendrites of the neurons. To obtain more information on expression levels of ciRS-7 and miR-135a, we cultured primary hippocampal neurons for different days *in vitro* (DIVs), harvested them and isolated their RNA for RT-qPCR analysis. We observed that the expression of miR-135a generally decreases during PHN maturation, whereas ciRS-7 levels increase (Figure 4B).

CiRS-7 and miR-135a expression after manipulation *in vitro*

CiRS-7 is a well-established circRNA to manipulate, allowing us to further investigate the expression correlation between ciRS-7 and miR-135a. Forty eight hours after siRNA-mediated knockdown of ciRS-7 in PCNs we observed a 50% decrease in the expression of ciRS-7 and a significant increase in the expression of miR-135a (Figure 4C). Vice versa, we observed that after overexpression of ciRS-7 using a construct, levels of miR-135a are significantly decreased (Figure 4D). Using two different overexpression vectors that contain pre-miR-135a, we were also able to overexpress miR-135a in Neuro 2A

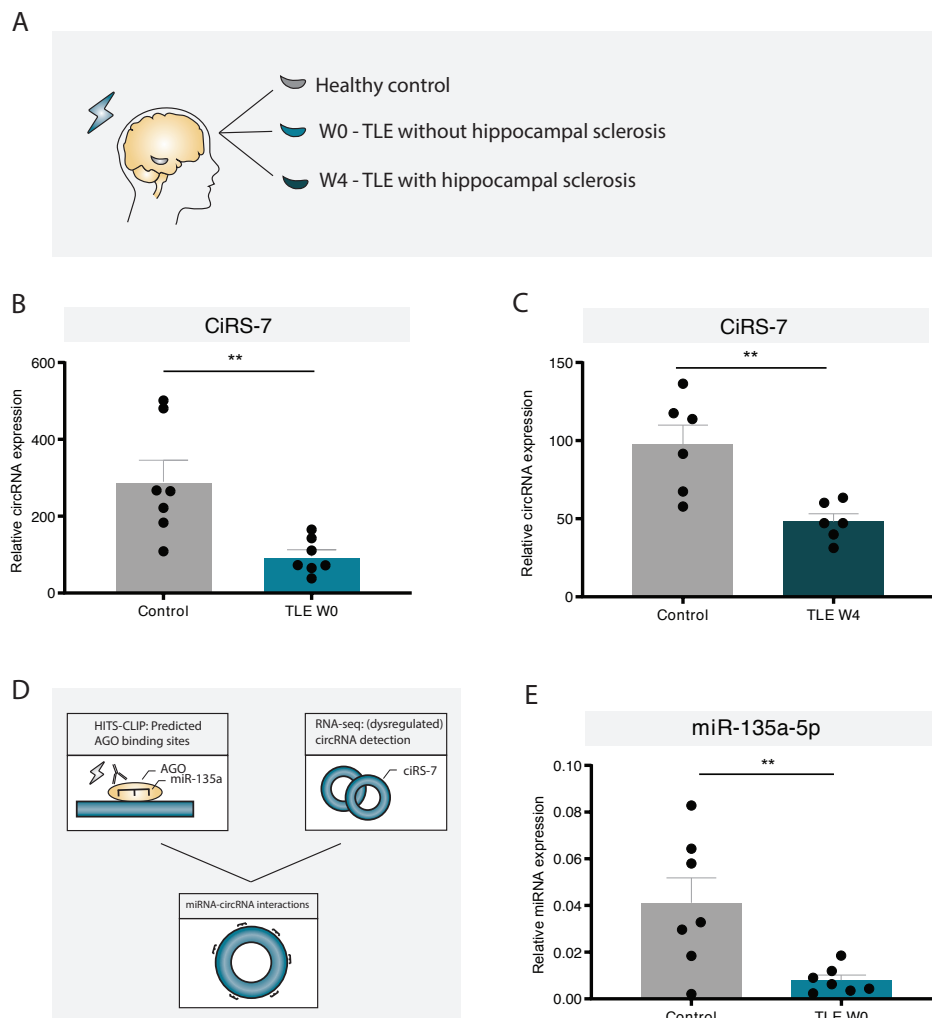


Figure 2 | CiRS-7, miR-7, miR-671 and miR-135a are downregulated in TLE patient material.
 (A) Schematic of human samples used for RT-qPCR analysis and high-throughput sequencing of RNA isolated by crosslinking immunoprecipitation (HITS-CLIP). For patients suffering from epileptogenic conditions in the temporal lobe area, hippocampal resection is often the only effective treatment against recurrent seizures 28. The resected TLE tissue can be characterized by reactive astrocytes and neuronal death, also known as hippocampal sclerosis. The severity of this hippocampal sclerosis is defined using the Wyler classification method defining W0 as hippocampal tissue without hippocampal sclerosis and W4 with the most severe sclerotic tissue. (B) CiRS-7 is downregulated in TLE W0 ($n = 7$, $p = 0.0061$) and (C) W4 ($n = 6$, $p = 0.0044$) patient material (unpaired t -test). (D) Schematic of the HITS-CLIP analysis for the identification of miRNA-circRNA interactions. (E) MiR-135a ($p = 0.0094$) is downregulated in HITS-CLIP data of TLE W0 patient samples ($n = 7$; unpaired t -test). * $p < 0.05$, ** $p < 0.01$, alpha = 0.05.

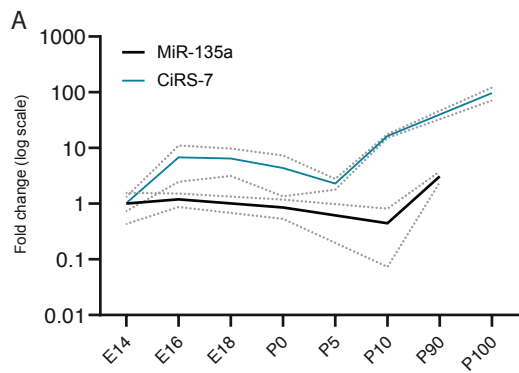
(N2a) cells, resulting in decreased expression of ciRS-7 (Figure 4E). In all, our *in vitro* observations suggest an inverse expression correlation between ciRS-7 and miR-135a that is comparable to the inverse expression detected in TLE tissue.

DISCUSSION

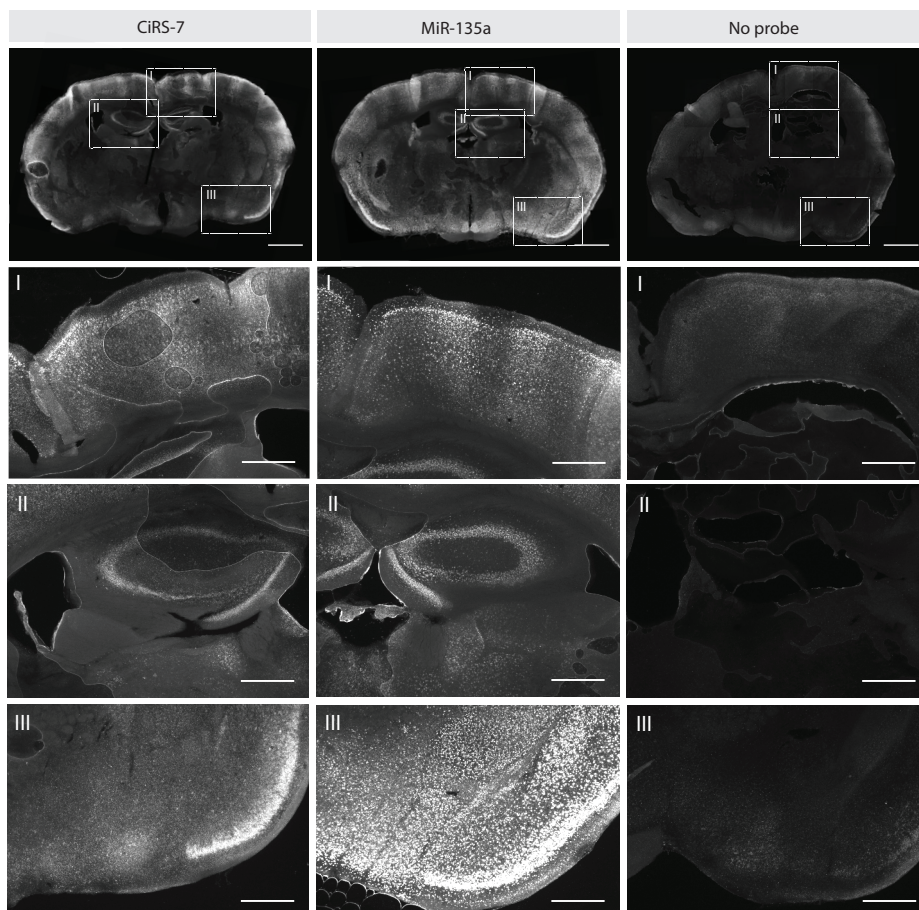
This and other studies show that miR-135a and ciRS-7 are specifically regulated in TLE patient material. In addition, expression correlation changes were observed in mice *in vitro* after manipulation of one the two molecules, whereas a positive correlation between ciRS-7 and miR-135a expression was observed in mouse *in vivo* systems (e.g. in the ciRS-7 knockout mouse). In all, the findings presented in this study suggest a possible functional link between ciRS-7 and miRNA-135a in the brain in health and disease and contribute to our understanding of the clinical significance of circRNAs in TLE pathology.

We investigated the expression of ciRS-7 and its binding miRNAs in TLE patient material and found that ciRS-7 in W4 patients is lower as compared to W0 patients. Previously it has been reported that miR-135a is increased in W4 TLE patient material²¹. W4 patient material is characterized by hippocampal sclerosis, which is characterized by neuronal death and reactive astrogliosis. As there are fewer neurons in W4 material and ciRS-7 is not expressed in glia, this could explain why we observed a lower expression of ciRS-7 in W4 samples as compared to W0 material¹⁰ (Chapter 2). In line with our findings, another study revealed that reduced expression of circRNA-0067835 was significantly correlated to increased seizure frequency and hippocampal sclerosis, suggesting that the downregulation of certain circRNAs (and subsequent upregulation of miRNAs) may be related to the sclerosis severity²³.

With the acquired expression data in this study, we hypothesized how interplay and disbalance between ciRS-7 and miR-135a could contribute to epileptogenesis (Figure 5). However, there are some major remarks concerning the hypothesized model. First, it is simplified. It does not only leave out the interaction of ciRS-7 with miR-7 and miR-671 but also those with other non-coding RNAs and RBPs. For instance the long non-coding RNA Cyran0 can bind miR-7 with unusually high complementarity and has been proposed to play a role in the gene-regulatory network of ciRS-7 and other non-coding RNAs^{24,25}. It is very likely that the interaction network of ciRS-7 and miR-135a consists



B



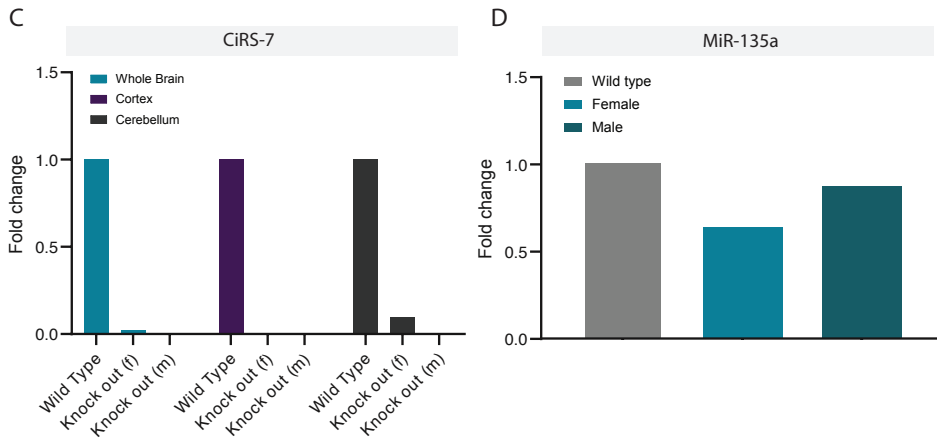


Figure 3 | CiRS-7 and miR-135a have a positive expression correlation *in vivo*.

(A) CiRS-7 and miR-135a have a positive expression correlation in the cortex during mouse brain development. MiR-135a data are adapted from van Battum et al., 2018 20. (B) ViewRNA single molecule fluorescent *in situ* hybridization (smFISH) of ciRS-7 and miR-135a in mouse coronal sections (Adult, P441). Scale bar upper row = 1 mm; lower rows = 500 μ m. (C) CiRS-7 is (almost) undetectable in the whole brain, cortex and cerebellum of female (f) heterozygous and male (m) homozygous ciRS-7 knockout mice. (D) MiR-135a is downregulated in ciRS-7 knock-out mice compared to wild type mice.

of many more players considering miR-135a (and miR-135b, that only differs by one nucleotide) has already many predicted RBP interaction partners. Second, the model does not distinguish between human and mouse systems. While both ciRS-7 and the described miRNAs are highly conserved across mammals, there are caveats in comparing the molecular expression between the two species; Mouse ciRS-7 has 130 miR-7 binding sites, compared to 70 in human. Moreover, the (sub)cellular localization of the molecules can be different between species. This could help explain why we do not observe an inverse correlation between the expression of ciRS-7 and miR-135a in ciRS-7 knockout mice and why the observed phenotype in this mouse is relatively mild. Lastly, there may also be differences in effect size when the molecules are knocked out (e.g. knockout mice) or knocked down (e.g. siRNA/plasmid).

The hypothesis needs more thorough testing given the broad expression of ciRS-7 and miR-135a in the brain, the specific spatial and temporal expression of the molecules and the diversity of the neural systems involved in TLE. To speculate on the role of ciRS-7 and miR-135a on neuronal activity, further studies are required. Preliminary data



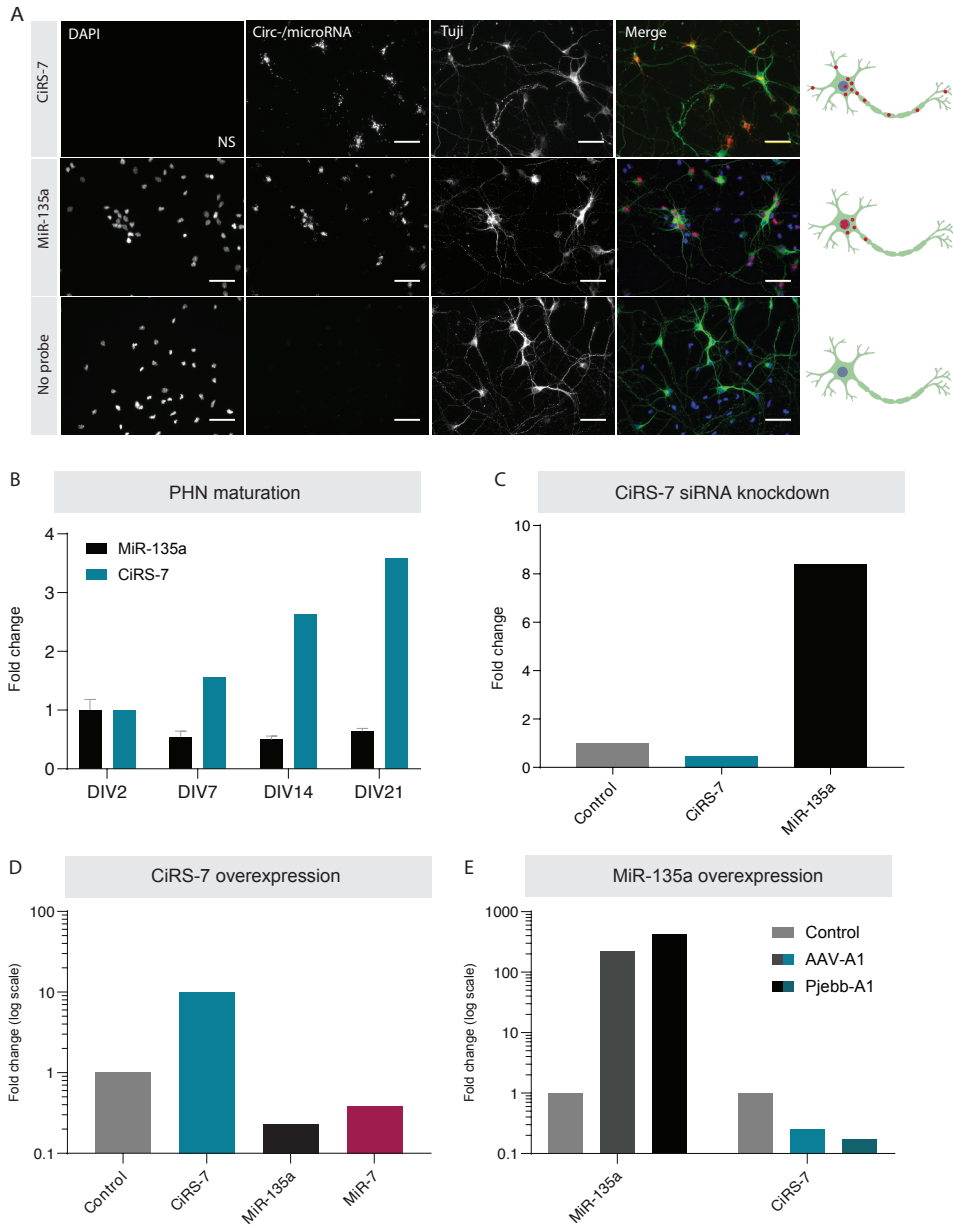


Figure 4 | CiRS-7 and miR-135a have an inverse expression correlation *in vitro*.

(A) Representative images of ViewRNA smFISH of *ciRS-7* and *miR-135a* in mouse primary cortical neurons (PCNs) (DIV7). Schematic summary of their subcellular localization *in vitro* on the right side. Scale bar = 100 μ m. NS = no signal. (B) *CiRS-7* and *miR-135a* have a negative expression correlation during the maturation of primary hippocampal neurons (PHN). *MiR-135a* data is adapted from van Battum et al., 2018 20. (C) *MiR-135a* expression is elevated after *ciRS-7* siRNA knockdown in primary cortical neurons (PCNs) (DIV2). (D) *MiR-135a* and *MiR-7* expression is decreased after *ciRS-7* overexpression (OE) in HEK293 cells compared to the empty vector control. (E) *CiRS-7* expression is decreased after *miR-135a* overexpression with two different strategies in N2a cells.

indicate that miR-135a expression is increased two weeks after intra-amygdala kainate injection in mice²¹ (Supplementary Figure 2E). Although the level of ciRS-7 expression in these experiments is currently unknown, it would be interesting to speculate whether overexpression of ciRS-7 (hence inducing sponging activity) in this animal model could have an influence on the epileptogenic phenotype, since altered levels of miR-135a are associated with TLE pathology²¹. Interestingly, we observed *in vitro* that enhanced neuronal activity induced by KCL does not affect ciRS-7 expression in PCNs and PHNs, while the expression of other circRNAs is increased (Supplementary Figure 2F; Chapter 3). Although we currently have no data on miR-135a expression in these activity assays it is interesting to examine whether ciRS-7 levels remain constant as a result of elevated neuronal activity, or whether ciRS-7 has an active role in neuronal activity regulation. To further explore the role of ciRS-7 and miR-135a in neuronal activity, it could be interesting to culture PCNs and PHNs from wildtype and/or ciRS-7 knockout mice on multi electrode assays and measure and manipulate their neuronal activity (e.g. by KCl, bicuculline, kainate addition), or overexpression/knockdown of ciRS-7/miR-135a. Moreover, it would be interesting to observe how epilepsy develops in ciRS-7 knockout mice after treatment with kainate and measure whether the expression of different miRNAs is altered. Lastly, it is interesting to speculate on the use the sponging abilities of ciRS-7 in therapeutic settings since silencing of miR-135a has been reported to reduce spontaneous recurrent seizures²¹.

A continued exploration of the functional relationship between ciRS-7 and miR-135a is necessary to uncover the function(s) of the associated circRNA/miRNA-target gene regulatory networks in the healthy and diseased brain. Based on the present findings, we conclude that ciRS-7 interacts with multiple miRNAs during brain development and we hypothesize how an interplay and disbalance between ciRS-7 and miR-135a could contribute to the neuronal phenotypes as observed in TLE. In combination with literature, the presented data provide evidence for a potential role for ciRS-7 and miR-135a as disease modulators or biomarkers in TLE pathology and could serve as a meaningful starting point from which to conduct further studies.

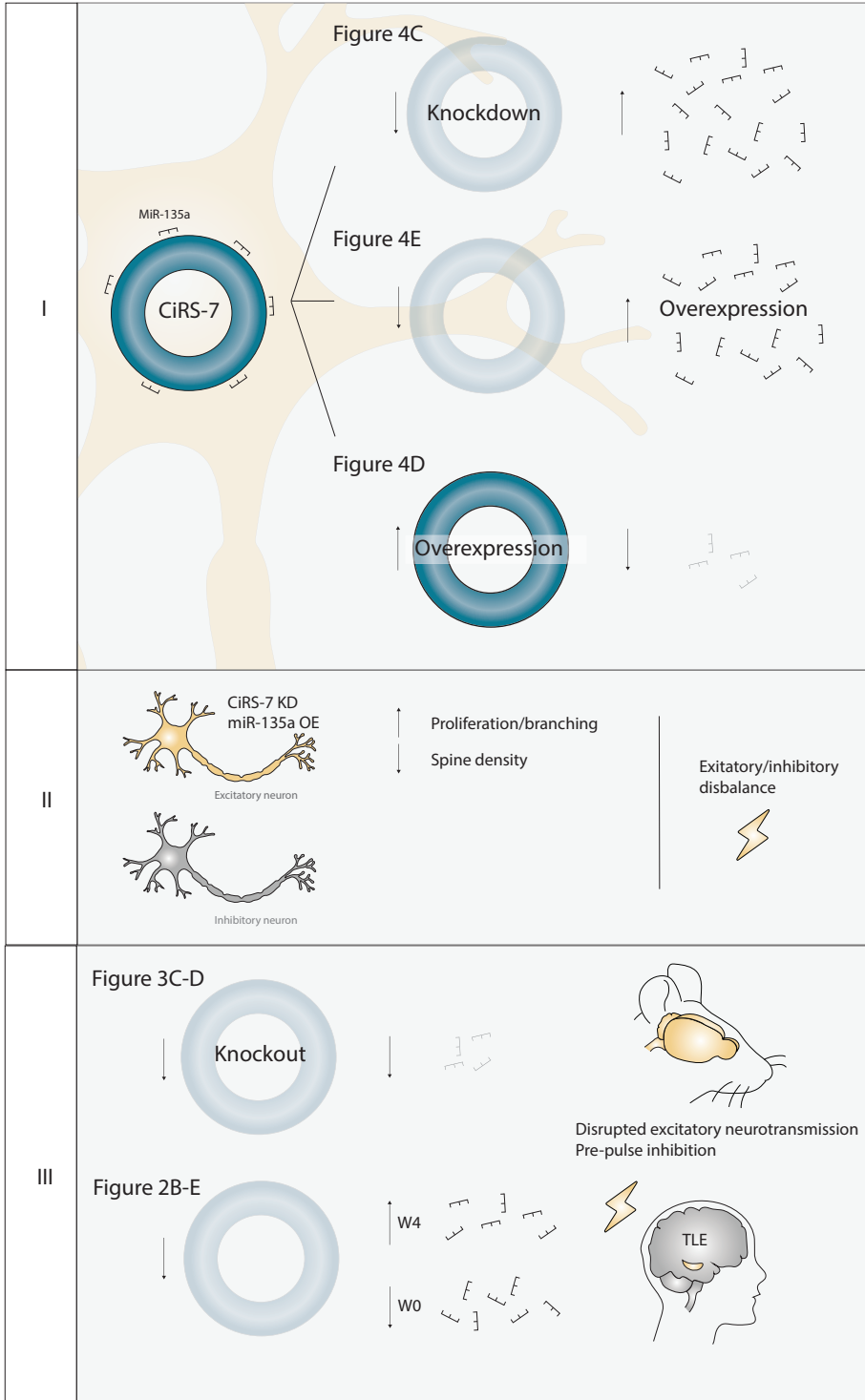


Figure 5 | CiRS-7/miR-135a interaction and neuronal activity.

Schematic of a hypothesized ciRS-7/miR-135a interaction proposed to contribute to disturbed neuronal activity. Downregulation of ciRS-7 in the epileptic brain—whether this happens as a cause or a result of the disease remains unknown—may result in reduced sponging of miR-135a (in W4), allowing more free miR-135a molecules to be able to target certain RNA binding proteins (RBPs). Using online tools, we predicted potential binding partners of miR-135a and subjected them to a gene ontology (GO) analysis (Supplementary Tables 3, 4). Interestingly, most RBPs potentially interacting with miR-135a were linked to a synaptic function. More importantly, some of the top predicted RBPs have in recent publication been linked to epilepsy providing further speculation on how elevated miR-135a levels could influence mRNA targets that play a role in the homeostasis of neuronal activation, which is disturbed in epilepsy^{29,30}. Next, we observed that manipulation of ciRS-7 or miR-135a results in an inverse expression of the other molecule in vitro (I). Other studies reported that ciRS-7 knockdown and miR-135a overexpression can lead to increased neuronal proliferation and branching and decreased spine density^{4,20,21}. Because ciRS-7 is only expressed in excitatory neurons (II), only these neurons will have a disturbed expression of one of the molecules²². As a result, a disbalance in excitability of inhibitory and excitatory neurons in a cellular network can lead to continuous dysfunction of excitatory synaptic transmission (III). Chronically altered neuronal network activity can contribute to disease phenotypes, possibly including the pathophysiology of TLE.

MATERIALS & METHODS

TLE patient selection and tissue collection

Hippocampal tissue samples of pharmaco-resistant TLE patients were obtained after hippocampal resection surgery was performed at the University Medical Centre Utrecht. Patients were selected for surgery according to the criteria of the Dutch Epilepsy Surgery Program. The excision was based on clinical evaluations, interictal and ictal EEG studies, MRI and intraoperative electrocorticography. Informed consent was obtained from all patients for all procedures approved by the Institutional Review Board. Immediately after *en bloc* resection of the hippocampus, tissue was cooled in physiological saline (4 °C) and cut on a precooled plate into three slices perpendicular to its longitudinal axis. Frozen and paraffin-embedded control hippocampal tissue samples were obtained from postmortem cases without hippocampal aberrations from the Netherlands Brain Bank. All control material was collected from donors with written informed consent for brain autopsy and the use of the material and clinical information for research purposes. Prior to dissection, brain pH was measured intraventricularly using an 18-GA 3.50-in. spinal needle. Detailed histological examination of the hippocampal material from all patients used in this study showed that all samples were devoid of tumor tissue. Hippocampal specimens were divided into three groups: a nonepileptic autopsy control group (control,

n = 7), a group of TLE patients without signs of hippocampal sclerosis (W0, n = 7) and a TLE group with hippocampal sclerosis (W4, n = 6). The severity of hippocampal sclerosis was determined by an experienced neuropathologist using the Wyler classification method defining W0 as hippocampal tissue without hippocampal sclerosis and W4 as tissue with the most severe type of hippocampal sclerosis.

RNA isolation TLE tissue

For the purpose of RNA isolation, 30 µm thick cryosections were cut until approximately 80-100 mg of tissue was collected. This material was stored at -80 °C until all the samples were collected. Later, all samples were thawed and processed by using Qiazol lysis reagent (Qiagen) to prevent RNA degradation. RNA was extracted using the miRNeasy kit (Qiagen) according to the manufacturer's protocol. RNA quality was assessed using a RNA 6000 Nano chip on the 2100 Bioanalyzer (Agilent) and RNA quantity was determined using Nanodrop (Thermo Scientific). All patient samples used in this study had RIN values above 6 (range 6.4–8.4; mean 7.2), confirming that all RNA samples were of excellent quality.

Ago CLIP-seq on deregulated circRNAs in TLE samples

Argonaute (Ago) Individual-nucleotide resolution UV crosslinking and immunoprecipitation (iCLIP) was utilized²⁶. Ago iCLIP was performed on resected hippocampal tissue from nine temporal lobe epilepsy (TLE) patients, six of which showed hippocampal sclerosis. Briefly, the data was demultiplexed, quality filtered and mapped to the human genome (GRCh38/hg38) using Bowtie2. The mapped position of crosslinking sites generated during iCLIP were checked for significant overrepresentation using CLIPper²⁷. With regards to deregulated circRNAs in TLE, miRNA targeting events were annotated to their sequence (FDR < 0.05).

Ethics statement

All animal experiments were performed in accordance to and approved by the CCD (Central Committee for animal research, The Netherlands), the University Medical Center Utrecht, the Dutch Law (Wet op Dierproeven 1996) and European regulation (Guideline 86/609/EEC).

Mouse tissue collection

Animals were housed under standard conditions and were provided food and water ad libitum. CiRS-7 knockout animals were generated using CRISPR as described in Piwecka *et al.*, 2017. The ciRS-7 knockout strain was maintained on a C57BL/6 background. Brains were collected from C57BL/6 mice at 7 time points (E12, E15, E18, P5, P25, P100 and P365) and meninges were removed. Samples were directly homogenized using a T10 basic ultra-turrax (IKA) in Qiazol (Qiagen), or frozen immediately in dry ice, and stored at -80 °C until further processing.

RNA isolation & reverse transcription

Total RNA was isolated from tissue samples and cultured cells using Qiazol reagent (Qiagen) and miRNeasy Mini Kit (Qiagen) following the manufacturer's instructions with minor modifications. RNA concentration was determined using a Nanodrop 2000 (Thermo Scientific).

CircRNA

Complementary DNA (cDNA) was generated from RNA using Superscript IV reverse transcriptase (RT) (Invitrogen) with random (hexamer) primers (Thermo Fisher Scientific) following the manufacturer's instructions. Unless stated otherwise, per 20 µl reaction, 1 µg RNA was used.

MiRNA

Complementary DNA (cDNA) was generated from 5 ng/µl total RNA with the miRCURY LNA RT Kit (Qiagen) following manufacturer's instructions.

Quantitative Real-time RT-PCR (qPCR)

circRNA

Complementary DNA was diluted 10-fold with RNase-free water. In a 10 µl PCR reaction using FastStart Universal SYBR Green Master ([ROX]; Roche) 4 µl cDNA was used. For circRNA amplification, primers followed a divergent amplification design in which the 5' primer was placed at the 3' end of the exon of interest and the 3' primer was placed at the 5' end. For linear RNA amplification, primers followed a standard convergent design. The reaction mix was added to a 96 or 384 well plate and amplification of the

product was measured after incubation steps at 50 °C for 2 minutes and 95 °C for 10 minutes during 40 PCR cycles (95 °C for 15 seconds and 60 °C for 1 minute) using a QuantStudio 6-flex Real-Time PCR system (Life Technologies). A melting curve was generated afterwards by ramping the temperature from 60 °C to 95 °C. Amplification curves were analyzed using QuantStudio 6 and 7 Flex Real-Time PCR System Software (v1.0). Ct values were normalized to the geometric mean of the reference genes (Hprt1, Actb, Pfkfb3, Tbp unless otherwise stated). Expression values were analyzed using the $2^{-\Delta\Delta Ct}$ method. If the fluorescent threshold was not reached after 40 PCR cycles, a value of 40 was used in the analysis. All qPCR reactions were conducted in technical triplicates. Primer (Integrated DNA Technologies) sequences are listed in Supplementary Table 1.

MiRNA

Complementary DNA was diluted 80-fold with RNase-free water, and 4 µl was then used in a 1 µl of PCR reaction using the miRCURY LNA miRNA PCR Assay (Qiagen). The reaction mix was added to a 96 or 384 well plate and amplification of the product was measured after incubation steps at 95 °C for 2 minutes and 95 °C for 15 seconds and 60 °C during 40 PCR cycles using a QuantStudio 6-flex Real-Time PCR system (Life Technologies). 5S rRNA was used for normalization. RT-qPCR probes used: hsa-miR-7-5p (YP00205877); hsa-miR-671-5p (YP00205649); hsa-miR-135a-5p (YP00204762)(Qiagen).

Cell culture

All cell lines were maintained at 37 °C in a humidified incubator with 5% CO₂.

Coating

Neurons were cultured on coverslips (VWR, 18Ø) in 12-well plates (Costar 3513/3524). Coverslips were etched in 1 N HCl (Emsure) for 1 hour at 65 °C and washed and stored in 100% EtOH (Emsure). The coverslips were coated with 20 µg/ml Poly-D-Lysine-ornithine (Sigma Aldrich) solution for 30 minutes at RT, washed with sterile PBS [1x] (Gibco) coated with 40 µg/ml Laminin (Gibco) for 1 hour at 37 °C, again washed with sterile PBS [1x] (Gibco) and used immediately to plate cells.

Primary cortical neurons (PCN)

Primary cortical neurons (PCNs) were prepared from 14 days old C57/BL6 mouse embryos (E14). The embryos were removed from the uterus and collected in Leibovitz's L-15 medium (Gibco). Cortices were separated and the meninges were removed before. The tissue was dissociated in 2.5% trypsin for 15 minutes at 37 °C. Following trypsinization, the supernatant was removed and dissociation medium added, consisting of 10% Fetal Bovine Serum (FBS) (Gibco), 0.2% DNase (0.012 mg/ml, Roche) in Leibovitz's L-15 medium (Gibco). The cells were triturated in the dissociation medium with a 200 µl pipette before being spun down for 1 minute at RT (IKA miniG). The supernatant was removed and the cells were resuspended in 1 ml Neurobasal Culture Medium (NB+) (Gibco) supplemented with 2% B27 (50x) (Gibco); 0.1% Pen/Strep (10 kU/ml Pen; 10 mg/ml Strep, Gibco); 0.1% Glutamine (Gibco); 5% 400 nm D-Glucose (Sigma Aldrich). Cells were plated on coated coverslips placed in 12-well plates. Cells were cultured for 2, 7, 14 and 21 days *in vitro* (DIV) with half the medium changed every week. The cells were washed with PBS [1x] and lysed in Qiazol (Qiagen) for further analysis.

Primary hippocampal neurons (PHN)

Primary hippocampal cultures were prepared from post-natal day 0 (P0) C57BL/6 mice. Mice were euthanized by decapitation and brains were dissected out in ice-cold L-15 medium (Gibco) with 7 mM HEPES (Gibco). Hippocampi were separated and the meninges removed in dissection medium containing 4.5 ml L-15 medium (Gibco) with 7 mM HEPES (Gibco). The tissue was incubated in 0.5 ml trypsin [10x] at 37 °C for 20 minutes. Following trypsinization, the supernatant was removed and cells were washed with a L-15 (Gibco), 7 mM HEPES (Gibco) mixture 3 times, removing as much supernatant as possible between washes. The cells were then exposed to 4 µl DNase (0.012 mg/ml, Roche) diluted in 1 ml NB+ medium (Gibco) supplemented with 18 µl HEPES 1 M (Gibco), 2.5 µl L-glutamine (Gibco), 1.8 µl 14.3 mM β-mercapto, and 20 µl B-27 (Gibco). Cells were triturated with a 200 µl pipette and filtered through a 70 µm nylon cell strainer (Falcon). A 1:10 dilution was made using 90 µl NB+ medium and 10 µl of the cell sample for cell counting. Hippocampal cultures were grown on coated coverslips in Neurobasal medium (NB) supplemented with B27, 14.3 mM β-mercapto, L-Glutamine and 1 M HEPES. The cells were washed with PBS [1x] and lysed in Qiazol (Qiagen) for further analysis.

Stable cell lines

N2a cells and HEK293 cells were cultured in DMEM high glucose containing 10% fetal calf serum, L-glutamine and penicillin /streptomycin. The cells were washed with PBS [1x] and lysed in Qiazol (Qiagen).

Overexpression and knockdown assays

Transfection of miR-135a mimics in N2a cells

N2a cells were transfected with pre-miR-135a-constructs (AAV-A1 and Pjebb-A1) using Lipofectamine 2000 (Thermo Fischer Scientific) following manufacturer's instructions. Cell lines were maintained at 37 °C in a humid-ified incubator with 5% CO₂. Cells were washed with PBS [1x], lysed in Qiazol (Qiagen) and processed for further analysis.

Transfection of ciRS-7 overexpression construct in HEK293 cells

HEK293 cells were transfected with overexpression constructs using Lipofectamine 2000 (Thermo Fischer Scientific) following manufacturer's instructions. Cell lines were maintained at 37 °C in a humidified incubator with 5% CO₂. Cells were washed with PBS [1x], lysed in Qiazol (Qiagen) and processed for further analysis.

CiRS-7 siRNA electroporation in PCNs

Cells were electroporated in OptiMem medium (Gibco) with ciRS-7 siRNAs [100 nM each] (UCUGCCGUAUCCAGGGUUU; CGUAUCCAGGGUUUCCAGU) in combination with a pCx-GFP construct [1 µg/µl]. MISSION® siRNA Fluorescent Universal Negative Control #1, Cyanine 3 (Sigma-Aldrich) scrambled siRNA was used as a negative control. PCNs were electroporated at DIV0 in suspension in pre-chilled electroporation cuvettes (Nepagene) in the NEPA21 electroporator (electroporation settings: Poring pulse 175 V, duration 5 milliseconds, interval 50 milliseconds, 2 pulses, decay 10%, one direction. Transfer pulse 20 V, duration 50 milliseconds, interval 50 milliseconds, 5 pulses, decay 40%, two directions). After electroporation, the cells were plated in NB+ medium. Adherent PCNs (> DIV0) were electroporated with a Napagene Culture Electrode in pre-warmed OptiMem (electroporation settings: Poring pulse 200 V, duration 5 milliseconds, interval 50 milliseconds, 2 pulses, decay 10%, two directions. Transfer pulse 30 V, duration 50 milliseconds, interval 50 milliseconds, 5 pulses, decay 40%, two directions.) After electroporation, fresh medium was added to the cells.

At 48 hours post electroporation, supernatant was removed, cells were lysed immediately in Qiazol reagent (Qiagen) and processed for further analysis.

ViewRNA

Tissue

Single molecule Fluorescent *In Situ* Hybridization (smFISH) was performed by using the ViewRNA miRNA ISH Cell Assay Kit (Invitrogen), according to the manufacturer's protocol with adjustments; Adult mice brains were dissected out of C57BL/6 mice and cut in 60 μm thick coronal sections on a vibratome in PBS [1x]. The sections were fixated in 4% RNase free PFA (Electron Microscopy Sciences) for 30 minutes at RT and incubated twice in crosslinking buffer QM (Thermo Fisher Scientific) for 10 minutes at RT. Next, sections were incubated in 0.16 M N-(3-Dimethylaminopropyl)-N'-ethylcarbodiimide hydrochloride (EDC; Sigma Aldrich) crosslinking buffer for an hour at RT. To permeabilize the sections they were exposed to detergent solution QM (Thermo Fisher Scientific) for 10 minutes at RT. The probes (Type I) (Thermo Fisher Scientific) were diluted in probe set solution (Thermo Fisher Scientific) at a ratio of 1:10 pipetted onto the sections, placed into a HybEZTM II Hybridization System and incubated for 3 hours at 40 °C. The sections were washed in wash buffer (Thermo Fisher Scientific) and left overnight at 4 °C in storage buffer (Thermo Fisher Scientific). The following day, the sections were incubated in Preamplifier mix QM (Thermo Fisher Scientific) for 1 hour at 40 °C in the HybEZTM II Hybridization System. The sections were washed in wash buffer (Thermo Fisher Scientific) and incubated in amplifier mix QM (Thermo Fisher Scientific) for 1 hour at 40 °C. Label Probe 1 Alkaline Phosphatase (LP1-AP; Thermo Fisher Scientific) was diluted to a 0.07% concentration in label probe diluent QF (Thermo Fisher Scientific) and added to the tissue sections. After incubation at 40 °C for 1 hour, the sections were washed in wash buffer (Thermo Fisher Scientific) and exposed to AP enhancer solution (Thermo Fisher Scientific) for 5 minutes at RT. Fast red (Thermo Fisher Scientific) was mixed with Naphthol buffer and added to the sections for 45 minutes at 40 °C. The sections were then washed in RNase free PBS [1x], re-fixed in RNase free 4% PFA (Electron Microscopy Sciences) for 10 minutes. Finally, samples were washed with PBS [1x], mounted on Superfrost Plus object glasses (VWR) with Fluorsave (Calbiochem) mounting medium and imaged.

Cells

Fluorescent *In Situ* Hybridization was performed by the ViewRNA miRNA ISH Cell Assay

Kit (Invitrogen), according to the manufacturer's protocol as described under tissue with minor adjustments; Primary cortical neurons were fixed in ultra clean PFA [4%] (PFA, Electron Microscopy Sciences) for 10 minutes and washed three times in PBS [1x]. The probes (Type I) (Thermo Fisher Scientific) were diluted in probe set solution (Thermo Fisher Scientific) at a ratio of 1:100 pipetted onto the cells. After the FISH protocol, the cells were blocked for 1 hour at RT with 5% Normal-Goat-Serum and 0.1% Triton-X in PBS [1x] (blocking buffer). Next, they were incubated in primary antibody in blocking buffer o/n at 4 °C. The coverslips were washed three times in PBS [1x] and cells were incubated in secondary antibody in PBS [1x] for 45 minutes at RT. The cells were washed three times in PBS [1x] followed by a 4',6-diamidino-2-phenylindole (DAPI) [1 µg/ml] (Sigma, D-9564-10MG) incubation for 10 minutes at RT. Lastly, the coverslips were washed with PBS [1x] and mounted on Superfrost Plus object glasses (VWR) with Fluorsave (Calbiochem) mounting medium before imaging. Primary antibody; β -tubulin IgG (SAB4200732, 1:1000); Secondary antibody; goat-anti-mouse Alexa Fluor 488 (Invitrogen A11029, 1:750).

Microscopes

All immunofluorescent images were acquired using an Axioscope epifluorescent microscope (Zeiss) and a LSM 880 confocal microscope (Zeiss). Brightfield images were acquired using a ZEISS Axio Scan.Z1 (Zeiss).

Statistical analysis

Statistical analyses were performed in GraphPad Prism version 8 (GraphPad Software). All data are represented as means and error bars represent as standard error of the mean (SEM). The significance is defined as * $p < 0.05$, ** $p < 0.01$.

Acknowledgements

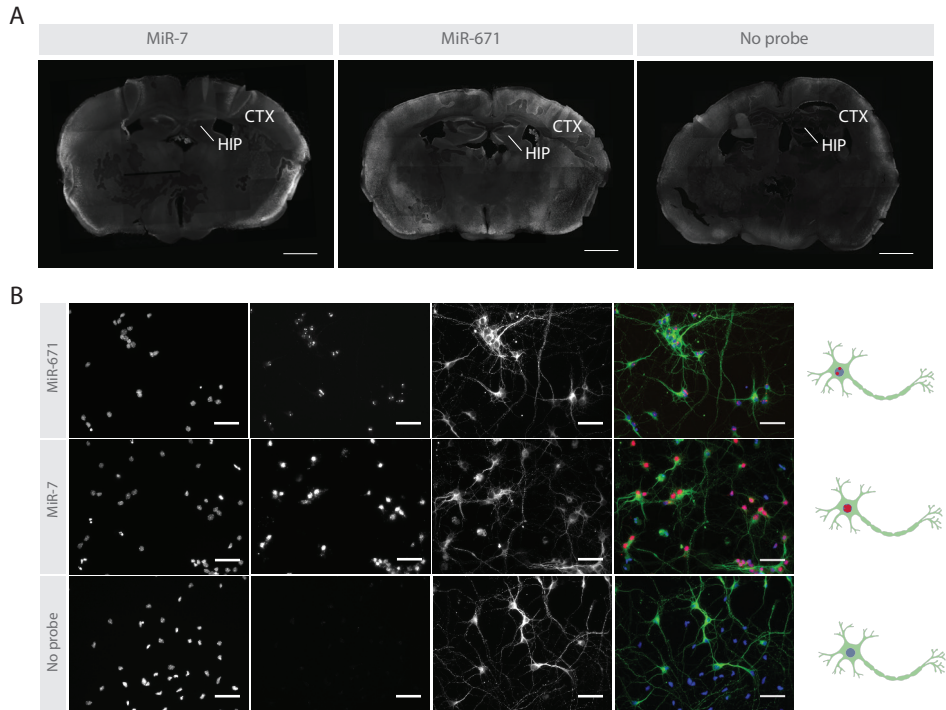
We like to thank Nikolaus Rajewsky for providing the ciRS-7 knock-out mice. This project has received funding from the Netherlands Organization of Scientific Research NWO (Personal grant DvR, part of Graduate Programme project (022.003.003) and NWO VICI to RJP) and the European Union's Horizon 2020 research and innovation programme under the Marie Skłodowska-Curie grant agreement No 721890 (circRTrain) and the EpimiRNA consortium, European Union's 'Seventh Framework' Programme (FP7) under Grant Agreement no. 654 602130 (to RJP).

REFERENCES

1. Westholm, J. O. et al. Genome-wide Analysis of *Drosophila* Circular RNAs Reveals Their Structural and Sequence Properties and Age-Dependent Neural Accumulation. *Cell Rep.* 9, 1966–1981 (2014).
2. Rybak-Wolf, A. et al. Circular RNAs in the Mammalian Brain Are Highly Abundant, Conserved, and Dynamically Expressed. *Mol. Cell* 870–885 (2014). doi:10.1016/j.molcel.2015.03.027
3. Jeck, W. R. et al. Circular RNAs are abundant, conserved, and associated with ALU repeats. *RNA* 19, 141–57 (2013).
4. Memczak, S. et al. Circular RNAs are a large class of animal RNAs with regulatory potency. *Nature* 495 VN-, 333–338 (2013).
5. Hansen, T. B., Kjems, J. & Damgaard, C. K. Circular RNA and miR-7 in Cancer. *Cancer Res.* 73, 5609–5612 (2013).
6. Capel, B. et al. Circular transcripts of the testis determining gene *Sry* in adult mouse testis. *Cell* 73, 1019–1030 (1993).
7. Wilusz, J. E. A 360° view of circular RNAs: From biogenesis to functions. *Wiley Interdiscip. Rev. RNA* 9, 1–17 (2018).
8. Chen, B. J., Huang, S. & Janitz, M. Changes in circular RNA expression patterns during human foetal brain development. *Genomics* 111, 753–758 (2019).
9. Pan, Z. et al. MicroRNA-1224 splicing circular-RNA-filip1l in an ago2-dependent manner regulates chronic inflammatory pain via targeting Ubr5. *J. Neurosci.* 39, 2125–2143 (2019).
10. Piwecka, M. et al. Loss of a mammalian circular RNA locus causes miRNA deregulation and affects brain function. *Science* (80-.). 357, (2017).
11. Hansen, T. B. et al. Natural RNA circles function as efficient microRNA sponges. *Nature* 495, 384–388 (2013).
12. Shao, Y. & Chen, Y. Roles of Circular RNAs in Neurologic Disease. *Front. Mol. Neurosci.* 9, 1–5 (2016).
13. Barrett, S. P. & Salzman, J. Circular RNAs: analysis, expression and potential functions. *Development* 143, 1838–1847 (2016).
14. Huang, C., Liang, D., Tatomer, D. C. & Wilusz, J. E. RESEARCH COMMUNICATION A length-dependent evolutionarily conserved pathway controls nuclear export of circular RNAs. 639–644 (2018). doi:10.1101/gad.314856.118.GENES
15. Lukiw, W. J. Circular RNA (circRNA) in Alzheimer’s disease (AD). *Front. Genet.* 4, 1–2 (2013).
16. Zhao, Y., Alexandrov, P. N., Jaber, V. & Lukiw, W. J. Deficiency in the ubiquitin conjugating enzyme UBE2A in Alzheimer’s Disease (AD) is linked to deficits in a natural circular miRNA-7 sponge (circRNA; ciRS-7). *Genes (Basel).* 7, (2016).
17. Junn, E. et al. Repression of alpha-synuclein expression and toxicity by microRNA-7. *Proc. Natl. Acad. Sci. U. S. A.* 106, 13052–7 (2009).
18. Yang, L., Fu, J. & Zhou, Y. Circular RNAs and Their Emerging Roles in Immune Regulation. *Front. Immunol.* 9, 2977 (2018).
19. Kan, A. A. et al. Genome-wide microRNA profiling of human temporal lobe epilepsy identifies modulators of the immune response. *Cell. Mol. Life Sci.* 69, 3127–3145 (2012).
20. Van Battum, E. Y. et al. An image-based miRNA screen identifies miRNA-135s as regulators of CNS axon growth and regeneration by targeting krüppel-like factor 4. *J. Neurosci.* 38, 613–630 (2018).
21. Vangoor, V. R. et al. Antagonizing increased miR-135a levels at the chronic stage of experimental TLE reduces spontaneous recurrent seizures. *J. Neurosci.* 39, 5064–5079 (2019).
22. Piwecka, M. et al. Loss of a mammalian circular RNA locus causes miRNA deregulation and affects brain function. *Sci.* 8526, 1–14 (2017).

23. Gong, G. H. et al. Comprehensive circular RNA profiling reveals the regulatory role of the CircRNA-0067835/miR-155 pathway in temporal lobe epilepsy. *Cell. Physiol. Biochem.* 51, 1399–1409 (2018).
24. Ulitsky, I., Shkumatava, A., Jan, C. H., Sive, H. & Bartel, D. P. Conserved function of lincRNAs in vertebrate embryonic development despite rapid sequence evolution. *Cell* 147, 1537–1550 (2011).
25. Kleaveland, B., Shi, C. Y., Stefano, J. & Bartel, D. P. A Network of Noncoding Regulatory RNAs Acts in the Mammalian Brain. *Cell* 174, 350–362. e17 (2018).
26. König, J. et al. ICLIP - transcriptome-wide mapping of protein-RNA interactions with individual nucleotide resolution. *J. Vis. Exp.* 2–8 (2011). doi:10.3791/2638
27. Lovci, M. T. et al. Rbfox proteins regulate alternative mRNA splicing through evolutionarily conserved RNA bridges. *Nat. Struct. Mol. Biol.* 20, 1434–1442 (2013).
28. Blümcke, I. et al. International consensus classification of hippocampal sclerosis in temporal lobe epilepsy: A Task Force report from the ILAE Commission on Diagnostic Methods. *Epilepsia* 54, 1315–1329 (2013).
29. Cukier, H. N. et al. Three Brothers With Autism Carry a Stop-Gain Mutation in the HPA-Axis Gene NR3C2. *Autism Res.* 13, 523–531 (2020).
30. Kjær, C. et al. Transcriptome analysis in patients with temporal lobe epilepsy. *Brain* 142, E55 (2019).

SUPPLEMENTARY DATA



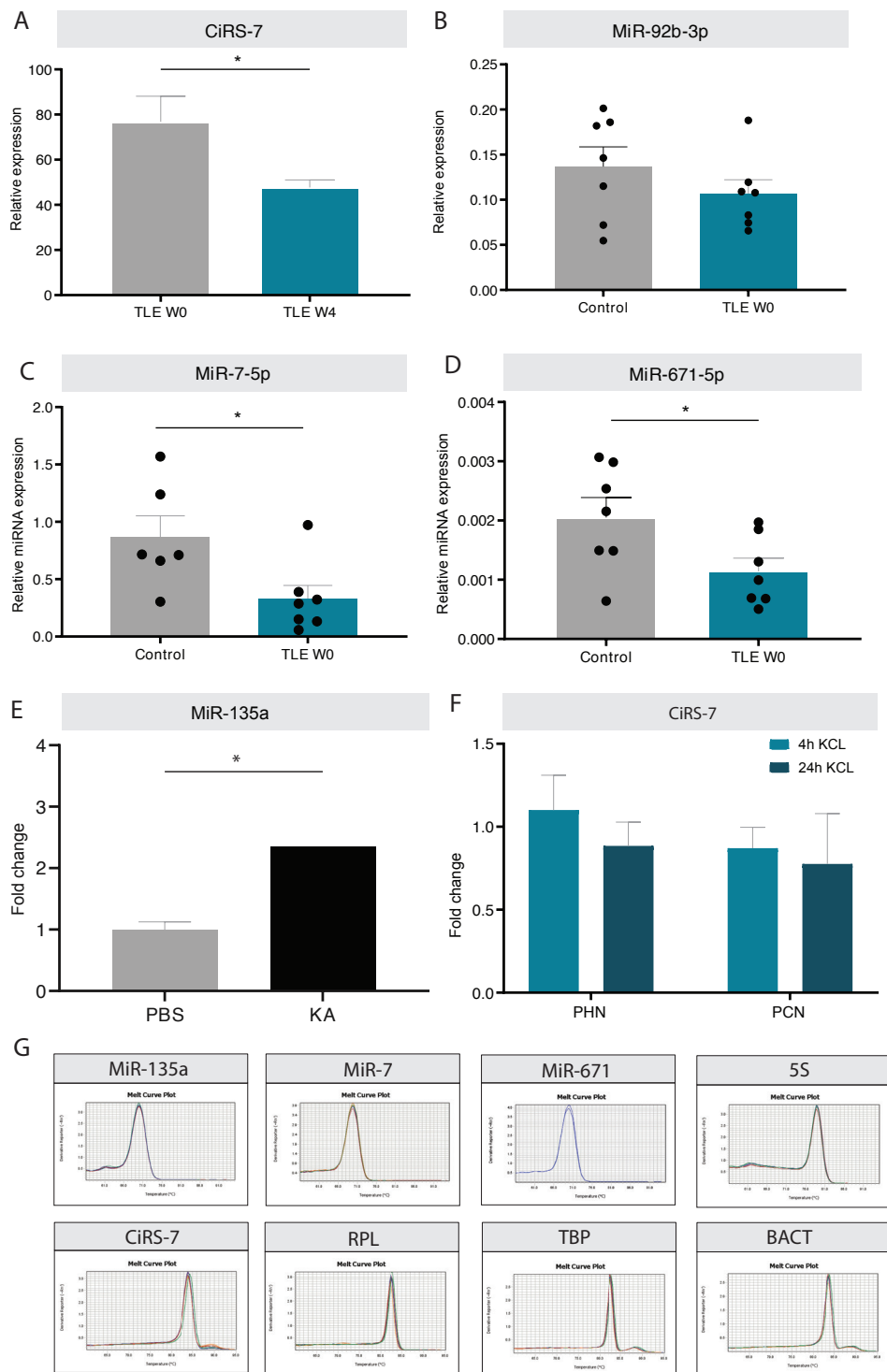
Supplementary Figure 1 | Single molecule fluorescent *in situ* hybridization.

(A) ViewRNA single molecule fluorescent *in situ* hybridization (smFISH) of miR-7 and miR-671 in mouse coronal sections (Adult, P441). Scale bar = 1 mm. (B) Representative images of ViewRNA smFISH of miR-7 and miR-671 in mouse primary cortical neurons (PCNs) (DIV7). miR-7 and miR-671 have a clear nuclear in expression, whereas ciRS-7 is expressed mainly cytosolic. Schematic summary of their subcellular localization *in vitro* on the right side of the panel. Scale bar = 100 μ m. HIP = Hippocampus; CTX = Cortex.

4

Supplementary Figure 2 | MiR-135a, ciRS-7 and neuronal activity.

(A) ciRS-7 is lower expressed in TLE W4 patients as compared to WO patients ($p = 0.0387$; $n = 4$; Unpaired *t*-test). (B) miR-92b-3p expression is not significantly altered in TLE WO patient samples as compared to control samples. (C) miR-7 ($p = 0.0282$) and (D) miR-671 ($p = 0.0434$) are downregulated in CLIP-seq data of TLE WO patient samples ($n = 7$; Unpaired *t*-test). (E) miR-135a expression is increased two weeks after intra-amygdala kainate injection in mice (unpaired *t*-test, $p = 0.0375$). Data adapted from 21. * $p < 0.05$, $\alpha = 0.05$. (F) Enhanced neuronal activity induced by KCL does not affect ciRS-7 expression in primary cortical neurons (PCN) and primary hippocampal neurons (PHN). (G) Melt curves of RT-qPCR runs.



Supplementary Table 1 | RT-qPCR Primer list

Target	Species	Forward Sequence	Reverse Sequence
CiRS-7	mmu	GGCGTTTGACATTGAGGTT	GGAAGATCACGATTGCTGGA
Actb	mmu	AGCCATGTACGTAGCCATCC	CTCTCAGCTGGTGGTGAA
Hprt1	mmu	ATGGGAGGCCATCACATTGT	ATGTAATCCAGCAGGTCAGCAA
Tbp	mmu	GAAGAACAATCCAGACTAGCAGCA	CCTTATAGGGAACCTCACATCACAG
Pgk	mmu	GATGGTGTCCCATGCCTGA	AGGCATTCTGACTTCTGGG
CiRS-7	hsa	CGTCTCCAGTGTGCTGATCT	AAGACCCGGAGTTGTTGGAA
GAPDH	hsa	TGGAAGGACTCATGACCACA	GGGATGATGTTCTGGAGAGC
BACT	hsa	GGACTTCGAGCAAGAGATGG	AGCACTGTGTTGGCGTACAG
RPII	hsa	GCACCACGTCCAATGACAT	GTGCGGCTGCTCCATAA
TBP	hsa	CCACGCTCTTCCACTACA	GCGGTACAATCCCAGAACTC

Target	Company	Mature miRNA seqence
hsa-miR-7-5p	Qiagen	UGGAAGACUAGUGAUUUUGUUGU
hsa-miR-671-5p	Qiagen	AGGAAGCCCUAGAGGGGCUAGGAG
hsa-miR-135a-5p	Qiagen	UAUGGCUUUUUUAUUCUAUGUGA
5S rRNA	Qiagen	NA

4

Supplementary Table 2 | HITS-CLIP ciRS miR-135a-5p

Chromo- some	Start	Stop	miR seed	miRNA	FDR	Antisense gene	circRNA
chrX	140784089	140784096	miR-135a- 5p_7mer-m8	miR-135a-5p	9,26E-7	CDR1	hsa_circ_0001946
chrX	140784359	140784366	miR-135a- 5p_7mer-m8	miR-135a-5p	5,17E-5	CDR1	hsa_circ_0001946

Supplementary Table 3 | Summary of the clinical data of all patients and controls included in the study

Gender	Age	Pathology	Hippocampal sclerosis
M	48	DMT I induced organ failure	No
F	78	Non demented control	No
M	93	Non demented control	No
F	82	Non demented control	No
F	72	Non demented control	No
F	89	Non demented control	No
F	75	Non demented control	No
F	23	mTLE Wyler scale 0	No
F	47	mTLE Wyler scale 0	No
M	60	mTLE Wyler scale 0	No
F	50	mTLE Wyler scale 0	No
F	63	mTLE Wyler scale 0	No
F	38	mTLE Wyler scale 0	No
M	44	mTLE Wyler scale 0	No
F	52	mTLE Wyler scale 4	Yes
M	41	mTLE Wyler scale 4	Yes
M	41	mTLE Wyler scale 4	Yes
M	42	mTLE Wyler scale 4	Yes
F	49	mTLE Wyler scale 4	Yes
F	42	mTLE Wyler scale 4	Yes

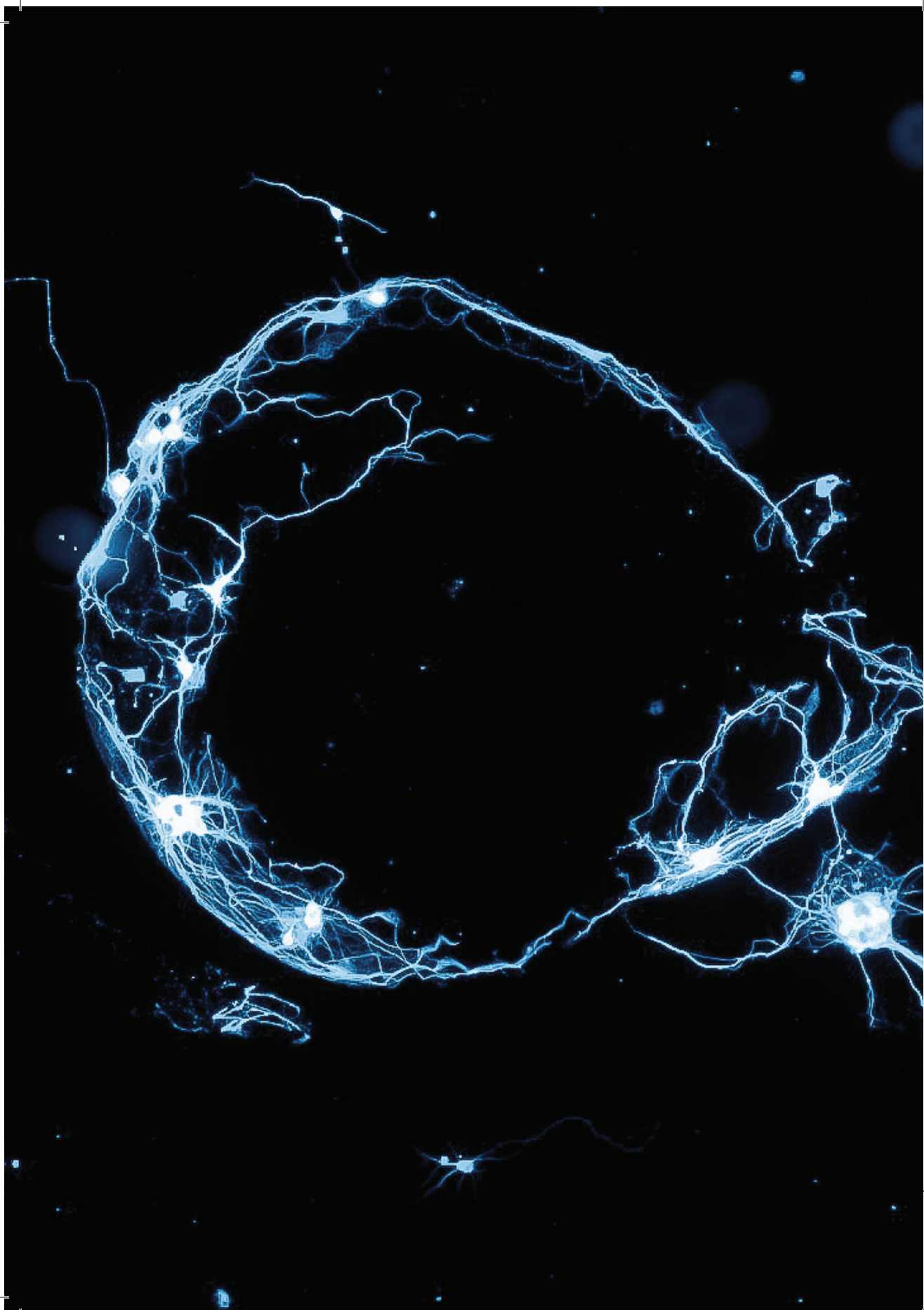
Supplementary Table 4 | Predicted RBPs for miR-135

Target Score	Gene Symbol	Target Score	Gene Symbol	Target Score	Gene Symbol
99	NR3C2	98	RBAK	97	DIP2C
99	SYT2	98	B3GLCT	97	ST6GAL2
99	SMIM13	98	RUNX2	97	DAG1
99	LZTS1	98	YWHAG	96	TNPO1
98	SLC24A2	98	KCNN3	96	SSR2
98	SHISA7	98	CPLX1	96	TCF7L2
98	TMEM168	98	STRBP	96	KALRN
98	FOXN3	97	CHD1	96	KCNQ5
98	CPLX2	97	KCNB1	96	SLC30A4

Supplementary Table 5 | GO analysis of predicted RBPs for miR-135a

GO term	Description	P-value	FDR q-value	Enrichment (N, B, n, b)	Top genes
GO:0048167	regulation of synaptic plasticity	2.02E-5	1.09E-1	12.27 (589,16,18,6)	SHISA7 SLC24A2 KCNB1 YWHAG CPLX2 LZTS1
GO:0099177	regulation of trans-synaptic signaling	2.16E-4	5.83E-1	7.16 (589,32,18,7)	SHISA7 SLC24A2 KCNB1 CPLX1 YWHAG CPLX2
GO:0050804	modulation of chemical synaptic transmission	2.16E-4	3.89E-1	7.16 (589,32,18,7)	SHISA7 SLC24A2 KCNB1 CPLX1 YWHAG CPLX2
GO:1903827	regulation of cellular protein localization	3.1E-4	4.2E-1	2.53 (589,24,155,16)	SHISA7 DAG1 ROCK2 PIK3R2 MFHAS1 TCF7L2
GO:1903305	regulation of regulated secretory pathway	3.28E-4	3.55E-1	4.57 (589,12,86,8)	SYT3 SYT2 CPLX1 PREPL KCNB1 CPLX2





DISCUSSION

Summary & general discussion

Primary cortical neurons in the shape of a circle (image taken with an epifluorescent microscope).

SUMMARY

CircRNAs are single stranded, circularized non-coding RNAs that can be derived from exonic and intronic parts of many genes. Because circRNAs often share parts of the sequence with their corresponding linear mRNA, they went unnoticed by researchers for a long time. After circRNAs were initially discovered, they were thought to be present at low abundance and were generally considered to represent splicing errors. However, after the development of high-throughput sequencing and computational tools for analyzing RNAs lacking a poly-A tail, this general view on circRNAs changed drastic. Quickly circRNAs were detected in most organisms, ranging from archaea to plants, and the number of studies on their expression and biogenesis increased¹⁻⁶. Although circRNAs were detected in many different tissue types, the most intriguing finding was their high expression in the brain, where they display very precise spatiotemporal expression, especially during development. With regard to their evolutionary conservation it is evident that circRNAs should fulfill important function(s) in and/or outside the brain. Yet, up until now only a few circRNAs have been extensively characterized and for only a handful a specific function has been described.

A recent study revealed that circRNAs from axon guidance genes are specifically upregulated during the development of the porcine brain⁷. Many of these axon guidance circRNAs were expressed in a tissue/developmental stage-specific manner and revealed a striking (up)regulation during brain development. This led to the question whether circRNAs from axon guidance genes may also play a role in neural circuit formation (like axon guidance proteins) or whether they fulfill other roles during development of the mammalian brain. In this thesis, we therefore aimed to investigate the expression and function of axon guidance circRNAs in the developing (mouse) brain. We used various techniques including RNA-seq, RT-qPCR, Nanostring and (sm)(F)ISH to study the spatiotemporal expression of a selected group of axon guidance circRNAs and we adapted various manipulation tools to investigate their function *in vitro* and *in vivo*.

In chapter 1, we identified which axon guidance circRNAs are expressed in the human adult brain using RNA-seq. After the selection of a group of axon guidance circRNAs, we characterized the expression of these circRNAs in the developing and adult mouse brain using RT-qPCR and Nanostring. We observed that axon guidance circRNAs are conserved

between mammalian species, can be expressed independently of their linear host genes and noted that they exhibit a dynamic spatial and temporal expression pattern *in vitro* and *in vivo*. We identified an expression peak for axon guidance circRNAs in the developing mouse cortex just before birth and observed accumulation of circRNAs with age.

Over the past years various (sm)(F)ISH techniques have been developed to specifically label and detect circRNAs *in vitro* and *in vivo*. In chapter 2, we discussed available (sm)(F)ISH techniques for the detection of circRNAs and covered their advantages and disadvantages in order to get a better understanding of axon guidance circRNA expression. Using smFISH, we were able to create an overview of the spatiotemporal expression of selected axon guidance circRNAs in primary cortical neuron cultures. This overview revealed that the expression levels and cellular localization of axon guidance circRNAs are dynamic and vary over the course of neuronal maturation. Moreover, we observed that the axon guidance circRNAs investigated were predominantly expressed in excitatory neurons, with no expression in glial cells.

In chapter 3, we described and utilized various tools for the manipulation of circRNAs derived from axon guidance genes. CircRNAs were successfully overexpressed in neuronal cells and in the mouse retina. For circRNA knockdown, we implemented different manipulation strategies from which knockdown with siRNAs was most reproducible *in vitro*. Sholl analysis following knockdown of circRNAs in primary cortical neurons hinted at a possible role for certain axon guidance circRNAs in neurite branching. siRNA-mediated knockdown in the mouse cortex using *in utero* electroporation did not induce obvious defects. Lastly, we reported that neuronal expression of axon guidance circRNAs is elevated as a result of cellular activation.

Previous research indicated that miR-135a (a miRNA that can bind circRNA ciRS-7 ((similar to miR-7 and miR-671)) is associated with temporal lobe epilepsy (TLE). However, the exact role of the interaction between ciRS-7 and miR-135a in a neurological disease-context remains unclear. In chapter 4, we systematically investigated the expression patterns of miR-7, miR-671 and ciRS-7 in the developing mouse brain. Furthermore, we analyzed ciRS-7 and miR-135a levels in TLE patient material (with and without hippocampal sclerosis) and found that ciRS-7 and miR-135a are significantly regulated. An inverse expression correlation between ciRS-7 and miR-135a was observed *in vitro* after knockdown or following overexpression of

one of the two molecules, suggesting a biological interaction between these RNAs. The functional meaning of the relationship between ciRS-7 and miR-135a in TLE pathology remains to be further explored, but the presented data could serve as a meaningful starting point from which to conduct further studies.

In summary, in this thesis we investigated the expression and function of axon guidance circRNAs in the developing (mouse) brain. We tested and optimized various assays to measure, label and overexpress or knockdown axon guidance circRNAs *in vitro* and *in vivo*. Our major findings are that axon guidance circRNAs i) are conserved between human and mice, ii) are dynamically expressed throughout the mammalian brain over the course of development, iii) reveal expression peaks in the mouse cortex before birth, iv) show age-related accumulation, v) are expressed in excitatory cells, vi) have no expression in glia and vii) are upregulated after cellular activation. These findings increase our understanding on axon guidance circRNA expression and function, but further studies are necessary to elucidate the exact function(s) of each axon guidance circRNA in neuronal development and their role(s) in neurological disease.

GENERAL DISCUSSION

This general discussion is structured in three main sections. In the first section, we discuss the expression (1) of axon guidance circRNAs in light of the latest findings in the circRNA research field. Next, we speculate on the potential function(s) (2) of axon guidance circRNAs in the brain in health and disease, and discuss the limitations that hamper investigating axon guidance circRNA function. Lastly, we give an overview on future directions (3) for further studies based on literature and the results described in this thesis.

1. Axon guidance circRNA expression

Spatiotemporal expression

A striking feature of circRNAs is their precise spatiotemporal expression and subcellular localization. As described throughout the chapters of this thesis, we aimed to create an expression overview of a select group of axon guidance circRNAs (and ciRS-7) in the developing brain, as information on their spatiotemporal expression could lead to better insight into their specific function(s). It is evident that the overview is far from complete, but we succeeded in creating a first overview of axon guidance circRNA expression at various stages in different areas of the developing mouse brain.

In order to select brain areas for functional analysis we first performed (sm)(F)ISH on axon guidance circRNAs in the developing brain (chapter 2). We investigated circRNA expression at different developmental timepoints in the brain as a whole and in the cortex and hippocampus, two major brain regions that were reported to have a high circRNA expression⁷. Our RT-qPCR and smFISH data revealed that axon guidance circRNAs have a very specific spatiotemporal expression and are predominantly expressed in excitatory neurons *in vitro* (chapter 2). As the cortex and hippocampus both consist of multiple different cell layers and different cell types, it would for future experiments be interesting to investigate the expression of axon guidance circRNAs in the individual layers and/or cell types of the cortex and hippocampus in order to discover their functional role(s).

In our RT-qPCR analysis all axon guidance circRNAs show an expression peak in the developing mouse cortex starting around E15, while levels are decreasing around birth

(chapter 1). In the mouse embryonic cortex a switch occurs around E16 that results in the splicing of exons linked to functions in synaptic transmission⁸. Around postnatal day 2 (P2) another switch occurs that includes exons involved in general synapse biology. Interestingly, these switches temporally correlate to when axon guidance circRNA expression is highest. The drop in circRNA expression around birth could also be linked to reduced neurogenesis and the start of glial development. Although glial cells (e.g. microglia, oligodendrocytes and astrocytes) have been demonstrated to have an impact on axon guidance (for instance by acting as guide post cells along migratory routes or by assisting in targeting synaptic partners) we found that circRNAs are not expressed in glia (chapter 2)^{9,10}. This suggests that the function of axon guidance circRNA is highly (neuronal)cell-type specific.

It was reported that circRNAs can be up- or downregulated in cultured neurons in response to changes in neuronal activity induced by addition of bicuculline (a GABAA receptor antagonist)¹¹. In our hands, the addition of bicuculline to cultured cortical cells had no effect on circRNA expression levels. Nonetheless, we demonstrated that neuronal activation using KCL treatment increases axon guidance circRNA levels *in vitro*, indicating that the neuronal expression of axon guidance circRNAs is activity-dependent (chapter 3). Whether axon guidance circRNAs play an active role in neuronal activity and cell-to-cell communication could be explored by further investigation of their subcellular localization. So far, we have only localized axon guidance circRNAs to the cell body and dendrites of developing neurons (chapter 2) (it is currently not clear whether the presence of the circRNAs in neurites is due to directed transport or is a consequence of diffusion). The finding that circRNAs localize to neurites is not surprising given 1) the occurrence of local and activity-dependent translation of mRNA in neurons, 2) the potential role that circRNAs have in regulating or influencing mRNA levels, and 3) the involvement of circRNAs in various cellular events like proliferation and differentiation¹¹⁻¹³. CircRNAs are overall reported to also be highly expressed in synaptoneurosomes¹¹. Although we did not localize axon guidance circRNAs to synapses (most likely due to the low sensitivity and resolution of our assays), we would expect axon guidance circRNAs to be expressed in synapses. Especially since our KCL experiments suggest that axon guidance circRNAs play a role in cellular activation and communication. A growing body of experimental evidence also indicates that circRNAs play a role in synaptic function. For instance, circGRIA1 was reported to regulate synaptic plasticity and synaptogenesis in the male macaque brain¹⁴. To investigate the role of axon guidance circRNAs in synaptic function, we need

more information on their subcellular localization. This can be achieved by investigating the expression of axon guidance circRNAs in synaptoneurosome fractions with RT-qPCR, or by using high resolution imaging in combination with smFISH on neurons that have developed active synapses. In addition, it would be interesting to monitor cell activation after circRNA manipulation *in vitro*, by using a multi electrode array (MEA) system, and *in vivo*. This would allow us to investigate neuronal activity on a network level and provide important information on the role of axon guidance circRNAs in cellular activation and communication.

Linear versus circular RNA

A big challenge in the RNA field is to distinguish linear mRNAs from circRNAs. This is difficult as most molecular tools that identify mRNA also detect circRNAs that contain the same exons. It is therefore very well possible that functions that have been ascribed to mRNAs in the past, are the result of circRNA behavior. A standardized way to investigate circRNAs specifically is using specific primers that identify the unique back-splice junction. Using this approach, we observed that axon guidance circRNAs are sometimes expressed at higher levels than their corresponding linear RNA. This is in line with the estimation that eukaryotic circRNAs can be present from 0.1 to 10-fold compared to linear transcripts (Chapter 1)^{15,16}. However, these findings raise the question what might be the advantage of an RNA to exist in a circular rather than in linear form, especially as back-splicing is far less efficient than canonical splicing¹⁷. It has been suggested that the balance between circular and linear transcripts is the result of splicing competition. In general, mammalian cells have been reported to have an inverse relationship between the abundance of circRNAs and their respective linear mRNAs, which can be time-and-place specific^{13,18}. We could speculate that splicing switches occur to retain a balance between the expression of the circular and linear transcripts, which both affect the regulation of specific neuronal processes in their own way. Our smFISH co-localization experiments were not successful, but other studies indicated that circRNAs and mRNAs from the same gene generally do not seem to co-localize¹¹. However, this doesn't mean that circRNAs and mRNAs from the same gene do not work together. For instance, upregulation of axon guidance circRNAs can result in lower axon guidance protein expression and vice versa. Another possibility is that active cooperation between the circular and linear molecules is necessary to establish proper neuronal growth and guidance. CircRNA and mRNA have different biological characteristics (mRNA can be stable up to 10 hours, where circRNA can have half-lives of longer than 48 hours and circRNAs are often smaller, therefore often

including only part of the genomic sequence) and could therefore fulfill different roles, while working together¹⁹.

Intronic circRNAs with retained introns were reported to function as positive regulators of RNA Pol II transcription in the nucleus. These so called EliciRNAs could promote the parental gene transcription via interaction with host U1 snRNP and RNA Polymerase II²⁰. The investigated circEfnb2 has an intronic part and could therefore potentially regulate the expression of the Efnb2 gene on a transcriptional level. This means this circRNA could influence the expression of the guidance molecule Efnb2 directly and specifically when the membrane receptor is required for neuronal pathfinding. We did not observe a specific upregulation of circEfnb2 in the nucleus and whether circEfnb2 (and other axon guidance circRNAs) would be capable of such a direct regulation remains to be validated. Nonetheless, it is interesting to speculate that an (axon guidance) circRNA can actively regulate the expression of its corresponding linear RNA via this pathway.

Axon guidance circRNAs in the aging brain

Even though circRNAs can have low basal transcription rates, their enhanced stability (mainly due to their circular nature) allows them to reach high levels in certain tissues, which is suggested to be the reason for their specific accumulation in the nervous system. It is not surprising that accumulation of axon guidance circRNAs occurs in the adult brain, which consists mostly of non-proliferating cells and has a very low turnover of neurons. Whether axon guidance circRNAs accumulate in the aging brain due to less efficient clearing mechanisms, or whether the accumulation of axon guidance circRNA in the brain has neuroprotective or toxic consequences is unclear.

It was reported that the majority of circRNAs derived from genes involved in calcium homeostasis and synaptic plasticity have high aging-specific expression²⁵. We observed that exposing cells to serum starvation or KCL, which can be cellular stressors, results in increased circRNA expression. These data suggest that cellular stress has an influence on circRNA expression (chapter 3). Different stressors may contribute to aging acceleration and age-related degenerative diseases, which could explain why circRNA levels are high in the aging brain. The immune system of the brain also deteriorates with age, leading to increased susceptibility to infection and higher levels of inflammation. Interestingly, the modification of certain circRNAs has been connected to immune responses²⁸. It is therefore possible that axon guidance circRNAs also play a role in the immune system in

the aging brain (although there is no evidence that the function of circRNAs and proteins from the same gene can be linked, it is known gene axon guidance molecules as such as Slits and Ephrins regulate immune cell migration, and Semaphorins were shown to play important roles in either stimulating or inhibiting inflammatory responses^{26,27}). Lastly, it is an interesting observation that the brain and testis have the highest expression of tissue-specific circRNAs and that both the reproductive and neuronal system have their own unique immune system²⁹.

The age-related circRNA accumulation hypothesis based on circRNA stability implies that circRNAs are passively accumulated over time due to low cellular turnover. This could be interesting for a cell, as the population of circRNAs at a given time could provide the cell with a memory of the transcriptional history/ancestry of a cell²⁴. Nonetheless, it is also possible that axon guidance circRNAs are actively expressed in the adult brain. Interestingly, alterations of splicing patterns during brain development (maturation and aging) are often temporally correlated to changes in circRNA levels⁸. For instance, it is known that alternative splicing happens more frequently in the adult brain, where circRNAs are also highly expressed²¹. We observed that axon guidance circRNAs are upregulated during two fundamentally different processes, embryonic/neonatal brain development and aging. This is not entirely surprising knowing that other molecules (like axon guidance proteins) can also play different roles in the developing brain (e.g. guiding growing axons) and the adult brain (e.g. controlling structural plasticity of synaptic connections) based on their spatiotemporal expression^{22,23}. Whether axon guidance circRNAs fulfill different functions in the young and the adult brain is unclear. We were unable to investigate axon guidance circRNA expression and function in the aging brain intensively due to limitations in our smFISH assays on mouse brain tissue, and because our manipulation tools were only suited for 'young' neurons.

Functional time-window

We selected key timepoints of neurodevelopmental processes to study axon guidance circRNAs, but axon guidance circRNAs are also expressed, and/or likely function at other timepoints that were not investigated. Key pre- and early postnatal brain development processes happen within hours in mice, which introduces the possibility that we missed crucial moments of axon guidance circRNA expression/function, especially with regard to their highly specific spatiotemporal expression. Moreover, this may have affected the experiments on the manipulation of axon guidance circRNAs *in vivo* (chapter 3). Therefore

we would ideally investigate the expression of the circRNAs with fewer time intervals, perhaps live in the developing brain and perform functional assays on timepoints where expression is highest or lowest.

2. Axon guidance circRNA function

Tools and circRNA isoforms

Like the quantitative detection of circRNAs, studies focusing on the visualization and function of circRNAs are often limited by traditional molecular biology techniques that fail to distinguish circRNAs from their linear counterparts. The general way to overcome this is by targeting the back-splice junction of circRNAs. However, because the back-splice junction represents a limited sequence region, probe design is often suboptimal. As described throughout the chapters of this thesis, this often results in off-target effects, low detection rates or inefficient manipulation (chapters 1-3). Another feature impeding the selective detection of specific circRNAs is that each axon guidance gene generates multiple different circRNA isoforms. The different circRNA isoforms that are generated from each gene are not expressed stochastically. Often there are one or few circRNAs isoform(s) predominantly expressed from each gene³⁰. We decided to select one of these predominantly expressed circRNA isoforms from each axon guidance gene (based on global conservation and expression level) for our analyses. Nevertheless, this doesn't mean that the other circRNA isoforms (that we did not investigate) may not have an important spatiotemporal expression or function. In addition, as the probe/primers/siRNAs that we used in our studies specifically detect the back-splice junction of the selected circRNA isoform, we may have underestimated the overall circRNA expression of a gene. Moreover, it is possible that our knockdown experiments did not result in large phenotypes due to functional redundancy of other circRNA isoforms from the same gene that were not knocked down. It is also important to note that due to alternative splicing there are also circRNA isoforms that have the same back-splice junction, but a different internal exon composition¹¹. If a circRNA has the same back-splice junction, but different exon composition, they may behave differently. This makes it difficult to delineate the function of a specific circRNA from other isoforms, by only looking at its back-splice junction, and shows that experimental determination of the full-length sequence of a circRNA is important. Because the axon guidance circRNA isoforms we studied have not been fully sequenced, we do not know whether they have similar back-splice junctions,

but different exon compositions. Long-read sequencing of single molecules using nanopore technology could be used in order to map and examine exon composition of circRNAs³¹.

Sponging, scaffolding or signaling?

A handful of circRNAs has been reported to be involved in post-transcriptional regulation by binding and sequestering miRNAs, thereby reducing their ability to target mRNAs (e.g. ciRS-7/miR-7/miR-671/miR135a, SRY/miR-138, circ-Foxo3)³²⁻³⁶. In order to function as a miRNA sponge, circular RNAs need to either harbor many miRNA binding sites or be expressed at very high levels in the cytosol (when they only contain a few binding sites), which is not the case for the majority of axon guidance circRNAs (chapter 3). Although miRNA sponging does not seem to be a general feature for axon guidance circRNAs, we could speculate that by sponging miRNAs, axon guidance circRNAs could contribute to enhanced protein synthesis in the growth cone or in synapses. This is interesting as axon guidance requires very specific timing, and transporting proteins along the axon takes time, while sponging can occur quick and locally^{32,33}. MiR-7, for instance, is predicted to bind to not only ciRS-7, but also circNeo1³⁷. It is likely that interactions of miRNAs with (axon guidance) circRNAs could play a role in neurodevelopmental processes.

Other suggested functions of circRNAs are binding of RBPs for transport in the cell, organization of RNA-protein complexes and/or regulation of RBP expression. Axon guidance proteins are known to interact with RBPs. For instance, IMP2 is required for local regulation of Robo1 and Robo2³⁸. Since axon guidance circRNAs are present in various subcellular compartments, it is interesting to speculate that they also interact with RBPs. Although axon guidance circRNAs show no enrichment in binding sites for RBPs and are not more likely to bind, store, sequester or act as scaffolds for the assembly of transcription factors or RBPs than linear mRNAs, based on nucleotide sequence alone, the tertiary structures of circRNAs may contribute to determining protein binding capacity³⁹⁻⁴¹. While linear RNAs are folded into dynamic unstable structures, most circRNAs form stable secondary structures with short imperfect duplexes⁴². A study on circFoxo3 suggested that this circRNA can display a variety of tertiary structures depending on different cell/tissue environments and it is therefore likely that the binding of RBPs/miRNAs is more complex than previously thought³⁶. This means that the function of axon guidance circRNAs could differ depending on their tertiary structure and their interaction with other molecules. Analysis following knockdown of circRNAs in PCNs

at different stages of maturation hinted at a possible role for specific axon guidance circRNAs in neurite branching at DIV2 but not at DIV9. Interestingly, this finding indicates that the Epha3 circRNA can fulfill diverse roles depending on the timing and context (which is something that is commonly observed in axon guidance, e.g. switching between attraction and repulsion or bidirectional signaling).

Although there is no evidence for the specific interaction between certain miRNAs or RBPs and axon guidance circRNAs, it is important to keep in mind that during neural circuit development, cooperation and crosstalk between various cues is essential. Thus, when investigating axon guidance circRNA function in future studies, it is important to also investigate their tertiary structure and their crosstalk between different molecules. An example of crosstalk between different RNA molecules in the brain is the gene regulatory axis of lncRNA(Cyrano)-miRNAs(miR-7/miR-671)-circRNA(ciRS-7). The interaction network of these molecules shows how different RNAs can collaborate to establish a complex posttranscriptional regulatory network⁴³. Another study demonstrated that the expression of certain circRNAs correlates with the expression of miR-7 target genes independent of whether the circRNAs harbor miR-7 binding sites, indicating not direct but indirect network communication⁴⁴. These Interaction networks between lncRNAs-miRNAs-circRNAs and circRNAs-miRNAs-mRNAs are likely to also occur for axon guidance circRNAs and it is therefore important to investigate their crosstalk and molecular consequences.

Biomarkers

Over the last few years, extracellular vesicles (EVs) have been established as crucial mediators of intercellular communication. Specific circRNAs were found highly expressed in EVs recovered from cell culture media^{45,46}. RNA-seq analyses revealed that these circRNAs were enriched by at least 2-fold in EVs compared to producer cells, which is not surprising regarding their stability and resistance to exonucleolytic degradation. Gene ontology analysis of up-regulated circRNAs in exosomes from the brain extracellular space after traumatic brain injury, suggested a role for circRNAs in the regulation of dendrite development, glutamatergic synapse and nervous system development⁴⁷. Since the active packing of circRNAs in EVs and the uptake by cells has to be very specific, large amounts of specific circRNAs need to be secreted. Based on our circRNA expression data, which identifies a few highly expressed circRNAs, this type of signaling may occur for axon guidance circRNAs.

Interestingly, circRNAs from the axon guidance genes SEMA4B and EPHB4 were already found expressed in EVs.

CircRNAs are enriched in body fluids including blood serum, plasma, cerebrospinal fluid, saliva and urine, and can also be specifically detected in free-floating cells inside body fluids and may therefore represent innovative circulating biomarkers^{48,49}. In addition, due to their cell-specific expression, circRNAs in EVs may be promising biomarkers for diagnosis of (neurological) diseases. A recent study showed that differentially expressed circRNAs in the brain were also similarly differentially expressed in blood at the respective time points. Many of these circRNAs identified in the blood were linked to pathways related to brain pathophysiology, including glutamate synapse and Alzheimer's disease⁵⁰. Blood circRNAs can therefore be considered as informative surroates (biomarkers) for brain circRNAs. Identifying these biomarkers could help the detection of brain diseases, which is valuable regarding the inaccessibility of brain tissue for biopsy. CircRNAs can pass through the blood-brain-barrier (in contrast to most drugs), which makes them also interesting candidates for brain interventions⁵¹. Future studies are required to demonstrate the relationships between the brain and these circulating circRNAs, and to investigate what their roles are in brain pathophysiology and could be in disease treatment.

Axon guidance circRNAs in neurological disorders

Although the functional interaction between ciRS-7 and miR-135a in TLE pathology remains to be further explored, the data discussed in chapter 4 illustrate how misregulation of circRNA ciRS-7 (and/or its binding miRNA miR-135a) could be linked to a disease phenotype. Other circRNAs, including circEFCAB2 and circDROSHA, were also reported to be significantly differentially expressed in the temporal lobe cortex of patients suffering from TLE. These circRNAs were suggested to act as sponges for miRNAs to retain the expression of target genes and impact TLE pathogenesis⁵². Increasing numbers of circRNA are also starting to be implicated in several neurodegenerative diseases, including Alzheimer's disease and Parkinson's disease^{53,54}. In Amyotrophic lateral sclerosis (ALS) the RNA-binding protein FUS has been recognized as an important modulator of circRNA expression⁵⁵. Interestingly, in brains from patients with bipolar disorder the axon guidance circRNA circEpha3 was found to be upregulated. Currently there is no other known connection between neurological disorders and the axon guidance circRNAs we studied. Nonetheless, as the altered expression and function of axon guidance molecules



as Semaphorins, Ephs and Slits are known to play a role in various neurological disease, it is interesting to speculate that circRNAs from these same genes could be interesting for the detection of neurological disorders and/or the design of therapeutic approaches for modulating neural injury and disease^{56,57}.

Conclusion

In this thesis, we took a first step in examining the expression and function of axon guidance circRNAs. We developed and optimized various assays to detect and measure axon guidance circRNA levels using RNA-seq, RT-qPCR and Nanostring, label and visualize expressed axon guidance circRNAs using (sm)(F)ISH, and manipulate axon guidance circRNA levels by overexpression and/or knockdown *in vitro* and *in vivo*. Developing these assays was challenging, and not all results from our studies are conclusive, but we can conclude on a few major observations. The expression patterns of the investigated axon guidance circRNAs are in general similar in the developing (mouse) brain (their expression peaks in the cortex before birth, they show age-related accumulation, expression in excitatory cells, no expression in glia and upregulation after cellular activation). We also observed differences between the expression and function of individual circRNAs. This includes heterogeneity in size and content (different exons/domains), difference in subcellular localization (e.g. around the nucleus vs. in neurites) and specific changes in cellular morphology after knockdown (e.g. circEpha3). In all, we managed to build a foundation from which (axon guidance) circRNA expression and function can be better studied in a more standardized way. Nonetheless, understanding the exact role of axon guidance circRNAs in neural circuit development remains a challenge. In combination with the finding by other researchers that the tertiary structure, and hence binding capacity, of circRNAs for other molecules (miRNAs/RBPs) can alter based on their spatiotemporal expression, it is likely that each of the studied axon guidance circRNA isoform fulfills a spectrum of different functions during neuronal development in a spatiotemporal specific manner. In order to study this, better tools need to be developed and more studies need to be performed to draw further conclusions on whether axon guidance circRNAs have active roles in neuronal developmental and/or aging processes, and if so, what these roles exactly are.

3. Future directions

The development of RNA-seq methods and advances in bioinformatics approaches to detect circRNAs have greatly aided the discovery of circRNAs. Yet, it is clear that the circRNA research field is still in its infancy. There is an urgent need for the development of better genetic, biochemical and imaging tools to further elucidate circRNA expression and function. For instance i) the development of RNA-seq algorithms and databases that focus on detecting tissue-specific circRNAs instead of only novel circRNAs can provide better insight into circRNA spatiotemporal expression, ii) experimental validation of databases that predict function(s) of circRNAs by interaction with cellular factors are necessary, iii) improved probe design is important to enhance circRNA detection sensitivity, and v) if we can tag circRNA in live cells (systems to visualize circRNA in live cells have been proposed, but not yet described), we could follow their expression dynamics and get a better understanding of their subcellular localization^{29,58}.

Main challenges in the field remain the identification of upstream regulators of axon guidance circRNA expression, and downstream targets that are regulated by circRNAs and affected by their dysregulation. Future work should focus on direct or indirect interactors of circRNAs that unveil underlying molecular networks. For this, development of both genetic tools and innovative *in vitro/in vivo* models are essential. During the course of this thesis work, some new techniques, like RIP, PAR-CLIP, HITS-CLIP, CRIP and circRNA precipitation followed by protein identification and/or small RNA sequencing were introduced into the field⁵⁹⁻⁶³. Also, machine learning algorithms to identify and predict circRNAs and its regulatory interactions are being improved⁶⁴. Another new approach is to examine certain post-transcriptional modifications including N6-methyladenosine²⁸. It could be important to determine which RNA modifications occur and how these may impact circRNA function.

CircRNAs play crucial roles in cell homeostasis and are implicated in disease phenotypes when they are dysregulated. Due to their high stability, tissue- and developmental stage-related expression, as well as their potential binding of proteins and RNAs, circRNAs are promising vehicles for targeted drug delivery. Because most circRNAs are not translated into peptides, the use of circRNA also provides a new direction for targeted therapy. One study already showed that it was possible to conjugate an expression plasmid

for circFoxo3 with gold nanoparticles⁶⁵. With the advantage of high delivery efficiency, delivery of siRNAs, shRNAs or antisense oligonucleotides against circular RNAs will be a valuable approach for future circular RNA studies. In addition, the development of circRNA specific knockout/knockdown mice, using Cas13 or other approaches could aid successful circRNA manipulation *in vitro* and *in vivo*. It is expected that in upcoming years we can foresee progress in single-cell profiling of circRNAs, studying and understanding circRNA localization, and gaining better insight in the circRNA interactome.

The results obtained in thesis, in combination with the literature, suggest that axon guidance circRNAs play roles in neurogenesis, ageing and cellular communication. We expect that in future studies the dysregulation of new axon guidance circRNA will be linked to disease phenotypes and more light will be shed on their interaction network by identifying interaction partners including lncRNAs, miRNAs and RBPs. In particular the role of axon guidance circRNAs in aging (for which human *post-mortem* samples could be analyzed), their synaptic expression and function and cell-to-cell communication (which can be done by employing e.g. MEA systems among others) are of interest for further exploration. Continued exploration of axon guidance circRNAs will help us to better understand their role in neuronal development and their contribution to other aspects of brain function in health and disease.

Coming full circle

In all, this thesis provides an overview of axon guidance circRNA expression in the developing (mouse) brain and presents different tools to manipulate circRNA levels *in vitro* and *in vivo*. Although we can only speculate on the exact function(s) of axon guidance circRNAs based on the data obtained in this thesis, the presented data paves a road for future experiments that, after the development of new techniques and experimental approaches, could lead to better insight in axon guidance circRNA function. For now the question remains; are we just facing hiccups in the start of an exciting and rapidly developing field of research, or are we trying to square a circle by investigating axon guidance circRNA function...?

REFERENCES

1. Danan, M., Schwartz, S., Edelheit, S. & Sorek, R. Transcriptome-wide discovery of circular RNAs in Archaea. *Nucleic Acids Res.* 40, 3131–3142 (2012).
2. Wang, G., Wu, J. & Song, H. LRIG2 expression and prognosis in non-small cell lung cancer. *Oncol. Lett.* (2014). doi:10.3892/ol.2014.2157
3. Broadbent, K. M. et al. Strand-specific RNA sequencing in *Plasmodium falciparum* malaria identifies developmentally regulated long non-coding RNA and circular RNA. *BMC Genomics* 16, 1–22 (2015).
4. Lu, T. et al. Transcriptome-wide investigation of circular RNAs in rice. *Rna* 21, 2076–2087 (2015).
5. Ji, P. et al. Expanded Expression Landscape and Prioritization of Circular RNAs in Mammals. *Cell Rep.* 26, 3444–3460.e5 (2019).
6. Hezroni, H. et al. A subset of conserved mammalian long non-coding RNAs are fossils of ancestral protein-coding genes. *Genome Biol.* 18, 1–15 (2017).
7. Venø, M. T. et al. Spatio-temporal regulation of circular RNA expression during porcine embryonic brain development. *Genome Biol.* 16, 245 (2015).
8. Weyn-Vanhenhenryck, S. M. et al. Precise temporal regulation of alternative splicing during neural development. *Nat. Commun.* 9, (2018).
9. Reemst, K., Noctor, S. C., Lucassen, P. J. & Hol, E. M. The indispensable roles of microglia and astrocytes during brain development. *Front. Hum. Neurosci.* 10, 1–28 (2016).
10. Liu, Y. P., Karg, M., Herrera-Carrillo, E. & Berkhout, B. Towards antiviral shRNAs based on the AgoshRNA design. *PLoS One* 10, 1–20 (2015).
11. You, X. et al. Neural circular RNAs are derived from synaptic genes and regulated by development and plasticity. *Nat. Neurosci. advance on*, 603–610 (2015).
12. Westholm, J. O. et al. Genome-wide Analysis of *Drosophila* Circular RNAs Reveals Their Structural and Sequence Properties and Age-Dependent Neural Accumulation. *Cell Rep.* 9, 1966–1981 (2014).
13. Rybak-Wolf, A. et al. Circular RNAs in the Mammalian Brain Are Highly Abundant, Conserved, and Dynamically Expressed. *Mol. Cell* 870–885 (2014). doi:10.1016/j.molcel.2015.03.027
14. Xu, K. et al. CircGRIA1 shows an age-related increase in male macaque brain and regulates synaptic plasticity and synaptogenesis. *Nat. Commun.* 11, 1–15 (2020).
15. Salzman, J., Chen, R. E., Olsen, M. N., Wang, P. L. & Brown, P. O. Cell-Type Specific Features of Circular RNA Expression. *PLoS Genet.* 9, (2013).
16. Lasda, E. & Parker, R. Circular RNAs: diversity of form and function. *RNA* 20, 1829–42 (2014).
17. Wilusz, J. E. A 360° view of circular RNAs: From biogenesis to functions. *Wiley Interdiscip. Rev. RNA* 9, 1–17 (2018).
18. Ashwal-Fluss, R. et al. CircRNA Biogenesis competes with Pre-mRNA splicing. *Mol. Cell* 56, 55–66 (2014).
19. Jeck, W. R. et al. Circular RNAs are abundant, conserved, and associated with ALU repeats. *RNA* 19, 141–57 (2013).
20. Zlotorynski, E. Non-coding RNA: Circular RNAs promote transcription. *Nat. Rev. Mol. Cell Biol.* 16, 206 (2015).
21. Gruner, H., Cortés-López, M., Cooper, D. A., Bauer, M. & Miura, P. CircRNA accumulation in the aging mouse brain. *Sci. Rep.* 6, 1–14 (2016).
22. Jongbloets, B. C. et al. Stage-specific functions of Semaphorin7A during adult hippocampal neurogenesis rely on distinct receptors. *Nat. Commun.* 8, 1–17 (2017).
23. Stoeckli, E. T. Understanding axon guidance: Are we nearly there yet? *Dev.* 145, (2018).
24. Patop, I. L., Wüst, S. & Kadener, S. Past, present, and future of circ RNA s. *EMBO J.* 38, 1–13 (2019).

25. Xu, K. et al. Annotation and functional clustering of circRNA expression in rhesus macaque brain during aging. *Cell Discov.* 1–18 (2018). doi:10.1038/s41421-018-0050-1
26. Sharfe, N., Freywald, A., Toro, A., Dadi, H. & Roifman, C. Ephrin stimulation modulates T cell chemotaxis. *Eur. J. Immunol.* 32, 3745–3755 (2002).
27. Nishide, M. & Kumanogoh, A. The role of semaphorins in immune responses and autoimmune rheumatic diseases. *Nat. Rev. Rheumatol.* 14, 91–103 (2018).
28. Chen, B. J., Huang, S. & Janitz, M. Changes in circular RNA expression patterns during human foetal brain development. *Genomics* 111, 753–758 (2019).
29. Xia, S. et al. Comprehensive characterization of tissue-specific circular RNAs in the human and mouse genomes. *Brief. Bioinform.* 18, 984–992 (2017).
30. Gokool, A., Anwar, F. & Voineagu, I. The Landscape of Circular RNA Expression in the Human Brain. *Biol. Psychiatry* 87, 294–304 (2020).
31. Rahimi, K., Venø, M. T., Dupont, D. M. & Kjems, J. Nanopore sequencing of full-length circRNAs in human and mouse brains reveals circRNA-specific exon usage and intron retention. *bioRxiv* 1–30 (2019). doi:10.1101/567164
32. Hansen, T. B. et al. Natural RNA circles function as efficient microRNA sponges. *Nature* 495, 384–388 (2013).
33. Memczak, S. et al. Circular RNAs are a large class of animal RNAs with regulatory potency. *TL - 495. Nature* 495 VN-, 333–338 (2013).
34. Jeck, W. R. & Sharpless, N. E. Detecting and characterizing circular RNAs. *Nat. Biotechnol.* 32, 453–61 (2014).
35. Guo, J. U., Agarwal, V., Guo, H. & Bartel, D. P. Expanded identification and characterization of mammalian circular RNAs. *Genome Biol.* 15, 409 (2014).
36. Du, W. W. et al. Foxo3 circular RNA retards cell cycle progression via forming ternary complexes with p21 and CDK2. *Nucleic Acids Res.* 44, 2846–2858 (2016).
37. Dudekula, D. B. et al. Circinteractome: A web tool for exploring circular RNAs and their interacting proteins and microRNAs. *RNA Biol.* 13, 34–42 (2016).
38. Preitner, N., Quan, J., Li, X., Nielsen, F. C. & Flanagan, J. G. IMP2 axonal localization, RNA interactome, and function in the development of axon trajectories. *Dev.* 143, 2753–2759 (2016).
39. Hentze, M. W. & Preiss, T. Circular RNAs: splicing's enigma variations. *EMBO J.* 32, 923–925 (2013).
40. Wilusz, J. E. & Sharp, P. a. A Circuitous Route to Are Gold Clusters in RF Fields. *Science* (80-.). 6–8 (2013). doi:10.1126/science.1238522
41. Salzman, J., Gawad, C., Wang, P. L., Lacayo, N. & Brown, P. O. Circular RNAs are the predominant transcript isoform from hundreds of human genes in diverse cell types. *PLoS One* 7, (2012).
42. Liu, J. J. et al. CasX enzymes comprise a distinct family of RNA-guided genome editors. *Nature* 566, 218–223 (2019).
43. Kleaveland, B., Shi, C. Y., Stefano, J. & Bartel, D. P. A Network of Noncoding Regulatory RNAs Acts in the Mammalian Brain. *Cell* 174, 350–362. e17 (2018).
44. Kristensen, L. S. et al. Spatial expression analyses of the putative oncogene ciRS-7 in cancer reshape the microRNA sponge theory. *Nat. Commun.* 11, (2020).
45. Lasda, E. & Parker, R. Circular RNAs Co-Precipitate with Extracellular Vesicles: A Possible Mechanism for circRNA Clearance. *PLoS One* 11, 1–11 (2016).
46. Preußner, C. et al. Selective release of circRNAs in platelet-derived extracellular vesicles. *J. Extracell. Vesicles* 7, (2018).

47. Zhao, R. T. et al. Circular ribonucleic acid expression alteration in exosomes from the brain extracellular space after traumatic brain injury in mice. *Journal of Neurotrauma* 35, (2018).
48. Sonnenschein, K. et al. Serum circular RNAs act as blood-based biomarkers for hypertrophic obstructive cardiomyopathy. *Sci. Rep.* 9, 1–8 (2019).
49. Wen, G., Zhou, T. & Gu, W. The potential of using blood circular RNA as liquid biopsy biomarker for human diseases. *Protein Cell* (2020). doi:10.1007/s13238-020-00799-3
50. Lu, D. et al. Identification of Blood Circular RNAs as Potential Biomarkers for Acute Ischemic Stroke. *Front. Neurosci.* 14, 1–15 (2020).
51. Memczak, S., Papavasileiou, P., Peters, O. & Rajewsky, N. Identification and characterization of circular RNAs as a new class of putative biomarkers in human blood. *PLoS One* 10, 1–13 (2015).
52. Li, J. et al. High-Throughput data of circular RNA profiles in human temporal cortex tissue reveals novel insights into temporal lobe epilepsy. *Cell. Physiol. Biochem.* 45, 677–691 (2018).
53. Zhao, Y., Alexandrov, P. N., Jaber, V. & Lukiw, W. J. Deficiency in the ubiquitin conjugating enzyme UBE2A in Alzheimer's Disease (AD) is linked to deficits in a natural circular miRNA-7 sponge (circRNA; ciRS-7). *Genes (Basel)*. 7, (2016).
54. Sang, Q. et al. CircSNCA downregulation by pramipexole treatment mediates cell apoptosis and autophagy in Parkinson's disease by targeting miR-7. *Aging (Albany, NY)*. 10, 1281–1293 (2018).
55. Errichelli, L. et al. FUS affects circular RNA expression in murine embryonic stem cell-derived motor neurons. *Nat. Commun.* 8, 1–11 (2017).
56. Van Battum, E. Y., Brignani, S. & Pasterkamp, R. J. Axon guidance proteins in neurological disorders. *Lancet Neurol.* 14, 532–546 (2015).
57. Luykx, J. J., Giuliani, F., Giuliani, G. & Veldink, J. Coding and non-coding RNA abnormalities in bipolar disorder. *Genes (Basel)*. 10, 1–14 (2019).
58. Bejugam, P. R., Das, A. & Panda, A. C. Seeing is believing: Visualizing circular rnas. *Non-coding RNA* 6, 1–18 (2020).
59. Li, Y., Chen, B. & Huang, S. Identification of circRNAs for miRNA targets by Argonaute2 RNA immunoprecipitation and luciferase screening assays. *Methods Mol. Biol.* 1724, 209–218 (2018).
60. König, J. et al. ICLIP - transcriptome-wide mapping of protein-RNA interactions with individual nucleotide resolution. *J. Vis. Exp.* 2–8 (2011). doi:10.3791/2638
61. Hafner, M. et al. PAR-CLIP - A method to identify transcriptome-wide the binding sites of RNA binding proteins. *J. Vis. Exp.* 2–6 (2010). doi:10.3791/2034
62. Licatalosi, D. D. et al. HITS-CLIP insights into processing. *Nature* 456, 464–469 (2009).
63. Zhang, K., Pan, X., Yang, Y. & Shen, H. Bin. Predicting circRNA-RBP interaction sites using a codon-based encoding and hybrid deep neural networks. *bioRxiv* 1604–1615 (2018). doi:10.1101/499012
64. Zhang, G. et al. Identifying Circular RNA and Predicting Its Regulatory Interactions by Machine Learning. *Front. Genet.* 11, 1–16 (2020).
65. Du, W. W. et al. Identifying and characterizing circRNA-protein interaction. *Theranostics* 7, 4183–4191 (2017).





ADDENDA

Nederlandse Samenvatting Curriculum Vitae Acknowledgements

'The dark light' - Photo by Bart van Dijk and Daniëlle van Rossum for the Art of Neuroscience competition 2018.

NEDERLANDSE SAMENVATTING

De hersenen zijn opgebouwd uit biljoenen zenuwcellen. Elke zenuwcel kan over een korte of lange afstand verbindingen maken met honderden andere zenuwcellen, waardoor hersengebieden met elkaar kunnen communiceren. Ondanks dat er zoveel zenuwcellen in het brein zijn, weten de uitlopers van individuele cellen precies waar zij heen moeten groeien. Dit komt deels doordat ze tijdens hun groei geleid worden door axon guidance moleculen. Axon guidance is een complex proces dat ervoor zorgt dat zenuwcellen op het juiste moment (temporeel) en op de juiste plek (spatieel) een bepaalde kant op worden gestuurd. De genen die betrokken zijn bij axon guidance produceren eiwitten die deze processen in goede banen leiden. Daarnaast is er onlangs bekend geworden dat deze genen ook zeer stabiele gesloten cirkels van RNA in zenuwcellen produceren. Verschillende studies tonen aan dat deze circulaire RNA's (circRNA's) van axon guidance genen op een heel precieze temporele en spatiele manier tot expressie worden gebracht tijdens de ontwikkeling van zenuwcellen, wat zou suggereren dat ze een rol spelen bij de ontwikkeling van het zenuwstelsel.

Over de precieze rol van axon guidance circRNA's bij de vorming van het complexe zenuwstelsel is nog weinig bekend. Het begrijpen van de functie van axon guidance circRNA's in de ontwikkelende hersenen kan helpen om inzicht te krijgen in de mechanismen die ten grondslag liggen aan de vorming van het zenuwstelsel en de ontwikkeling van bepaalde hersenaandoeningen. Hieruit is vraag ontstaan wat de precieze expressie en functie van axon guidance circRNA's in het ontwikkelende brein zijn. In dit proefschrift onderzochten we daarom de expressie van axon guidance circRNA's in de zenuwcellen van het brein door gebruik te maken van verschillende moleculaire en cellulaire benaderingen. Daarnaast is dit proefschrift gericht op het onderzoeken van de functie van een axon guidance circRNA's *in vitro* (buiten het lichaam van een organisme) en *in vivo* (binnen het lichaam van een organisme) door het toepassen van verschillende manipulatie technieken.

In hoofdstuk 1 van dit proefschrift karakteriseerden we de expressie van axon guidance circRNA's in het volwassen menselijke brein met behulp van RNA-sequencing (een techniek die het mogelijk maakt om genexpressie in kaart te brengen) en in het ontwikkelende- en volwassen muizenbrein met behulp van verschillende moleculaire

technieken. We hebben gevonden dat axon guidance circRNA's geconserveerd zijn tussen verschillende diersoorten (o.a. mens en muis), onafhankelijk van de conventionele 'lineaire' RNA's van hetzelfde gen tot expressie worden gebracht (van een gen kunnen zowel lineaire als circulaire RNA's afkomen) en dat ze een dynamisch spatiaal en temporeel expressiepatroon vertonen. Daarnaast identificeerden we een expressiepiek van axon guidance circRNA's in de hersenen van de muis net voor de geboorte en observeerden we een trend in accumulatie van circRNA's gedurende de maturatie van de hersenen.

Afgelopen jaren zijn er verschillende *In situ* hybridisatie (ISH) technieken ontwikkeld om circRNA's *in vitro* en *in vivo* aan te kleuren en te detecteren. Om meer inzicht te krijgen in de spatiale en temporele expressie patronen van axon guidance circRNA's maakten we gebruik van verschillende ISH technieken en bespraken hun voor en nadelen in hoofdstuk 2. Met behulp van de ISH techniek ViewRNA waren we in staat om een overzicht te maken van de spatiotemporele expressie van een geselecteerde groep axon guidance circRNA's in zenuwcellen *in vitro*. Dit overzicht laat zien dat de expressie niveaus en cellulaire lokalisatie van deze circRNA's dynamisch zijn en dat deze variëren tijdens maturatie van zenuwcellen. Daarnaast vonden we dat de onderzochte circRNA's voornamelijk tot expressie komen in excitatoire (activerende) zenuwcellen en niet in gliacellen (zenuwcel-ondersteunende cellen die ook in grote getalen in het brein voorkomen).

In hoofdstuk 3 maakten we gebruik van verschillende technieken voor de manipulatie van de expressieniveaus van axon guidance circRNA's. CircRNA's werden met succes tot overexpressie gebracht *in vitro* (in celkweken) en *in vivo* (in het netvlies van de muis). Voor de uitschakeling van axon guidance circRNA's hebben we verschillende manipulatie strategieën geïmplementeerd, waarvan het gebruik van siRNA's (hele kleine RNA's die de expressie van genen kunnen beïnvloeden) tot een betrouwbare uitschakeling *in vitro* leidde. Sholl-analyse (een manier om de complexiteit van zenuwcellen te meten) na uitschakeling met siRNA's suggereerde een mogelijke rol voor bepaalde axon guidance circRNA's bij de vertakking van zenuwuitlopers. Uitschakeling van circRNA's met behulp van siRNA's in de muis-cortex, de buitenste laag van de hersenen, met behulp van *in utero* elektroporatie veroorzaakte geen duidelijke defecten. Ten slotte observeerden we dat de expressie van axon guidance circRNA's is verhoogd *in vitro* als gevolg van cellulaire activatie.

CiRS-7 is het eerst en meest bestudeerde circRNA. CiRS-7 kan meerdere kleine RNA's zoals microRNA's (miRNA's) aan zich binden (waaronder miR-7, miR-671 en miR-135a) en dit proces staat bekend staat als het sponzen van miRNAs. Op basis van eerder gepubliceerde data is gebleken dat miR-135a wordt geassocieerd met temporaalkwabepilepsie (TLE). De exacte rol van de interactie tussen ciRS-7 en miR-135a in het verloop of ontstaan van TLE blijft echter nog onduidelijk. In hoofdstuk 4 hebben we daarom eerst systematisch de expressiepatronen van miR-7, miR-671 en ciRS-7 onderzocht in de ontwikkelende muizenhersenen. Daarna hebben we ciRS-7 en miR-135a expressieniveaus in TLE patiëntmateriaal geanalyseerd en ontdekten we dat ciRS-7 en miR-135a significant lager aanwezig zijn in WO TLE weefsel. We namen een tegengestelde expressiecorrelatie tussen ciRS-7 en miR-135a waar *in vitro* na uitschakeling of overexpressie van een van de twee moleculen, wat suggereert dat ze een biologische interactie hebben. De functionele betekenis van de relatie tussen ciRS-7 en miR-135a in TLE pathologie moet nog verder worden onderzocht, maar de gepresenteerde resultaten kunnen dienen als een uitgangspunt voor verdere studies.

Samenvattend bieden de resultaten in dit proefschrift een overzicht van de expressie axon guidance circRNA's in de hersenen van mensen en muizen en zetten we een eerste stap in het onderzoeken van de functie van axon guidance circRNA's. Alhoewel de ontwikkeling van betere technieken om circRNAs te besturen nodig is en verder onderzoek moet worden gedaan om achter de functie(s) van axon guidance circRNA's in het (ontwikkelende) zenuwstelsel te komen, dragen de verkregen inzichten in dit proefschrift bij aan onze kennis over de regulatie van genexpressie tijdens de ontwikkeling van de hersenen.



CURRICULUM VITAE

About the author

Daniëlle Samantha van Rossum was born on February 2nd 1991 in Zoetermeer, the Netherlands. In 2009 she graduated high school and received her gymnasium diploma at the Erasmus College Zoetermeer. Later that year she started the Bachelor programme “Biology” at Leiden University where she followed a variety of different courses. In her third year she did an internship in the group of Prof. Carel ten Cate at the Institute of Biology Leiden (IBL) where she worked on a translational study on grammar learning in zebrafishes and humans that resulted in a publication. With a growing curiosity for Neuroscience research, she next went on exchange to Uppsala University in Zweden to follow courses of the master programme “Genes, Brain and Behaviour”. After returning from Zweden in 2013 she obtained her Bachelor degree in Biology and got accepted to the research master “Neuroscience and Cognition” at Utrecht University. During her master programme Daniëlle performed an internship in the group of Prof. R. Jeroen Pasterkamp at the Utrecht Brain Center of the University Medical Center Utrecht (UMCU) where she investigated the prion properties of the ALS associated proteins FUS and TDP-43. In addition, she wrote a grant proposal together with Prof. R. Jeroen Paterkamp as



Picture by Bart van Dijk

part of the NWO graduate program and got awarded with a 4-year personal PhD grant. Before starting her PhD, Daniëlle finished her Master studies with an internship at the ETH/University of Zürich in Switzerland, where she worked in the group of Prof. Martin Schwab on the role of Nogo-A exosomes in spinal cord injury under the supervision of Dr. Mea Holm. After completion of her Master, Daniëlle continued her scientific career in 2016 as a PhD candidate in de group of Prof. R. Jeroen Pasterkamp at the Utrecht Brain Center UMCU, where she focused on the expression and function of axon guidance circRNAs during brain development. The results of these studies are presented in this thesis. Currently Daniëlle is working as a project coordinator and policy officer education at the Department of Developmental Origins of Disease at the Wilhelmina Children’s hospital (WKZ) in Utrecht.

List of publications

van Rossum D, Verheijen BM, Pasterkamp RJ (2016) Circular RNAs: Novel Regulators of Neuronal Development. *Front Mol Neurosci* 9:1–7 Available at: <http://journal.frontiersin.org/Article/10.3389/fnmol.2016.00074/abstract>.

Chen J, van Rossum D, ten Cate C (2015) Artificial grammar learning in zebra finches and human adults: XYX versus XXY. *Anim Cogn* 18:151–164.

Poster presentations

2016	Berlin Summer Meeting: Brave New RNA	Berlin, Germany
	BCRM PhD Day	Utrecht, the Netherlands
2017	AXON meeting	Vienna, Austria
	Non-coding RNAs in Nervous System	
	Development, Plasticity and Disease meeting	Marburg, Germany
	ONWAR retraite	Woudschoten, the Netherlands
2018	Molecular Mechanisms of Neuronal	
	Connectivity meeting	Cold Spring Harbour, USA
	BCRM research day	Utrecht, the Netherlands
	ONWAR retraite	Woudschoten, the Netherlands



ACKNOWLEDGEMENTS

The road towards creating this book has been an immense journey and the appreciation for the inner circle that contributed the most - my fun and caring colleagues, students, lab shenanigans and fellow scientists who turned into amazing friends, out-of-work-friends who were the biggest cheerleaders imaginable, my Christmas CD's that were making the days with bad data a little brighter (apologies for any harm caused) and my family, without whose love and support I wouldn't be where I am today - is impossible for me to describe without adding another 'chapter' to this book. Therefore, I will thank everyone with a personal note for their incredible support throughout the years and for making my days as a PhD student joyful and memorable.



SAMENSTELLING BEOORDELINGSCOMMISSIE

Prof. dr. K.P.J. Braun

Prof. dr. J.P.H. Burbach

Prof. dr. J. Kjemis

Prof. dr. J.P.G. Sluiter

Dr. C.J. Wierenga

"The circle is now complete" - Star Wars